

SYNTHESIS OF SIMPLIFIED DISCODERMOLIDE ANALOGS

by

Daniel Michael Brody

B.S., Marquette University, 2006

Submitted to the Graduate Faculty of
the Kenneth P. Dietrich School of Arts and Sciences in partial fulfillment
of the requirements for the degree of
Master of Science

University of Pittsburgh

2013

UNIVERSITY OF PITTSBURGH
Dietrich School of Arts and Sciences

This thesis was presented

by

Daniel M. Brody

It was defended on

November 19th, 2013

and approved by

Chair: Dennis P. Curran, Professor, Department of Chemistry

Kazunori Koide, Associate Professor, Department of Chemistry

Kay Brummond, Professor, Department of Chemistry

Barry Gold, Professor, Department of Pharmaceutical Sciences

Copyright © by Daniel M. Brody

2013

Synthesis of Simplified Discodermolide Analogs

Daniel M. Brody, MS

University of Pittsburgh, 2013

Discodermolide was discovered in 1990 and with its discovery set off an expansive medicinal chemistry program fueled by many groups' research. It acts as a microtubule stabilizer, which makes it a potential anti-cancer agent. The synthesis of simplified discodermolide analogs is reported here. These analogs use simplified versions of the lactone and carbamate fragments, which are then coupled via olefin metathesis. Hologram quantitative structure-activity relationship (HQSAR) is also used to show that an olefin linker inserted by olefin metathesis as viable simple alternatives to the complex middle portion usually found in the parent molecule.

TABLE OF CONTENTS

PREFACE.....	X
1.0 INTRODUCTION.....	1
1.1 EARLY SYNTHETIC STUDIES.....	2
1.2 SYNTHETIC WORK OF DISCODERMOLIDE	3
1.3 MECHANISM OF ACTION AS A MICROTUBULE STABILIZER.....	6
1.3.1 The Microtubule System and Discodermolide	6
1.3.2 The Mechanism of Action of Discodermolide	7
1.3.3 Discodermolide Activity in Combination with Other Agents.....	10
1.4 CONFORMATIONAL ANALYSES OF DISCODERMOLIDE	11
1.4.1 Docking Studies of Discodermolide.....	13
1.5 SYNTHETIC ANALOGS OF DISCODERMOLIDE.....	15
1.5.1 Analogs of the Lactone Fragment	16
1.5.2 Analogs of the Carbamate Fragment.....	17
1.5.3 Analogs of the Linker Fragment	18
1.5.4 Dictyostatin.....	19
1.5.5 Hybrid Microtubule Stabilizer Analogs	20
1.6 GOALS OF STUDY	22
2.0 MOLECULAR MODELING OF NEW DISCODERMOLIDE ANALOGS	24

2.1	INTRODUCTION	24
2.2	RESULTS	25
2.3	CONCLUSION	34
3.0	SYNTHESIS OF SIMPLIFIED DISCODERMOLIDE FRAGMENTS.....	35
3.1	INTRODUCTION	35
3.2	RESULTS	36
3.2.1	Synthesis of the Common Precursor 29.....	36
3.2.2	Synthesis of the Simplified Carbamate Fragment 24.....	38
3.2.3	Redesigned Scheme for the Simple Carbamate Fragment 24	39
3.2.4	Synthesis of the Phenyl Replacement Carbamate Fragment 20	41
3.2.5	Synthesis of Courmarin Lactone 15.....	43
3.2.6	Synthesis of the Phenol Lactone Replacement 22.....	44
3.2.7	Synthesis of Short-Chain Lactone 23.....	45
3.3	SUMMARY	46
4.0	SYNTHESIS OF DISCODERMOLIDE ANALOGS	47
4.1	INTRODUCTION	47
4.2	RESULTS	48
4.2.1	Final Steps of Analogue Synthesis.....	48
5.0	SUMMARY	52
6.0	EXPERIMENTAL SECTION	53
APPENDIX 1.....		84
BIBLIOGRAPHY		155

LIST OF TABLES

Table 1-Fragments Used for HQSAR Studies	27
Table 2-HQSAR Model Parameters	28
Table 3-HQSAR pIC ₅₀ predictions, Models 1 and 2	30
Table 4-HQSAR Results, Models 3 and 4	31

LIST OF FIGURES

Figure 1- (+)-Discodermolide and its constituent moieties. Stereotriad is identified by starts.	2
Figure 2- Schreiber Synthesis of (+)-Discodermolide, the Correct Enantiomer of the Natural Product	3
Figure 3- Common Precursor Synthetic Scheme used by Smith and Novartis for Scale-up Synthesis	5
Figure 4- Formation of Microtubules by the α,β tubulin heterodimer (<i>Reprinted by permission from Macmillan Publishing Ltd: Nat. Rev. Cancer, 2004, 4, 253-265. Copyright 2004</i>)	7
Figure 5- Turbidity Assay Result Comparing Discodermolide (3), Paclitaxel (2) and Untreated Microtubules (1). (<i>Adapted with permission from ter Haar et al. Biochemistry, 1996, 35 pp243-250. Copyright 1996, American Chemical Society</i>).....	9
Figure 6- Discodermolide Crystal Structure that Shows the Hairpin Structure (<i>Journal of Organic Chemistry, 1990, 55, pp 4912-4915</i>)	12
Figure 7- Two Distinct Poses of Discodermolide in the Taxane Binding Site (<i>Reprinted with permission from the Journal of Medicinal Chemistry vol 53, 2010, pp 155-165. Copyright 2010, American Chemical Society</i>).....	14
Figure 8- SAR of the Lactone Ring of Discodermolide and Possible Replacement Groups	17
Figure 9- SAR of the Carbamate Fragment of Discodermolide	18

Figure 10- SAR of the Linker Region of Discodermolide and Other Additions	19
Figure 11- The Marine Natural Product Dictyostatin	20
Figure 12- Paterson Discodermolide/Dictyostatin/Paclitaxel Hybrids containing the C8-C24 portion of Discodermolide, C1-C7 portion of Dictyostatin, and the side chains of Paclitaxel or Docetaxel	22
Figure 13- Experimental Design for Discodermolide Analogs using Simple Linker Groups	23
Figure 14- Assembly of Analogs for HQSAR Screening	26
Figure 15- Virtual Analogs the have a pIC ₅₀ value above 7.0 in 3 out of 4 models	32
Figure 16- A. Analogue C-1 Structure. B. C-1 Overlaid on the 3-D structure of Discodermolide to Demonstrate the Hairpin Conformation of the Analogue	33
Figure 17- Fragments Targeted for Synthesis of Discodermolide Analogs	36
Figure 18- Synthesis of the Common Precursor Lactone 29	37
Figure 19- First Attempt for Simple Carbamate 24	39
Figure 20- Revised Route to Carbamate Fragment 24	41
Figure 21- Synthesis of Simple Carbamate Fragment 20 Containing a Phenyl End Group	43
Figure 22- Synthesis of the Coumarin Fragment 15 as a Lactone Replacement	44
Figure 23- Synthesis of Phenol Fragment 22 as a Lactone Replacement	45
Figure 24- Synthesis of Short Chain Lactone Fragment 23	45
Figure 25- Analogue Containing Short Chain Lactone and Phenyl Carbamate Groups	49
Figure 26- Synthesis of Analogue Containing Coumarin and Phenyl Carbamate Groups	50
Figure 27- Synthesis of Analogue Containing Two Phenyl Groups	51

PREFACE

A thank you is necessary for Prof. Adriano Andricopulo and Dr. Livia Salum for performing the HQSAR screen for my discodermolide analogs. I thank all those who worked on the discodermolide project with me, including Amy Short, Wanli Pu, Amanda Gavin, Kate Adams, and Sevara Zayitova. I thank Dr. Lee McDermott for editorial help in preparation of this manuscript. Thank you to the American Chemical Society Division of Medicinal Chemistry for a Pre-doctoral fellowship. Thank you to all the members of the Day laboratory for help along the way with research, especially Dr. Prema Iyer. Thank you to my committee for insight and advice during my years in graduate school. Thank you to Prof. Billy Day for mentorship and allowing me to work in your lab. And thank you to my family and friends, especially my wife Andrea, for all the love and support throughout school. I could not have done this without her.

1.0 INTRODUCTION

Discodermolide **1** (**Figure 1**) was first discovered in 1990 by researchers at the Harbor Branch Oceanographic Institution, Inc. from the marine sponge *Discodermia dissoluta*.¹ The molecule is a complex polyketide containing thirteen stereocenters, four double bonds (a terminal diene and two internal *Z*-olefin linkages), four hydroxy groups, a δ -lactone and a carbamate. The first biological screens of the molecule identified discodermolide as a potential immunosuppressive agent.¹ Initial studies compared discodermolide with the immunosuppressive agents cyclosporin A and FK506 (a novel immunosuppressive agent at the time, now known as tacrolimus). *In vitro* studies showed that discodermolide was nearly as potent in suppressing proliferation in a mixed lymphocyte reaction assay as cyclosporin A, but not as potent as FK506.² Follow-up *in vivo* studies identified discodermolide to be more potent than cyclosporin A.³ The relative configuration of discodermolide was elucidated by using an acetylated form of the molecule by 1D and 2D NMR techniques,¹ but the absolute stereochemistry was unknown for some time. Although the potential for discodermolide as a drug was exciting, the excitement was tempered because it represented only 0.002 % by weight of the *Discodermia* sponge.¹ The supply problem, as well as the potential of discodermolide as an active compound, led many groups to undertake its total synthesis and pursue further biological studies.

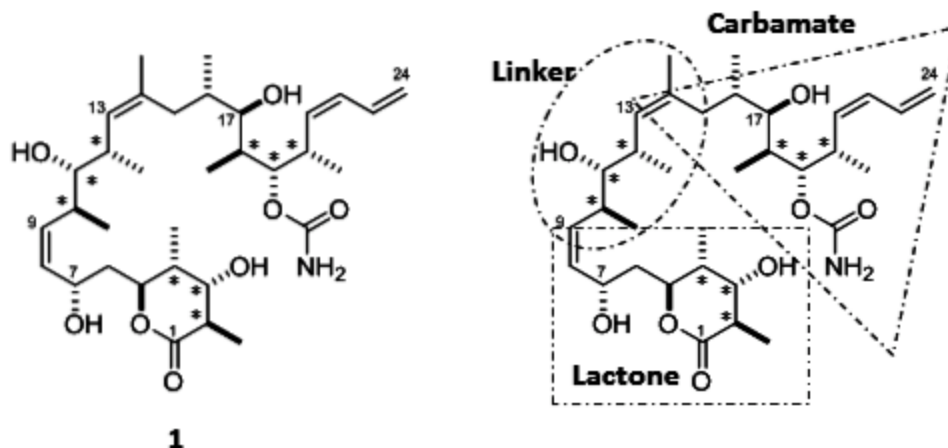


Figure 1- (+)-Discodermolide and its constituent moieties. Stereotriad is identified by stars.

1.1 EARLY SYNTHETIC STUDIES

The first total synthesis of discodermolide was reported in 1993 by the Schreiber group.⁴ The synthesis began with the now common disconnection of discodermolide into three fragments **5**, **6**, and **7** (**Figure 1** and **Figure 2**), all of which contain the same *syn*, *anti*, methyl-hydroxy-methyl stereotriad (stars in **figure 1**). The three fragments are separated by the double bonds at C8-9 and C13-14. The synthesis by Schreiber used a common starting material, the enantiomers of 3-hydroxy-2-methylpropionate **2** (a.k.a., Roche ester), to synthesize both the (–) and the (+) enantiomers of the natural product in a highly convergent synthetic scheme (**Figure 2**).^{5,6} From the starting ester, they made two homoallylic alcohols **3** and **4** that could be transformed into fragments containing the C1-C7 lactone **6**, C8-C15 linker **5**, and the C16-C24 carbamate **7** (numbering for discodermolide begins with the lactone carbonyl group, see **figure 1**). A revised strategy called for coupling of the lactone and linker portions via a Nozaki-Kishi reaction, and

then an alkylation with the *E*-enolate at C16 and the combined lactone-linker portion. With both enantiomers of **1** in hand, Schreiber identified (+)-discodermolide as the natural product by comparison of optical rotation values of the synthesized enantiomers to the value reported by Gunasekera. Also, Schreiber compared the anti-proliferative potencies of the synthesized compounds to the isolated compound to confirm (+)-discodermolide as the correct enantiomer.⁵ The first total synthesis of **1** was completed in 36 total steps, with a yield of 4.3 % over a 24 step longest linear sequence.⁶

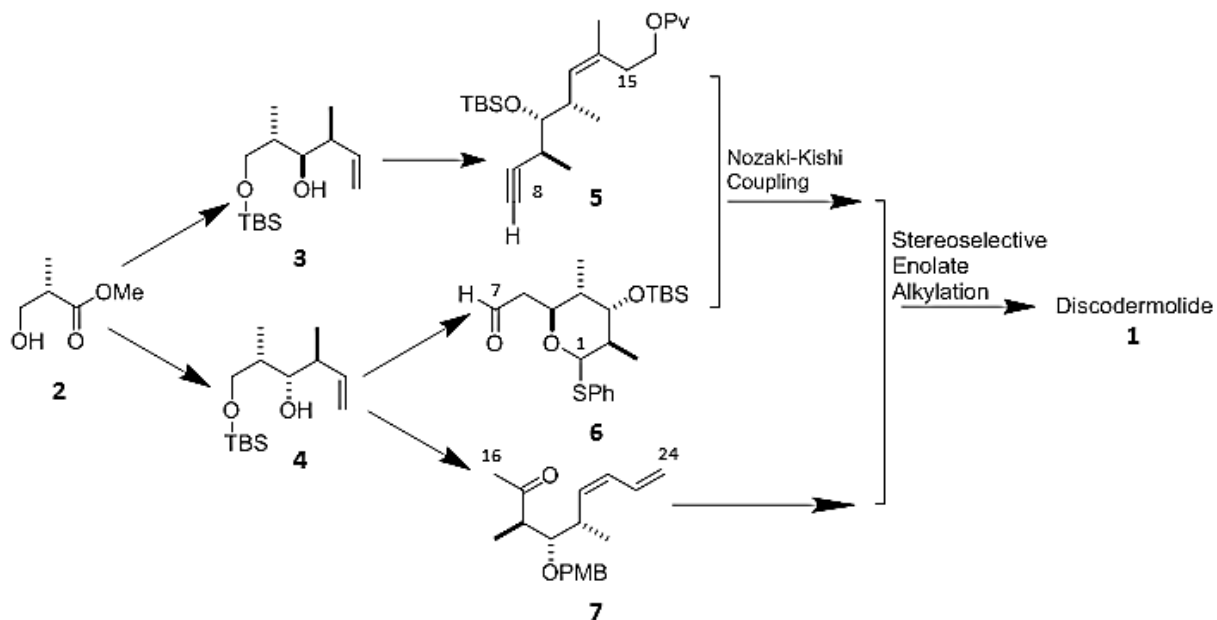


Figure 2- Schreiber Synthesis of (+)-Discodermolide, the Correct Enantiomer of the Natural Product

1.2 SYNTHETIC WORK OF DISCODERMOLIDE

Following Schreiber's total synthesis, many other groups worked on discodermolide synthesis. Four total syntheses have been completed by Amos Smith's group.⁷ Their syntheses use a

“common precursor” to synthesize three fragments that contain the stereotriad of discodermolide starting from Roche’s ester **2**. The result of the first synthesis was the antipode of discodermolide.⁷ In 1999, Smith published a synthetic route that resulted in one gram of the natural form of discodermolide using the common precursor scheme as before with the correct enantiomer of Roche ester as the starting material (**Figure 3**).⁸ Briefly, the common precursor synthesis began with *para*-methoxybenzyl protection of the primary alcohol **2** to yield ether **8**. The ester moiety of **8** is reduced with lithium aluminum hydride to yield **9**. Alcohol **9** is oxidized with Swern conditions to yield aldehyde **10**. Aldehyde **10** undergoes an Evans syn-aldol condensation with **11** to yield **12**. Finally, **12** is transformed to Weinreb amide **13** with treatment of trimethylaluminum. The Evans auxiliary **11** can be recycled, which helps in the scale-up of the synthesis. They improved on their initial synthesis by employing only 24 steps in the longest linear sequence, and 6 % overall yield. A third approach was disclosed in 2003,⁹ and in 2005 a fourth approach was reported that reduced the total number of steps (longest linear sequence 17 steps) and increased the overall yield to 9%.¹⁰ Novartis Pharma, needing many grams of discodermolide to perform clinical trials, used Smith’s common precursor **13** to make the three fragments of discodermolide. This was followed by coupling methods found in the syntheses by Smith and Paterson. This impressive feat resulted in 60 g over 39 steps and required only 17 chromatographic purifications, allowing Novartis to begin clinical trials of discodermolide as a potential anti-cancer medicine.^{11–15}

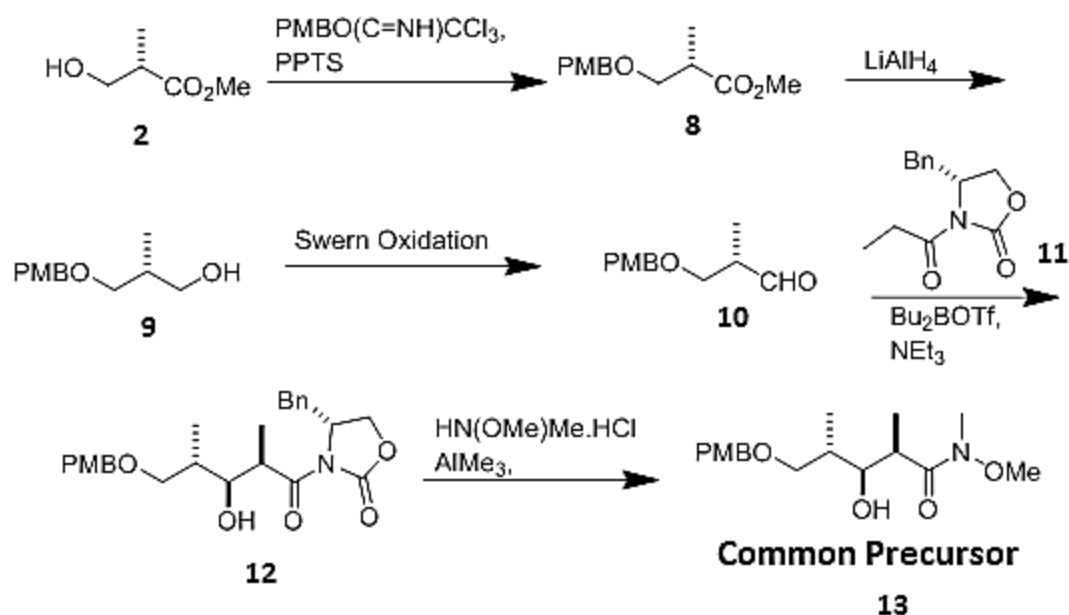


Figure 3- Common Precursor Synthetic Scheme used by Smith and Novartis for Scale-up Synthesis

In a first synthesis,¹⁶ the Paterson group made discodermolide with an overall yield of 10.3% over 23 steps for the longest linear sequence (42 steps overall).¹⁶ The same group reported two other total syntheses of discodermolide. The 3rd route completes discodermolide in an overall yield of 11.3% from the chiral Roche ester.¹⁷ The Myles group reported a total synthesis of the enantiomer of discodermolide in 1997¹⁸ and followed that with the preparation of the naturally occurring compound in 2003.¹⁹ Marshall and Johns disclosed their total synthesis of discodermolide in 1998.²⁰ Arefalov and Panek reported a total synthesis of discodermolide in 2005 in 42 steps with 2.1 % overall yield.²¹ The Ardisson group published a total synthesis in 2008 that completed the natural product in a 21-step longest linear sequence in a yield of 1.6 %.²² These innovative total syntheses testify to the importance of discodermolide **1** as a drug candidate, since many groups devised ways to make the natural product.

1.3 MECHANISM OF ACTION AS A MICROTUBULE STABILIZER

1.3.1 The Microtubule System and Discodermolide

Microtubules are a crucial part of the cytoskeleton that has a role in many cellular functions. These hollow tubes consist of polymerized α , β tubulin heterodimers organized into thirteen protofilaments that form a 25 nm inner diameter tube (**Figure 4**). Tubulin is a 55 kDa protein that appears in 5 isoforms (α , β , γ , δ , and ϵ). Two isoforms (α and β) make up the majority of the protein found in cells. Microtubules have the ability to grow up to a few micrometers in length or to shrink depending on the need at a particular moment. During mitosis, microtubules undergo rapid polymerization/depolymerization to search and capture kinetochores (the center of chromatids available for microtubule attachment) of sister chromatid pairs during prometaphase of mitosis. Cells cannot undergo normal division until all chromosomes are attached and able to be separated by the two microtubule-anchoring centrosomes. Microtubule-perturbing agents act during this stage, causing cell-cycle arrest and apoptosis.²³ Because microtubules are crucial for cell division, they are validated targets for cancer drugs.

Drugs that target the microtubule system fall into two categories: microtubule stabilizers and destabilizers. Microtubule destabilizers, such as colchicine and the vinca alkaloids, act by arresting the polymerization of microtubules and disrupting the dynamics of the system.²⁴ Microtubule stabilizers act by inhibiting the depolymerization of microtubules. The inhibition arrests mitosis because of microtubule bundling and inhibition of the search and capture mechanism needed to separate sister chromatid pairs.²⁵ The best studied microtubule-stabilizing agent is paclitaxel, a compound whose mechanism of action was determined in 1979.²⁶

Paclitaxel, used clinically as an anticancer drug, binds to polymerized microtubules and causes cell cycle arrest but exhibits some problems as a drug due to low solubility.

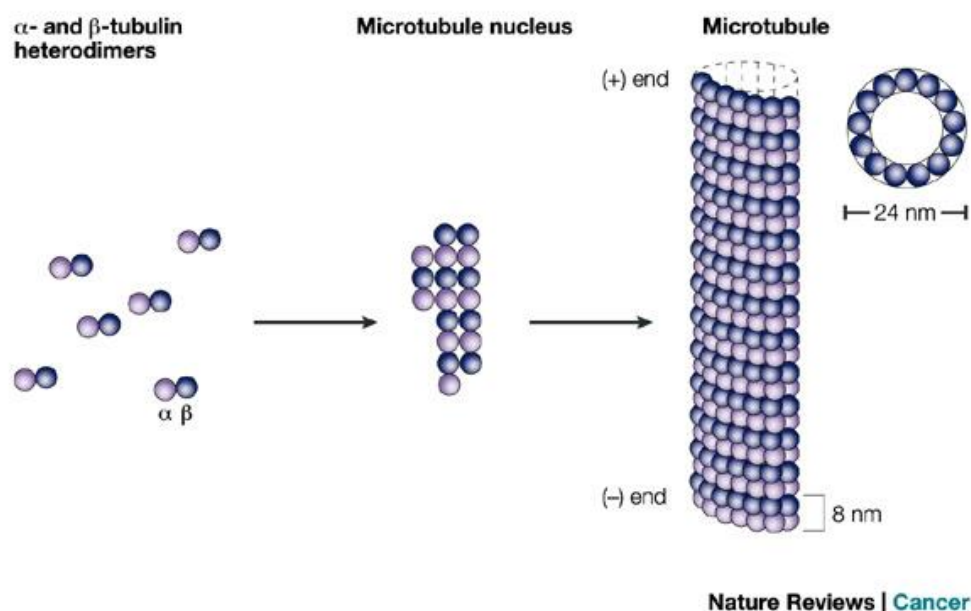


Figure 4- Formation of Microtubules by the α,β tubulin heterodimer (Reprinted by permission from Macmillan Publishing Ltd: *Nat. Rev. Cancer*, **2004**, 4, 253-265. Copyright 2004)

1.3.2 The Mechanism of Action of Discodermolide

In conjunction with the synthesis of both antipodes of discodermolide, Schreiber first reported in 1994⁵ that both enantiomers arrested the cell cycle of MG63 human osteoblasts, but in different phases. The natural (+)-antipode arrests the cell cycle in the G2/M (mitosis) phase, while the unnatural (-)-antipode arrests the cell cycle in the S (synthesis) phase.

A QSAR (quantitative structure-activity relationship) screen of multiple libraries looking for molecules with potential microtubule-perturbing activity by the Day group unexpectedly

identified discodermolide as a possible microtubule stabilizer.²⁷ The Day group then performed initial *in vitro* studies that showed that discodermolide acted as a microtubule stabilizer.²⁸ Microtubule stabilizers at that time included only paclitaxel, docetaxel and the epothilones, but since then the class has grown to include dictyostatin and several others. Although structurally diverse, all of these microtubule-stabilizing agents have shown strong preclinical activity as potential anti-cancer therapeutics.²⁵

The Day group compared discodermolide and paclitaxel in cell assays. The GI₅₀ (50% growth inhibition of cells) value was 2.4 nM for discodermolide compared to 2.1 nM for paclitaxel in the estrogen-responsive cell line MCF-7. A turbidity assay was performed to investigate the ability of discodermolide to alter the assembly of tubulin *in vitro* (**Figure 5**). Discodermolide caused tubulin assembly at 0 °C in the presence of microtubule associated proteins and GTP (**Figure 5, curve 3**). Without test agents, polymerization occurs at 37 °C (**Figure 5 curve 1**), and at about 17 °C when paclitaxel is added (**Figure 5, curve 2**). Also, the discodermolide-induced polymer does not disassemble when the temperature is dropped to 0 °C, unlike test agent-untreated and paclitaxel-treated microtubules.²⁸ It was also confirmed by Day that (+)-discodermolide arrests MCF-7/LY2 breast carcinoma cells in the G2/M phase of the cell cycle, confirming the findings of Schreiber.²⁹

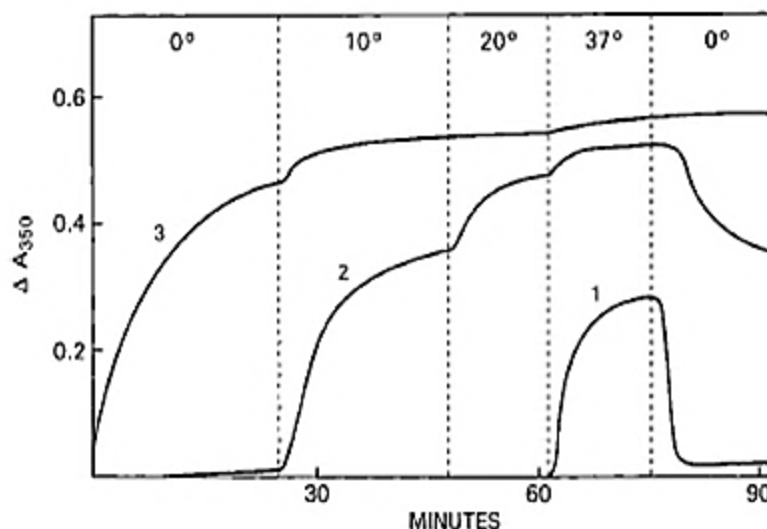


Figure 5- Turbidity Assay Result Comparing Discodermolide (3), Paclitaxel (2) and Untreated Microtubules (1). (Adapted with permission from ter Haar et al. *Biochemistry*, 1996, 35 pp243-250. Copyright 1996, American Chemical Society)

Discodermolide also shows activity as an anti-proliferative agent in multi-drug resistant cells and retains potency against paclitaxel-drug resistant cancer cell types.³⁰ In SW620 colon carcinoma cells, discodermolide is about 10-fold less potent than paclitaxel. But in the multi-drug resistant variant of the same cell line, discodermolide is 4-fold more potent than paclitaxel. This is because discodermolide is not a substrate for the P-glycoprotein efflux pump, while paclitaxel is a substrate. Additionally, in a variant of 1A9 ovarian cancer cells that need paclitaxel to survive, discodermolide is not a substitute of the drug, and cells are not viable. Etoposide B, another microtubule stabilizing, can substitute for paclitaxel and allows for cell viability.³⁰

Discodermolide causes cell death in breast carcinoma cells via an apoptosis mechanism.³¹ This is the case with both estrogen dependent and independent cell types.²⁹ Treatment with

discodermolide in A549 cells results in shorter microtubules and more bundles as well as the induction of accelerated cell senescence.³² Accelerated cell senescence is a unique finding for discodermolide treatment compared to treatment with other microtubule stabilizers.^{33,32} Recent studies trying to pinpoint the mechanism of cell death with discodermolide treatment show that usual apoptotic cell markers are not up-regulated in cells after discodermolide treatment.³⁴ Additionally, a discodermolide-resistant cell type has been isolated in which the level of the protein 4E-BP1 is decreased.³⁵ This protein is important for accelerated cell senescence, so it is believed that resistance to discodermolide can be obtained by decreasing the incidence of this cell mechanism.

1.3.3 Discodermolide Activity in Combination with Other Agents

Discodermolide binds microtubules differently from other microtubule stabilizing agents; discodermolide shows a higher affinity for the taxane-binding site on β -tubulin than paclitaxel. In competition binding experiments with [³H]-paclitaxel, discodermolide displaces paclitaxel from the binding site and forms shorter microtubule polymers at a faster rate.³⁰ Despite these differences and the higher affinity of discodermolide for the paclitaxel binding site, discodermolide and paclitaxel act synergistically when used in tandem against ovarian, breast, and lung cancer cells.^{36,37} This synergy was unexpected, because discodermolide displaces paclitaxel from microtubules in competition binding experiments. Discodermolide does not act synergistically with other microtubule stabilizing agents that bind in the paclitaxel or other sites.³⁸ In studies of the effect of microtubule destabilizing agents in pre-stabilized microtubules, discodermolide-stabilized microtubules resisted the destabilizing tendencies of many microtubule destabilizing agents better than paclitaxel- or epothilone B-stabilized microtubules.³⁹

Although discodermolide performed well in many *in vitro* assays and showed many positive characteristics that differ from classic microtubule stabilizing agents, Novartis halted studies of discodermolide in Phase I/II clinical trials due to pneumotoxicity.⁴⁰ This lessened the interest in the development of discodermolide as a clinical candidate, but increased interest in the synthesis of analogs that may not have the toxicities associated with the natural product.

1.4 CONFORMATIONAL ANALYSES OF DISCODERMOLIDE

The desire to determine how discodermolide binds in microtubules led to great number conformational studies. Several microtubule stabilizers with very different structures were discovered at about the same time as discodermolide, so a link between all the compounds of this class was sought. In 1999, it was hypothesized that discodermolide, paclitaxel, docetaxel and the epothilone family fit a common pharmacophore model for the paclitaxel binding site.⁴¹ Using molecular dynamics simulations, the important aspects needed for binding were proposed to be the lactone region, the C13-C14 area, and the terminal double bond. Even with a possible common pharmacophore model, the lack of a co-crystal structure of discodermolide in the α , β tubulin dimer led to more studies aimed at discovering the exact binding mode and conformation of discodermolide. In 2001, the Smith group matched NOE peaks from a ROESY 2D spectrum of discodermolide with corresponding energy minimized conformations of molecules to give a solution structure of discodermolide in acetonitrile. The Smith group (or The same group) found that discodermolide in solution closely resembles the conformation of discodermolide in the crystalline state (**Figure 6**). Despite the many rotatable bonds, the solution preference of discodermolide for a fairly rigid hairpin type conformation was rationalized by the A^{1,3} strain at

C13-16 and C8-10, as well as *syn*-pentane interactions in the backbone at C10-12, C16-C18 and C18-C20.⁴²

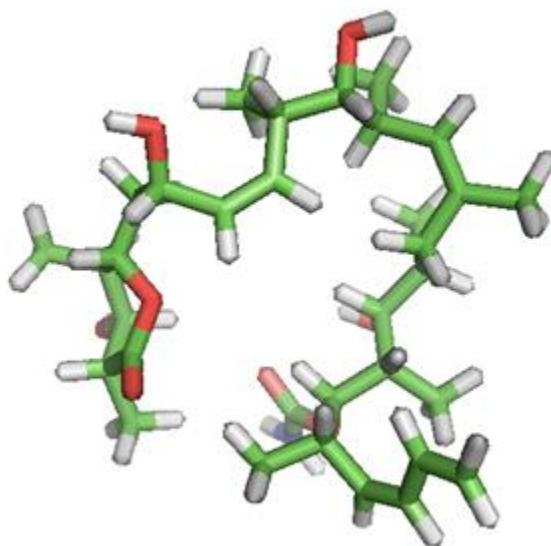


Figure 6- Discodermolide Crystal Structure that Shows the Hairpin Structure (*Adapted with permission from The Journal of Organic Chemistry, 1990, 55, pp 4912-4915, Copyright 1990, American Chemical Society*)

Shortly after the solution-based study by Smith, Snyder and co-workers employed 1D and 2D NMR experiments to find the conformation of discodermolide in DMSO and correlated the data with the modeling protocol NAMFIS (*NMR analysis of molecular flexibility in solution*).⁴³ Whereas in acetonitrile only one general conformation is put forth, Snyder specifies 12 conformations that were possible for discodermolide in DMSO. These conformations were classified into three groups. The most populated conformation was called a corkscrew, in which the molecule forms a helical shape. This general shape occurred 58% of the time, and is the

closest in resemblance to the hairpin conformation set forth by Smith. The two other less populated shapes were the sickle and extended forms of the molecule.

The Carlomagno and Jimenez-Barbaro groups then determined the conformation of discodermolide bound in soluble tubulin in DMSO⁴⁴ and in D₂O.⁴⁵ Discodermolide kept the hairpin conformation identified by Smith upon binding to β -tubulin as determined by 2D NMR experiments. Snyder and co-workers revisited their binding conformation using four force fields for modeling experiments of the bound-conformation of discodermolide instead of just one used previously. In this instance, Snyder's results more closely resembled the conformations that are found in both D₂O and acetonitrile. Indeed, they find that the X-ray motif shows up more than 50 % of the time in the NAMFIS calculations.⁴⁶ Although these studies differ in various aspects, there is a steady consensus that the hairpin conformer of discodermolide is important.

1.4.1 Docking Studies of Discodermolide

Two potential taxane binding sites on β -tubulin are hypothesized; an inner luminal site that is the major site for activity of the taxanes, and a possible pore site found on the outside of formed microtubules.⁴⁷ Because many microtubule stabilizing agents only bind to polymerized microtubules, one hypothesis states that microtubule stabilizing agents bind first to the external pore site, and then move to the internal luminal site as a final resting place. This hypothesis is supported by two observations. First, a fluorinated analogue of paclitaxel, hexaflutax, has trouble entering the luminal site on β -tubulin, instead stopping at the pore site.⁴⁸ A second experiment uses cyclostreptin, a microtubule stabilizing agent that binds covalently to β -tubulin. Using mass spectrometry techniques, researchers found that cyclostreptin was bound to peptides in both the pore and the luminal sites.⁴⁹

It is not yet known whether discodermolide binds at the pore or luminal taxane binding site. Canales and co-workers used 2D NMR conformational studies and the program AUTODOCK to generate the first binding pose/model of discodermolide in β -tubulin.⁴⁵ In this model, important polar contacts occur with His229, Pro274, Thr276, Ser277, Gln282 and Gly330 (blue molecule, **figure 7**) in the luminal site of β -tubulin, with the lactone and carbamate being responsible for many of these contacts. The Snyder group used their own conformational studies to dock discodermolide into the taxane binding site.⁴⁶ They used three programs to generate binding poses; Glide, RosettaLigand and AUTODOCK (v 4.0). In addition to the pose generated by Canales, they generated a pose that flips discodermolide in the luminal binding pocket, making the linker region exposed to solvent rather than making contacts with the protein (green molecule, **Figure 7**). The residues identified in the second pose show Pro272, Thre274 and Arg276 making important contacts with the C3 hydroxyl, the C17 hydroxyl and the C19 nitrogen of the carbamate.

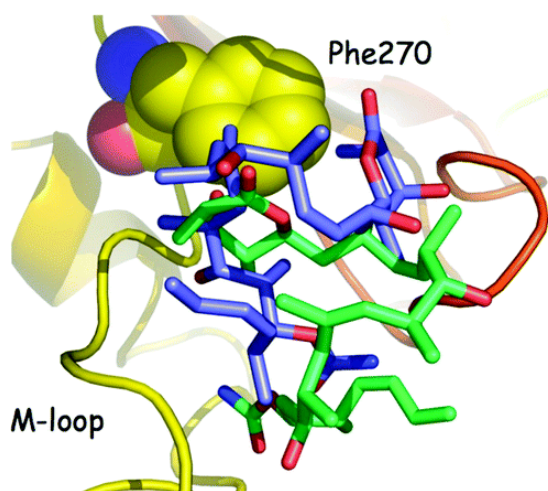


Figure 7- Two Distinct Poses of Discodermolide in the Taxane Binding Site (*Reprinted with permission from the Journal of Medicinal Chemistry vol 53, 2010, pp 155-165. Copyright 2010, American Chemical Society*)

The Xiao and Horwitz groups used hydrogen-deuterium exchange (HDX) experiments followed by LC-ESI-MS analysis and then SURFLEX docking to identify and confirm the amino acid residues in the binding pocket for discodermolide.⁵⁰ The investigators found that the amino acids that are protected from deuterium incorporation upon binding with paclitaxel and discodermolide are very different. They also find that some of the amino acids that Canales described as contacts in pose-1 (blue, **figure 7**) are not blocked from deuterium incorporation. Based on results from the HDX experiments, they found that discodermolide binds best in the taxane binding pocket instead of the pore site. Contacts are made between the C19 nitrogen of discodermolide and Leu361 and Gly360, between the C7 hydroxyl group and Asp224, and the C11 hydroxyl and Glu22.

1.5 SYNTHETIC ANALOGS OF DISCODERMOLIDE

Although discodermolide shows potent activity in cell-based assays, researchers have synthesized analogs to attempt to make a compound that could become a drug. A thorough structure-activity relationship (SAR) has been developed based on hundreds of analogs. Analogs can be classified into categories based on the fragment of discodermolide that was modified (see **Figure 1**). The categories include derivatives of the lactone fragment, derivatives of the linker fragment, derivatives of carbamate fragment, and hybrid analogs of discodermolide with other microtubule stabilizers.

Gunasekera and coworkers contributed some of the first analogs of discodermolide through semi-synthesis and by isolating analogs from natural sponge sources of the *Discodermia*

family. Acetylation of the C17 and C11 hydroxyl positions decreases activity compared with discodermolide, but acetylated versions at C3 and C7 hydroxyl positions retain potency close to the parent molecule.^{51,52} Natural analogs isolated consisted of the C2 epimer of the parent molecule, a C2 desmethyl analogue, a C19 desaminocarbonyl analogue, the open chain form of the δ -lactone, and the C9-C13 cyclopentane form of discodermolide.⁵³ All of these analogs had nanomolar activity in anti-proliferative assays except for the cyclopentane modification which was only weakly active. Following the work of Gunasekera, many more analogs were made by total synthesis that contained changes the three regions of discodermolide.

1.5.1 Analogs of the Lactone Fragment

The area of discodermolide that has been targeted the most for potential improvements or simplification is the lactone region (SAR is summarized in **Figure 8**). Analogs typically alter individual positions on the lactone ring or replace the δ -lactone moiety entirely. An α , β -unsaturated lactone (removal of the C3-OH and C2-methyl group) made by Smith showed the same potency as the parent molecule in cell based assays.³³ This was the first significantly simplified lactone that retained potency similar to discodermolide.

Complete replacement of the δ -lactone fragment of discodermolide with simpler lactones was tested soon after by a Smith group/Kosan Biosciences collaboration. Favorable groups included the five-membered butyrolactone **14**, which showed better activity in cell-based assays than the parent molecule.⁵⁴ Another possible replacement of the δ -lactone is a coumarin group **15**, which also has higher potency than discodermolide.⁵⁵ Additionally, a phenol group **16** in place of the lactone retained potency seen near the parent molecule.⁵⁴ Based on the activity of

these analogs, a hypothesis was stated that the carbonyl of the lactone ring is the important aspect of discodermolide binding to microtubules.

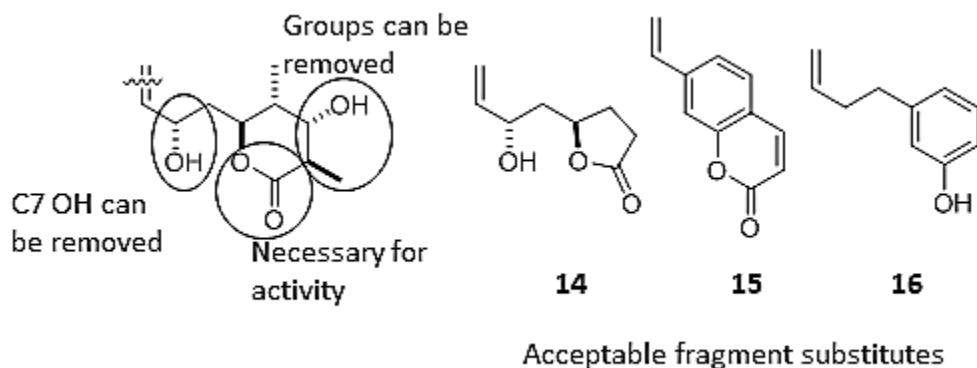


Figure 8- SAR of the Lactone Ring of Discodermolide and Possible Replacement Groups

1.5.2 Analogs of the Carbamate Fragment

The SAR of the carbamate fragment is summarized in **Figure 9**; Changes were made to the carbamate region of discodermolide at the terminal diene, the C19 carbamate, the C17 hydroxyl position and various methyl groups. The terminal diene was appended with extensions for possible photo-analogs or fluorescent probes. These extensions did not decrease activity of the molecule.⁶ In addition to appendages to the terminal diene, saturating the C23-C24 double bond led to an improvement of activity. Although the C23-C24 bond can be saturated, the Z C21-C22 double bond is necessary to keep the potency discodermolide.⁵⁶

Smith and colleagues again added to the SAR of discodermolide when they prepared analogs with bulkier C19 carbamate moieties.⁵⁷ A wide range of phenyl carbamate analogs were

advantageous in terms of biological activity in normal cells but not in multi-drug resistant cell lines. Analogs with bulky carbamate groups were less potent when compared to discodermolide. The only carbamate that allowed for retention of activity against multi-drug resistant cells was an aniline carbamate moiety.⁵⁷

Positions modified include the C17 hydroxyl position and the methyl groups at C16 and C14. In the synthesis of discodermolide by Schreiber, it was reported that the epimer of C17 OH as has low activity.⁵ Schreiber reported that the C16 desmethyl analogue was almost as potent as the parent molecule.⁶ The C14 desmethyl form of discodermolide, reported by Smith, shows good activity, but not as good as discodermolide.³³

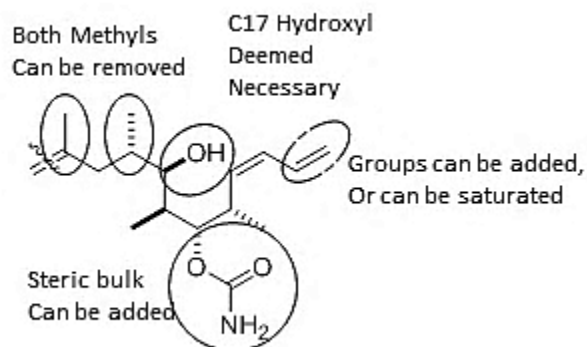


Figure 9- SAR of the Carbamate Fragment of Discodermolide

1.5.3 Analogs of the Linker Fragment

Although the two end regions of discodermolide have been investigated thoroughly, the linker fragment has not been investigated to the same extent. Analogs with a connection between C9 and C13 on the discodermolide backbone (**Figure 10**) were isolated by Gunasekera as

byproducts after the final deprotection step during the Novartis synthesis of discodermolide. The analogs had lower activity than discodermolide.⁵⁸ Smith synthesized two diastereomeric C13-14 cyclopropyl analogs of discodermolide. These analogs had some activity, but not near the level of discodermolide.⁵⁹ Finally, Gunasekera also reported that the C8-C9 bond can be saturated without affecting activity, whereas saturation of the C13-C14 double bond causes loss of activity compared to discodermolide.⁵³

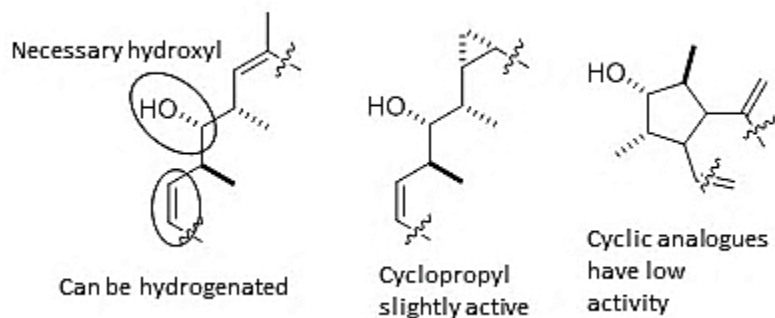


Figure 10- SAR of the Linker Region of Discodermolide and Other Additions

1.5.4 Dictyostatin

In 1994, the marine natural product dictyostatin **17** (**Figure 11**) was isolated by Pettit and colleagues from the marine sponge *Spongia* family.⁶⁰ Although dictyostatin is a macrocycle, the backbone of dictyostatin matches up to the C8-C24 backbone of discodermolide, minus the C13-14 olefin and the C16 methyl group. In that context, dictyostatin can be considered as a cyclic discodermolide derivative. The total synthesis of dictyostatin was reported concurrently by the Paterson⁶¹ and Curran⁶² groups in 2004. Further studies with this marine product revealed that it

acts in a similar way to discodermolide, and that analogs of dictyostatin and discodermolide have a similar SAR.⁶³

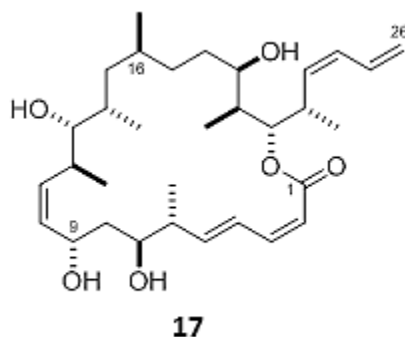


Figure 11- The Marine Natural Product Dictyostatin

The most important analogue of dictyostatin that can be applied to the discodermolide SAR is saturation of the terminal double bond at C25-26⁶⁴ (the dictyostatin backbone is 2 carbons longer than discodermolide, so this would correspond to C23-24 of discodermolide). Other changes to the dictyostatin backbone that are beneficial for its biological activity include epimerization of the C6 methyl group,⁶⁵ and removal of the C16 methyl group.⁶⁶ These changes concur with the SAR that emerged through the synthesis of discodermolide analogs.

1.5.5 Hybrid Microtubule Stabilizer Analogs

The unique biological properties of discodermolide compared to other microtubule stabilizers and the potential overlap in the taxane binding pocket^{37,50} led to the pursuit of hybrid molecules of this class. Hybrids of discodermolide and dictyostatin were first made by cyclizing discodermolide with simple alkyl chains to result in a macrolide like dictyostatin.⁶⁷ These

analogs showed much lower potency than discodermolide and dictyostatin. In another hybrid designed by Paterson, the C2-C24 backbone of discodermolide and the *Z*-enolate of dictyostatin were used, but the analogue showed lower activity than discodermolide.⁶⁸ Paterson also reported a hybrid where the C6-C24 fragment of discodermolide was coupled with the C1-C7 fragment of dictyostatin, which showed activity intermediate to that of the two individual natural products.⁶⁹ Paterson describes the synthesis of a paclitaxel-discodermolide-dictyostatin analogue. In this work, the C6-C24 backbone of discodermolide was connected to the C1-C7 fragment of dictyostatin, and the side chains of either paclitaxel and docetaxel were attached to either of the hydroxy groups (**18, 19, Figure 12**).⁷⁰ These analogs were about five times less active than the natural products. Smith and Horwitz recently prepared and tested discodermolide/paclitaxel hybrid molecules. These molecules paired the discodermolide base structure with aromatic groups similar to the chain of paclitaxel added to the carbamate position of the molecule. The hybrids performed better than parent discodermolide in anti-proliferative assays against A549 lung carcinoma cells and MCF-7 breast carcinoma cells.⁷¹ Construction of hybrid derivatives represents the most recent approach to the investigation of the discodermolide and dictyostatin SAR.

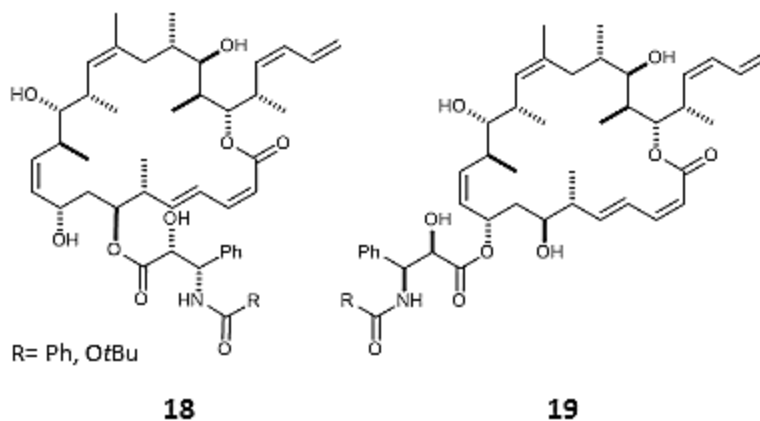


Figure 12- Paterson Discodermolide/Dictyostatin/Paclitaxel Hybrids containing the C8-C24 portion of Discodermolide, C1-C7 portion of Dictyostatin, and the side chains of Paclitaxel or Docetaxel

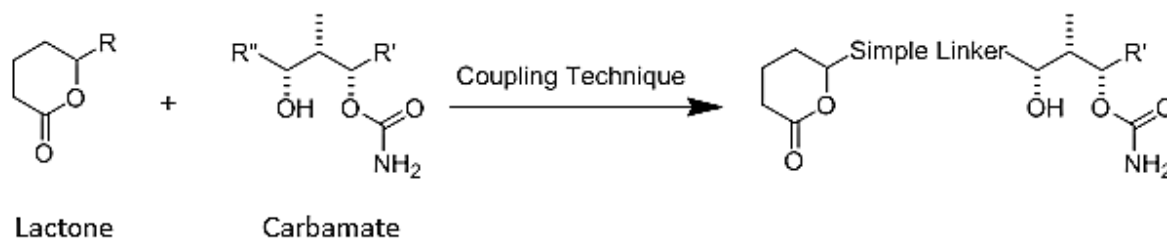
1.6 GOALS OF STUDY

Although there is much research on attempting to make discodermolide into a promising drug, I saw a lack of exploration into the SAR of the linker region of discodermolide. The long term goals of this project are to design and synthesize simplified versions of discodermolide that have new middle fragments. If analogs retain the hairpin conformation of the parent natural product then the compounds will retain potency. Simplifying the discodermolide structure will also reduce the total number of steps needed to complete an active molecule. Such simplified molecules that are devoid of pneumotoxicity but retain the potency and biological characteristics of discodermolide are quite attractive as potential drugs.

To achieve these long term goals, I designed simple discodermolide analogs containing an olefin linkage and optimized a synthetic scheme to synthesize a few simple analogs. I

designed virtual analogs, and screened them in a hologram quantitative structure-activity relationship (HQSAR). These analogs are predicted to have activity in cell-based screens at levels near the activity of discodermolide. Also, I worked toward synthesizing two carbamate and three lactone fragments derived from the SAR of discodermolide. Some fragments were coupled together using olefin cross metathesis (**Figure 13**), resulting in the synthesis of simplified analogs ready for testing in both protein and cell-based screens

A. General Discodermolide Analogue Design



B. Example of Analogue Synthesis

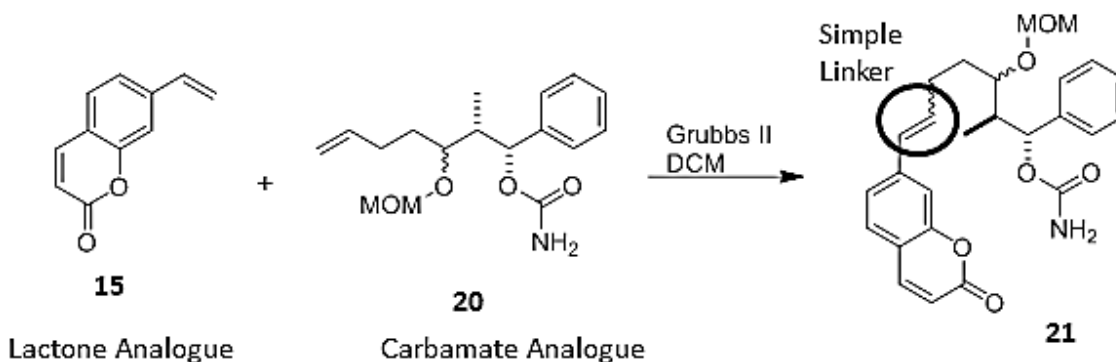


Figure 13- Experimental Design for Discodermolide Analogs using Simple Linker Groups

2.0 MOLECULAR MODELING OF NEW DISCODERMOLIDE ANALOGS

2.1 INTRODUCTION

As documented in section 1.4, discodermolide keeps the same hairpin conformation in a variety of solvents.^{42,43,45} However, the structure of discodermolide bound in the taxane site of the β -tubulin subunit of microtubules has not yet been elucidated, leaving ambiguity on what key residues interact with discodermolide. The high resolution cryo-electron microscopy structure of paclitaxel bound to β -tubulin⁷² has yet to be helpful in modeling the binding of discodermolide analogs in the taxane binding site. So we looked to QSAR methods to predict the activity of novel analogs.

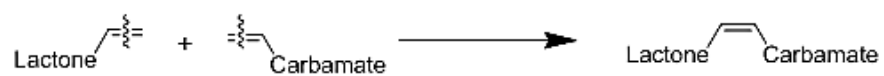
Quantitative structure-activity relationship (QSAR) analysis is a process in which numerical predictions of activity can be obtained by using the structures and activities of analogs that have already been tested. Salum and colleagues⁷³ built an HQSAR (hologram quantitative structure-activity relationship) for analogs of discodermolide to predict activity of new discodermolide analogs. This fragment-based approach used the activity of discodermolide and 46 analogs in A549 non-small cell lung carcinoma cells to generate a predictive model. They hypothesized that the C19 carbamate, C14 methyl, C11 hydroxyl, C7 hydroxyl and C1 carbonyl group of the lactone all should make important contacts in the binding site because they are repeatedly found in analogs that have excellent activity.

The modeling portion of my work has two parts. The first part involves the design of analogs and the identification of their low energy conformations via molecular mechanics minimization. Here we are looking for new analogs that mimic the hairpin conformation well. The second part involves the prediction of activities for designed analogs using the HQSAR model for discodermolide analogs created by Salum and Andricopulo.

2.2 RESULTS

Sixteen new discodermolide analogs were assembled by taking one carbamate fragment and one lactone fragment to form a virtual analogue via an olefin linkage (**Figure 14**). The four possible carbamate fragments are identified by Arabic numerals 1-4 and the four lactone fragments are identified by letters A-D in **Table 1**. In the lab, such analogs could be made by performing a cross metathesis reaction using terminal alkenes of the two fragments. For example, coupling of lactone B with carbamate 2 would yield analogue B-2 shown in **Figure 14B**. The designed analogs then underwent energy minimization by molecular mechanics models using the Tripos forcefield.

A. General Assembly of Virtual Analogues



B. Specific Example of Virtual Analogue Assembly

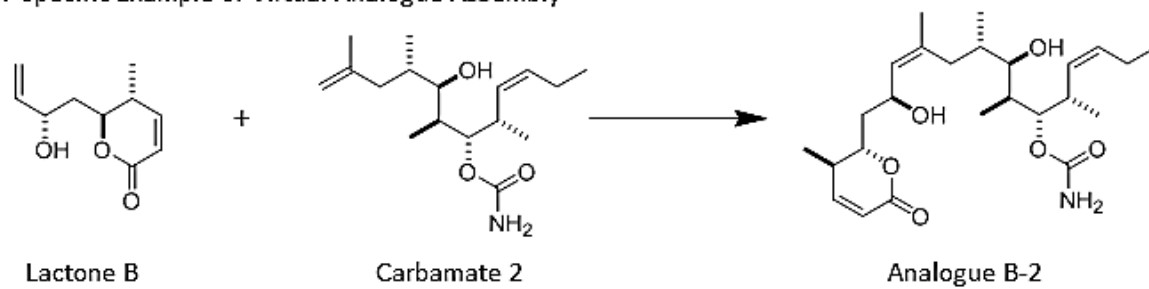
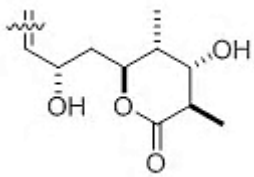
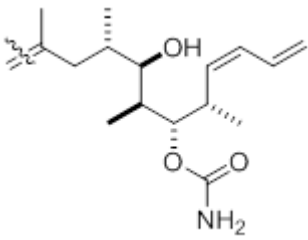
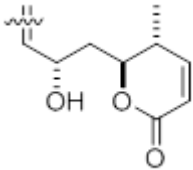
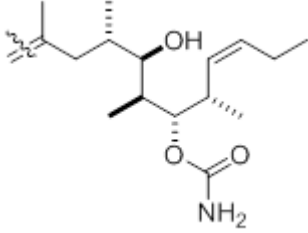
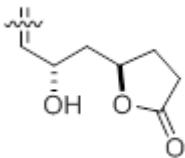
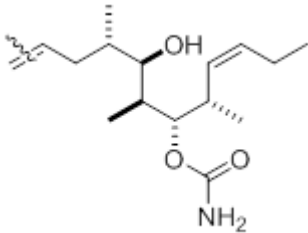
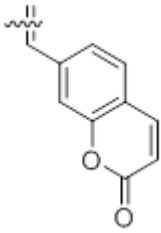
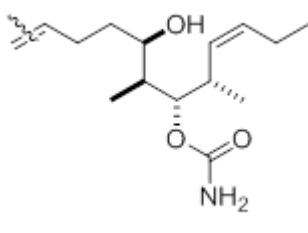


Figure 14- Assembly of Analogs for HQSAR Screening

Table 1-Fragments Used for HQSAR Studies

Lactone Fragment	Carbamate Fragment
 <p>A</p>	 <p>1</p>
 <p>B</p>	 <p>2</p>
 <p>C</p>	 <p>3</p>
 <p>D</p>	 <p>4</p>

The energy minimized virtual analogs were then screened *in silico* for predicted activity with the HQSAR method designed by Salum and colleagues.⁷³ Four different HQSAR models were used to evaluate the compounds using various parameters (**Table 2**). For the HQSAR, six parameters are available to comprise a testing model. They are atoms (A) that occur in the molecule, they types of bonds (B) connecting the different atoms in the molecule, and connections (C), meaning how the atoms are connected to one another. Additionally, hydrogen atoms (H) found in the atom, the chirality (Ch) of individual positions and the donor or acceptor ability (DA) of atoms are also considered. In principle, any combination of parameters can be used to form a model, and different combinations may result in a different predicted potency values. In the first HQSAR model (model 1) atoms, bonds and connections were used. In model 2, the same three parameters, plus hydrogen atoms and chirality were used. In model 3, all six parameters mentioned above were used, whereas in model 4 atoms, connections and donor/acceptor ability were only used (**Table 2**).

Table 2-HQSAR Model Parameters

Parameters	Statistical Parameters					
	q^2_{LOO}	r^2	SEE	HL	N	Size
1. A/B/C	0.59	0.74	0.49	61	4	4-7
2. A/B/C/H/Ch	0.64	0.88	0.33	199	5	6-9
3. A/B/C/H/Ch/DA	0.59	0.89	0.32	151	6	4-7
4. A/C/DA	0.58	0.81	0.43	61	5	4-7

q^2_{LOO} -leave-on-out cross-validated correlation coefficient; r^2 -non-cross-validated correlation coefficient; SEE-standard error of estimate; HL-hologram length; N -optimal number of components, Size-range of number of components used to build holograms. Parameters: A-atoms, B-bonds, C-connections, H-hydrogen atoms, Ch-chirality, DA-donor and acceptor

The methodology behind this HQSAR study involves breaking down a test set of virtual analogs into molecular fragments. These molecular fragments can then be comparatively screened against the fragments found in the training set, which consist of discodermolide and the 46 analogs disclosed by the Smith group with IC_{50} values against A549 lung carcinoma cell types. The 16 virtual analogs that resulted from the combination of the fragments shown in **Table 1** were screened in the HQSAR method of Salum to obtain predicted IC_{50} values. These pIC_{50} ($pIC_{50} = -\log[IC_{50} \text{ value in A549 cells}]$) and the percent fragments missing for analogs are shown in **Tables 3 and 4**. In **Tables 3 and 4**, virtual analogs are identified by two characters representing the lactone and carbamate fragment that were combined to form a new analogue. Percent fragments missing are the percentage of virtual fragments found in the test molecule that do not occur in the training set of analogs. These values were extrapolated for the final calculations of pIC_{50} . IC_{50} values correspond to the predicted micromolar concentration of these analogs for 50 % inhibition of A549 lung carcinoma cells. **Table 3** shows the values for models 1 and 2 from **Table 2**. **Table 4** shows the values from models 3 and 4 from **Table 2**. Active molecules will have high pIC_{50} values and low IC_{50} values.

Table 3-HQSAR pIC₅₀ predictions, Models 1 and 2

	Model 1			Model 2		
Compound	pIC₅₀	% Missing	IC₅₀ Value	pIC₅₀	% Missing	IC₅₀ Value
Name	value	Fragments	(μM)	value	Fragments	(μM)
A-1	7.0	5	0.100	6.6	9	0.251
B-1	7.4	1	0.040	6.6	2	0.251
C-1	7.9	1	0.013	7.2	2	0.063
D-1	6.6	50	0.251	5.5	21	3.162
A-2	7.4	0	0.040	5.2	6	6.310
B-2	7.4	1	0.040	6.2	6	0.631
C-2	7.9	1	0.013	6.8	7	0.159
D-2	6.6	50	0.251	5.1	20	7.943
A-3	6.3	4	0.501	5.8	8	1.585
B-3	6.6	0	0.251	5.7	1	1.995
C-3	7.1	0	0.079	6.3	1	0.501
D-3	6.2	49	0.631	4.9	19	12.59
A-4	6.9	0	0.126	6.1	2	0.794
B-4	7.0	0	0.100	6.5	2	0.316
C-4	7.5	0	0.032	7.1	2	0.079
D-4	6.5	53	0.316	5.6	23	2.512

Table 4-HQSAR Results, Models 3 and 4

	Model 3			Model 4		
Compound	pIC₅₀	% Missing	IC₅₀ value	pIC₅₀	% Missing	IC₅₀ Value
Name	value	Fragments	(μM)	Value	Fragments	(μM)
A-1	8.1	3	0.008	7.0	4	0.100
B-1	7.5	1	0.032	7.4	1	0.040
C-1	7.7	1	0.020	7.3	1	0.050
D-1	6.3	17	0.501	5.4	12	3.981
A-2	7.0	1	0.100	6.7	1	0.200
B-2	7.1	2	0.079	7.1	1	0.079
C-2	7.4	2	0.040	7.0	1	0.100
D-2	6.0	17	1.000	5.1	12	7.943
A-3	7.1	2	0.079	6.2	3	0.631
B-3	6.5	0	0.316	6.6	0	0.251
C-3	6.7	0	0.200	6.6	0	0.251
D-3	5.2	17	6.310	4.5	11	31.62
A-4	6.2	1	0.631	6.4	0	0.398
B-4	6.3	1	0.501	6.8	0	0.159
C-4	6.6	1	0.251	6.8	0	0.159
D-4	5.1	19	7.943	4.9	12	12.59

The data generated by all four HQSAR models show that many of the proposed virtual analogs have high pIC_{50} values. Out of sixteen analogs screened, one (C-1) has a predicted pIC_{50} above 7.0 in all four models. Four analogs (A-1, B-1, B-2 and C-2) have a predicted pIC_{50} value above 7.0 in all four models. Four analogs (A-1, B-1, B-2 and C-2) have a predicted pIC_{50} value above 7.0 in three out of four models. Five analogs (A-2, A-3, B-4, C-3 and C-4) have a predicted pIC_{50} value above 7.0 in at least one out of four models. A pIC_{50} value of 7.0 corresponds to an IC_{50} value of 100 nM, so analogs with a pIC_{50} in that range are potentially active anti-proliferative agents against A549 lung carcinoma cells.

The structures of the four analogs that have a pIC_{50} value greater than 7.0 in three out of the four models are shown in **Figure 15**. Two of the analogs (A-1 and B-1) contain the complete carbamate fragment, while the other two (B-2 and C-2) are saturated at the C23-24 position. Three different lactone portions (A, B and C) are represented, with only the coumarin lactone replacement (D) not appearing in this set of analogs.

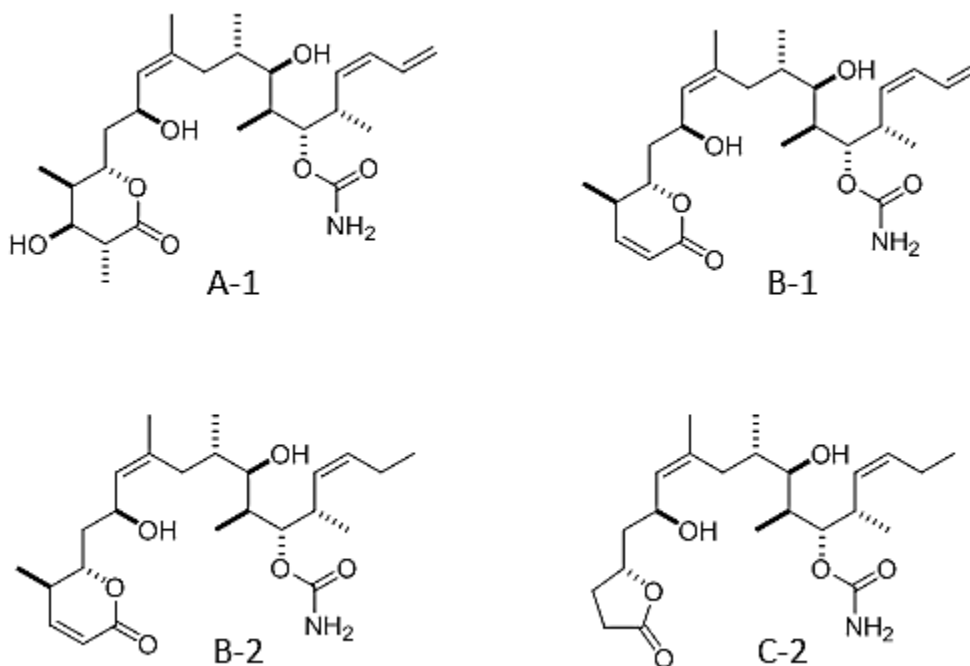


Figure 15- Virtual Analogs the have a pIC_{50} value above 7.0 in 3 out of 4 models

Analogue C-1 (**Figure 16A**) is the virtual compound that scores above 7.0 in all models. It consists of butyrolactone fragment C (**Table 1**) coupled to the complete C14-C24 carbamate fragment 1 (**Table 1**). Considering the comparative way the HQSAR method works, it is not surprising that this particular virtual analogue scores well in all four HQSAR models. Even without the complete middle fragment of discodermolide, both sides of this virtual molecule mimic portions of discodermolide found in analogs that are very potent in biological assays. The energy minimization of C-1 shows that it can mimic the hairpin conformation of discodermolide to a great degree (**Figure 16B**).

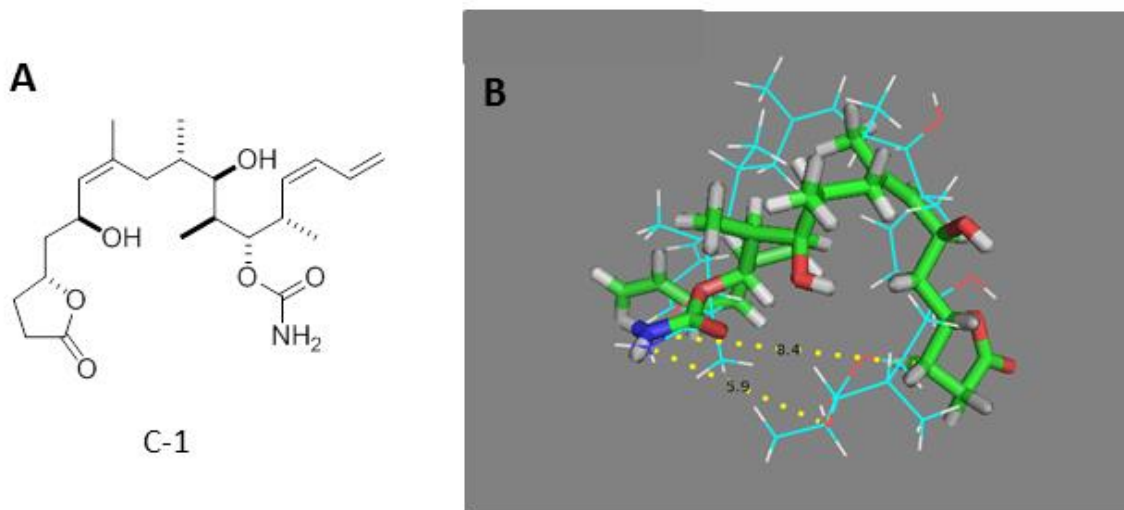


Figure 16- A. Analogue C-1 Structure. B. C-1 Overlaid on the 3-D structure of Discodermolide to Demonstrate the Hairpin Conformation of the Analogue

Virtual analogs containing the coumarin moiety consistently had much lower pIC_{50} values. A discodermolide analogue with coumarin in place of the naturally occurring lactone has

been synthesized and its biological activity has been disclosed by Smith.⁵⁵ Unfortunately, this compound was never tested against the A549 lung carcinoma cell line, so it is not in the training set of 46 compounds that provide biological data for the IC₅₀ predictions of the HQSAR model(s). The absence of a coumarin moiety in the training set for the HQSAR can be seen by the high percent missing fragments value for all coumarin virtual analogs. A high percentage of missing fragments means that the pIC₅₀ value was extrapolated from the data. Therefore, we can attribute the low pIC₅₀ values of the coumarin fragment to its lack of inclusion in the training set. This means that although the model predicts low activity, the coumarin analogs may still be active compounds.

2.3 CONCLUSION

New virtual analogs of discodermolide were screened in a HQSAR experiment for predicted IC₅₀ values, using four different parameter model sets. A high percentage of the virtual analogs are predicted to have a high pIC₅₀ values. One analogue (C-1) displays pIC₅₀ value greater than 7 in all four model systems, while four more analogs (A-1, B-1, B-2, C-1) display pIC₅₀ values greater than 7 in three out of the four model systems. Another four analogs resulted in a pIC₅₀ value greater than 7 in at least one of the model systems. These predictions are encouraging results for the use of an alkene linker as a substitute for the natural compound linker region.

3.0 SYNTHESIS OF SIMPLIFIED DISCODERMOLIDE FRAGMENTS

3.1 INTRODUCTION

The synthetic strategy used here is related to those developed in the Day group,⁷⁴ Smith,⁸ and Novartis.^{75,76} Using the discodermolide SAR in chapters 1 and 2, target fragments were identified by activity of the regions and simplicity of synthesis. Three fragments were selected as lactone groups **15**, **22**, and **23** along with two simplified carbamate fragments **20** and **24** (**Figure 17**). The synthetic schemes for the fragments were designed to result in terminal olefins that could then be coupled together via olefin cross metathesis.

A coumarin group **15**, the phenol group **22**, and the complete lactone from the natural product **23** with an allylic chain were chosen as lactone groups. These groups were chosen based on the number of new steps needed to make the fragment. Two carbamates were chosen for synthesis that retain three (**20**) or four (**24**) of the stereocenters found in the carbamate portion of discodermolide. A benzene ring was used in place of the C20 methyl and C21-22 olefin for fragment **20**. This phenyl group could be an isostere to the terminal diene in biological studies. Carbamate fragment **24** contains the saturated C23-24. Neither of these carbamate fragments contains either the C16 or C14 methyl groups found in discodermolide.

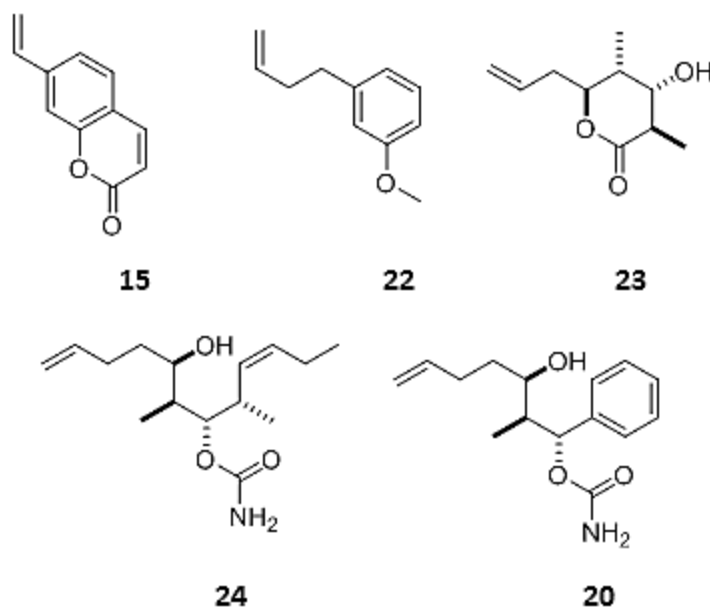


Figure 17- Fragments Targeted for Synthesis of Discodermolide Analogs

3.2 RESULTS

3.2.1 Synthesis of the Common Precursor 29

The known common precursor **29**^{74,75} for the fragments **23**, and **24** was prepared as shown in **Figure 18** by combining the routes of Day⁷⁴ and Novartis.⁷⁵ The synthesis of **29** starts with the reaction of Evans chiral oxazoladinone **25** (**Figure 18**) which was synthesized from (D)-phenylalanine.⁷⁷ Acylation of **25** with *n*-butyllithium (BuLi) and propionyl chloride⁷⁸ gave the acyl-auxiliary **11** in 80%. Enolization of **11** with dibutylboron triflate (Bu₂BOTf) and diisopropylethyl amine (DIPEA) under typical Evans aldol condensation conditions⁷⁹ followed by the addition of methacrolein gave the *syn* aldol adduct **26** along with a minor *anti* isomer in a

ratio of about 90/10. Pure *syn*-isomer **26** was isolated in 66% yield by flash chromatography. An additional 6.3% of the *anti*-isomer was isolated. The alcohol of **26** was protected with *t*-butyldimethylsilyl triflate (TBSOTf) generating **27** in 87% yield as a white solid. Without purification, **27** was hydroborated with 9-BBN in THF according to Novartis⁷⁵ to give unstable intermediate **28**. Alcohol **28** was prone to spontaneous lactonization, so it was directly exposed to potassium *t*-butoxide to complete the conversion to **29**. This lactone was isolated in 55% yield. The isolation of **29** as a single isomer shows that the hydroboration to give **28** was both regioselective (for the 1°-alcohol) and stereoselective (for the *anti*-isomer).

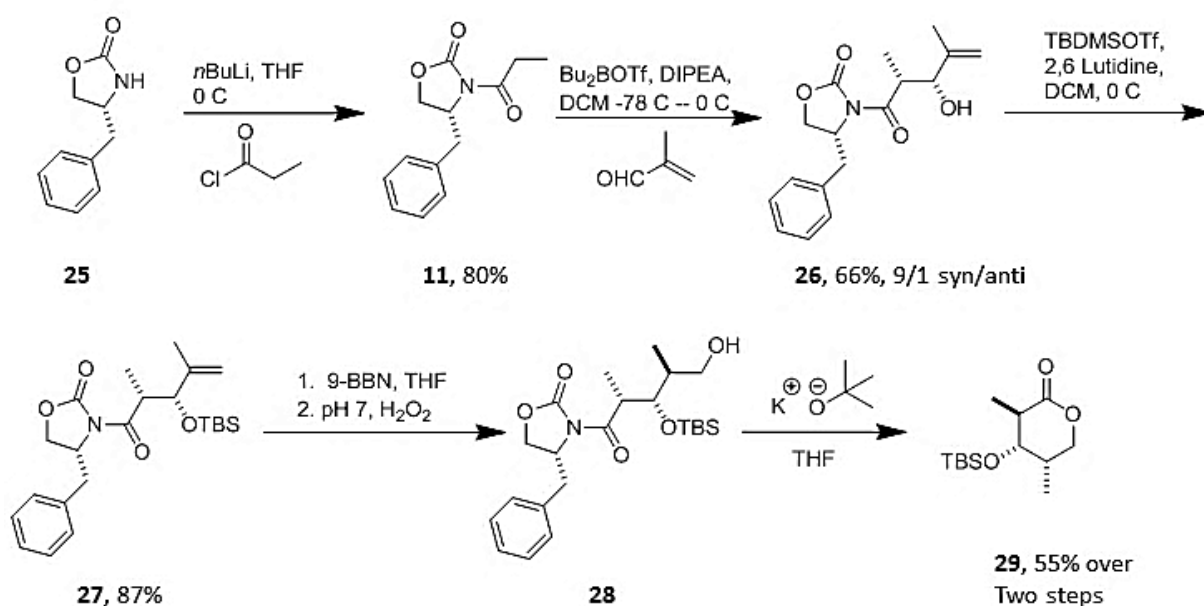


Figure 18-Synthesis of the Common Precursor Lactone 29

3.2.2 Synthesis of the Simplified Carbamate Fragment 24

The first attempt to make carbamate fragment **24** is shown in **Figure 19**. Treatment of **29** with *N,O*-dimethylhydroxylamine and isopropylmagnesium chloride⁷⁶ gave Weinreb amide **30**. To minimize the chance for relactonization, crude **30** was immediately treated with sulfur trioxide-pyridine (Parikh-Doehring oxidation⁸) to afford aldehyde **31** in 80% yield. The Wittig reaction of aldehyde **31**⁸⁰ with propyltriphenylphosphonium bromide and BuLi was not reproducible. Alkene **32** was isolated in yields up to 61%, but typical yields were less than 25%. The ¹H NMR spectrum of alkene **32** showed resonances at 5.2-5.6 ppm, but the *E/Z* ratio could not be determined due to overlapping of peaks. The *Z*-isomer should be favored based on the methodology.⁸¹ Moving forward with limited amounts of **32**, DIBAL-H reduction⁷⁶ gave aldehyde **33** in 61% yield. From this point, all intermediates are new compounds en route to discodermolide fragments. Direct Grignard addition of **33** with 3-butenylmagnesium bromide⁸² gave alcohol **34** in 43% yield. A Felkin-Ahn analysis⁸³ based on sterics suggested that the (*R*)-isomer at C17 would be favored, and product **34** proved to be a ratio of 2/1 of inseparable isomers. This was seen by the two NMR peaks at 3.61 and 3.62 ppm corresponding to a CH-O hydrogen shift.

The mixture of alcohols **34** was protected with methoxymethyl chloride (MOMCl)⁸⁴ to give **35** in 70% yield. Desilylation of **35** with tetrabutylammoniumfluoride (TBAF)⁸⁵ gave alcohol **36** in 48% isolated yield. The final installation of the carbamate to give **24** was then abandoned due to the mounting problems with this route. Specifically, the low yielding Wittig reaction and the inability to separate the diastereomeric Grignard products were significant detractors.

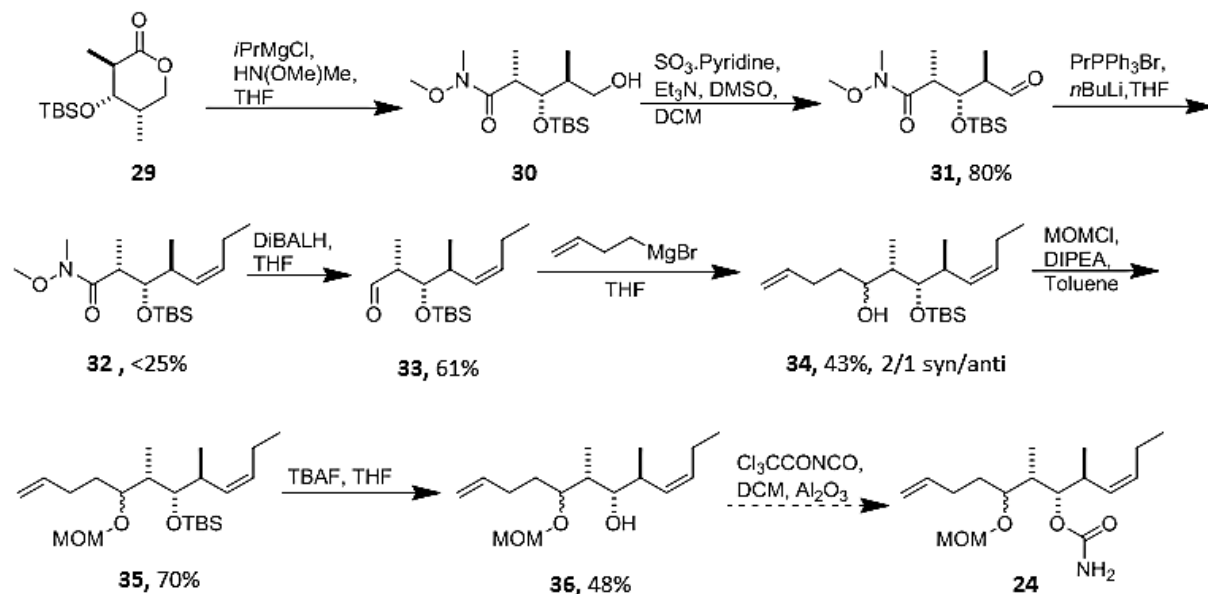


Figure 19- First Attempt for Simple Carbamate 24

3.2.3 Redesigned Scheme for the Simple Carbamate Fragment 24

The revised route to carbamate fragment **24** is shown in **Figure 20**. In this route, the butenyl side chain and the *Z*-alkene are introduced in reverse order. This should solve the yield problem with the Wittig reaction because the new aldehyde partner **42-syn** has only one carbonyl group (unlike **31**, which has two). Additionally, all compounds in this reaction sequence are new except for Weinreb amide **37** and aldehyde **38**.

The common precursor **29** was again converted to the Weinreb amide **30**. Attempts to protect the primary alcohol of **30** with *para*-methoxybenzyl (PMB) and *tert*-butyldimethylsilyl (TBS) groups were not successful. However, treatment of **30** with triethylsilyl chloride⁸⁶ (TES-

Cl), dimethylaminopyridine (DMAP) and imidazole gave the bis-silyl ether **37** in 59% yield along with 31% of lactone **29**.

The Weinreb amide **37** was reduced with DIBAL-H⁷⁴ to form aldehyde **38** in 86% yield. Reaction of crude aldehyde **38** with 3-butenylmagnesium bromide led to olefin **39** in 70 % yield with a d.r. of 2:1 in favor of the target isomer **39-syn** as assigned by ¹H NMR spectroscopy. For example, the protons on the carbinol carbon of **39-syn** and **39-anti** were observed at 3.84 and 3.89 ppm. The major isomer was assigned as syn by Felkin-Ahn model analysis.⁸³ Separation by flash chromatography gave 40% yield of pure **39-syn** with an additional 30% of a syn/anti mixture. Alcohol **39-syn** was protected with MOMCl⁸⁴ to provide the triether **40** in 43% yield.

Selective desilylation of triether **40** with acetic acid formed 1°-alcohol **41** in 48% yield. This was oxidized under Parikh-Doering conditions to yield aldehyde **42**. The crude aldehyde **42** was treated with the ylide derived from triphenylpropylphosphonium bromide and *n*BuLi to afford diene **35-syn** in 70% with a *Z/E* ratio of 5:1 as determined by integration of peaks of the methylene hydrogen in the 2.4-3.0 ppm range in the ¹H NMR spectrum. These conditions are known to be *Z*-selective, so the major isomer was assigned as *Z*.⁸¹

The diene **35-syn** was treated with TBAF⁸⁵ to result in alcohol **36-syn** in 11% yield. The resonances in the ¹H and ¹³C NMR spectra of **35-syn** and **36-syn** matched one of the two sets of resonances in the spectra of the syn/anti mixtures of **35** and **36-syn** in Scheme 20. The other set was absent, so **17-syn** and **18-syn** are isomerically pure. Installation of the carbamate by the Kocovsky protocol⁸⁷ with trichloroacetoisocyanate in dichloromethane resulted in **24** in 11% yield. The route to **24** in **Figure 20** has two more steps than the route in **Figure 19**, but it is better because the Wittig reaction occurred in much higher yield and because the needed syn-isomer could be separated after the Grignard reaction.

The synthesis of **20** started with preparation of aldehyde **47** by a similar route to the synthesis of fragment **24**. An Evans aldol reaction⁷⁵ of chiral auxiliary **11** and benzaldehyde **43** gave alcohol **44** in 65% yield as a single diastereomer. The alcohol **44** was protected with TBSOTf to result in ether **45** in 95% yield. The chiral auxiliary was removed with lithium borohydride¹⁰ to give 62% yield of alcohol **46**. Finally, alcohol **46** was oxidized⁸ with sulfur trioxide-pyridine to yield crude aldehyde **47** quantitatively.

Direct Grignard reaction⁸² of crude aldehyde **47** with 3-butenylmagnesium bromide gave the new alcohol **48** as a mixture of diastereomers in 64% yield over two steps. The desired diastereomer **48**-syn was favored in a ratio of 3.5:1 as determined by ¹H NMR spectroscopy. peaks occurring at 3.80 and 3.71 ppm. These diastereomers could not be separated by either flash chromatography or chiral supercritical fluid chromatography; however, the needed isomer predominates according to Felkin-Ahn steric arguments,⁸³ so we proceeded with the mixture.

Alcohol **48** was protected with MOM-Cl, resulting in diether **49** in 74% yield.⁸⁴ This diether was treated with TBAF⁸⁵ to give alcohol **50** in 63% yield. Finally, the carbamate group was installed by the Kocovsky protocol,⁸⁷ resulting in carbamate fragment **20** in 52% yield. Unfortunately, the diastereomers were not separable at any point, so the final sample of **20** was about a 3.5/1 ratio of syn/anti isomers. The route to **5** has only eight steps, compared to the 15 steps needed to make **24** from the acyl-auxiliary. If the phenyl group is an active structural modification, then this would be a useful simplification in the synthesis of discodermolide analogs.

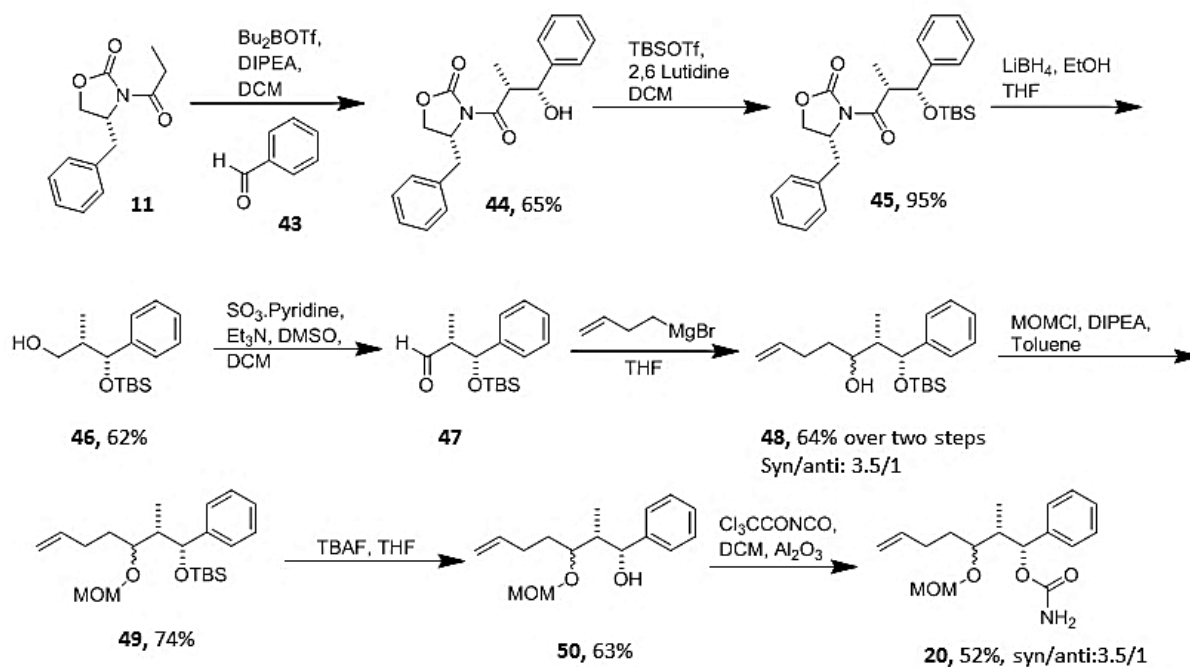


Figure 21- Synthesis of Simple Carbamate Fragment 20 Containing a Phenyl End Group

3.2.5 Synthesis of Coumarin Lactone 15

A coumarin lactone fragment with a terminal olefin was made in four steps from 7-methylcoumarin **51** (Figure 22). 7-Methylcoumarin **51** was brominated with *N*-bromosuccinamide (NBS) to yield **52** as prepared by my colleague Ms. Amy Short. 7-Bromomethylcoumarin **52** was hydrolyzed to yield alcohol **53** quantitatively. The primary alcohol **53** was oxidized via Parikh-Doering conditions⁸ to result in aldehyde **54** in 66% yield. Methyltriphenylphosphonium bromide was treated with BuLi ⁸⁸ and added to crude aldehyde **54** to yield **15** in 16% yield. This route was not optimized because enough material was obtained for coupling reactions.

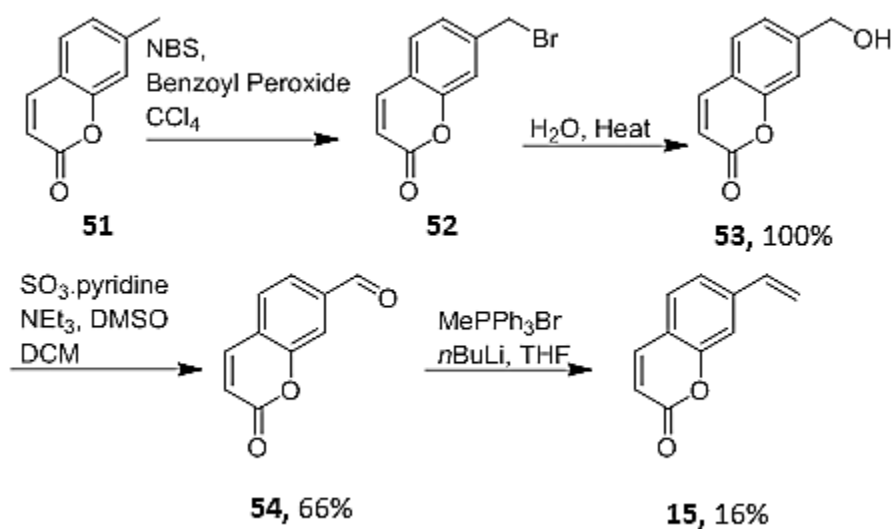


Figure 22- Synthesis of the Coumarin Fragment 15 as a Lactone Replacement

3.2.6 Synthesis of the Phenol Lactone Replacement 22

Another lactone replacement group identified by the discodermolide SAR is a phenol group, so we targeted simple fragment **22**. The alcohol **55** was oxidized under Parikh-Doering conditions⁸ to result in aldehyde **56** in 77% yield. Crude aldehyde **56** underwent a Wittig coupling reaction⁸⁰ with the ylide of methyltriphenylphosphonium bromide to result in olefin **22** in 50% yield (Figure 23).

3.3 SUMMARY

Five new fragments were synthesized for use in cross metathesis reactions. The key steps for synthesis of simple fragments include aldol condensations using Evans' oxazoladinone auxiliary to install two of the stereocenters found in the common precursor and a Grignard addition with 3-butenylmagnesium bromide. Lactone groups were prepared primarily with a Parikh-Doering oxidation followed by a Wittig addition with methyltriphenylphosphonium bromide.

4.0 SYNTHESIS OF DISCODERMOLIDE ANALOGS

4.1 INTRODUCTION

The fragments described in chapter 3 were designed to be coupled together using olefin cross metathesis. An alkene linker is suggested to be a viable connector by the HQSAR studies found in chapter 2. The possible advantages of an alkene linker compared to the full linker in discodermolide are 1) to remove three stereocenters found in the natural product; 2) to place both the lactone and carbamate fragments in a similar conformation as discodermolide; and 3) to use a robust synthetic method that cuts down on the total number of steps to complete chemical synthesis of analogs.

Olefin metathesis has been used in the synthesis of natural products, including other microtubule stabilizers.⁸⁹ A ring closing olefin metathesis approach was attempted for the C10-C11 double bond by the Curran group,⁹⁰ but other routes were more robust, and this route was not included in the total synthesis. Hoveyda, Schrock and co-workers used a Z-selective ring-closing metathesis in the synthesis of epothilone B.⁹¹ Recent examples have been seen using metathesis in the synthesis of the complex molecules such as tularin C,⁹² and leiodermatolide.⁹³

Olefin cross metathesis was therefore used to prepare analogs of discodermolide that contain an alkene linker instead of the naturally occurring *syn*, *anti*-stereotriad. The analogs

were made by coupling the three lactone groups with the phenyl replacement carbamate **20** that were discussed in chapter 3.

4.2 RESULTS

4.2.1 Final Steps of Analogue Synthesis

Grubbs II ruthenium olefin metathesis catalyst was used to couple two fragments directly together to make simplified discodermolide analogs. The short chain lactone **23** and carbamate **20** were coupled with Grubbs II catalyst in methylene chloride by heating at reflux for 8 h to yield 13 mg of **57** in 24% yield (**Figure 25**) as a complex mixture of inseparable isomers at the new alkene and the stereocenter containing a MOM ether. Deprotection of analogue **57** was done by treatment with 4 M HCl overnight, yielding the mono-hydroxy product **58** in 60% yield (5.2 mg), as well as the di-alcohol product **59** in 54% (4.2 mg). Analysis of the ^1H NMR spectrum of **58** shows a mixture of *E/Z* isomers. The ratio is unclear due to overlapping peaks in the 5.4-5.6 ppm range, but the *E* isomer is generally favored in cross metathesis reaction.⁹⁴ The complete syntheses for the new analogs **58** and **59** only took 17 total steps, beginning with the aldol condensation using Evans chiral oxazoladinone auxiliary.

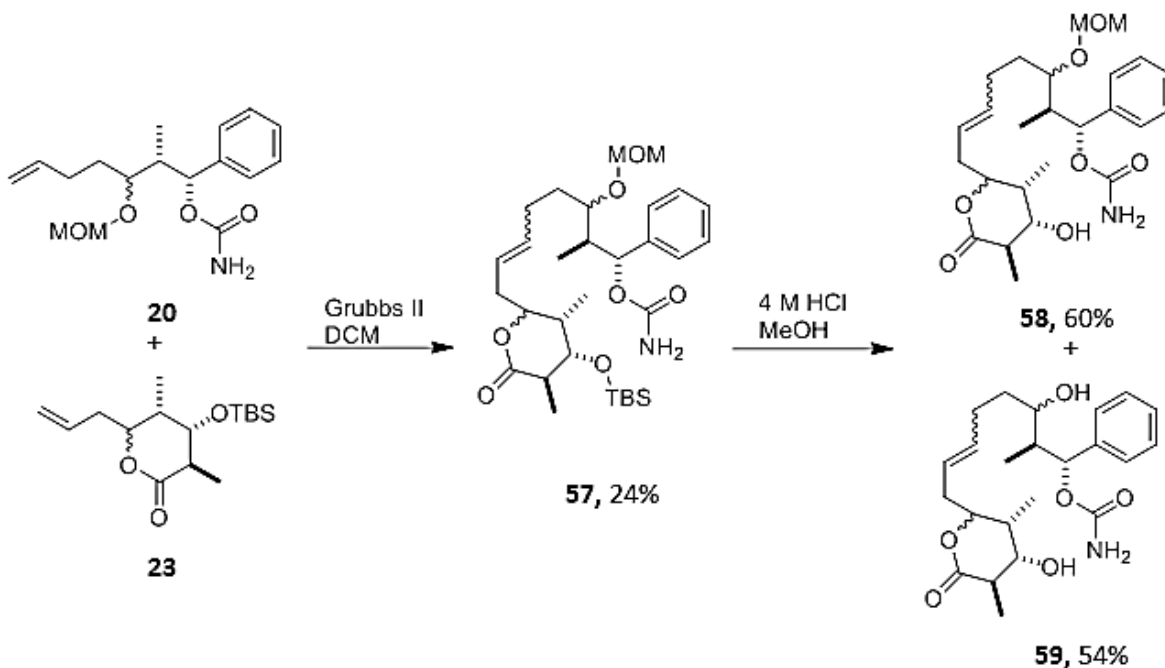


Figure 25- Analogue Containing Short Chain Lactone and Phenyl Carbamate Groups

Synthesis of a new coumarin analogue is shown in **Figure 26**. Coumarin **15** and phenyl carbamate **20** were heated to reflux in the presence of Grubbs II catalyst to yield **21** in 38% (16.6 mg) as a mixture of isomers (**Figure 26**). The ratio was again undetermined due to overlapping peaks in the 6.23-6.28 ppm region. Alkene **21** was treated with 6 M HCl to yield 1.6 mg of **60** (31%). The complete synthesis of this analogue was completed in 14 total steps.

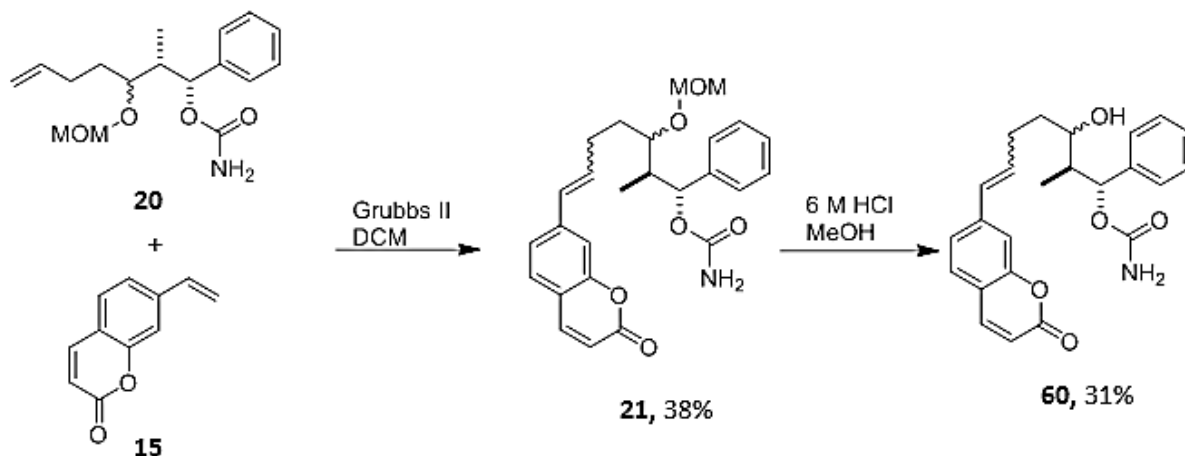


Figure 26- Synthesis of Analogue Containing Coumarin and Phenyl Carbamate Groups

A third new analogue was prepared as shown in **Figure 27**. Phenol lactone mimetic **22** and phenyl carbamate fragment **20** (**Figure 27**) underwent olefin metathesis with Grubbs II catalyst to yield **61** in 33% yield (12 mg). Again, the ratio of *E/Z* isomers was unclear by ^1H NMR spectroscopy, but the presence of new alkene protons showed that the cross metathesis succeeded. Alkene **61** was treated with 6 M HCl to yield **62** in 29% (1.5 mg). The entire scheme to reach **62** took only 13 overall steps.

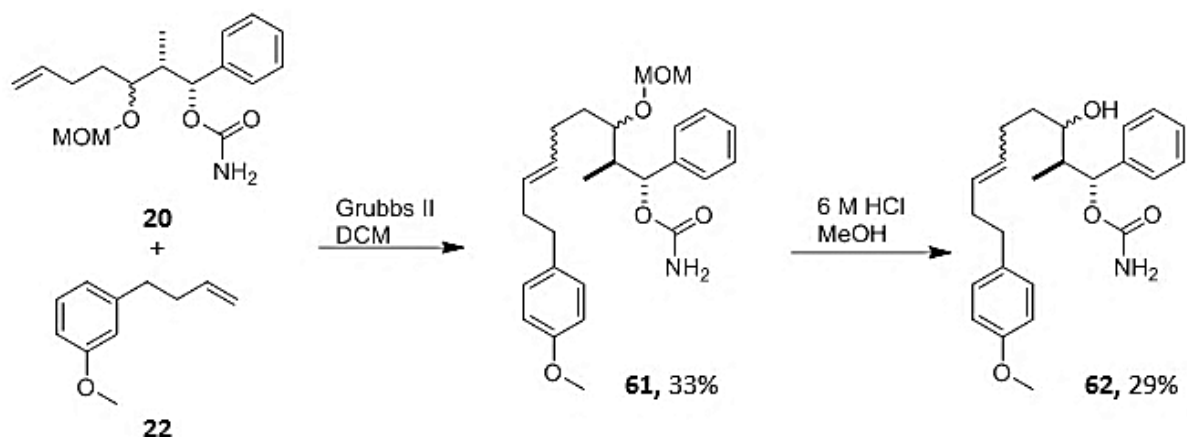


Figure 27- Synthesis of Analogue Containing Two Phenyl Groups

In total, six compounds were made that will be used for testing in biological screening in breast cancer cell types. The synthetic schemes used to make these compounds drastically limit the number of steps used to make the end product compared to the total synthesis of discodermolide. The routes also were completed without any in-depth optimization. Any analogue with potency as a microtubule stabilizer has potential for scale-up synthesis with optimization of the synthetic scheme. Unfortunately, the cross metathesis method used for coupling was not stereoselective, and both *cis* and *trans* alkene isomers were apparent in product mixtures. Although the *cis*-form of coupled product was desired in the initial design of the project, the *trans*-isomer may place the lactone and carbamate moieties in proper position, since carbamate **20** contains two rotatable methylenes, unlike the rigid backbone of discodermolide. Additionally, if the isomers are separated chromatographically, more compounds are available for biological testing. Unfortunately, purification of the isomers was not an easy task, and with only small amounts of compound, the analogs are not isomerically pure compounds.

5.0 SUMMARY

The goal of the project was to synthesis simplified analogs of discodermolide. To achieve that end, I first designed 16 virtual analogs of discodermolide that contained a simple alkene linker. These analogs were screened in the HQSAR of Salum and Andricopulo for predicted activities using four different models. One analogue (C-1) had pIC₅₀ values above 7.0 in all four model sets, while four analogs (A-1, B-1, B-2 and C-2) had pIC₅₀ values above 7.0 in three out of the four model sets.

Three simple analogs of discodermolide were completed by total synthesis. These analogs were made from the carbamate **20** and three simple lactones **15**, **22**, and **23**. The fragments were coupled together using olefin cross metathesis. Unfortunately, the stereochemical isomers could not be separated, so they are reported here as isomeric mixtures. The total synthesis of these analogs took between 13 and 17 steps, much shorter than the total synthesis of discodermolide (usually 32 steps at minimum). Optimization of the synthetic route and biological testing of the analogs can still be done to establish if these simple discodermolide analogs have potential as drugs.

6.0 EXPERIMENTAL SECTION

Modeling Experimental

General

All simulations were done using SYBYL 8.0 platform run on Red Hat Enterprise Linux workstations. Analogs were built using ChemDraw Ultra 12.0, and converted to correct .mol files on Chem 3D Pro 12.0. PyMOL was used as viewing software for 3D rendering of analogs.

HQSAR Predictions

Discodermolide analogs were energy minimized employing the TRIPOS forcefield using 10000 iterations in a gradient of 0.005 kcal/mol. The previously developed HQSAR was used to predict the pIC_{50} ($-\log IC_{50}$; IC_{50} is the concentration of 50% inhibition of A549 lung carcinoma cells) of analogs of discodermolide. A training set of 47 analogs was broken into fragments six to nine atoms in length, which were then differentiated according to the parameters of atoms, bonds, connectivity, chirality and hydrogen atoms. These were then used for building molecular holograms and HQSAR models which identified positive atomic contributions to biological activity. Analogs were used as a test set, and evaluated with the same parameters, using the same process.

Chemistry

General Information: All reactions were performed under an inert atmosphere of N₂ gas in oven-dried glassware using anhydrous solvents unless stated otherwise. Anhydrous THF was obtained from sodium/benzophenone distillation. Anhydrous CH₂Cl₂ was obtained by distillation from CaH₂. All other anhydrous solvents were purchased from Sigma-Aldrich. Melting points for all compounds were obtained from a Fisher-Johns melting point apparatus. ¹H NMR spectra were obtained from a 600 MHz Bruker Ultrashield Plus spectrometer equipped with a cryoprobe. ¹³C NMR spectra were obtained in the same spectrometer at 150 MHz. Spectra were obtained using CDCl₃ as solvent (unless stated otherwise) and reported relative to residual CHCl₃ shift (7.26 ppm) for ¹H NMR spectra and CDCl₃ (77.2 ppm) for ¹³C NMR spectra. Low-resolution mass spectra were obtained on an Applied Biosciences API 2000 ESI-triple quadrupole mass spectrometer with a Shimadzu UFLC inlet system. Gas chromatography was performed using a 5890 Series II Gas Chromatograph equipped with a Hewlett-Packard 5971 Series Mass Selective Detector.

D-Phenylalanol: D-Phenylalanine (10.0 g, 60.5 mmol) was added to a 500-mL 3-neck flask and dissolved in THF (30 mL). A reflux condenser, an addition funnel and a septum were attached to the flask. BF₃•OEt₂ (7.50 ml in ether, 60.5 mmol) was added dropwise to the flask by addition funnel, and after complete addition, the flask was heated at reflux for 2 h. BH₃•SMe₂ (13.9 mL, 5M in diethyl ether) was then added by slow dropwise addition (about 1 h) to the flask via the addition funnel. The solution was then heated to reflux an additional 6 h. The mixture was cooled overnight for 14 h, and then a 1:1 THF/EtOH (7.6 mL) mixture was added, followed by addition of 5 M NaOH solution (45 mL). This mixture was refluxed for 12 h. Upon cooling, the slurry was filtered, and the filtrate washed with THF (2 x 25 mL). The organic phase was

evaporated, and the resulting slurry was extracted with CH₂Cl₂ (1 x 50 mL, 1 x 25 mL), dried with MgSO₄, filtered, and concentrated in vacuo. The crude mixture was crystallized from hot ethyl acetate resulting in 4.77 g (52%) of white crystalline solid: m.p. 90-92 °C ¹H NMR (600 MHz, CDCl₃) δ 7.31 (t, *J* = 10.8 Hz, 2 H), 7.23 (d, *J* = 10.8 Hz, 1 H), 7.19 (d, *J* = 10.2 Hz, 2 H), 3.63 (dd, *J* = 15.9, 6 Hz, 1 H), 3.38 (dd, *J* = 16.2, 10.8 Hz, 1 H), 3.11 (m, 1 H), 2.79 (dd, *J* = 20.1 Hz, 7.8 Hz, 1 H), 2.53 (dd, *J* = 20.1, 13.2 Hz, 1 H).

4(*R*)-4-Phenylmethyl-2-oxazolidinone (25): The amino alcohol **25** (4.00 g, 26.5 mmol), diethyl carbonate (6.62 mL, 54.6 mmol) and potassium carbonate (0.366 g, 2.65 mmol) were all added to a small round bottom flask. A distillation apparatus was attached, and the flask was lowered into a sand bath pre-heated to 135 °C for 3.5 h. After cooling, workup for the reaction began with the addition of CH₂Cl₂ (25 mL). The contents of the reaction flask were added to a separatory funnel and the organic and aqueous phases were separated. The organic portion was washed with water (25 mL), dried with MgSO₄, filtered, and concentrated in vacuo. Recrystallization of the crude material in 2:1 hot hexane-ethyl acetate solvent resulted in 1.96 g (42%) of **25** as white crystals: m.p. 87.5-89 °C; ¹H NMR (600 MHz, CDCl₃) δ 7.34 (t, *J* = 7.2 Hz, 2 H), 7.29 (t, *J* = 7.2 Hz, 1 H), 7.18 (d, *J* = 7.2 Hz, 2 H), 4.98 (br s, 1 H), 4.90 (t, *J* = 8.4 Hz, 1 H), 4.16 (dd, *J* = 9.0, 5.4 Hz, 1 H), 4.09 (m, 1 H), 2.87 (qd, *J* = 13.5, 5.4 Hz, 2 H)

3-(1-Oxopropyl)-4-(phenylmethyl)-(4*R*)-2-oxazolidinone (11): The auxiliary **25** (1.77 g, 10.0 mmol) was dissolved in dry THF, placed under N₂ gas, and cooled in an ice bath at 0 °C. *n*-BuLi (6.88 mL, 11.0 mmol, 1.6 M in THF) was added dropwise to the solution. This was followed by addition of propionyl chloride (1.04 mL, 12.0 mmol), and the solution was stirred overnight with

gradual warming to room temperature (about 14 h). Workup proceeded with addition of saturated aq. NH_4Cl (60 mL) and the solution was diluted with diethyl ether (60 mL). The mixture was transferred to a separatory funnel. The layers were separated, and the organic fraction was washed with 1 M HCl (2 x 50 mL), 1 M NaOH (2 x 50 mL), and saturated aq. NaCl (50 mL). The organic fraction was then dried with MgSO_4 , filtered, and concentrated *in vacuo*. Pure product **11** was isolated as a yellow gel by flash chromatography (5:1 hexane-ethyl acetate). Yellow crystals were obtained by placing product on vacuum with seed crystal resulting in 1.86 g (80%): m.p. 41-46 °C, ^1H NMR (600 MHz, CDCl_3) δ 7.34 (t, $J = 7.2$ Hz, 2 H), 7.28 (t, $J = 7.2$ Hz, 1 H), 7.21 (d, $J = 7.2$ Hz, 2 H), 4.67 (m, 1 H), 4.18 (m, 2 H), 3.30 (dd, $J = 13.2$, 3 Hz, 1 H), 2.96 (m, 2 H), 2.76 (dd, $J = 13.5$, 9.6 Hz, 1 H), 1.20 (t, $J = 7.2$ Hz, 3 H)

3-[(2*R*,3*R*)-3-Hydroxy-2,4-dimethyl-1-oxo-4-penten-1-yl]-4-(phenylmethyl)-(4*R*)-2-

oxazolidinone (26): The acyl-auxiliary **11** (2.00g, 8.57 mmol) was dissolved in dry CH_2Cl_2 (19 mL), and cooled to 0 °C in an ice bath. Dibutylboron triflate (10.28 mL, 10.28 mmol, 1 M in CH_2Cl_2) was added dropwise over 10 minutes to the solution, followed by the addition of DIPEA (1.94 mL, 11.1 mmol). This solution was then cooled to -78 °C in an acetone/dry ice bath, and methacrolein (1.59 mL, 19.3 mmol) was added to the solution with slow addition over 20 minutes. The mixture was stirred for 20 min in the dry ice/acetone bath, warmed to 0 °C in an ice bath, and stirred an additional hour at this temperature. After this time, pH 7 phosphate buffer was added (13.3 mL), followed by the addition of CH_3OH (20 mL). After 5 min of stirring, 30% H_2O_2 (13.3 mL) was added, followed by more CH_3OH (26 mL). This was stirred for 1 h. The reaction flask was then concentrated *in vacuo*, resulting in yellow slurry. The slurry was transferred to a separatory funnel and was extracted with diethyl ether (2 x 25 mL). The

organic layers were combined, washed with saturated aq. NaCl (2 x 25 mL), dried with MgSO₄, filtered and concentrated in vacuo. Purified product was isolated by flash chromatography (5:1 hexane-ethyl acetate) resulting in 1.72 g (66%) product **26** as a clear gel: ¹H NMR (600 MHz, CDCl₃) δ 7.34 (t, *J* = 7.8 Hz, 2 H), 7.29 (t, *J* = 7.2 Hz, 1 H), 7.21 (d, *J* = 7.2 Hz, 2 H), 5.13 (s, 1 H), 4.99 (s, 1 H), 4.71 (m, 1 H), 4.46 (s, 1 H), 4.21 (m, 2 H), 3.96 (qd, *J* = 7.2, 3 Hz, 1 H), 3.27 (dd, *J* = 13.8, 3.6 Hz, 1 H), 2.96 (d, *J* = 3 Hz, 1 H), 2.80 (dd, *J* = 13.2, 9.6 Hz, 1 H), 1.74 (s, 3 H), 1.19 (d, *J* = 6.6 Hz, 3 H)

3-[(2*R*,3*R*)-3-[(1,1-Dimethylethyl)dimethylsilyl]oxy]-2,4-dimethyl-1-oxo-4-penten-1-yl]-4-(phenylmethyl)-(4*R*)-2-oxazolidinone (27): The auxiliary starting material **26** (1.80 g, 5.93 mmol) was placed in a round bottom flask, dissolved in CH₂Cl₂ (10 mL), placed in an atmosphere of N₂ gas and cooled to 0 °C in an ice bath. 2,6-Lutidine (0.96 mL, 8.30 mmol) was added dropwise via syringe, followed by the dropwise addition of TBDMSOTf (1.50 mL, 6.52 mmol). This reaction mixture was stirred at 0 °C. The reaction was monitored by TLC. After 1.5 h, the reaction was quenched with the addition of 20 mL of hexane and 10 mL of 1 M HCl. After transferring the contents of the reaction mixture to a separatory funnel, the aqueous layer was then extracted with hexane (2 x 10 mL). The organic layers were then combined and washed with 1 M HCl (2 x 15 mL), saturated NaHCO₃ (2 x 15 mL), and saturated NaCl (2 x 15 mL). The organic fraction was then dried with MgSO₄, filtered and the solvent evaporated. The result was a crude white solid **27** (1.65g, 82%) that was carried on without any purification: m.p. 73-76 °C; ¹H NMR (600 MHz, CDCl₃) δ 7.33 (t, *J* = 7.2 Hz, 2 H), 7.29 (d, *J* = 4.2 Hz, 1 H), 7.21 (d, *J* = 7.2 Hz, 2 H), 4.93 (s, 1 H), 4.983 (s, 1 H), 4.56 (m, 1 H), 4.34 (d, *J* = 6.0 Hz, 1 H), 4.15

(m, 2 H), 4.0 (quin. $J = 7.2$ Hz, 1 H), 3.27 (dd, $J = 13.2, 3$ Hz, 1 H), 2.96, 2.75 (dd, $J = 13.5, 10.2$ Hz, 1 H), 1.71 (s, 3 H), 1.20 (d, $J = 7.2$ Hz, 3 H), 0.90 (s, 9 H), 0.005 (s, 3 H) -0.02 (s, 3 H).

3-[(2*R*,3*R*,4*S*)-3-[[*(1,1*-Dimethylethyl)dimethylsilyl]oxy]-2,4-dimethyl-5-hydroxy-1-oxo-pentan-1-yl]-4-(phenylmethyl)-(4*R*)-2-oxazolidinone (28): The TBDMS ether **27** (1.60 g, 3.83 mmol) was dissolved in dry THF (15 mL), cooled to 0 °C in an ice bath, and put in an atmosphere of N₂ gas. 9-BBN (15.3 mL, 0.5 M in THF) was then added dropwise. The solution was stirred for 15 min at 0 °C, and then for 5 h at room temperature. EtOH-THF (1:1, 5.1 mL), pH 7 phosphate buffer (5.1 mL) and 30% hydrogen peroxide (5.1 mL) were added sequentially to the flask, which had been cooled to 0 °C. The contents were stirred for 30 min at this temperature, then overnight at room temperature. The reaction was quenched with the addition of 20% aq. NaHSO₃ (40 mL) and heptanes (50 mL). The layers were separated, and the aqueous layer was extracted with heptane (3 x 35 mL). These organic layers were combined, and washed with saturated aq. NaCl (2 x 40 mL). The organic fractions were then dried with MgSO₄, filtered and concentrated in vacuo, resulting in **28**. It was carried forward without any further purification.

(3*R*,4*S*,5*S*)-4-(*tert*-Butyldimethylsilanyloxy)-3,5-dimethyltetrahydropyran-2-one (29): The crude alcohol **28** (0.100 g, 0.23 mmol) was dissolved in dry THF (2.4 mL), placed in a round-bottom flask under an atmosphere of N₂ gas, and the flask was cooled to 0 °C in an ice bath. Potassium *tert*-butoxide (0.516 mg, 0.0046 mmol) was added to the flask, and the solution was allowed to stir for 1 h. Workup proceeded with addition of hexane (10 mL). The organic fraction was washed with saturated aq. NaCl (1 x 10 mL), dried with MgSO₄, filtered, and

concentrated in vacuo. Crude product was then subjected to flash chromatography (SiO₂; 9:1 hexane-ethyl acetate) to yield the lactone **29** in 55% yield (59.4 mg): m.p. 53-57 °C ¹H NMR (600 MHz, CDCl₃) δ 4.25 (t, *J* = 10.2, 1 H), 4.12 (dd, *J* = 10.8, 4.8 Hz, 1 H), 3.68 (br. t, *J* = 3 Hz, 1 H), 2.62 (qd, *J* = 3.6 Hz, 7.5 Hz, 1 H), 2.20 (m, 1 H), 1.30 (d, *J* = 7.8 Hz, 3 H), 0.97 (d, *J* = 7.2 Hz, 3 H), 0.90 (s, 9 H), 0.08 (d, *J* = 8.4 Hz, 6 H).

(2*R*,3*S*,4*S*)-3-(*tert*-Butyldimethylsilanyloxy)-5-hydroxy-2,4-dimethylpentanoic acid methoxymethylamide (30): The δ-lactone **29** (1.10 g, 4.26 mmol) and methoxy methyl amide (0.644 g, 6.60 mmol) were placed in a round bottom flask, dissolved in dry THF (14 mL), placed in an atmosphere of N₂ gas, and cooled to ~-15 °C in an acetone/dry ice bath. *i*-PrMgCl (6.65 mL, 13.3 mmol, 2M in THF) was added with dropwise addition via syringe, and the reaction was allowed to stir for 1 h and 20 min. Workup began with addition of diethyl ether (12 mL), followed by 1:1 saturated aq. NH₄Cl-water (24 mL). The layers were separated, and the aqueous phase was extracted with diethyl ether (12 mL). The organic layers were combined, washed with saturated aq. NaCl (3 x 15 mL), dried with MgSO₄, filtered and evaporated, resulting in a clear oil **30**, which was carried forward without any further purification: ¹H NMR (600 MHz, CDCl₃) δ 4.09 (dd *J* = 9.6 Hz, 3 Hz, 1 H), 3.73 (s, 3 H), 3.58 (m, 1 H), 3.25 (m, 1 H), 3.17 (br s, 3 H), 3.12 (m, 1 H), 2.86 (m, 1 H), 1.91 (m, 1 H), 1.18 (d, *J* = 7.2 Hz, 3 H), 0.92 (s, 9 H), 0.11 (d, *J* = 3.6 Hz, 6 H).

(2*R*,3*S*,4*S*)-3-(*tert*-Butyldimethylsilanyloxy)-5-oxo-2,4-dimethylpentanoic acid methoxymethylamide (31): The crude alcohol **30** (1.36 g, 4.26 mmol) was dissolved in dry CH₂Cl₂ (4.3 mL), placed in an atmosphere of N₂ gas, and cooled to 0 °C in an ice bath. Then, in

succession, triethylamine (2.38 mL, 17.08 mmol), DMSO (1.51 mL), and SO₃-pyridine (2.04 g, 12.82 mmol) dissolved in DMSO (7.0 mL) were added to the flask. The reaction was stirred for 1.5 h. Workup began with addition of diethyl ether (32 mL). This was followed by addition of 1 M NaHSO₄ (16.4 mL) in water (4.6 mL). This was stirred for 10 min on ice. After this time, the layers were separated, and the aqueous phase was extracted with diethyl ether (30 mL). The organic layers were combined, washed with 8% aq. NaHCO₃ (30 mL) and saturated aq. NaCl (40 mL). The organic layer was then dried with MgSO₄, filtered and evaporated resulting in a clear oil. This was purified using flash chromatography (SiO₂, 9:1 hexane-ethyl acetate) resulting in a clear oil **31** (80% over two steps): ¹H NMR (600 MHz, CDCl₃) δ 9.71 (s, 1 H), 4.25 (dd, *J* = 9.0, 1.8 Hz, 1 H), 3.71 (s, 3 H), 3.13 (br s, 4 H), 2.47 (q, *J* = 5.4 Hz, 1 H), 1.28 (d, *J* = 7.8 Hz, 3 H), 1.13 (d, *J* = 6.6 Hz, 3 H), 0.90 (s, 9 H), 0.12 (d, *J* = 3.6 Hz, 6 H).

(2*R*,3*S*,4*S*,*Z*)-3-(*tert*-Butyldimethylsilanyloxy)-2,4-dimethyloct-5-enoic acid methoxymethylamide (32): Propyltriphenylphosphonium bromide (1.22 g, 3.16 mmol) was dissolved in THF (7.4 mL), and cooled in an acetone-dry ice bath to -78 °C. *n*-Butyl lithium (1.98 mL, 3.16 mmol, 1.6 M in THF) was added dropwise to the solution, and the reaction mixture was warmed to room temperature and stirred for 40 min. During this time, the aldehyde **31** (0.600 g, 1.89) was dissolved in THF (9.45 mL) and cooled in the dry ice/acetone bath. The phosphonium ylide was transferred via syringe until the reaction mixture took on an orange color. This was stirred at 0 °C for 1 h. Workup was done with addition of saturated aq. NH₄Cl (0.9 mL) and hexane (40 mL). The layers were separated, and the organic layer was washed with water (2 x 15 mL) and saturated aq. NaCl (2 x 15 mL). The organic layer was dried with MgSO₄, filtered, and concentrated in vacuo. Purification was done via flash chromatography

(SiO₂, 9:1 hexane-ethyl acetate) resulting in 0.388 g (60%) of Wittig product as a clear oil **32**: ¹H NMR (600 MHz, CDCl₃) δ 5.46 (t, *J* = 10.2 Hz, 1 H), 5.35 (m, 1 H), 3.87 (d, *J* = 8.4 Hz, 1 H), 3.64 (br s, 3 H), 3.13 (br s, 3 H), 2.90 (m, 1 H), 2.60 (m, 1 H), 1.99 (m, 1 H), 1.92 (m, 1 H), 1.11 (d, *J* = 7.2, 3 H), 0.97 (d, *J* = 6.6 Hz), 0.91 (s, 9 H), 0.07 (d, *J* = 7.8 Hz, 6 H); ¹³C NMR (150 MHz, CDCl₃) δ 177.5, 132.2, 130.5, 61.4, 40.6, 36.5, 32.4, 26.4, 21.0, 19.6, 18.7, 15.8, 14.7, – 3.2; *m/z* (ESI) [M + H]⁺ 344.2.

(2R,3S,4S,Z)-3-(tert-Butyldimethylsilanyloxy)-2,4-dimethyloct-5-enal (33): The methoxyxymethyl amide starting material **32** (0.345 g, 1.00 mmol) was dissolved in THF (1.02 mL) and cooled in an acetone/dry ice bath to ~ –30 °C. DIBAL-H (1.15 mL, 1 M in toluene) was added dropwise, and the mixture was stirred for 45 min. CH₃OH (0.5 mL) was added, followed by saturated aq. sodium potassium tartrate (12 mL) and hexane (12 mL). The layers were separated, and the aqueous fraction was extracted with hexane (2 x 7 mL). The organic layers were combined, washed with saturated aq. NaHCO₃ (2 x 7 mL) and saturated aq. NaCl (2 x 7 mL). The organic layer was dried with MgSO₄, filtered and concentrated *in vacuo*. The crude product was purified by flash chromatography (SiO₂, 19:1 hexane-ethyl acetate) resulting in 0.175 g (61%) of clear oil **33**: ¹H NMR (600 MHz, CDCl₃) δ 5.35 (m, 1 H), 5.30 (t, *J* = 10.2 Hz, 1 H), 3.94 (t, *J* = 10.2 Hz, 1 H), 2.66 (m, 1 H), 2.47 (m, 1 H), 2.00 (m, 1 H), 1.95 (m, 1 H), 1.06 (d, *J* = 6.6 Hz, 3 H), 0.99 (d, *J* = 6.6 Hz, 3 H), 0.90 (s, 12 H), 0.09 (s, 3 H), 0.05 (s, 3 H); ¹³C (150 MHz, CDCl₃), δ 204.66, 133.19, 129.92, 76.42, 51.75, 35.24, 25.78, 21.21, 19.14, 14.16, 9.78, –4.03, –4.13.

(6*S*, 7*S*, 8*S*, *Z*)-7-((*tert*-Butyldimethylsilyl)oxy)-6,8-dimethyldodeca-1,9-dien-5-ol (34):

Magnesium turnings (0.084 g, 3.47 mmol) and a crystal of I₂ were placed in a round bottom flask. 4-Bromo-1-butene (0.32 ml, 3.15 mmol) was dissolved in anhydrous THF (3.15 ml), and added to the reaction flask slowly, allowing for the initiation of the reaction as evidenced by a color change from brown to grey. The formation of the Grignard reagent was stirred for 1 h at room temperature. In the meantime, aldehyde **33** (0.300g, 1.05 mmol) was dissolved in anhydrous THF (8.75 ml), and cooled to 0 °C in an ice bath. The Grignard reagent was added via syringe, and this reaction was stirred for 1.5 h at 0 °C. The reaction was quenched with the addition of saturated NH₄Cl (5.3 ml). The reaction mixture was then extracted with ethyl acetate (3 x 10 ml). The organics were combined and washed with brine (10 ml). The organics were then dried over Na₂SO₄, were filtered, and concentrated. The crude mixture was purified by flash chromatography (SiO₂, 0-100% ethyl acetate :hexane over 16 minutes) to yield 0.151 g (43%) of diastereomeric mixture of product **34**: ¹H NMR (600 MHz, CDCl₃) δ 5.84-5.80 (m, 1 H), 5.54 (t, *J* = 10.7 Hz, 1 H), 5.47-5.41 (m, 1 H), 5.03 (d, *J* = 17.2 Hz, 1 H), 4.94 (d, *J* = 10.0 Hz, 1 H), 3.79-3.68 (m, 1 H), 3.61 (s, 1 H), 2.75-2.69 (m, 1 H), 2.26-2.13 (m, 1 H), 2.13-1.98 (m, 3 H), 1.94 (s, 1 H), 1.75-1.69 (m, 2 H), 1.41-1.30 (m, 1 H), 1.01-0.97 (m, 6 H), 0.97 (s, 12 H), 0.07 (d, *J* = 12.3 Hz, 6 H); ¹³C NMR (150 MHz, CDCl₃) δ 138.70, 132.46, 131.22, 114.55, 78.93, 70.50, 42.42, 34.83, 34.76, 30.66, 26.04, 20.93, 19.34, 18.27, 14.27, 9.35, -4.03, -4.05; these resonances are the major peaks found in the ¹³C spectrum; *m/z* (ESI) [M – TBS + H]⁺ 227.2.

(2*R*,3*S*,4*S*)-3-((*tert*-Butyldimethylsilyl)oxy)-*N*-methoxy-*N*,2,4-trimethyl-5-

((triethylsilyl)oxy)pentanamide (37): Weinreb's amide **30** (2.891 g, 9.05 mmol) was dissolved

in anhydrous pyridine (161 ml). N, N-dimethyl-4-aminopyridine (0.221 g, 1.81 mmol) was added to the reaction flask, followed by the addition of chlorotriethylsilane (3.2 ml, 19.01 mmol). The reaction was stirred overnight for 17.5 h. Workup was done by dilution of the reaction mixture with methylene chloride (320 ml). This was washed with a 1:1 mixture of saturated aqueous $\text{NaHCO}_3\text{:H}_2\text{O}$ (160 ml). The organics were dried over Na_2SO_4 , were filtered and concentrated. Purification of crude diether **37** was done by flash chromatography (SiO_2 , 19:1 hexane: ethyl acetate), to yield 2.331 g of product (59%). Additionally, 0.731 g of lactone **29** (31%) was recovered from the reaction mixture: ^1H NMR (600 MHz, CDCl_3) δ 3.91 (dd, J = 7.1, 3.8 Hz, 1 H), 3.74 (dd, J = 9.8, 4.5 Hz, 1 H), 3.69 (s, 3 H), 3.27 (t, J = 9.3 Hz, 1 H), 3.16 (s, 3 H), 3.10 (m, 1 H), 1.76 (m, 1 H), 1.11 (d, J = 7.0 Hz, 3 H), 0.97 (d, J = 6.9 Hz, 3 H), 0.94 (t, J = 7.9 Hz, 9 H), 0.90 (s, 9 H), 0.57 (q, J = 8.0 Hz, 6 H), 0.05 (d, J = 12.1 Hz, 6 H); ^{13}C NMR (150 Hz, CDCl_3) δ 75.46, 64.50, 61.19, 41.49, 38.90, 32.12, 32.12, 26.11, 18.33, 14.62, 14.31, 6.57, 5.77, 4.34, -3.92, -4.02.

(2R,3S,4S)-3-((tert-Butyldimethylsilyl)oxy)-2,4-dimethyl-5-((triethylsilyl)oxy)pentanal (38):

Weinreb amide **37** (0.714 g, 1.65 mmol) was dissolved in anhydrous THF (12.5 ml) and cooled to $-78\text{ }^\circ\text{C}$ in an acetone/dry ice bath. DiBAL-H (3.5 ml, 1M in toluene) was added drop-wise to the cooled solution, and the reaction was stirred for 6 h in the acetone/dry ice bath. The reaction was quenched after this time with the addition of MeOH (2.5 ml). Saturated aqueous sodium potassium tartrate (12.5 ml) and ethyl acetate (25 ml) were added to the reaction flask. The flask was stirred an additional 2 h at room temperature. After this, the layers were separated and the organic portion was washed with saturated aqueous NaHCO_3 (50 ml) and brine (50 ml). The organic portion was then dried over MgSO_4 , was filtered and concentrated, yielding 0.534 g

(86%) of crude aldehyde **38**: ^1H NMR (600 MHz, CDCl_3) δ 9.72 (s, 1 H), 4.19 (dd, $J = 6, 3.6$ Hz, 1 H), 3.65 (dd, $J = 9.6, 5.4$ Hz, 1 H), 3.47 (dd, $J = 10.2, 6$ Hz, 1 H), 2.50 (qd, $J = 7.2, 3.6$ Hz, 1 H), 1.10 (d, $J = 7.2$ Hz, 3 H), 0.96 (t, $J = 7.8$ Hz, 9 H), 0.92 (d, $J = 7.2$ Hz, 3 H), 0.86 (s, 9 H), 0.59 (q, $J = 7.8$ Hz, 6 H), 0.07 (s, 3 H), -0.01 (s, 3 H); ^{13}C NMR (150 MHz, CDCl_3) 205.14, 72.17, 64.50, 50.00, 40.39, 25.90, 18.22, 13.84, 8.02, 6.80, 4.38, -4.18, -4.35.

(5R,6S,7S,8S)-7-((tert-Butyldimethylsilyl)oxy)-6,8-dimethyl-9-((triethylsilyl)oxy)non-1-en-5-ol (39): The Grignard reagent was prepared by placing magnesium turnings (0.634 g, 26.07 mmol) in an oven-dried round bottom flask, along with a crystal of iodine. 4-Bromo-1-butene (2.4 ml, 23.70 mmol) was dissolved in anhydrous THF (23.7 mL) and added to the reaction flask slowly. After complete addition, the reaction was deemed to have initiated by the change in color from brown to grey. This flask was stirred for 1 h at room temperature. The aldehyde **38** (2.960 g, 7.90 mmol) was dissolved in anhydrous THF (66 mL) and cooled to 0 °C in an ice bath. The Grignard reagent was added to this reaction flask, and stirred for 2 h. The reaction was quenched with the addition of saturated aqueous NH_4Cl (39.5 mL). This mixture was then extracted with ethyl acetate (3 x 79 mL). The organics were combined, and washed with brine (79 mL). It was dried over Na_2SO_4 , was filtered, and concentrated *in vacuo*. The mixture was purified by flash chromatography (SiO_2 , 19:1 hexane: ethyl acetate), yielding the correct isomer of **39** (1.36 g, 40%). Additionally, another 1.01 g of a mixture of both diastereomers was isolated (30% yield): ^1H NMR (600 MHz, CDCl_3) δ 5.85-5.81 (m, 1 H), 5.03 (d, $J = 17.1$ Hz, 1 H), 4.95 (d, $J = 10.1$ Hz, 1 H), 3.83 (t, $J = 4.0$ Hz, 1 H), 3.72-3.70 (m, 1 H), 3.64 (dd, $J = 7.9, 9.9$ Hz, 1 H), 3.43 (dd, $J = 6.1, 10.0$ Hz, 1 H), 2.66, (d, $J = 3.1$ Hz, 1 H), 2.26-2.20 (m, 1 H), 2.10-2.05 (m, 1 H), 2.05-2.00 (m, 1 H), 1.72-1.70 (m, 1 H), 1.58-1.54 (m, 1 H), 1.49-1.43 (m, 1 H),

0.94 (t, $J = 8.0$, 9 H), 0.91 (d, $J = 7.3$ Hz, 3 H), 0.90 (s, 9 H), 0.88 (d, $J = 7.1$ Hz, 3 H), 0.59 (q, $J = 8.0$ Hz, 6 H), 0.07 (s, 6 H); ^{13}C NMR (150 MHz, CDCl_3) δ 138.81, 114.51, 76.30, 73.33, 65.16, 40.54, 40.25, 34.18, 30.59, 26.01, 18.27, 14.02, 9.37, 6.78, 4.26, -3.78, -4.37; m/z (ESI) $[\text{M} + \text{H}]^+$ 431.2.

(5*R*,6*S*,7*S*,8*S*)-5-(But-3-en-1-yl)-7-((*tert*-butyldimethylsilyl)oxy)-11,11-diethyl-6,8-dimethyl-2,4,10-trioxa-11-silatridecane (40): Alcohol **39** (1.362 g, 3.16 mmol) is dissolved in anhydrous toluene (3.0 mL). Chloromethoxymethane (0.48 mL, 6.32 mmol) was added to the reaction flask, followed by addition of Hunig's base (0.69 mL, 3.95 mmol). The reaction was stirred for 3 h at room temperature. Work up was done by diluting the reaction with ethyl acetate (5.4 mL) and quenching the reaction with saturated aqueous NH_4Cl (5.4 mL). The layers were separated, and the aqueous phase was extracted with ethyl acetate (2 x 11 mL). The organics were combined and washed with saturated aqueous NaHCO_3 (2 x 11 mL) and brine (2 x 11 mL). The organic phase was then dried over MgSO_4 , filtered and concentrated, resulting in a crude oil. This was purified via flash chromatography (SiO_2 , 19:1 hexane: ethyl acetate) resulting in 0.288 g of **40** (19%). Also isolated was 0.486 g of alcohol **41**, a yield of 43% based on the amount of starting material **39**. ^1H NMR (600 MHz, CDCl_3) δ 5.84-5.79 (m, 1 H), 5.03 (d, $J = 17.1$ Hz, 1 H), 4.95 (d, $J = 10.1$ Hz, 1 H), 4.62 (q, $J = 7.0$ Hz, 2 H), 3.70 (t, $J = 4.3$ Hz, 1 H), 3.66 (dd, $J = 5.3, 9.8$ Hz, 1 H), 3.49 (q, $J = 5.8$ Hz, 1 H), 3.38 (s, 3 H), 2.12-2.07 (m, 2 H), 1.90-1.88 (m, 1 H), 1.83-1.80 (m, 1 H), 1.68-1.63 (m, 2 H), 0.95 (t, $J = 8.0$ Hz, 9 H), 0.91 (d, $J = 7.0$ Hz, 6 H), 0.89 (s, 9 H), 0.58 (q, $J = 8.0$ Hz, 6 H), 0.05 (d, $J = 4.5$ Hz, 6 H); ^{13}C NMR (150 MHz, CDCl_3) δ 138.64, 114.51, 101.15, 96.38, 79.73, 73.80, 64.73, 55.79, 40.92, 38.73, 31.48, 29.43, 26.13, 18.47, 14.30, 10.84, 6.82, 4.37, -3.77, -3.78; m/z (ESI) $[\text{M} + \text{H}]^+$ 475.0.

(2*S*,3*S*,4*S*,5*R*)-3-((*tert*-Butyldimethylsilyl)oxy)-5-(methoxymethoxy)-2,4-dimethylnon-8-en-1-ol (41): Triether **40** (0.288 g, 0.607 mmol) was dissolved in anhydrous THF (0.49 mL), and MeOH (0.49 mL). The reaction was cooled to 0 °C by an ice bath, and H₂O (0.15 mL) was added, followed by addition of acetic acid (52 µl, 0.91 mmol). The reaction was stirred for 4 h in the ice bath. After this, the reaction was diluted with H₂O (2 mL) and was extracted with ethyl acetate (3 x 4 mL). The organics were combined, and washed with saturated aqueous NaHCO₃ (2 x 2 mL) and H₂O (2 x 2.4 mL). The organics were dried over MgSO₄, filtered and concentrated *in vacuo*. The product was purified by flash chromatography (SiO₂, 7:1 hexane: ethyl acetate), yielding 0.105 g of isolated alcohol **41** (48%): ¹H NMR (600 MHz, CDCl₃) δ 5.83-5.79 (m, 1 H), 5.04 (d, *J* = 16.7 Hz, 1 H), 4.97 (d, *J* = 10.2 Hz, 1 H), 4.62 (dd, *J* = 17.5, 6.8 Hz, 2 H), 3.82 (dd, *J* = 5.5, 3.5 Hz, 1 H), 3.69-3.66 (m, 1 H), 3.54-3.51 (m, 1 H), 3.39 (s, 3 H), 2.62 (t, *J* = 6.0 Hz, 1 H), 2.13-2.06 (m, 2 H), 1.99-1.97 (m, 1 H), 1.95-1.91 (m, 1 H), 1.65 (q, *J* = 6.9 Hz, 1 H), 0.98 (d, *J* = 7.1 Hz, 3 H), 0.95 (d, *J* = 7.0 Hz, 3 H), 0.92 (s, 9 H), 0.10 (d, *J* = 11.4 Hz, 6 H); ¹³C NMR (150 MHz, CDCl₃) δ 167.51, 138.28, 114.90, 79.52, 75.81, 65.22, 55.94, 39.21, 38.91, 30.97, 30.08, 26.16, 18.38, 14.52, 11.56, -3.46, -3.91; *m/z* (ESI) [M + H]⁺ 361.3, [M + Na]⁺ 383.1.

(2*R*,3*R*,4*S*,5*R*)-3-((*tert*-Butyldimethylsilyl)oxy)-5-(methoxymethoxy)-2,4-dimethylnon-8-enal (42): Alcohol **41** (0.591 g, 1.64 mmol) was dissolved in anhydrous methylene chloride (4.1 mL) and DMSO (8.2 mL), and cooled to 0 °C in an ice bath. Triethylamine (1.1 mL, 7.77 mmol) was added, followed by addition of sulfur trioxide-pyridine (0.968 g, 6.08 mmol). The reaction was stirred for 1.5 h at 0 °C. Work up was done by diluting the reaction with diethyl ether (21 mL).

The reaction mixture was then washed with H₂O (16 mL) saturated aqueous NaHCO₃ (16 mL) H₂O (16 mL) again and brine (16 mL). It was dried over MgSO₄, was filtered and concentrated *in vacuo*, resulting in 0.532 g of crude **42**. No purification was done on this aldehyde: ¹H NMR (600 MHz, CDCl₃) δ 9.76 (s, 1 H), 5.81-5.78 (m, 1 H), 5.03 (d, *J* = 17.2 Hz, 1 H), 4.9 (d, *J* = 10.2 Hz, 1 H) 4.59 (dd, *J* = 20.6, 6.8 Hz, 2 H), 3.96 (dd, *J* = 6.3, 3.4 Hz, 1 H), 3.55 (dd, *J* = 10.2, 6.1 Hz, 1 H) 3.36 (s, 3 H) 2.70 (m 1 H), 2.08-2.05 (m, 2 H), 1.90-1.87 (m, 1 H), 1.70-1.63 (m, 2 H), 1.11 (d, *J* = 7.0, 3 H), 0.97 (d, *J* = 7.0, 3 H), 0.88 (s, 9 H), 0.08 (d, *J* = 6.1 Hz, 6 H); ¹³C NMR (150 MHz, CDCl₃) δ 204.66, 138.14, 114.94, 96.11, 78.54, 74.87, 55.84, 50.65, 40.23, 31.12, 29.92, 29.79, 25.98, 18.31, 11.76, 11.77, -3.82 *m/z* (ESI) [M + H]⁺ 359.1.

(6*S*, 7*S*)-5-(But-3-en-1-yl)-7-((*S*,*Z*)-hex-3-en-2-yl)-6,9,9,10,10-pentamethyl-2,4,8-trioxa-9-silaundecane (35): Propyltriphenylphosphonium bromide (0.855 g, 2.22 mmol) was suspended in anhydrous THF (5.2 mL), and cooled to -78 °C in an acetone/dry ice bath. *n*BuLi (1.4 mL, 2.24 mmol, 1.6 M) was added, and the contents of the flask were stirred for 2 h at room temperature. The aldehyde **42** (0.241 g, 0.673 mmol) was dissolved in anhydrous THF (3.4 mL). The phosphonium reagent was added to the aldehyde reaction flask cooled to 0 °C in an ice bath. This was stirred 18 h overnight, gradually warming to room temperature. The reaction was quenched with the addition of saturated aqueous NH₄Cl (1.4 mL), and then diluted with hexane (10 mL). The reaction mixture was washed with H₂O (2 x 10 mL) and brine (2 x 10 mL). The aqueous portions were combined, and extracted once more with hexane (10 mL). The organics were combined, dried over MgSO₄, were filtered and concentrated. The crude mixture was purified by flash chromatography (SiO₂, 19:1 hexane: ethyl acetate), yielding 0.182 g of **35** (70% yield): ¹H NMR (600 MHz, CDCl₃) δ 5.84-5.77 (m, 1 H), 5.39-5.34 (m, 2 H), 5.01 (d, *J* = 17.0

Hz, 1 H), 4.95 (d, $J = 9.6$ Hz, 1 H), 4.61 (dd, $J = 30.3, 6.8$ Hz, 2 H), 3.61 (dd, $J = 5.8, 3.2$ Hz, 1 H), 3.48, (dd, $J = 10.8, 6.0$ Hz, 1 H), 3.39, (s, 3 H), 2.75-2.70 (m, 1 H), 2.08-1.99 (m, 4 H), 1.72-1.69 (m, 1 H), 1.64-1.56 (m, 2 H), 0.99-0.96 (m, 6 H), 0.92 (s, 12 H), 0.07 (d, $J = 3.4$ Hz, 6 H); ^{13}C NMR (150 MHz, CDCl_3) δ 138.53, 131.56, 131.00, 114.53, 95.98, 78.99, 76.03, 55.79, 39.44, 36.19, 29.77, 26.22, 26.17, 20.98, 18.62, 18.50, 14.44, 10.97, -3.35, -3.60; m/z (ESI) $[\text{M} - \text{TBS} - \text{CH}_3 + \text{Na}]^+ 279.0$ $[\text{M} - \text{CH}_3 + \text{Na}]^+ 393.3$.

(5*S*, 6*S*, 7*R*, *Z*)-8-(Methoxymethoxy)-5,7-dimethyldodeca-3,11-dien-6-ol (36): Diene **35** (0.101g, 0.262 mmol) was dissolved in anhydrous THF (1.1 mL). *tetrabutylammoniumfluoride* (TBAF, 0.87 mL, 1 M in THF). The reaction was stirred for 3 days at room temperature. The reaction was quenched with the addition of saturated aqueous NH_4Cl (0.8 mL). The mixture was extracted with diethyl ether (2 x 2 mL). It was dried over MgSO_4 , filtered, and concentrated *in vacuo*. The crude product was purified via flash chromatography (SiO_2 , 9:1 hexane: ethyl acetate) resulting in 7.6 mg of isolated product **36** (11% yield): ^1H NMR (600 MHz, CDCl_3) δ 5.85-5.80 (m, 1 H), 5.54-5.52 (m, 1 H), 5.23, (t, $J = 10.2$ Hz, 1 H), 5.03 (d, $J = 17.0$ Hz, 1 H), 4.96 (d, $J = 10.1$ Hz, 1 H), 4.68 (dd, $J = 31.2, 6.8$ Hz, 2 H), 3.63 (dd, $J = 11.2, 5.8$ Hz, 1 H), 3.40, (s, 3 H), 2.66-2.60 (m, 1 H), 2.51 (s, 1 H), 2.12-2.06 (m, 4 H), 1.86-1.84 (m, 1 H), 1.76-1.74 (m, 1 H), 1.66-1.66 (m, 1 H), 1.00-0.94 (m, 6 H), 0.91 (d, $J = 6.7$ Hz, 3 H); ^{13}C (150 MHz, CDCl_3) δ 138.46, 133.49, 131.93, 114.67, 96.12, 81.58, 55.95, 53.48, 36.88, 35.63, 30.67, 29.66, 17.45, 14.44, 7.59; m/z (ESI) $[\text{M} + \text{Na}]^+ 293.4$, $[\text{M} + \text{K}]^+ 309.1$.

(5*S*,6*S*,7*S*,8*R*,*Z*)-8-(Methoxymethoxy)-5,7-dimethyldodeca-3,11-dien-6-yl carbamate (24): Diene **36** (31.4 mg, 0.116 mmol) was dissolved in anhydrous methylene chloride (0.24 mL).

Trichloroacetoisocyanate (14.5 μ l, 0.122 mmol) was dissolved in anhydrous benzene (0.12 mL) and added to the reaction flask at room temperature. The reaction was stirred for 3 h. After this time, the reaction mixture was diluted with DCM (5 mL) and was poured over a bed of alumina (Al_2O_3), and left for 15 min. The alumina was washed with DCM (25 mL, 10 mL) and hexane (10 mL). The organics were then evaporated, resulting in **24** (4.0 mg) in 11%. ^1H NMR (600 MHz, CDCl_3) δ 5.84-5.75 (m, 1 H), 5.40-5.30 (m, 2 H), 5.01 (d, J = 17.1 Hz, 1 H), 4.95 (d, J = 10.2 Hz, 1 H), 4.61-4.59 (m, 3 H), 3.62-3.61 (m, 1 H), 3.49 (q, J = 4.4 Hz, 1 H), 3.39 (s, 3 H), 2.73-2.71 (m, 1 H), 2.09-1.96 (m, 4 H), 1.68-1.64 (m, 3 H), 1.63-1.59 (m, 3 H), 0.99-0.94 (m, 9 H); m/z (ESI) $[\text{M} + \text{H}]^+$ 314.3, $[\text{M} + \text{Na}]^+$ 336.2.

(*R*)-4-Benzyl-3-((2*R*,3*R*)-3-hydroxy-2-methyl-3-phenylpropanoyl)oxazolidin-2-one (44):

Auxiliary **11** (6.02 g, 25.81 mmol) was dissolved in anhydrous methylene chloride (56.1 mL), and cooled to 0 $^\circ\text{C}$ in an ice bath. Dibutylboron triflate (31.0 mL, 31.0 mmol, 1M in DCM) was added to the reaction flask, followed by addition of Hunig's base (5.8 mL, 33.55 mmol). The reaction flask was moved to an acetone/dry ice bath cooled to -78 $^\circ\text{C}$, and benzaldehyde **43** (5.9 mL, 58.07 mmol) was added to the reaction flask. This was stirred for 20 min at -78 $^\circ\text{C}$, and for 1 h at 0 $^\circ\text{C}$. At this time, pH 7 phosphate buffer (37.4 mL), MeOH (56.1 mL) and 30 % H_2O_2 in MeOH (37.4 mL in 84.2 mL) were added to the reaction flask, and it was stirred an additional hour at 0 $^\circ\text{C}$. After this, the reaction flask was concentrated. The residue was extracted with diethyl ether (2 x 85 mL). The organic portions were combined, and washed with brine (2 x 85 mL). The organics were then dried over MgSO_4 , were filtered and concentrated. Purification was done by flash chromatography (SiO_2 , 9:1 hexane: ethyl acetate), yielding 5.30 g of product **44** (61%): ^1H NMR (600 MHz, CDCl_3) δ 7.39 (d, J = 7.4 Hz, 2 H), 7.33 (q, J = 7.4 Hz, 4 H) 7.28

(q, $J = 7.5$ Hz, 2 H), 7.20 (d, $J = 7.1$ Hz, 2 H), 5.10 (d, $J = 3.8$ Hz, 1 H), 4.62-4.58 (m, 1 H), 4.16-4.07 (m, 4 H), 3.24 (dd, $J = 13.4, 3.2$ Hz, 1 H), 3.09 (bs, 1 H), 2.77 (dd, $J = 13.4, 9.6$ Hz, 1 H), 1.17 (d, $J = 7.0$ Hz, 3 H); ^{13}C NMR (150 MHz, CDCl_3) δ 176.70, 152.88, 141.25, 135.00, 129.40, 128.95, 128.23, 127.52, 127.41, 126.09, 73.80, 66.13, 55.21, 44.52, 37.74, 10.89; m/z (ESI) $[\text{M} + \text{H}]^+$ 340.1, $[\text{M} + \text{Na}]^+$ 362.1.

(*R*)-4-Benzyl-3-((2*R*,3*R*)-3-((*tert*-butyldimethylsilyl)oxy)-2-methyl-3-

phenylpropanoyl)oxazolidin-2-one (45): Alcohol **44** (5.303 g, 15.63 mmol) was dissolved in anhydrous DCM (26.1 mL) and cooled to 0 °C in an ice bath. 2,6 Lutidine (2.5 mL, 21.88 mmol) was added, followed by the addition of TBDMSOTf (4.0 mL, 17.19 mmol). The reaction was stirred for 1.5 h at 0 °C. Work up was done with the addition of 1 M HCl (26 mL) and hexane (52 mL). The layers were separated, and the aqueous phase was extracted with hexane (52 mL). The organics were combined, and washed with 1 M HCl (2 x 52 mL), saturated aqueous NaHCO_3 (2 x 52 mL) and brine (52 mL). It was dried over MgSO_4 , was filtered and concentrated, resulting in 6.734 g of crude product **45** as a white solid (95%). No purification was done on the crude product: ^1H NMR (600 MHz, CDCl_3) δ 7.35 (d, $J = 7.2$ Hz, 2 H), 7.31 (t, $J = 7.2$ Hz, 2 H), 7.27 (t, $J = 7.2$ Hz, 3 H), 7.21 (t, $J = 7.2$ Hz, 1 H), 7.17 (d, $J = 7.2$ Hz, 2 H), 4.83 (d, $J = 7.2$ Hz, 1 H) 4.27-4.23 (m, 1H), 4.15 (p, $J = 6.6$ Hz, 1 H), 3.98 (dd, $J = 9, 1.8$ Hz, 1 H), 3.68 (t, $J = 8.4$ Hz, 1 H), 3.20 (dd, $J = 13.2, 3.6$ Hz, 1 H), 2.69 (dd, $J = 13.2, 9.6$ Hz, 1 H), 1.29 (d, $J = 6.6$ Hz, 3 H) 0.88 (s, 9 H), 0.01 (s, 3 H) -0.23 (s, 3 H); ^{13}C NMR (150 MHz, CDCl_3) δ 152.88, 142.85, 135.38, 129.42, 128.90, 127.86, 127.40, 127.28, 126.68, 104.43, 99.96, 96.39, 76.57, 65.86, 55.73, 46.69, 37.69, 25.72, 18.10, 12.87, -4.68, -5.28; m/z (ESI) $[\text{M} + \text{Na}]^+$ 476.0

(2*S*,3*R*)-3-((*tert*-Butyldimethylsilyl)oxy)-2-methyl-3-phenylpropan-1-ol (46): Silyl ether **45** (6.734 g, 14.84 mmol) was dissolved in anhydrous THF (118 mL), and cooled to -78 °C in an acetone/dry ice bath. Ethanol (1.3 mL, 22.26 mmol) was added to the reaction flask, followed by the addition of lithium borohydride (11.1 mL, 2M in THF). The reaction was stirred for 1 h at -78 °C, and 16.5 h at room temperature. After this time, diethyl ether (177 mL) and 1 M NaOH (59 mL) were added to the reaction flask, and the reaction was stirred for an additional 4 h. The reaction was quenched with the addition of saturated aqueous NH₄Cl (59 mL). The layers were separated, and the aqueous portion was extracted with diethyl ether (3 x 120 mL). The organics were combined, washed with brine (2 x 150 mL) and dried over Na₂SO₄. It was filtered and concentrated. The crude mixture was taken up in hot hexane: ethyl acetate (9:1) to crystalize the oxazolidinone auxiliary as a white solid (1.36 g, 52 % recovered). The mother liquor was then purified by flash chromatography (SiO₂, 9:1 hexane: ethyl acetate) to yield 2.59 g of alcohol **46** 62%. An additional 0.266 g of auxiliary was isolated with flash chromatography, totaling in 62 % recovery of auxiliary: ¹H NMR (600 MHz, CDCl₃) δ 7.33-7.26 (m, 4 H), 7.25 (t, *J* = 7.2 Hz, 1 H), 4.83 (d, *J* = 4.2 Hz, 1 H), 3.60-3.56 (m, 1 H), 3.44 (p, *J* = 5.4 Hz, 1 H), 2.44 (t, *J* = 4.8 Hz, 1 H), 2.09-2.04 (m, 1H) 0.91 (s, 9H), 0.77 (d, *J* = 7.2 Hz, 3 H), 0.05 (s, 3 H), -0.18 (s, 3 H); ¹³C NMR (150 MHz, CDCl₃) δ 142.28, 127.81, 127.10, 126.75, 77.50, 65.51, 42.82, 25.80, 18.12, 11.90, -4.69, -5.33; *m/z* (ESI) [*M* + *H*] 280.9.

(2*R*,3*R*)-3-((*tert*-Butyldimethylsilyl)oxy)-2-methyl-3-phenylpropanal (47): Alcohol **46** (2.58 g, 9.20 mmol) was dissolved in anhydrous DCM (23 mL) and DMSO (46 mL), and cooled to 0 °C in an ice bath. Triethylamine (6.1 mL, 43.61 mmol) was added, followed by sulfur trioxide-pyridine (5.43 g, 34.13 mmol). The reaction was stirred for 1.5 h at 0 °C. The reaction was

diluted with diethyl ether (115 mL). The reaction mixture was washed with H₂O (92 mL), 1 M NaHCO₃ (92 mL), H₂O (92 mL) and brine (92 mL). It was dried over MgSO₄, was filtered and concentrated, resulting in 2.758 g of crude aldehyde **47**, which was used immediately in the next reaction step: ¹H NMR (600 MHz, CDCl₃) δ 9.76 (s, 1 H), 7.34-7.27 (m, 4 H), 7.26-7.25 (m, 1 H), 5.15 (d, *J* = 4.3 Hz, 1 H), 2.61-2.56 (m, 1 H), 1.04 (d, *J* = 7.0 Hz, 3 H), 0.89 (s, 9 H), 0.03 (s, 3 H), -0.18 (s, 3 H).

(1*R*,2*S*)-1-((*tert*-Butyldimethylsilyl)oxy)-2-methyl-1-phenylhept-6-en-3-ol (48): Magnesium turnings (0.738 g, 30.36 mmol) and a crystal of I₂ were placed in a round bottom flask. 4-bromo-1-butene (2.8 mL, 27.60 mmol) was dissolved in anhydrous THF (27.6 mL). This solution was added slowly to the flask containing turnings. The formation of the Grignard reagent was stirred for 1 h at room temperature. In the meantime, Aldehyde **47** (2.562 g, 9.20 mmol) was dissolved in anhydrous THF (76.7 mL). The Grignard reagent was added to the aldehyde solution cooled to 0 °C. The reaction was stirred an hour at 0 °C. Work up was done by quenching the reaction with saturated NH₄Cl (46 mL). The mixture was extracted with EtOAc (3 x 93 mL). The organics were combined and washed with brine (93 mL). The organic portion was dried over Na₂SO₄, filtered and concentrated. Purification was done by flash chromatography (SiO₂, 19:1 hexane: ethyl acetate), yielding 1.98 g (64 %) of both diastereomers **48** (3.5:1 *Z/E*): ¹H NMR (600 MHz, CDCl₃) δ 7.32-7.29 (m, 3 H), 7.27-7.26 (m, 1 H), 7.25-7.22 (m, 1 H), 5.83-5.78 (m, 1 H), 5.00 (d, *J* = 17.1 Hz, 1 H), 4.94 (d, *J* = 11.2 Hz, 1 H), 4.81 (d, *J* = 4.7 Hz, 1 H), 3.74-3.70 (m, 1 H), 2.34 (s, 1 H), 2.16-2.08 (m, 1 H), 2.06-2.00 (m, 1 H), 1.68-1.65 (m, 1 H), 1.45-1.42 (m, 1 H), 0.91 (s, 9 H), 0.88 (d, *J* = 6.8 Hz, 3 H), 0.07 (s, 3 H), -0.27 (s, 3H); ¹³C NMR (150 MHz,

CDCl₃) δ 143.58, 138.47, 127.91, 127.07, 126.41, 114.63, 79.45, 73.50, 45.29, 34.47, 30.39, 25.85, 18.04, 6.47, -4.42, -5.20; m/z (ESI) $[M + H]^+$ 335.2.

(6*S*,7*R*)-5-(But-3-en-1-yl)-6,9,9,10,10-pentamethyl-7-phenyl-2,4,8-trioxa-9-silaundecane

(49): Chloromethoxymethane (0.88 mL, 11.56 mmol) was added to a round bottom flask. Alcohol **48** (1.935 g, 5.78 mmol) was dissolved in anhydrous toluene (5.5 mL) and added to the reaction flask. Hunig's base (1.3 mL, 7.23 mmol) was added to the reaction flask, and the reaction was stirred for 3 hours at room temperature. Work up was done by diluting the reaction mixture with ethyl acetate (8 mL), followed by quenching the reaction with saturated NH₄Cl (8 mL). The layers were separated, and the aqueous was extracted with EtOAc (2 x 17 mL). The organics were combined, and washed with saturated aqueous NaHCO₃ (2 x 17 mL) and brine (2 x 17 mL). The organics were dried over MgSO₄, filtered and concentrated. The residue was purified by flash chromatography (SiO₂, 19:1 hexane: ethyl acetate) yielding 1.61 g of **49** (74 %): ¹H NMR (600 MHz, CDCl₃) δ 7.32-7.28 (m, 4 H), 7.28-7.21 (m, 1 H), 5.70-5.61 (m, 1 H), 4.90 (d, J = 18.8 Hz, 1 H), 4.85 (d, J = 10.1 Hz, 1 H), 4.60 (d, J = 7.3 Hz, 1 H), 4.58 (d, J = 6.8 Hz, 1 H), 4.55 (d, J = 6.8 Hz, 1 H), 3.39 (s, 3 H), 3.18-3.16 (m, 1 H), 1.95-1.91 (m, 2 H), 1.84 (td, J = 7.0, 3.3 Hz, 1 H), 1.68-1.64 (m, 1 H), 1.63-1.58 (m, 1 H), 1.05 (d, J = 6.9 Hz, 3 H), 0.85 (s, 9 H), 0.02 (s, 3 H), -0.29 (s, 3 H); ¹³C NMR (150 MHz, CDCl₃) δ 144.59, 138.22, 127.88, 127.11, 126.55, 114.56, 96.88, 79.27, 76.43, 55.58, 44.89, 31.99, 29.84, 25.84, 18.13, 9.90, -4.42, -4.96; m/z (ESI) $[M + H]^+$ 379.2, $[M + K]^+$ 418.2

(1*R*,2*R*)-3-(Methoxymethoxy)-2-methyl-1-phenylhept-6-en-1-ol (50): Diether **49** (0.387 g, 1.02 mmol) was dissolved in anhydrous THF (4.1 mL) and cooled to 0 °C in an ice bath. TBAF

(2.04 mL, 1M in THF) was added, and the reaction was stirred for 5 minutes at 0 °C, and 6 h at room temperature. After this, the reaction was quenched with saturated NH₄Cl (2.5 mL). This mixture was extracted with diethyl ether (2 x 5 mL). The organics were combined, and dried over MgSO₄. This was filtered off, and the solvent was concentrated. Purification was done by flash chromatography (SiO₂, 19:1 hexane: ethyl acetate) yielding 0.170 g of **50** (63 %): ¹H NMR (600 MHz, CDCl₃) δ 7.35-7.33 (m, 4 H), 7.26-7.24 (m, 1 H), 5.81-5.76 (m, 1 H), 5.02 (d, *J* = 17.1 Hz, 1 H), 4.97 (d, *J* = 10.4 Hz, 1 H), 4.94 (s, 1 H), 4.76 (d, *J* = 6.7 Hz, 1 H), 4.66 (d, *J* = 6.7 Hz, 1 H), 3.79-3.77 (m, 1 H), 3.43 (s, 3 H), 3.22 (s, 1 H), 2.05-2.03 (m, 2 H), 1.94-1.92 (m, 1 H), 1.83-1.80 (m, 1 H), 1.64-1.61 (m, 1 H), 0.90 (d, *J* = 7.0 Hz, 3 H); ¹³C NMR (150 MHz, CDCl₃) δ 143.70, 137.87, 128.09, 126.94, 125.91, 114.98, 95.86, 81.63, 55.93, 42.36, 30.84, 29.89, 9.94, 5.95; *m/z* (ESI) [M + H]⁺ 265.2, [M + Na]⁺ 287.0.

(1*R*,2*S*)-3-(Methoxymethoxy)-2-methyl-1-phenylhept-6-en-1-yl carbamate (20): Alcohol **50** was dissolved in anhydrous DCM (1.3 mL). Trichloroacetoisocyanate (83 μl, 0.699 mmol) was dissolved in anhydrous benzene (0.7 mL) and added to the reaction flask. The reaction was stirred for 1 h at room temperature. After this, the reaction mixture was diluted with DCM (5 mL) and poured over a pad of alumina. After 5 minutes, the alumina was washed with DCM (25 mL, 10 mL) and then the organics were concentrated *in vacuo*. Purification was done by flash chromatography (SiO₂, 3:1 hexane: ethyl acetate) yielding 0.119 g of **20** (52 %): ¹H NMR (600 MHz, CDCl₃) δ 7.35-7.30 (m, 4 H), 7.28-7.26 (m, 1 H), 5.74 (d, *J* = 7.3 Hz, 1 H), 5.73-5.70 (m, 1 H), 4.95 (d, *J* = 17.0 Hz, 1 H), 4.90 (d, *J* = 10.1 Hz, 1 H), 4.66 (bs, 2 H), 4.60 (d, *J* = 6.8 Hz, 1 H), 4.51 (d, *J* = 6.9 Hz, 1 H), 3.40 (s, 3 H), 3.26-2.24 (m, 1 H), 2.12 (td, *J* = 7.0, 3.4 Hz, 1 H), 2.00 (q, *J* = 7.3 Hz, 2 H), 1.71-1.67 (m, 1 H), 1.64-1.59 (m, 1 H), 1.03 (d, *J* = 6.8 Hz, 3 H); ¹³C

NMR (150 MHz, CDCl₃) δ 156.14, 138.08, 128.35, 126.92, 114.82, 101.16, 98.77, 96.78, 78.96, 77.81, 55.75, 41.75, 31.39, 9.64; m/z (ESI) [M + H]⁺ 308.1, [M + Na]⁺ 330.2.

7-(Hydroxymethyl)-2H-chromen-2-one (53): 7-(Bromomethyl)-2H-chromen-2-one **52** (0.250 g, 1.05 mmol) was dissolved in H₂O (10.5 mL) and THF (10.5 mL). It was heated at reflux overnight. Work-up was done by extracting the reaction mixture with methylene chloride (2 x 10 mL). The organic portions were combined, and washed with saturated aqueous NaHCO₃ (10 mL) and brine (10 mL). The organic portion was then dried over MgSO₄, filtered and was concentrated *in vacuo*. Purification of the crude mixture was done by flash chromatography (SiO₂, 3:1 hexane: ethyl acetate) yielding 0.237 g of product **53**: ¹H NMR (600 MHz, CDCl₃) δ 7.70 (d, J = 9.5 Hz, 1 H), 7.47 (d, J = 7.9 Hz, 1 H), 7.36 (s, 1 H), 7.29 (d, J = 7.0 Hz, 1 H), 6.41 (d, J = 9.5 Hz, 1 H), 4.82 (d, J = 5.8 Hz, 2 H).

2-Oxo-2H-chromene-7-carbaldehyde (54): Alcohol **53** (0.237 g, 1.34 mmol) was dissolved in anhydrous methylene chloride (3.4 mL) and DMSO (6.7 mL). The reaction flask was cooled to 0 °C in an ice bath. Triethylamine (0.89 mL, 6.35 mmol) was added, followed by the addition Sulfur trioxide-pyridine (0.79 g, 4.97). The reaction was stirred for 1.5 h. Work-up was begun by addition of diethyl ether (17 mL). The reaction mixture was then washed with H₂O (14 mL), saturated aqueous NaHCO₃ (14 mL), H₂O (14 mL), and brine (14 mL). The organic portion was then dried over MgSO₄, was filtered and concentrated *in vacuo*, resulting in 0.154 g of the crude aldehyde **54** (66%): ¹H NMR (600 MHz, CDCl₃) δ 10.09 (s, 1 H), 7.81 (d, J = 7.2 Hz, 2 H), 7.76 (d, J = 9.8 Hz, 1 H), 7.65 (d, J = 8.1 Hz, 1 H), 6.57 (d, J = 9.5 Hz, 1 H).

7-Vinyl-2H-chromen-2-one (15): Methyltriphenylphosphonium bromide (1.04 g, 2.88 mmol) was suspended in anhydrous THF (6.8 mL). This reaction flask was cooled to -78 °C in an acetone/dry ice bath. *n*Butyl Lithium (1.8 mL, 2.88 mmol, 1.6 M in hexane) was added to the flask. The acetone/dry ice bath was removed, and the reaction was stirred for 3 h at room temperature. In the meantime, aldehyde **54** (0.154 g, 0.883 mmol) was dissolved in anhydrous THF (4.4 mL). It was cooled in an ice bath to 0 °C, and the methyl ylide was added to the aldehyde flask. The reaction was allowed to stir overnight, gradually warming to room temperature. The reaction was quenched with the addition of saturated aqueous NH₄Cl (1.8 mL). The reaction was diluted with hexane (13.5 mL), and washed with H₂O (2x 13.5 mL) and brine (13.5 mL). The aqueous portions were combined and extracted once with hexane (13.5 mL). The organics were combined, dried over MgSO₄, filtered and concentrated *in vacuo*. The crude reaction mixture was purified by flash chromatography (SiO₂, 9:1 hexane: ethyl acetate), resulting in 25 mg of isolated **15** (16%): ¹H NMR (600 MHz, CDCl₃) δ 7.68 (d, *J* = 9.5 Hz, 1 H), 7.43 (d, *J* = 8.5 Hz, 1 H), 7.34 (s, 1 H), 7.34 (d, *J* = 7.1 Hz, 1 H), 6.75 (dd, *J* = 17.5, 10.9 Hz, 1 H), 6.39 (d, *J* = 9.5 Hz, 1 H), 5.88 (d, *J* = 17.5 Hz, 1 H), 5.43 (d, *J* = 10.9 Hz, 1 H).

3-(3-Methoxyphenyl)propanal (56): Alcohol **55** (0.549 g, 3.30 mmol) was dissolved in anhydrous methylene chloride (8.3 mL) and DMSO (16.5 mL). The reaction was cooled to 0 °C in an ice bath. Triethylamine (2.2 mL, 15.64 mmol) was added to the reaction flask, followed by addition of sulfur trioxide-pyridine (1.95 g, 12.24 mmol). The reaction was stirred for 1.5 h at 0 °C. Work up was done with addition of diethyl ether (42 mL). The reaction mixture was washed with H₂O (33 mL), saturated NaHCO₃ (33 mL), H₂O (33 mL) and brine (33 mL). The organic phase was then dried over MgSO₄, filtered, and concentrated *in vacuo*, resulting 0.419 g

of crude aldehyde **56** (77%): ^1H NMR (600 MHz, CDCl_3) δ 9.81 (s, 1 H), 7.19 (m, 1 H), 6.76 (m, 3 H), 3.78 (s, 3 H), 2.93 (t, $J = 7.5$ Hz, 1 H), 2.77 (t, $J = 7.8$ Hz, 1 H) 2.67 (m, 1 H), 1.90 (m, 1 H).

1-(But-3-en-1-yl)-3-methoxybenzene (22): Methyltriphenylphosphonium bromide (3.00 g, 8.42 mmol) was suspended in anhydrous THF (20 mL). The reaction flask was cooled to -78°C in an acetone/dry ice bath. *n*Butyl lithium (5.3 mL, 8.48 mmol, 1.6 M in THF) was added and the mixture was stirred for 3 h, turning orange in color. Crude aldehyde **56** (0.419 g, 2.55 mmol) was then dissolved in anhydrous THF (13 mL), and cooled to 0°C . The orange ylide mixture was added to the aldehyde flask, and the reaction was stirred overnight, gradually warming to room temperature. The reaction was quenched by the addition of saturated aqueous NH_4Cl (5.3 mL). The reaction was diluted hexane (40 mL). This was then washed with H_2O (2 x 40 mL) and brine (2 x 40 mL). The aqueous portions were combined, and extracted once with hexane (40 mL). The organics were combined, dried over MgSO_4 , filtered and concentrated *in vacuo*. The product was purified by flash chromatography (SiO_2 , 19:1 hexane: ethyl acetate) yielding 0.207 g of product **22** at 50 % yield as a colorless oil: ^1H NMR (600 MHz, CDCl_3) δ 7.21 (t, $J = 7.7$ Hz, 1 H), 6.80 (d, $J = 7.5$ Hz, 1 H), 6.76 (s, 1 H), 6.76 (d, $J = 8.4$ Hz, 1 H), 5.88 (m, 1 H), 5.07 (d, $J = 17.2$, 1 H), 4.99 (d, $J = 10.3$ Hz, 1 H), 3.81 (s, 3 H), 2.71 (t, $J = 7.6$ Hz, 2 H), 2.39 (dd, $J = 15.0$, 6.8 Hz, 2 H).

(3R,4S,5S)-6-Allyl-4-((tert-butyldimethylsilyl)oxy)-3,5-dimethyltetrahydro-2H-pyran-2-one (23): Aldehyde **31** (0.656 g, 2.07 mmol) was dissolved in anhydrous DCM (19.7 mL) and cooled to -78°C . Titanium tetrachloride (0.23 mL, 2.11 mmol) was dissolved in anhydrous DCM (2.11

mL) and added drop-wise to the reaction flask. This was followed by addition of allyltrimethylsilane (0.43 mL, 2.69 mmol). The reaction was allowed to warm gradually to -20 °C over 3 hours and 40 minutes. A 2nd aliquot of allyltrimethylsilane (0.33 mL, 2.07 mmol) was added at this point, and the reaction was allowed to warm to 0 °C over 2 hours. The reaction was quenched at this point by addition of saturated aqueous NaHCO₃ (16.4 mL) and was extracted with DCM (4 x 16 mL). The organics were combined, and trifluoroacetic acid (0.33 mL) was added to the organic phase. This was shaken vigorously, and was then washed with saturated aqueous NaHCO₃ (2 x 30 mL) and brine (2 x 30 mL). This was then dried over MgSO₄, was filtered, and concentrated *in vacuo*. Purification was done via flash chromatography (SiO₂, 19:1 hexane: ethyl acetate) yielding 0.240 g of **23** (39%) as a mixture of two diastereomers: ¹H NMR (600 MHz, CDCl₃) δ 5.86 (m, 1 H), 5.17 (d, *J* = 6.5 Hz, 1 H), 5.15 (s, 1 H), 4.42 (m, 1 H), 3.66 (t, *J* = 2.5, 1 H), 2.63 (qd, *J* = 7.62, 2.9 Hz, 1 H), 2.56 (dt, *J* = 14.9, 4.7 Hz, 1 H), 2.30 (m, 1 H), 1.96 (m, 1 H), 1.25 (d, *J* = 7.6 Hz, 3 H), 0.98 (d, *J* = 6.8 Hz, 3 H), 0.88 (s, 9 H), 0.07 (d, *J* = 7.5 Hz, 6 H); ¹³C NMR (150 MHz, CDCl₃) δ 174.14, 132.56, 118.58, 80.12, 74.47, 43.94, 36.95, 32.42, 25.70, 17.95, 16.32, 13.62, -4.53, -4.82.

(1*R*,2*S*,*E*)-8-((3*S*,4*S*,5*R*)-4-((*tert*-butyldimethylsilyl)oxy)-3,5-dimethyl-6-oxotetrahydro-2*H*-pyran-2-yl)-3-(methoxymethoxy)-2-methyl-1-phenyloct-6-en-1-yl carbamate (57):

Carbamate **20** (29.2 mg, 0.0950 mmol) and lactone **23** (42.5 mg, 0.1425 mmol) were dissolved in anhydrous methylene chloride (1.9 mL). Grubbs II ruthenium catalyst (8.1 mg, 0.00950 mmol) was dissolved in DCM (0.48 mL), and then added to the reaction flask. A reflux condenser was attached, and the reaction was heated at reflux for 7 h. After this, the heating was stopped, and the DCM was evaporated from the reaction mixture. The residue was purified by flash

chromatography, (SiO₂, 3:1 hexane: ethyl acetate) to yield 13 mg of **57** (24%): ¹H NMR (600 MHz, CDCl₃) δ 7.34-7.27 (m, 5 H), 5.76 (d, *J* = 6.8 Hz, 1 H), 5.48-5.46 (m, 2 H), 4.65 (bs, 2 H), 4.56 (dd, *J* = 39.4, 6.8 Hz, 2 H), 3.64 (t, *J* = 2.4 Hz, 1 H), 3.39 (s, 3 H), 3.28-3.23 (m, 1 H), 2.64 (qd, *J* = 7.7, 2.9 Hz, 1 H), 2.46-2.42 (m, 1 H), 2.21-2.14 (m, 1 H), 2.13-2.08 (m, 1 H), 2.06-1.96 (m, 2 H), 1.96-1.90 (m, 1 H), 1.66-1.58 (m, 3 H), 1.24 (d, *J* = 7.7 Hz, 3 H), 0.99 (d, *J* = 6.8 Hz, 3 H), 0.96 (d, *J* = 6.7 Hz, 3 H), 0.88 (s, 9 H), 0.06 (d, *J* = 7.1 Hz, 6 H); ¹³C NMR (150 MHz, CDCl₃) 174.31, 156.08, 140.36, 133.85, 128.25, 126.79, 126.67, 124.14, 96.72, 80.54, 79.24, 79.17, 65.84, 55.76, 43.90, 42.09, 32.61, 31.77, 25.77, 25.62, 17.95, 16.27, 15.27, 13.76, 9.66, -4.55, -4.81; *m/z* (ESI) [M + H]⁺ 578.2, [M + Na]⁺ 600.2.

(1*R*,2*S*,*E*)-8-((3*R*,4*S*,5*R*)-4-Hydroxy-3,5-dimethyl-6-oxotetrahydro-2*H*-pyran-2-yl)-3-

(methoxymethoxy)-2-methyl-1-phenyloct-6-en-1-yl carbamate (58**):** Analogue **57** (10.8 mg, 0.0187 mmol) was dissolved in MeOH (4.7 mL). HCl (4.7 mL, 4 M in H₂O) was added to the reaction flask, and the reaction was stirred for 14 h. After this time, the reaction was diluted with H₂O (10 mL) and poured into a separating funnel containing ethyl acetate (15 mL). The acid was neutralized with the addition of saturated aqueous NaHCO₃. The aqueous was then extracted with EtOAc (3 x 10 mL). The organics were combined, washed with brine (10 mL) and dried over MgSO₄. This was filtered and then concentrated *in vacuo*. The crude mixture was purified by flash chromatography (SiO₂, 3% MeOH in methylene chloride) to yield **58** (60%) and **59** (54%): ¹H NMR (600 MHz, CDCl₃) δ 7.33-7.27 (m, 5 H), 5.76 (d, *J* = 6.7 Hz, 1 H), 5.48-5.46 (m, 2 H), 4.70 (bs, 2 H), 4.56 (dd, *J* = 38.2, 6.9 Hz, 2 H), 4.36-4.32 (m, 1 H), 3.72 (bs, 1 H), 3.40 (s, 3 H), 3.26 (td, *J* = 6.3, 3.7 Hz, 1 H), 2.68 (qd, *J* = 7.2, 4.5 Hz, 1 H), 2.41 (dt, *J* = 14.0, 4.3 Hz, 1 H), 2.25-2.19 (m, 1 H), 2.11 (td, *J* = 6.8, 3.2, 1 H), 2.00-1.90 (m, 4 H), 1.66-1.62 (m, 2 H), 1.30

(d, $J = 7.3$ Hz, 3 H), 1.04 (d, $J = 6.9$, 3 H), 1.02 (d, $J = 6.9$ Hz, 3 H); ^{13}C NMR (150 MHz, CDCl_3) δ 156.09, 133.90, 128.34, 127.68, 126.73, 124.19, 99.97, 98.77, 96.70, 79.97, 79.11, 73.20, 55.80, 43.09, 41.93, 35.69, 33.92, 31.75, 29.70, 28.69, 15.65, 12.41, 9.71; m/z (ESI) $[\text{M} + \text{H}]^+ 464.2$, $[\text{M} + \text{Na}]^+ 486.1$, $[\text{M} - \text{H}]^- 462.1$.

(1*R*,2*S*,*E*)-3-Hydroxy-8-((3*R*,4*S*,5*R*)-4-hydroxy-3,5-dimethyl-6-oxotetrahydro-2*H*-pyran-2-yl)-2-methyl-1-phenyloct-6-en-1-yl carbamate (59): ^1H NMR (600 MHz, CDCl_3) 7.34-7.28 (m, 5 H), 5.75 (d, $J = 6.4$ Hz, 1 H), 5.51-5.49 (m, 2 H), 4.74 (bs, 2 H), 4.35-4.31 (m, 1 H), 3.73 (t, $J = 3.4$ Hz, 1 H), 3.51-3.49 (m, 1 H), 2.67 (qd, $J = 7.4, 3.9$ Hz, 1 H), 2.44 (dt, $J = 14.5, 5.6$ Hz, 1 H), 2.25-2.19 (m, 1 H), 2.12-2.08 (m, 2 H), 1.98-1.90 (m, 2 H), 1.64-1.48 (m, 4 H), 1.30 (d, $J = 7.4$ Hz, 3 H), 1.05 (d, $J = 6.8$ Hz, 3 H), 0.98 (d, $J = 6.8$ Hz, 3 H); ^{13}C NMR (150 MHz, CDCl_3) δ 139.98, 133.92, 128.39, 128.34, 127.68, 126.40, 124.38, 120.35, 104.34, 98.77, 79.96, 78.67, 73.38, 71.37, 44.04, 43.25, 35.61, 34.42, 33.80, 29.70, 29.12, 15.82, 12.50, 8.58; m/z (ESI) $[\text{M} + \text{H}]^+ 420.3$, $[\text{M} + \text{Na}]^+ 442.0$, $[\text{M} - \text{H}]^- 418.2$.

(1*R*,2*S*,*E*)-3-(Methoxymethoxy)-2-methyl-7-(2-oxo-2*H*-chromen-7-yl)-1-phenylhept-6-en-1-yl carbamate 21: Carbamate **20** (30 mg, 0.0976 mmol) and lactone **15** (25mg, 0.117 mmol) were dissolved in anhydrous methylene chloride (1.6 mL). Grubbs II catalyst (8.3 mg, 0.00976 mmol) was dissolved in DCM (0.41 mL) and added to the reaction flask. The reaction was heated at reflux for 10 hours. After this, the DCM was evaporated, and the residue was purified by flash chromatography (SiO_2 , 2:1 hexane: ethyl acetate) to yield 16.6 mg of **21** (38%): ^1H NMR (600 MHz, CDCl_3) δ 7.66 (d, $J = 9.5$ Hz, 1 H), 7.38 (d, $J = 8.5$ Hz, 1 H), 7.32-7.28 (m, 5 H), 7.20 (s, 2 H), 6.36 (d, $J = 9.5$ Hz, 1 H), 6.35 (d, $J = 16.1$ Hz, 1 H), 6.28-6.24 (m, 1 H), 5.76

(d, $J = 7.4$ Hz, 1 H), 4.62 (bs, 2 H), 4.58 (dd, $J = 52.7, 6.9$ Hz, 2 H), 3.41 (s, 3 H), 3.30-3.27 (m, 1 H), 2.22 (q, $J = 3.4$ Hz, 2 H), 2.14 (td, $J = 7.1, 3.4$ Hz, 1 H), 1.81-1.73 (m, 2 H), 1.06 (d, $J = 6.8$ Hz, 3 H); ^{13}C NMR (150 MHz, CDCl_3) 161.01, 155.99, 154.46, 143.12, 141.66, 140.12, 133.86, 129.05, 128.39, 127.87, 127.79, 126.90, 122.18, 117.58, 115.70, 113.79, 104.34, 98.77, 96.91, 78.91, 77.74, 60.39, 55.82, 41.89, 31.64, 29.24, 14.19, 9.72; m/z (ESI) $[\text{M} + \text{Na}]^+$ 474.1.

(1*R*,2*S*,*E*)-3-Hydroxy-2-methyl-7-(2-oxo-2*H*-chromen-7-yl)-1-phenylhept-6-en-1-yl

carbamate (60): Analogue **21** (5.8 mg, 0.0128 mmol) was dissolved in MeOH (3.2 mL). HCl (3.2 mL, 6 M in H_2O) was added in 0.2 mL aliquots over 4 hours. The reaction was then stirred for an additional 21 hours. Work up was done by diluting the reaction mixture with H_2O (6 mL). This was then poured into a separating funnel containing ethyl acetate (9 mL). The acid was neutralized by addition of saturated aqueous NaHCO_3 . The aqueous portion was then extracted with ethyl acetate (3 x 6 mL). The organics were combined and washed with brine (6 mL). The organics were then dried over MgSO_4 , was filtered and concentrated. The crude mixture was purified by flash chromatography (SiO_2 , 3 % MeOH in DCM) to yield **60** (1.6 mg, 31%): ^1H NMR (600 MHz, CDCl_3) δ 7.66 (d, $J = 9.5$ Hz, 1 H), 7.38 (d, $J = 8.5$ Hz, 1 H), 7.34-7.28 (m, 5 H), 6.40-6.35 (m, 3 H), 5.74 (d, $J =$, 1 H), 4.63 (bs, 2 H), 3.54-3.52 (m, 1 H), 2.36-2.31 (m, 1 H), 2.28-2.21 (m, 1 H), 2.01-1.94 (m, 1H), 1.70-1.65 (m, 1 H), 1.65-1.62 (m, 2 H), 1.04 (d, $J = 6.8$ Hz, 3 H); m/z (ESI) $[\text{M} + \text{Na}]^+$ 430.2, $[\text{M} - \text{H}]^-$ 406.2.

(1*R*,2*S*,*E*)-3-(Methoxymethoxy)-9-(4-methoxyphenyl)-2-methyl-1-phenylnon-6-en-1-yl

carbamate (61): Carbamate **20** (25 mg, 0.0813 mmol) and lactone **22** (15.8 mg, 0.0976 mmol) were dissolved in anhydrous methylene chloride (1.6 mL). Grubbs II catalyst (6.9 mg, 0.00813

mmmol) was dissolved in anhydrous DCM (0.41 mL) and added to the reaction flask. The reaction was refluxed for 10 hours. After this, the DCM was evaporated, and the residue was purified by flash chromatography (SiO₂, 4:1 hexane: ethyl acetate) to yield 12 mg of **61** (33%): ¹H NMR (600 MHz, CDCl₃) δ 7.33-7.28 (m, 5 H), 7.23-7.18 (m, 1 H), 6.77-6.72 (m, 3 H), 5.73 (d, *J* = 7.5 Hz, 1 H), 5.37-5.34 (m, 2 H), 4.58 (bs, 2 H), 4.54 (dd, *J* = 50.7, 6.9 Hz, 2 H), 3.80 (s, 3 H), 3.37 (s, 3 H), 3.22 (td, *J* = 6.4, 3.2 Hz, 1 H), 2.59 (t, *J* = 7.5 Hz, 2 H), 2.24 (q, *J* = 6.9 Hz, 2 H), 2.09 (td, *J* = 7.1, 3.2 Hz, 1 H), 1.92 (q, *J* = 7.3 Hz, 2 H), 1.64-1.63 (m, 2 H), 1.02 (d, *J* = 6.8 Hz, 3 H); ¹³C NMR (150 MHz, CDCl₃) δ 159.52, 156.04, 143.72, 140.25, 130.03, 129.92, 129.18, 128.33, 127.77, 126.96, 120.87, 114.24, 110.91, 101.95, 101.16, 96.76, 94.79, 78.89, 77.88, 55.74, 55.11, 41.71, 35.98, 34.17, 32.01, 28.58, 9.65, 1.00; *m/z* (ESI) [M + Na]⁺ 464.1.

(1*R*,2*S*,*E*)-3-Hydroxy-9-(4-methoxyphenyl)-2-methyl-1-phenylnon-6-en-1-yl carbamate

(62): Analogue **61** (5.9 mg, 0.0128 mmol) was dissolved in MeOH (3.4 mL). HCl (3.4 mL, 6 M in H₂O) was added in 0.2 mL aliquots over 2.5 h. The reaction was then stirred for an additional 20 hours. Work up was done by diluting the reaction mixture with H₂O (7 mL). This was then poured into a separating funnel containing ethyl acetate (10.5 mL). The acid was neutralized by addition of saturated aqueous NaHCO₃. The aqueous portion was then extracted with ethyl acetate (3 x 10 mL). The organics were combined and washed with brine (10 mL). The organics were then dried over MgSO₄, was filtered and concentrated. The crude mixture was purified by flash chromatography (SiO₂, 1 % MeOH in DCM) to yield **62** (1.5 mg, 29%): ¹H NMR (600 MHz, MeOD) δ 7.34-7.28 (m, 4 H), 7.26-7.24 (m, 1 H), 7.15 (t, *J* = 7.7 Hz, 1 H), 6.72-6.70 (m, 3 H), 5.61 (d, *J* = 7.9 Hz, 1 H), 5.39-5.34 (m, 2 H), 3.77 (s, 3 H), 2.54 (t, *J* = 7.6 Hz, 2 H), 2.19 (q, *J* = 6.9 Hz, 2 H), 2.01-1.98 (m, 1 H), 1.92-1.87 (m, 2 H), 1.51-1.45 (m, 2 H), 1.31-1.27 (m, 3 H),

1.00 (d, $J = 6.8$ Hz, 3 H); ^{13}C NMR (150 MHz, MeOD) δ 161.12, 144.93, 142.19, 131.28, 131.11, 130.19, 129.23, 128.59, 127.99, 121.88, 115.19, 112.05, 81.40, 79.39, 71.24, 55.53, 45.46, 37.18, 35.88, 35.59, 29.95, 9.57; m/z (ESI) $[\text{M} + \text{Na}]^+ 420.1$, $[\text{M} - \text{H}]^- 395.8$.

APPENDIX 1

SPECTRA OF NEW COMPOUNDS

EXPNO	1
PROCNO	1

1.11116	10.20
INSTRUM	spect

PULPROG Zg30

NS	16

SWH	12376.237
FTDPES	0 188846

RG 18

[illegible]

TD0 1

-----	CHANNEL 11	----
NUC1		1H

PLT	4.00
PLT	4.00

210-	000 • 400	0000
SI		32768

WDW	EM
0.00	0.00
0.01	0.01
0.02	0.02
0.03	0.03
0.04	0.04
0.05	0.05
0.06	0.06
0.07	0.07
0.08	0.08
0.09	0.09
0.10	0.10
0.11	0.11
0.12	0.12
0.13	0.13
0.14	0.14
0.15	0.15
0.16	0.16
0.17	0.17
0.18	0.18
0.19	0.19
0.20	0.20
0.21	0.21
0.22	0.22
0.23	0.23
0.24	0.24
0.25	0.25
0.26	0.26
0.27	0.27
0.28	0.28
0.29	0.29
0.30	0.30
0.31	0.31
0.32	0.32
0.33	0.33
0.34	0.34
0.35	0.35
0.36	0.36
0.37	0.37
0.38	0.38
0.39	0.39
0.40	0.40
0.41	0.41
0.42	0.42
0.43	0.43
0.44	0.44
0.45	0.45
0.46	0.46
0.47	0.47
0.48	0.48
0.49	0.49
0.50	0.50
0.51	0.51
0.52	0.52
0.53	0.53
0.54	0.54
0.55	0.55
0.56	0.56
0.57	0.57
0.58	0.58
0.59	0.59
0.60	0.60
0.61	0.61
0.62	0.62
0.63	0.63
0.64	0.64
0.65	0.65
0.66	0.66
0.67	0.67
0.68	0.68
0.69	0.69
0.70	0.70
0.71	0.71
0.72	0.72
0.73	0.73
0.74	0.74
0.75	0.75
0.76	0.76
0.77	0.77
0.78	0.78
0.79	0.79
0.80	0.80
0.81	0.81
0.82	0.82
0.83	0.83
0.84	0.84
0.85	0.85
0.86	0.86
0.87	0.87
0.88	0.88
0.89	0.89
0.90	0.90
0.91	0.91
0.92	0.92
0.93	0.93
0.94	0.94
0.95	0.95
0.96	0.96
0.97	0.97
0.98	0.98
0.99	0.99
1.00	1.00

0 GB

1

7.260

5.478

5.461

5.444

5.361

5.348

3.876

3.862

3.648

3.129

2.902

2.604

2.592

2.579

2.016

2.004

1.992

1.981

1.931

1.930

1.918

1.907

1.906

1.895

1.119

1.107

0.977

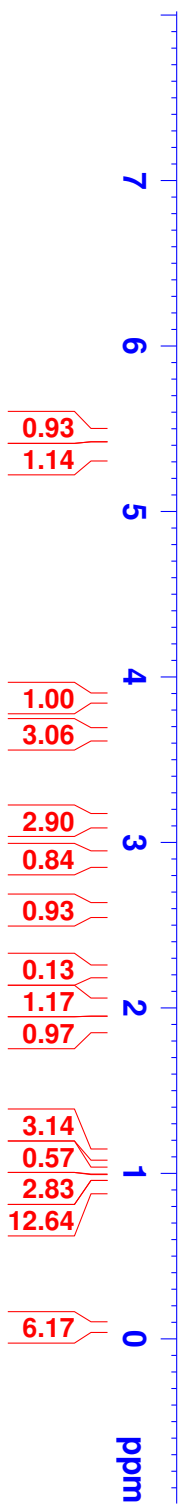
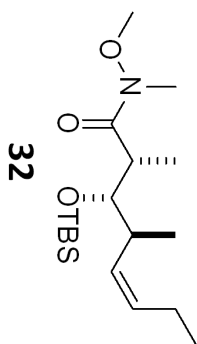
0.965

0.918

0.915

0.084

0.071



DMB1-153f6-15 carbon

177.33

132.06
130.69
130.39

77.38
77.16
77.04
76.95

61.29

40.45
39.37
36.35
32.25
26.33
26.28
25.90
20.90
19.43
18.58
18.54
15.67
14.53

-3.33
-3.40



NAME DMB1-153f6

EXPNO 3

PROCNO 1

Date_ 20100816

Time 9.34

INSTRUM spect

PROBHD 5 mm CPTCI 1H-

PULPROG zgpg30

TD 65536

SOLVENT CDCl3

NS 528

DS 2

SWH 35971.223 Hz

FIDRES 0.548877 Hz

AQ 0.9110143 sec

RG 14596.5

DW 13.900 usec

DE 6.50 usec

TE 289.0 K

D1 2.00000000 sec

D11 0.03000000 sec

TD0 1

===== CHANNEL f1 =====

NUC1 13C

P1 12.00 usec

PL1 -0.70 dB

PL1W 82.63385773 W

SFO1 150.9178988 MHz

===== CHANNEL f2 =====

CPDPRG2 waltz16

NUC2 1H

PCPD2 80.00 usec

PL2 4.00 dB

PL12 24.00 dB

PL13 27.00 dB

PL2W 7.00000000 W

PL12W 0.07000000 W

PL13W 0.03508311 W

SFO2 600.1324005 MHz

SI 32768

SF 150.9027942 MHz

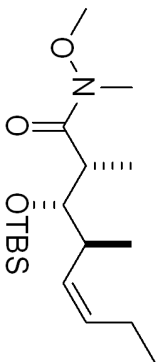
WDW EM

SSB 0

LB 1.00 Hz

GB 0

PC 1.40

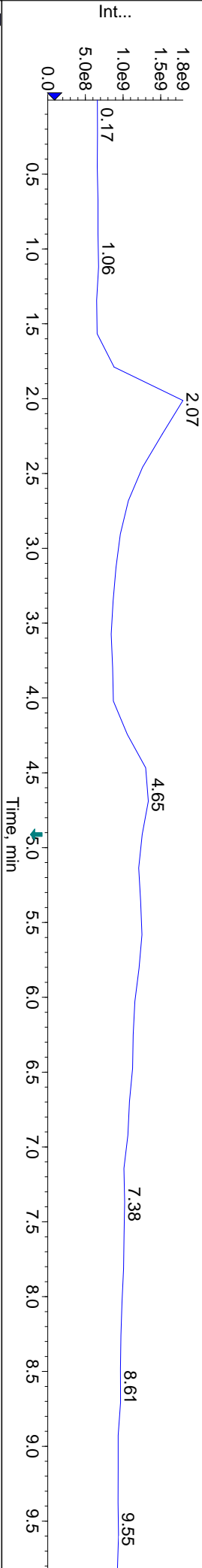


32



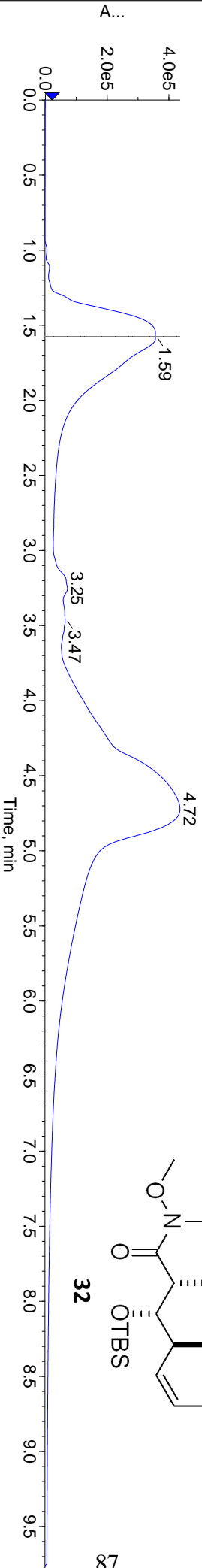
TIC: from Sample 1 (DMB) of DMB10.18.10.153.wiff (Turbo Spray)

Max. 1.8e9 cps.



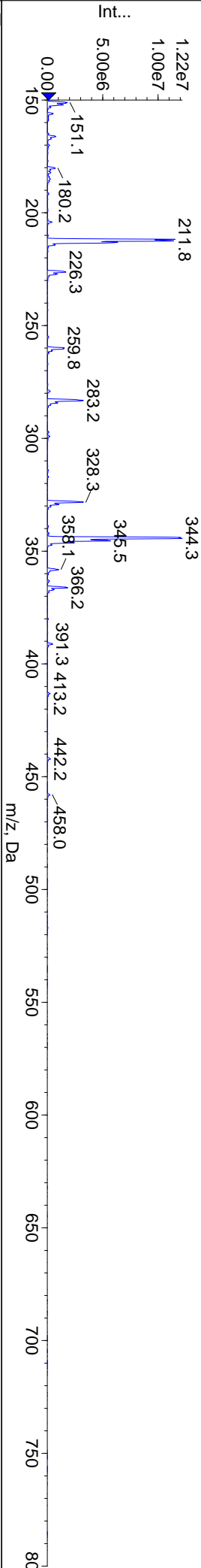
Shimadzu LC Controller Detector A, Channel 1 from Sample 1 (DMB) of DMB10.18.10.153.wiff

Max. 4.4e5 .



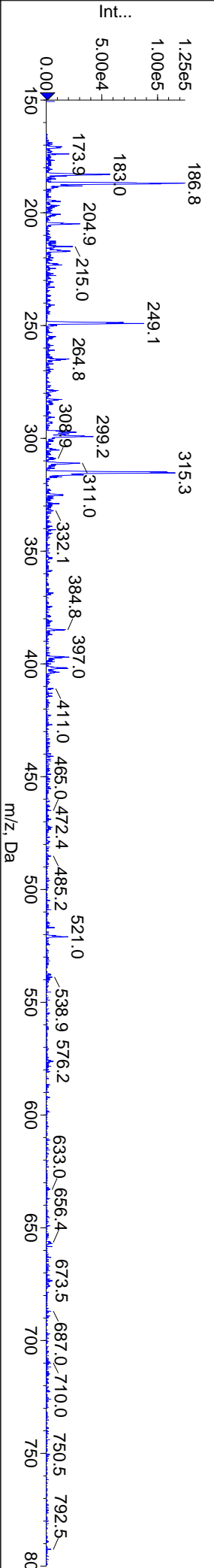
+Q1: Exp 1, 1.566 min from Sample 1 (DMB) of DMB10.18.10.153.wiff (Turbo Spray)

Max. 1.2e7 cps.

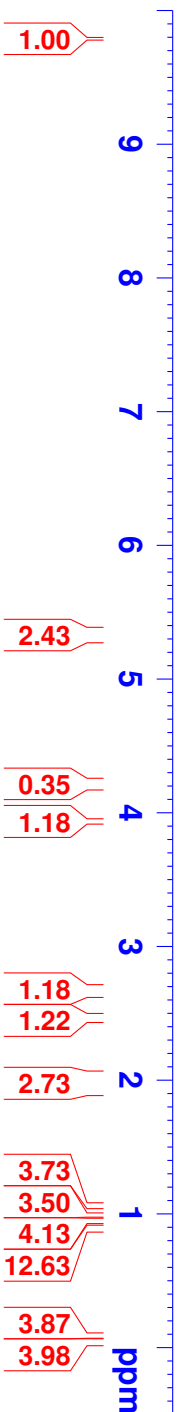
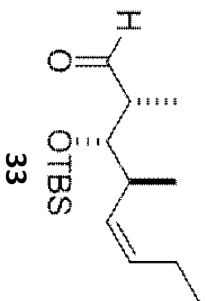
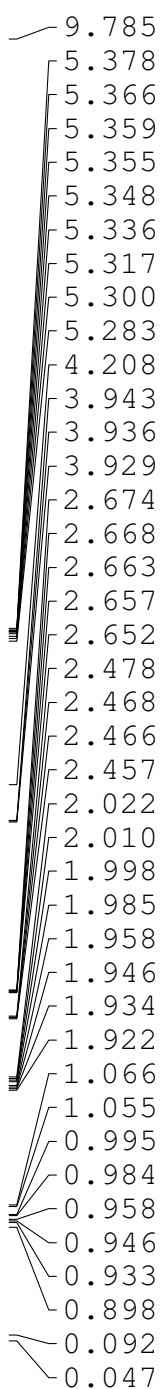


-Q1: Exp 2, 1.678 min from Sample 1 (DMB) of DMB10.18.10.153.wiff (Turbo Spray)

Max. 1.2e5 cps.



DMB1-154f4-9



```

NAME DMB1-154f4
EXPNO 1
PROCNO 1
Date_ 20100819
Time 8.05
INSTRUM spect
PROBHD 5 mm CPTCI 1H-
PULPROG zg30
TD 65536
SOLVENT CDCl3
NS 16
DS 2
SWH 12376.237 Hz
FIDRES 0.188846 Hz
AQ 2.6477449 sec
RG 20.2
DW 40.400 usec
DE 6.50 usec
TE 298.0 K
D1 1.00000000 sec
TD0 1

===== CHANNEL f1 =====
NUC1 1H
P1 8.00 usec
PL1 4.00 dB
PL1W 7.00000000 W
SFO1 600.1337060 MHz
SI 32768
SF 600.1300170 MHz
WDW EM
SSB 0
LB 0.30 Hz
GB 0
PC 1.00
  
```

DMB1-154 carbon for comp



33

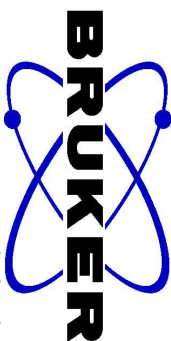
200 180 160 140 120 100 80 60 40 20 0 ppm

NAME DMB1-154
EXPNO 4
PROCNO 1
Date_ 20101016
Time 22.13
INSTRUM spect
PROBHD 5 mm CPTCI 1H-
PULPROG zgpg30
TD 65536
SOLVENT CDCl3
NS 512
DS 2
SWH 35971.223 Hz
FIDRES 0.548877 Hz
AQ 0.9110143 sec
RG 16384
DE 13.900 usec
TE 289.3 K
D1 2.00000000 sec
D11 0.03000000 sec
TD0 1

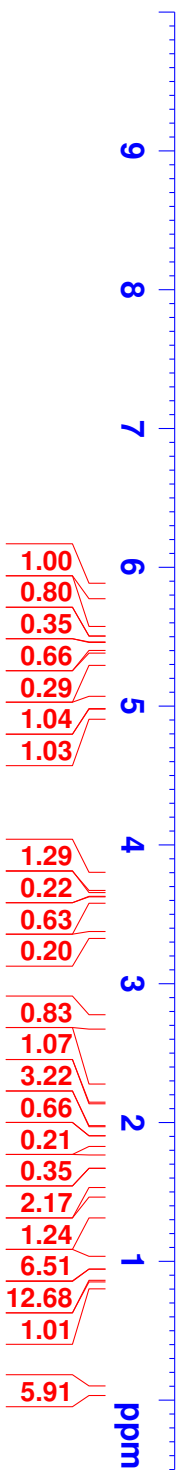
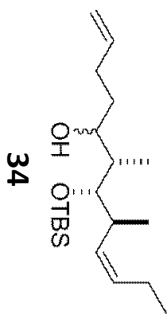
===== CHANNEL f1 =====
NUC1 13C
P1 12.00 usec
PL1 -0.70 dB
PL1W 82.63385773 W
SFO1 150.9178988 MHz

===== CHANNEL f2 =====
CPDPRG2 waltz16
NUC2 1H
PCPD2 80.00 usec
PL2 4.00 dB
PL12 24.00 dB
PL13 27.00 dB
PL2W 7.00000000 W
PL12W 0.07000000 W
PL13W 0.03508311 W
SFO2 600.1324005 MHz
SI 32768
SF 150.9027933 MHz
WDW EM
SSB 0
GB 1.00 Hz
PC 1.40

DMB2-97f8-9



5.830
5.819
5.537
5.521
5.435
5.417
5.040
5.011
4.954
4.938
3.753
3.749
3.612
3.607
2.727
2.189
2.076
2.064
2.051
2.049
2.038
2.036
1.937
1.619
1.616
1.607
1.592
1.388
1.384
1.378
1.000
0.995
0.989
0.983
0.970
0.915
0.834
0.822
0.111
0.090
0.084
0.070
0.063



NAME DMB2-97f8
EXPNO 1
PROCNO 1
Date_ 20120201
Time 8.55
INSTRUM spect
PROBHD 5 mm CPTCI 1H-
PULPROG zg30
TD 65536
SOLVENT CDCl3
NS 16
DS 2
SWH 12376.237 Hz
FIDRES 0.188846 Hz
AQ 2.6477449 sec
RG 8
DW 40.400 usec
DE 6.50 usec
TE 298.0 K
D1 1.0000000 sec
TD0 1

===== CHANNEL f1 =====
NUC1 1H
P1 8.00 usec
PL1 4.00 dB
PL1W 7.0000000 W
SFO1 600.1337060 MHz
SI 32768
SF 600.1300155 MHz
WDW EM
SSB 0
LB 0.30 Hz
GB 0
PC 1.00

DMB2-97F8-9 13C

139.10
138.70
132.46
131.41
131.22
130.78

114.55
114.34

— 78.93
 — 72.45
 — 70.50

Website Type	Average Visits
1	43.04
2	42.42
3	34.83
4	34.76
5	34.50
6	34.40
7	33.97
8	30.66
9	29.18
10	26.04
11	20.93
12	19.34
13	18.27
14	17.83
15	14.27
16	13.80
17	13.51
18	9.35
19	-3.87
20	-4.03
21	-4.05
22	-4.34



BRUKER

34

NAME	DMB2-97f8
EXPNO	1
PROCNO	2
Date_	20120201
Time	9.24
INSTRUM	spect
PROBHD	5 mm CPTCI 1H-
PULPROG	zgpg30
TD	65536
SOLVENT	CDCl3
NS	512
DS	4
SWH	35971.223 Hz
FIDRES	0.548877 Hz
AQ	0.9110143 sec
Rg	4.5
DW	13.900 usec
DE	6.50 usec
TE	298.0 K
D1	2.00000000 sec
D11	0.03000000 sec
TD0	1

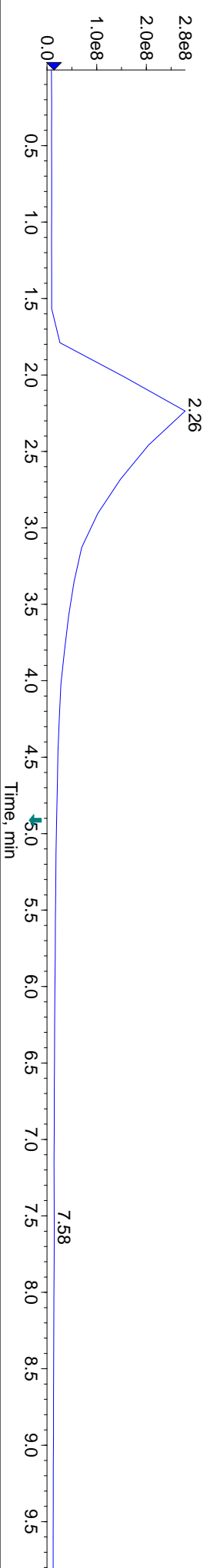
	CHANNEL	f1
=====		=====
NUC1		13C
P1		12.00 usec
PL1		-0.70 dB
PLW		82.63385773 W
SFO1		150.9178988 MHz

```
===== CHANNEL f2 =====
CPDPRG2          waltz16
NUC2             1H
PCPD2            80.00 usec
PL2              4.00 dB
PL12             24.00 dB
PL13             27.00 dB
PL1W             7.00000000 W
PL12W            0.07000000 W
PL13W            0.03508311 W
SF02             600.1324005 MHz
SI              32768
SF              150.9028123 MHz
WDW             EM
SSB             0
LB             1.00 Hz
GB             0
PC             1.40
```



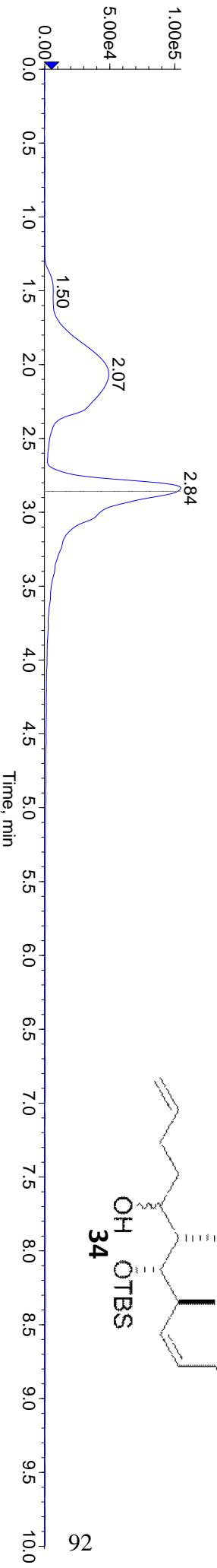
TIC: from Sample 1 (DMB2-97f8-9) of DMB2-97f8-9.wiff (Turbo Spray)

Max. 2.8e8 cps.



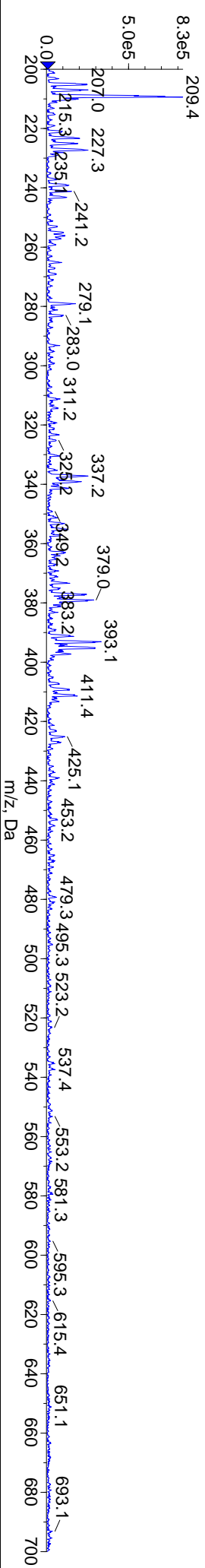
Shimadzu LC Controller Detector A, Channel 1 from Sample 1 (DMB2-97f8-9) of DMB2-97f8-9.wiff

Max. 1.0e5 .



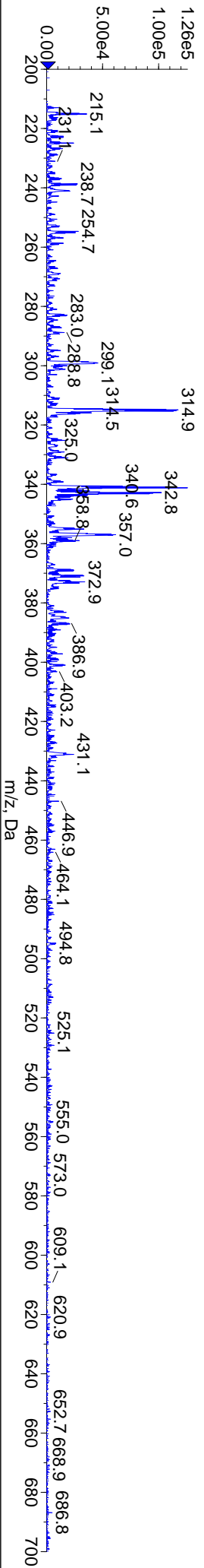
+Q1: Exp 1, 2.682 min from Sample 1 (DMB2-97f8-9) of DMB2-97f8-9.wiff (Turbo Spray)

Max. 8.3e5 cps.

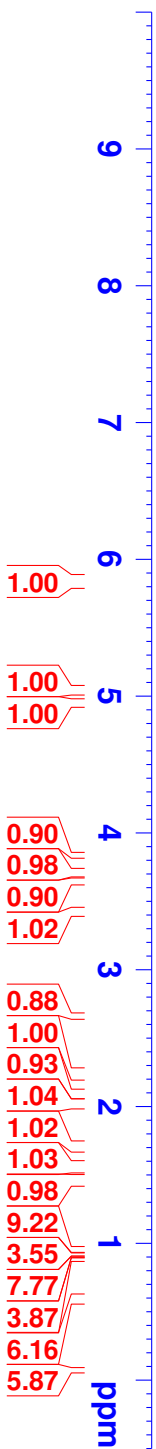
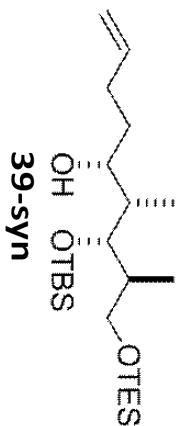
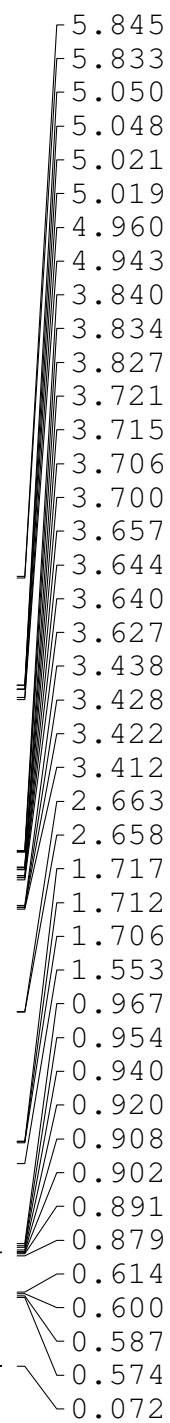


-Q1: Exp 2, 2.793 min from Sample 1 (DMB2-97f8-9) of DMB2-97f8-9.wiff (Turbo Spray)

Max. 1.3e5 cps.



DMB2-296f7-10 600 MHz



NAME DMB2-296f7
EXPNO 2
PROCNO 1
Date_ 20130124
Time 13.46
INSTRUM spect
PROBHD 5 mm CPTCI 1H-
PULPROG zg30
TD 65536
SOLVENT CDCl3
NS 16
DS 2
SWH 12376.237 Hz
FIDRES 0.188846 Hz
AQ 2.6477449 sec
RG 10.1
DW 40.400 usec
DE 6.50 usec
TE 293.0 K
D1 1.00000000 sec
TD0 1

===== CHANNEL f1 =====
NUC1 1H
P1 8.00 usec
PL1 4.00 dB
PL1W 7.00000000 W
SFO1 600.1337060 MHz
SI 32768
SF 600.1300161 MHz
WDW EM
SSB 0
LB 0.30 Hz
GB 0
PC 1.00

DMB2-296f7-10 125 MHz

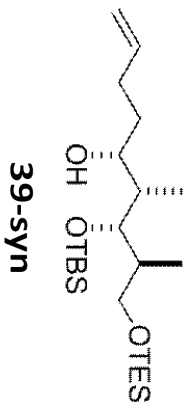
138.81
114.51
76.30
73.33
65.16
40.54
40.25
34.18
30.59
26.01
18.27
14.02
9.37
6.78
4.26
-3.78
-4.37

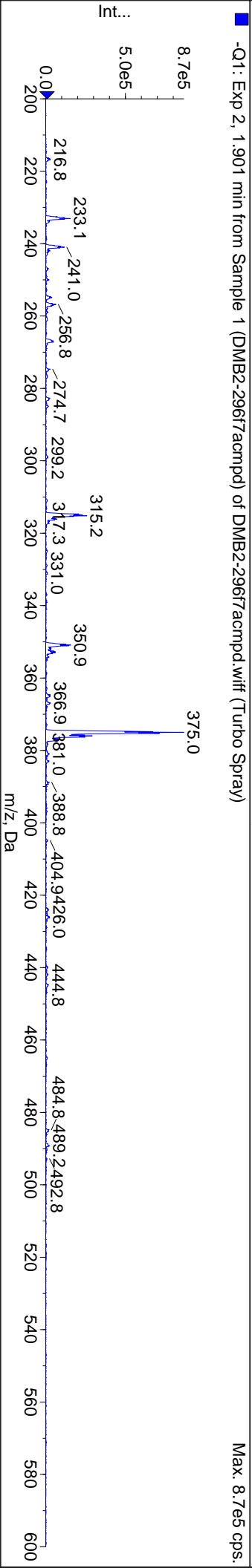
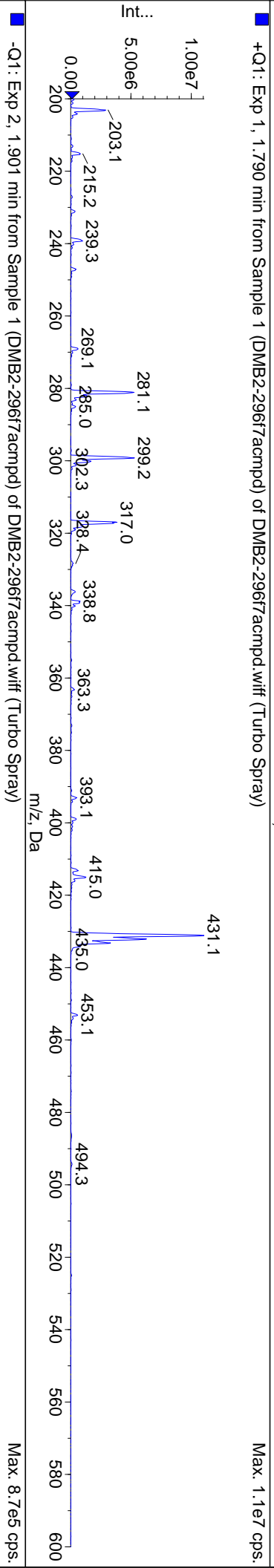
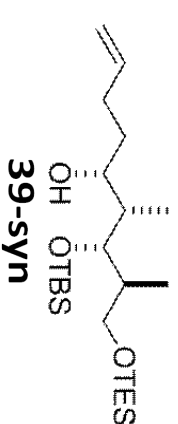
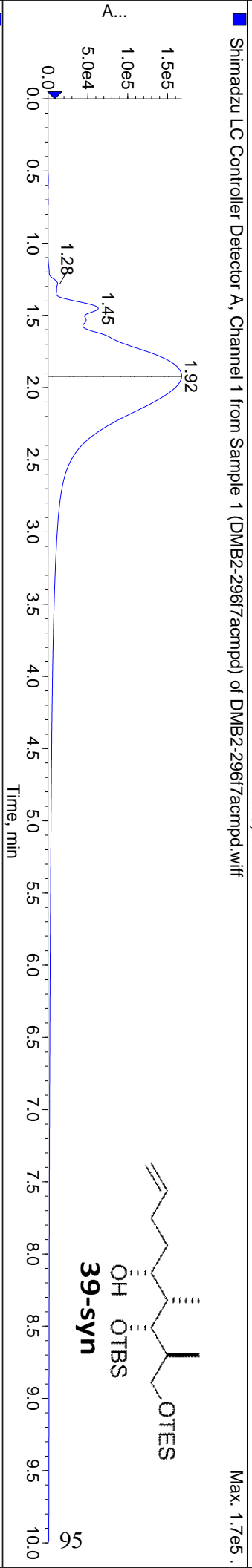
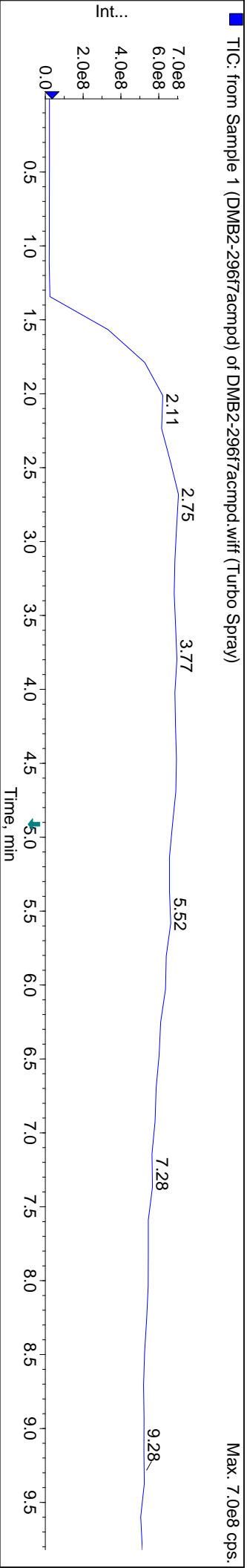


NAME DMB2-296f7
EXPNO 3
PROCNO 1
Date_ 20130124
Time 14.14
INSTRUM spect
PROBHD 5 mm CPTCI 1H-
PULPROG zgpg30
TD 65536
SOLVENT CDCl3
NS 512
DS 4
SWH 35971.223 Hz
FIDRES 0.548877 Hz
AQ 0.9110143 sec
RG 5.7
DE 13.900 usec
TE 293.0 K
D1 2.00000000 sec
D11 0.03000000 sec
TD0 1

===== CHANNEL f1 =====
NUC1 13C
P1 12.00 usec
PL1 -0.70 dB
PL1W 82.63385773 W
SFO1 150.9178988 MHz

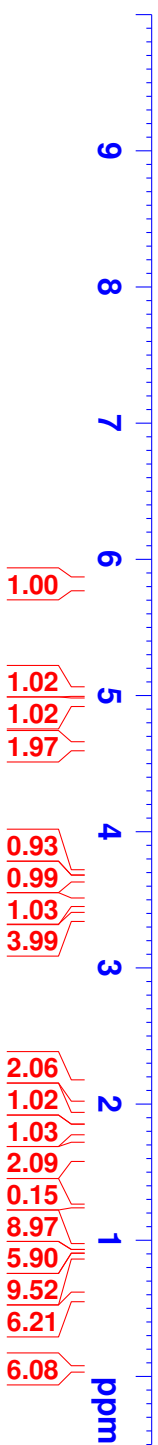
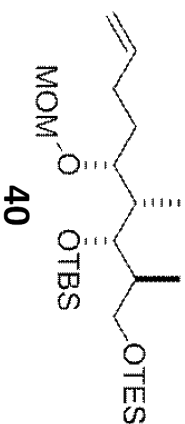
===== CHANNEL f2 =====
CPDPRG2 waltz16
NUC2 1H
PCPD2 80.00 usec
PL2 4.00 dB
PL12 24.00 dB
PL13 27.00 dB
PL2W 7.00000000 W
PL12W 0.07000000 W
PL13W 0.03508311 W
SFO2 600.1324005 MHz
SI 32768
SF 150.9028153 MHz
WDW EM
SSB 0
LB 1.00 Hz
GB 0
PC 1.40






NAME	DMB2-220f2
------	------------

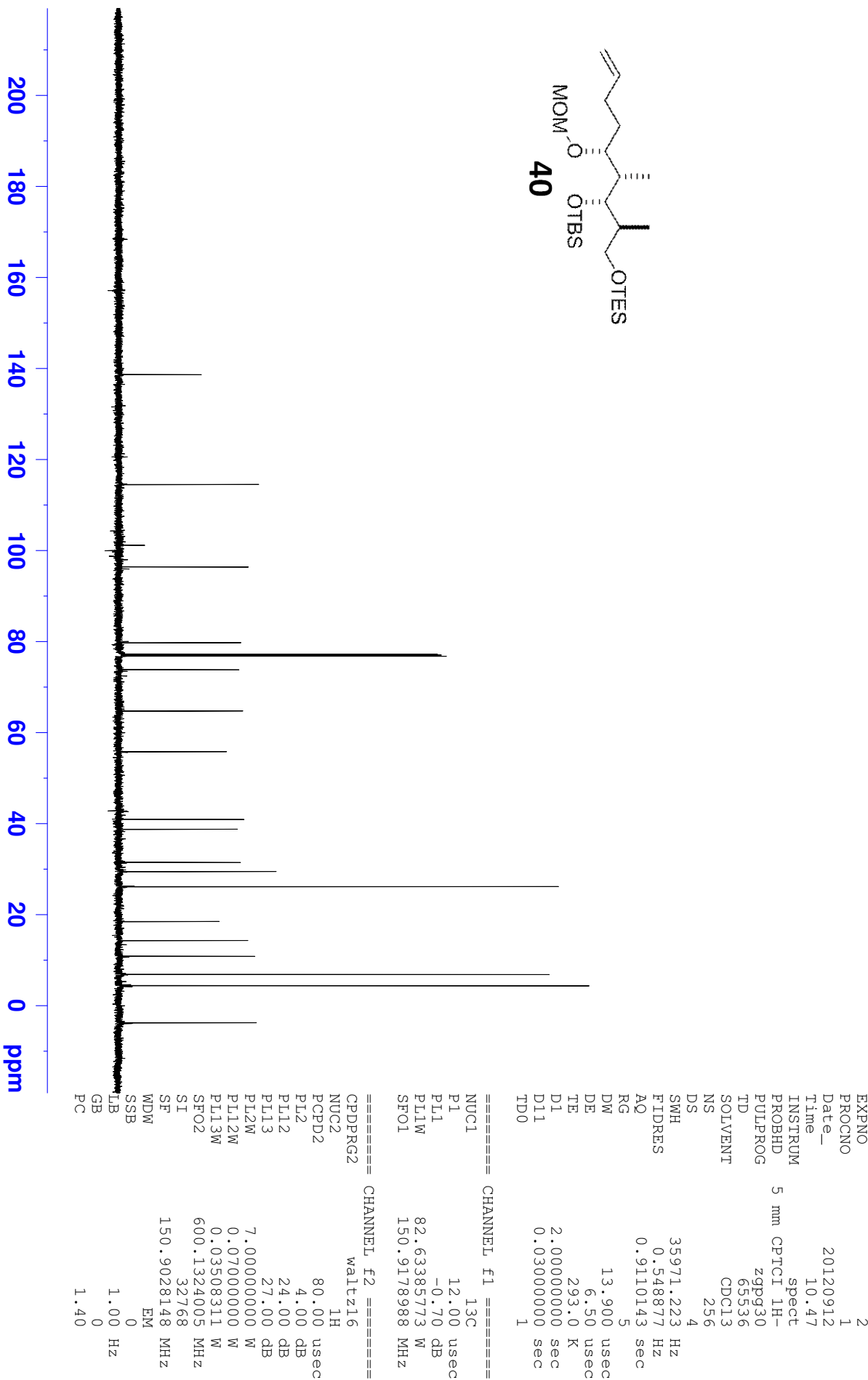
6

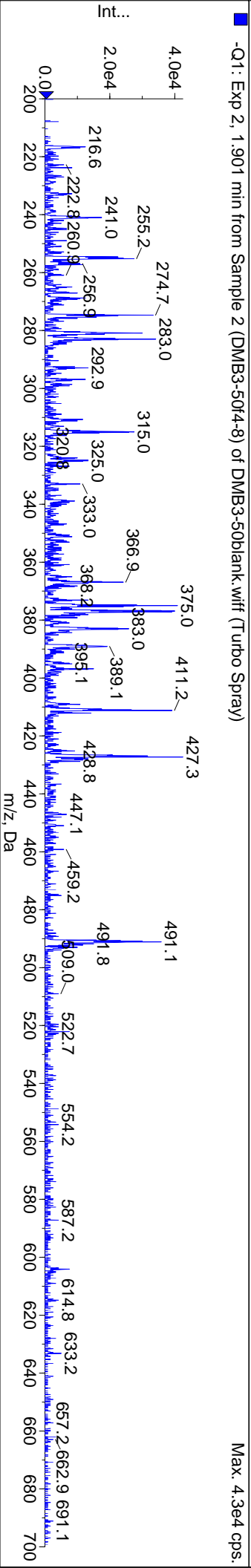
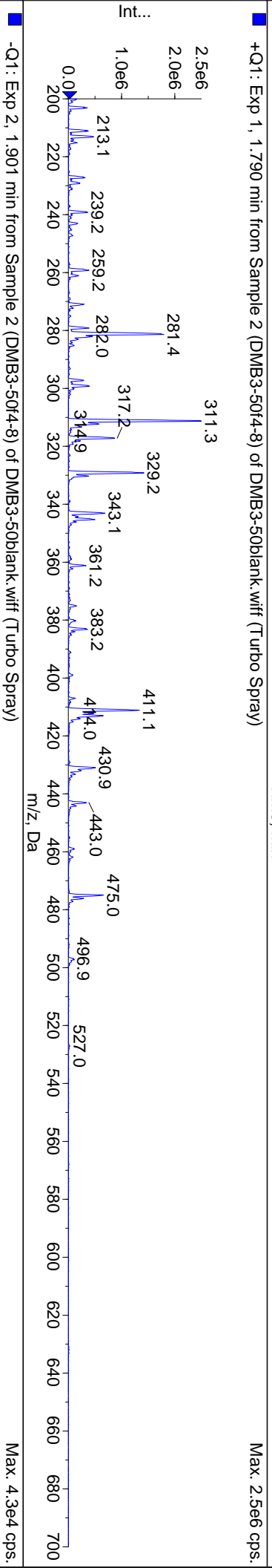
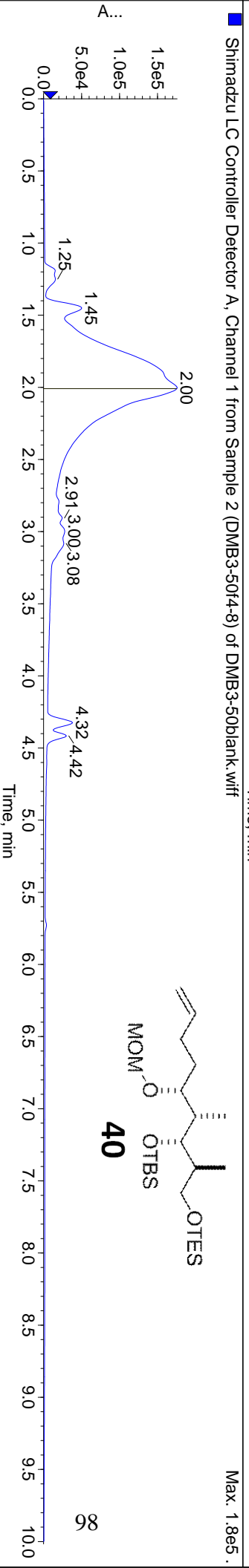
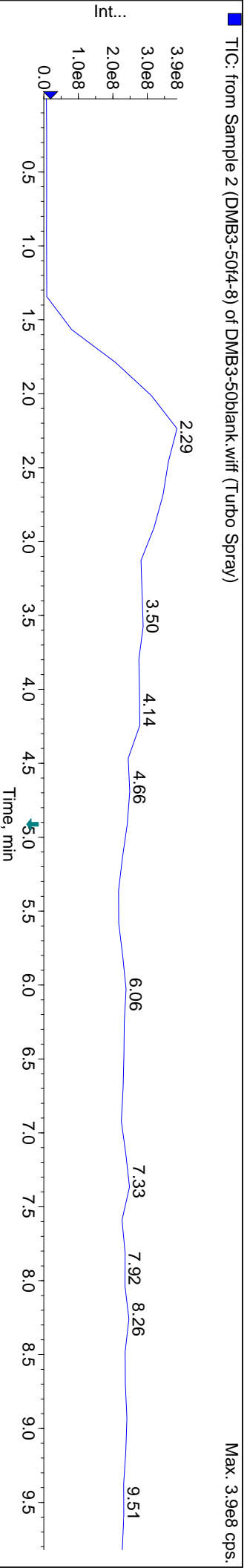


```
===== CHANNEL f1 =====
NUC1      1H
P1         8.00 usec
PL1        4.00 dB
PL1W       7.00000000 W
SF01       600.1337060 MHz
SI         32768
SF         600.1300172 MHz
WDW        EM
SSB        0
LB         0.30 Hz
GB         0
PC         1.00
```

The Bruker logo, featuring the word "BRUKER" in a bold, black, sans-serif font, oriented vertically. To the right of the text is a stylized blue graphic consisting of two intersecting loops, resembling an atomic orbital or a figure-eight shape, with small blue dots at the intersection points.C[C@H](O[Si](C)(C)C)[C@@H](O[Si](C)(C)C)[C@H](OC(=O)c1ccc(C(F)(F)F)c1)[C@@H](O[Si](C)(C)C)CCCC=C

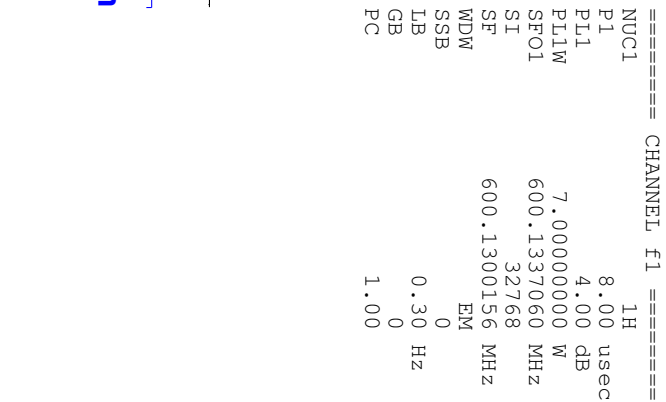
40





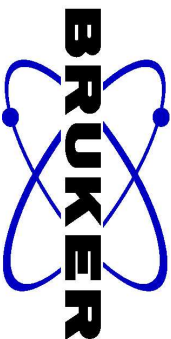
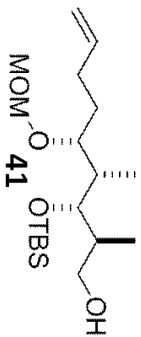
NAME	DMB3-50F60
------	------------

99



DMB2-224f16-26 carbon

167.51
138.28
114.90
101.19
98.01
96.12
95.62
79.52
75.81
65.22
55.94
39.21
38.91
30.97
30.08
26.16
18.38
14.52
11.56
0.01
-3.46
-3.91



NAME DMB2-224f16
EXPNO 2
PROCNO 1
Date_ 20121003
Time 11.09
INSTRUM spect
PROBHD 5 mm CPTCI 1H-
PULPROG zgpg30
TD 65536
SOLVENT CDCl3
NS 512
DS 4
SWH 35971.223 Hz
FIDRES 0.54877 Hz
AQ 0.9110143 sec
RG 6.3
DW 13.900 usec
DE 6.50 usec
TE 298.0 K
D1 2.0000000 sec
D11 0.0300000 sec
TD0 1

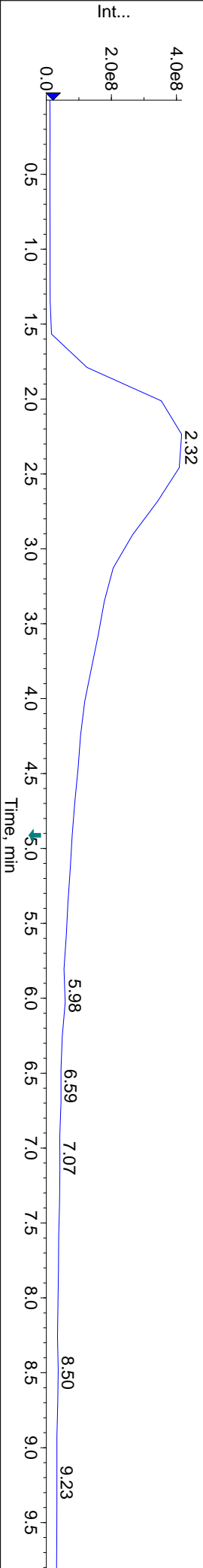
===== CHANNEL f1 =====
NUC1 13C
P1 12.00 usec
PL1 -0.70 dB
PL1W 82.63385773 W
SFO1 150.9178988 MHz

===== CHANNEL f2 =====
CPDPRG2 waltz16
NUC2 1H
PCPD2 80.00 usec
PL2 4.00 dB
PL12 24.00 dB
PL13 27.00 dB
PL2W 7.00000000 W
PL12W 0.07000000 W
PL13W 0.03508311 W
SFO2 600.1324005 MHz
SI 32768
SF 150.9028090 MHz
WDW EM
SSB 0
LB 1.00 Hz
GB 0
PC 1.40

200 180 160 140 120 100 80 60 40 20 0 ppm

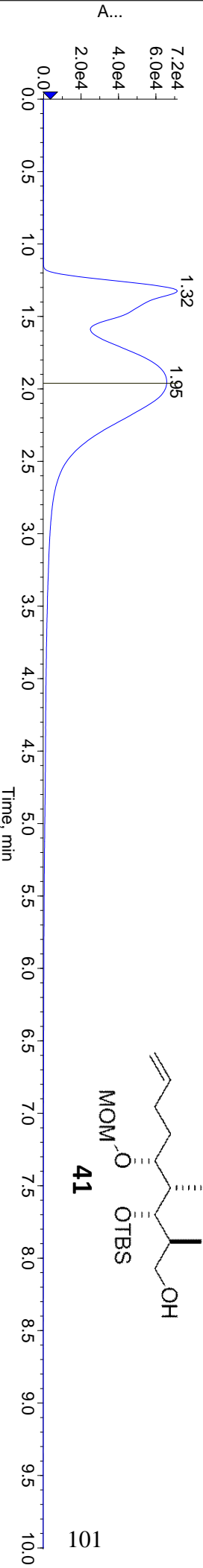
TIC: from Sample 1 (DMB2-224f17-26) of DMB2-224f17-26.wiff (Turbo Spray)

Max. 4.2e8 cps.



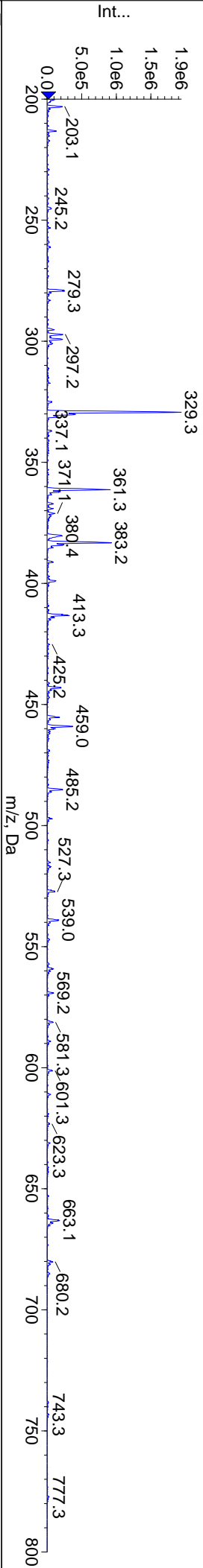
Shimadzu LC Controller Detector A, Channel 1 from Sample 1 (DMB2-224f17-26) of DMB2-224f17-26.wiff

Max. 7.2e4.



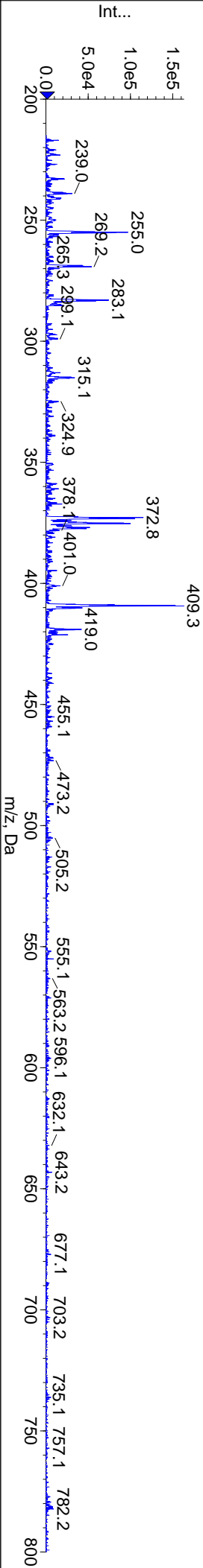
+Q1: Exp 1, 1.790 min from Sample 1 (DMB2-224f17-26) of DMB2-224f17-26.wiff (Turbo Spray)

Max. 1.9e6 cps.

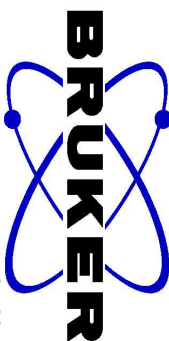


-Q1: Exp 2, 1.901 min from Sample 1 (DMB2-224f17-26) of DMB2-224f17-26.wiff (Turbo Spray)

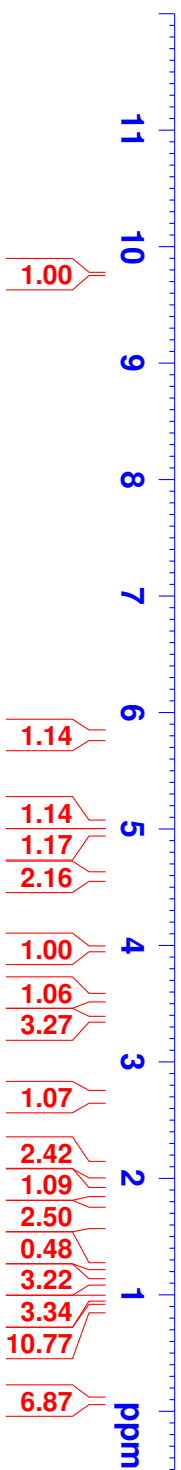
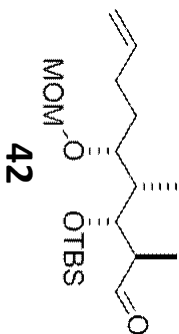
Max. 1.6e5 cps.



DMB3-69crude



9.764	NAME	DMB3-69
9.761	EXPNO	1
5.809	PROCNO	1
5.798	Date_	20130405
5.049	Time	9.44
5.047	INSTRUM	spect
5.021	PROBHD	5 mm CPTCI 1H-
5.019	PULPROG	zg30
4.982	TD	65536
4.965	SOLVENT	CDCl3
4.614	NS	16
4.603	DS	2
4.580	SWH	12376.237 Hz
4.568	FIDRES	0.188846 Hz
3.975	AQ	2.6477449 sec
3.969	RG	18
3.964	DW	40.400 usec
3.959	DE	6.50 usec
3.552	TE	298.0 K
3.545	D1	1.00000000 sec
3.363	TD0	1



```

===== CHANNEL f1 =====
NUC1      1H
P1         8.00 usec
PL1        4.00 dB
PL1W       7.00000000 W
SFO1       600.1337060 MHz
SI         32768
SF         600.1300148 MHz
WDW        EM
SSB        0
LB         0.30 Hz
GB         0
PC         1.00
  
```


DMB2-295crude

204.66
204.50

138.46
138.14

114.94
114.72

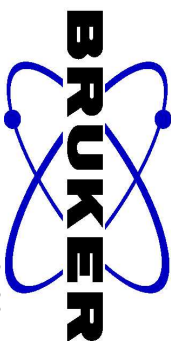
96.11
96.03

78.94
78.54
74.87
73.54

55.84
52.16
50.65

40.23
40.09
31.12
29.92
29.78
28.74
25.98
18.31
11.76
11.17

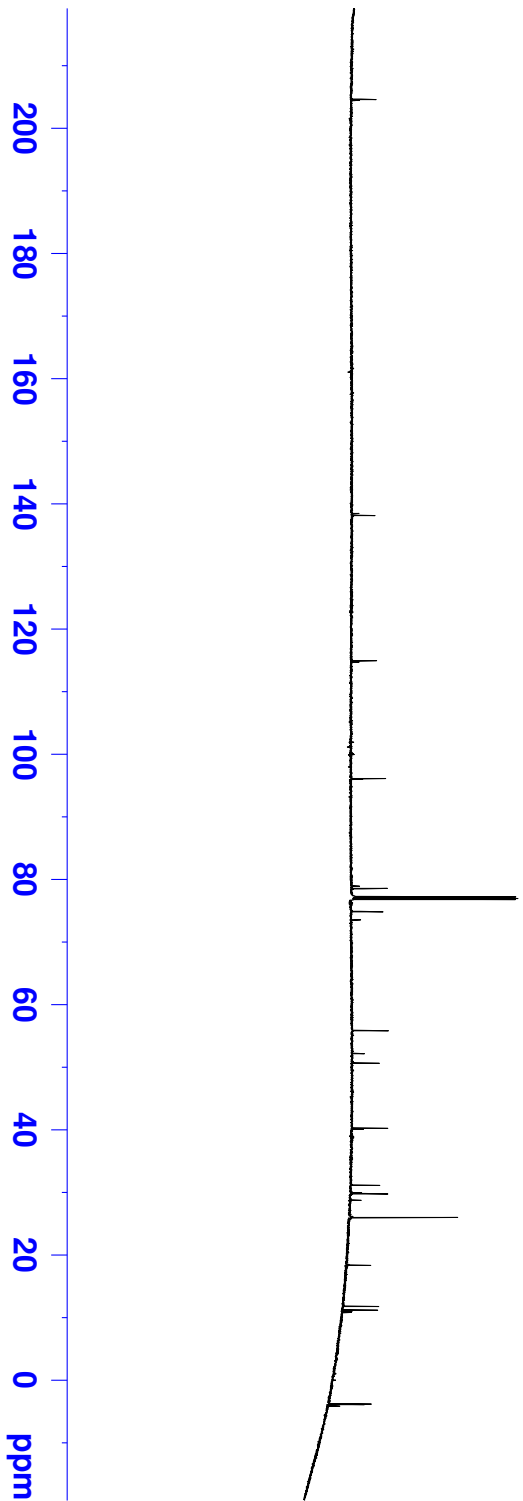
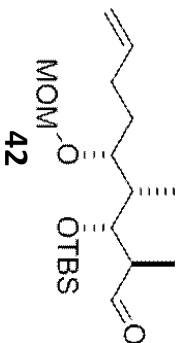
-3.82



NAME DMB2-295
EXPNO 2
PROCNO 1
Date_ 20130108
Time 19.21
INSTRUM spect
PROBHD 5 mm CPTCI 1H-
PULPROG zgpg30
TD 65536
SOLVENT CDCl3
NS 512
DS 4
SWH 35971.223 Hz
FIDRES 0.548877 Hz
AQ 0.9110143 sec
RG 7.1
DW 13.900 usec
DE 6.50 usec
TE 298.0 K
D1 2.00000000 sec
D11 0.03000000 sec
TD0 1

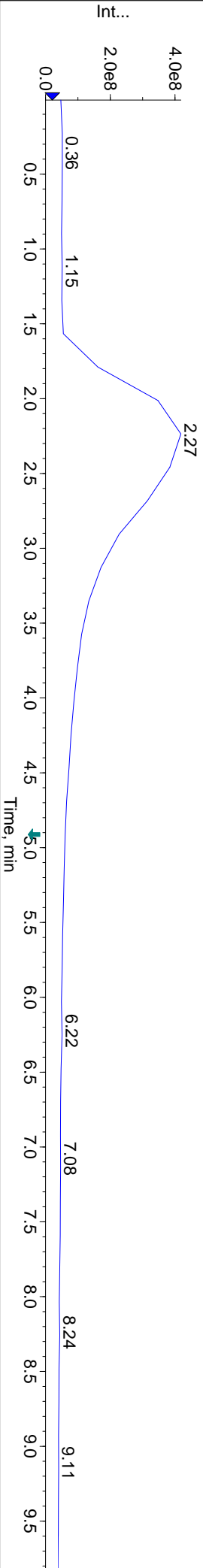
===== CHANNEL f1 =====
NUC1 13C
P1 12.00 usec
PL1 -0.70 dB
PL1W 82.63385773 W
SFO1 150.9178988 MHz

===== CHANNEL f2 =====
CPDPRG2 waltz16
NUC2 1H
PCPD2 80.00 usec
PL2 4.00 dB
PL12 24.00 dB
PL13 27.00 dB
PL12W 7.00000000 W
PL12W 0.07000000 W
PL13W 0.03508311 W
SFO2 600.1324005 MHz
SI 32768
SF 150.9028133 MHz
WDW EM
SSB 0
LB 1.00 Hz
GB 0
PC 1.40



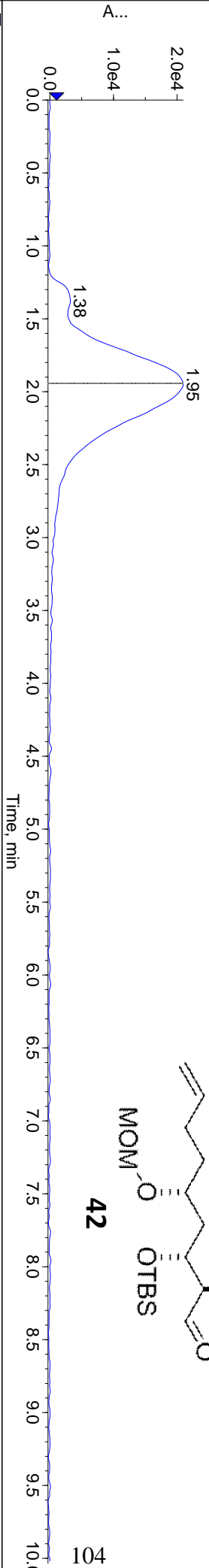
TIC: from Sample 1 (DMB2-295sample) of DMB2-295sample.wiff (Turbo Spray)

Max. 4.2e8 cps.



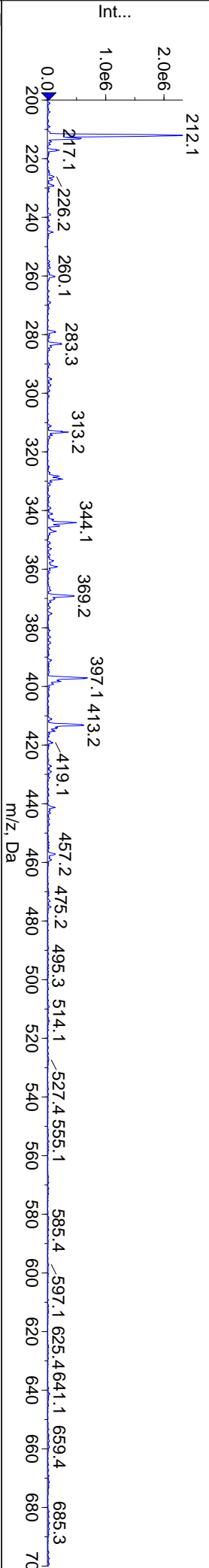
Shimadzu LC Controller Detector A, Channel 1 from Sample 1 (DMB2-295sample) of DMB2-295sample.wiff

Max. 2.1e4 .



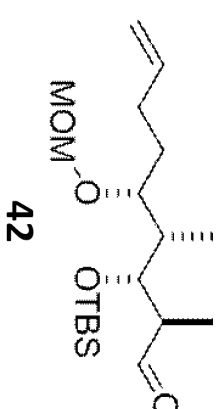
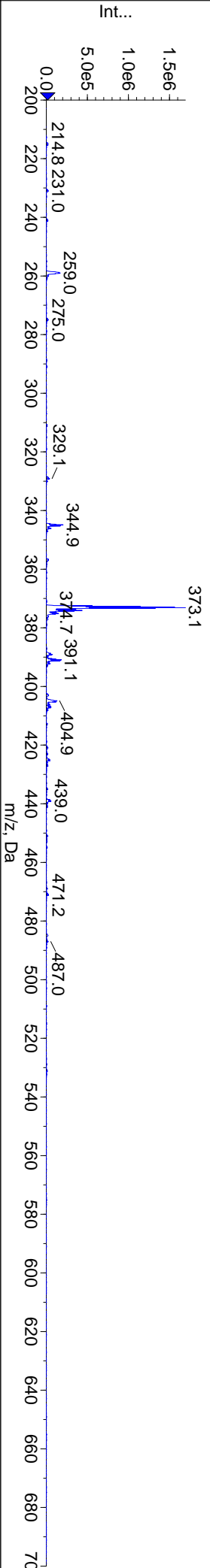
+Q1: Exp 1, 1.790 min from Sample 1 (DMB2-295sample) of DMB2-295sample.wiff (Turbo Spray)

Max. 2.3e6 cps.

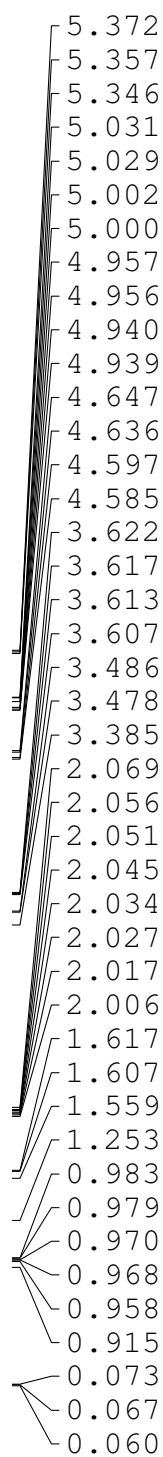


-Q1: Exp 2, 1.901 min from Sample 1 (DMB2-295sample) of DMB2-295sample.wiff (Turbo Spray)

Max. 1.7e6 cps.



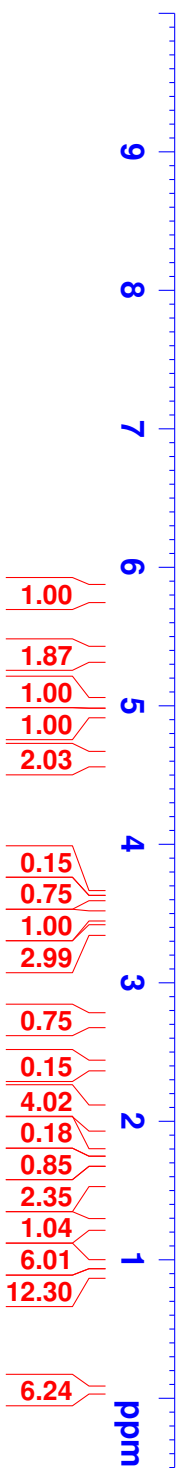
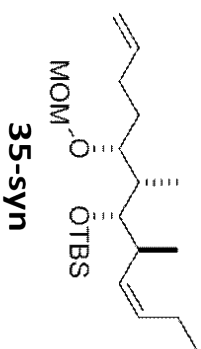
DMB3-70f4-11




```

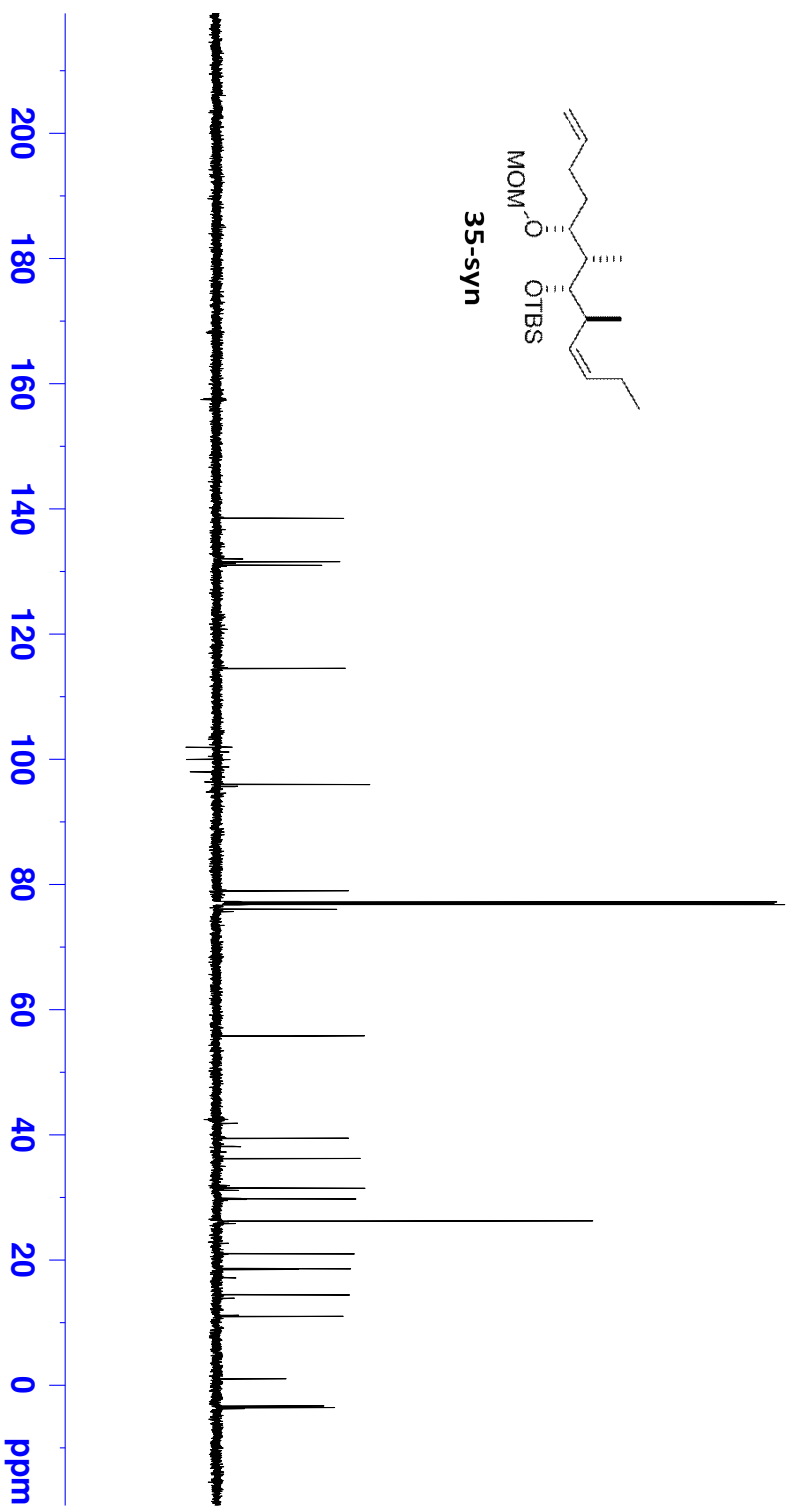
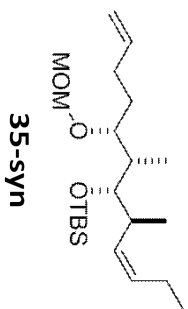
NAME DMB3-70f4
EXPNO 1
PROCNO 1
Date_ 20130408
Time 17.18
INSTRUM spect
PROBHD 5 mm CPTCI 1H-
PULPROG zg30
TD 65536
SOLVENT CDCl3
NS 16
DS 2
SWH 12376.237 Hz
FIDRES 0.188846 Hz
AQ 2.6477449 sec
RG 22.6
DE 40.400 usec
TE 298.0 K
D1 1.0000000 sec
TD0 1

===== CHANNEL f1 =====
NUC1 1H
P1 8.00 usec
PL1 4.00 dB
PL1W 7.00000000 W
SFO1 600.1337060 MHz
SI 32768
SF 600.1300152 MHz
WDW EM
SSB 0
LB 0.30 Hz
GB 0
PC 1.00
  
```





NAME	DMB3-70f4
EXPNO	3
PROCNO	1
Date_	20130916
Time	10.19
INSTRUM	spect
PROBHD	5 mm CPTCI 1H-
PULPROG	zgpg30
TD	65536
SOLVENT	CDCl3
NS	256
DS	2
SWH	35971.223 Hz
FIDRES	0.548877 Hz
AQ	0.9110143 sec
RG	7.1
DW	13.900 usec
DE	6.50 usec
TE	298.0 K
D1	2.00000000 sec
D11	0.03000000 sec
TD0	1

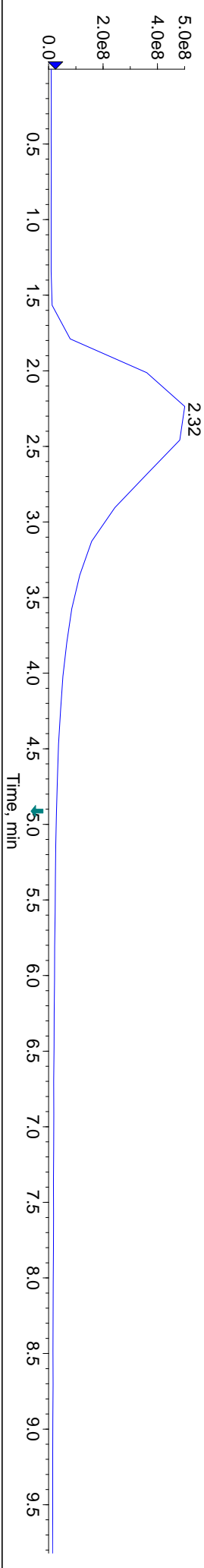


```
===== CHANNEL f1 =====
NUC1      13C
P1         12.00 usec
PL1        -0.70 dB
PL1W       82.63385773 W
SFO1       150.9178988 MHz

===== CHANNEL f2 =====
CPDPRG2    waltz16
NUC2        1H
PCPD2      80.00 usec
PL2         4.00 dB
PL12        24.00 dB
PL13        27.00 dB
PL1W        7.00000000 W
PL12W       0.07000000 W
PL13W       0.03508311 W
SFO2        600.1324005 MHz
SI          32768
SF          150.9028126 MHz
WDW         EM
SSB         0
LB          1.00 Hz
GB          0
DC          1.40
```

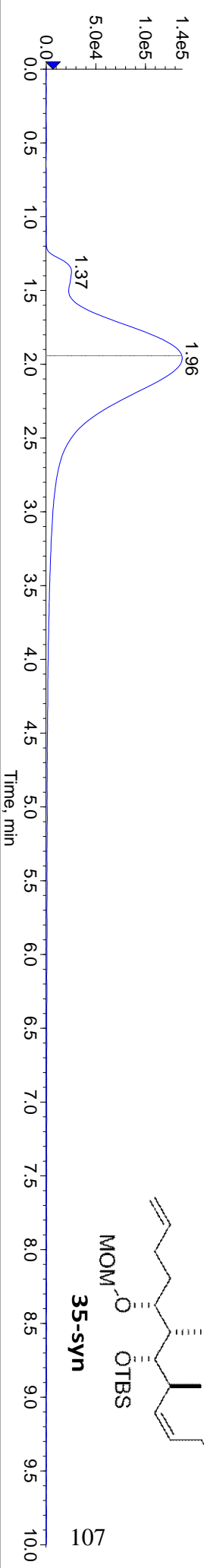
TIC: from Sample 1 (DMB3-70f4-11) of DMB3-70f4-11.wiff (Turbo Spray)

Max. 5.0e8 cps.



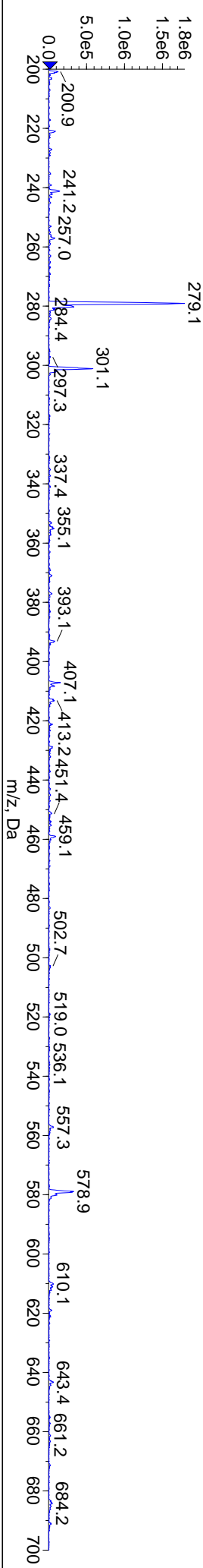
Shimadzu LC Controller Detector A, Channel 1 from Sample 1 (DMB3-70f4-11) of DMB3-70f4-11.wiff

Max. 1.4e5 .



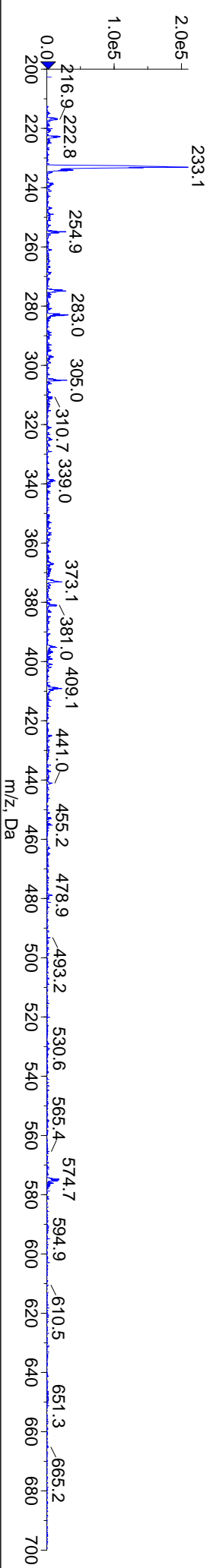
+Q1: Exp 1, 1.790 min from Sample 1 (DMB3-70f4-11) of DMB3-70f4-11.wiff (Turbo Spray)

Max. 1.8e6 cps.

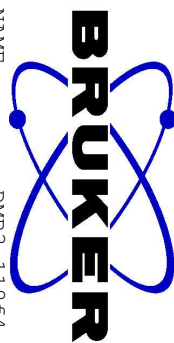
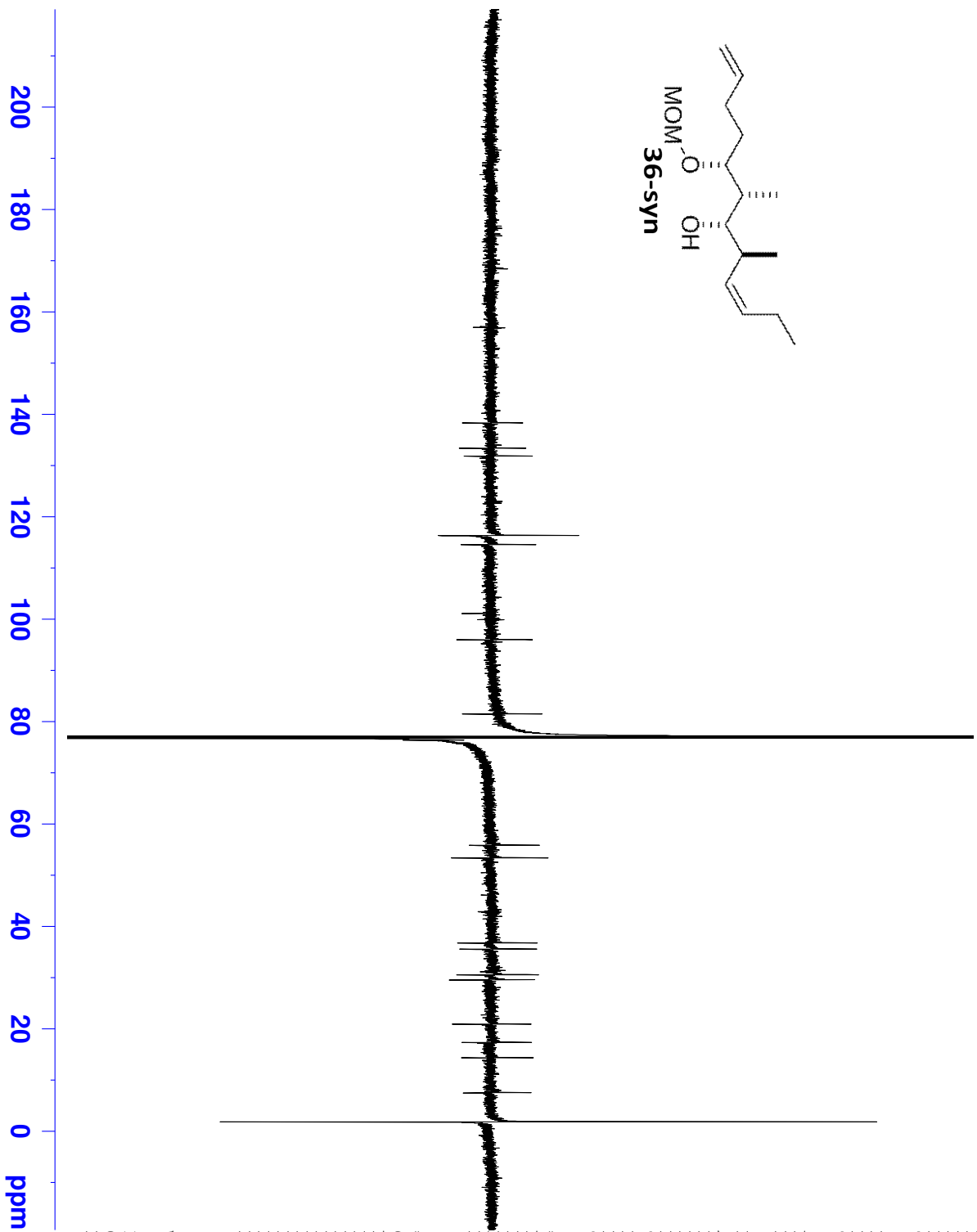
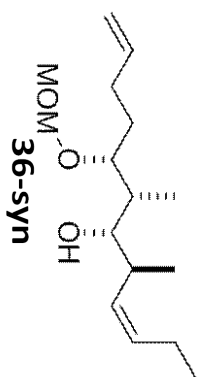


-Q1: Exp 2, 1.901 min from Sample 1 (DMB3-70f4-11) of DMB3-70f4-11.wiff (Turbo Spray)

Max. 2.1e5 cps.



DMB3-118f4-7



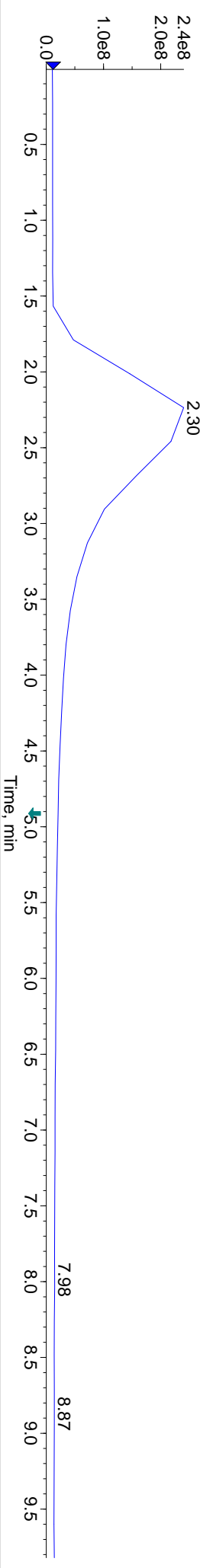
NAME DMB3-118f4
EXPNO 3
PROCNO 1
Date_ 20130914
Time 14.18
INSTRUM spect
PROBHD 5 mm CPTCI 1H-
PULPROG zgpg30
TD 65536
SOLVENT CDCl3
NS 1024
DS 4
SWH 35971.223 Hz
FIDRES 0.548877 Hz
AQ 0.9110143 sec
RG 7.1
DW 13.900 usec
DE 6.50 usec
TE 298.0 K
D1 2.00000000 sec
D11 0.03000000 sec
TD0 1

===== CHANNEL f1 =====
NUC1 13C
P1 12.00 usec
PL1 -0.70 dB
PL1W 82.63385773 W
SFO1 150.9178988 MHz

===== CHANNEL f2 =====
CPDPRG2 waltz16
NUC2 1H
PCPD2 80.00 usec
PL2 4.00 dB
PL12 24.00 dB
PL13 27.00 dB
PL2W 7.00000000 W
PL12W 0.07000000 W
PL13W 0.03508311 W
SFO2 600.1324005 MHz
SI 32768
SF 150.9028224 MHz
WDW EM
SSB 0
LB 1.00 Hz
GB 0
PC 1.40

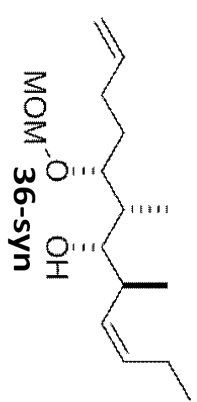
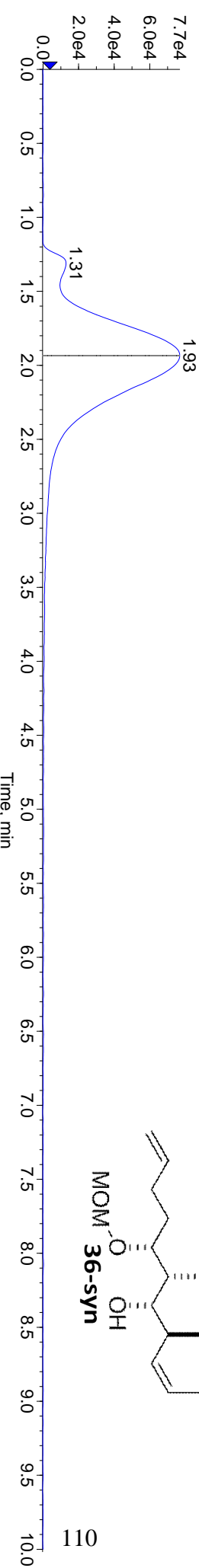
TIC: from Sample 1 (DMB3-118f4-11) of DMB3-118f4-11.wiff (Turbo Spray)

Max. 2.4e8 cps.



Shimadzu LC Controller Detector A, Channel 1 from Sample 1 (DMB3-118f4-11) of DMB3-118f4-11.wiff

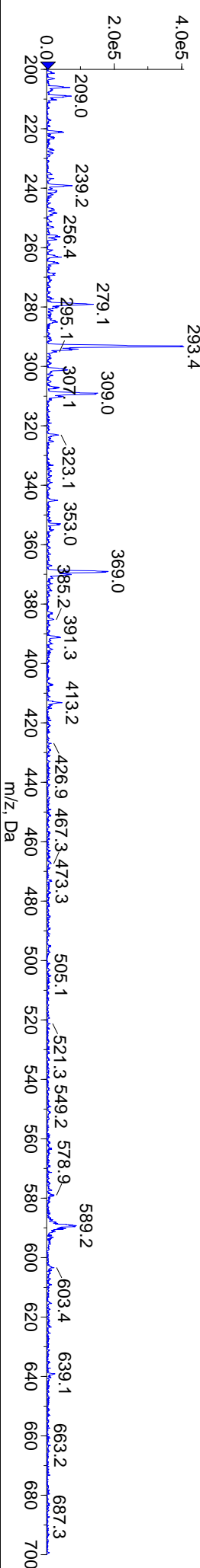
Max. 7.7e4.



110

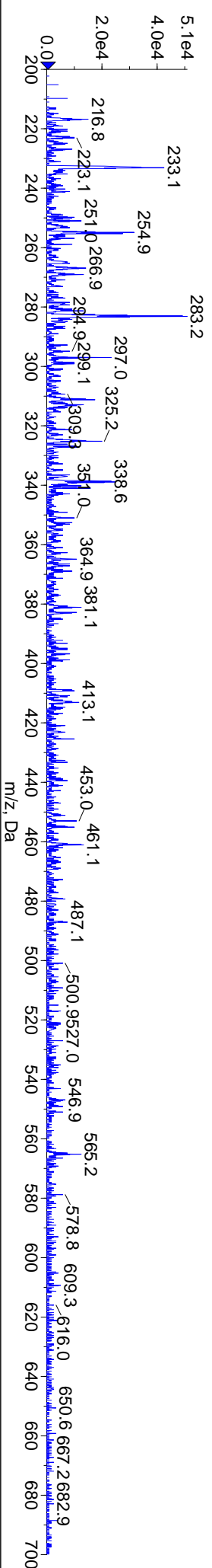
+Q1: Exp 1, 1.790 min from Sample 1 (DMB3-118f4-11) of DMB3-118f4-11.wiff (Turbo Spray)

Max. 4.1e5 cps.



-Q1: Exp 2, 1.901 min from Sample 1 (DMB3-118f4-11) of DMB3-118f4-11.wiff (Turbo Spray)

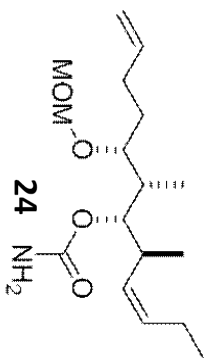
Max. 5.1e4 cps.



DMB3-134



5.357
4.647
4.636
4.597
4.585
3.413
3.386
3.381
2.045
2.034
2.026
2.022
2.017
2.009
2.004
1.704
1.665
1.657
1.632
1.616
1.606
1.601
1.596
1.590
1.542
1.252
1.167
1.124
1.107
0.978
0.975
0.970
0.967
0.920
0.915
0.909
0.901
0.899
0.890
0.887
0.879
0.867



9 8 7 6 5 4 3 2 1 ppm

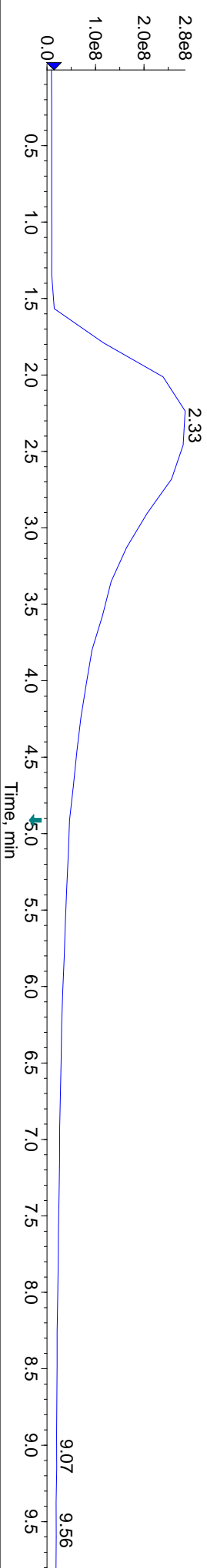
1.28
2.00
1.38
1.23
0.23
3.02
0.64
0.28
0.07
0.25
0.15
0.11
0.59
0.94
1.20
2.79
0.27
0.59
0.09
0.25
0.70
0.75
5.43
0.96
3.13
2.81
9.56
10.65
13.54

NAME DMB3-134
EXPNO 5
PROCNO 1
Date_ 20130914
Time 15.36
INSTRUM spect
PROBHD 5 mm CPTCI 1H-
PULPROG zg30
TD 65536
SOLVENT CDCl3
NS 512
DS 0
SWH 12376.237 Hz
FIDRES 0.188846 Hz
AQ 2.6477449 sec
RG 8
DW 40.400 usec
DE 6.50 usec
TE 298.0 K
D1 2.0000000 sec
TD0 1

===== CHANNEL f1 =====
NUC1 1H
P1 8.00 usec
PL1 4.00 dB
PL1W 7.00000000 W
SFO1 600.1337060 MHz
SI 32768
SF 600.1300159 MHz
WDW EM
SSB 0
LB 0.30 Hz
GB 0
PC 1.00

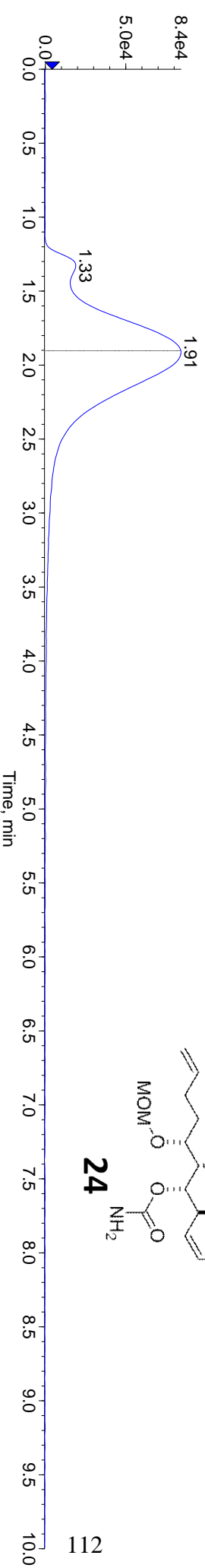
TIC: from Sample 1 (DMB3-29f12) of DMB3-29f12.wiff (Turbo Spray)

Max. 2.8e8 cps.



Shimadzu LC Controller Detector A, Channel 1 from Sample 1 (DMB3-29f12) of DMB3-29f12.wiff

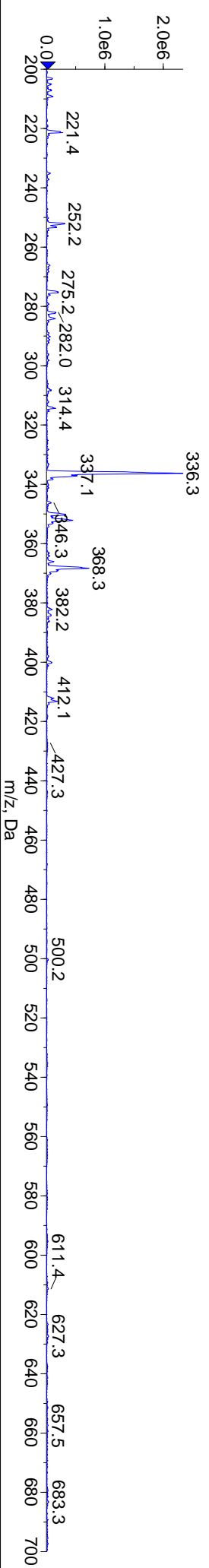
Max. 8.4e4 .



112

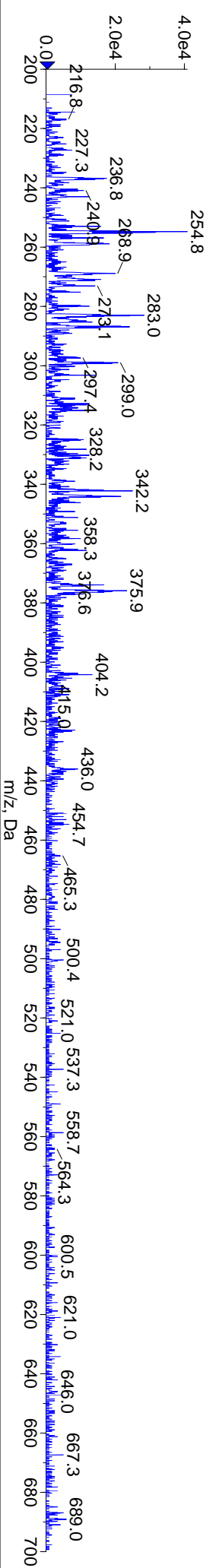
+Q1: Exp 1, 1.790 min from Sample 1 (DMB3-29f12) of DMB3-29f12.wiff (Turbo Spray)

Max. 2.3e6 cps.

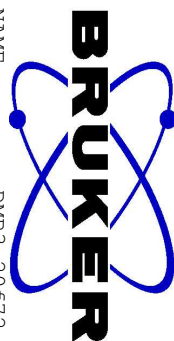
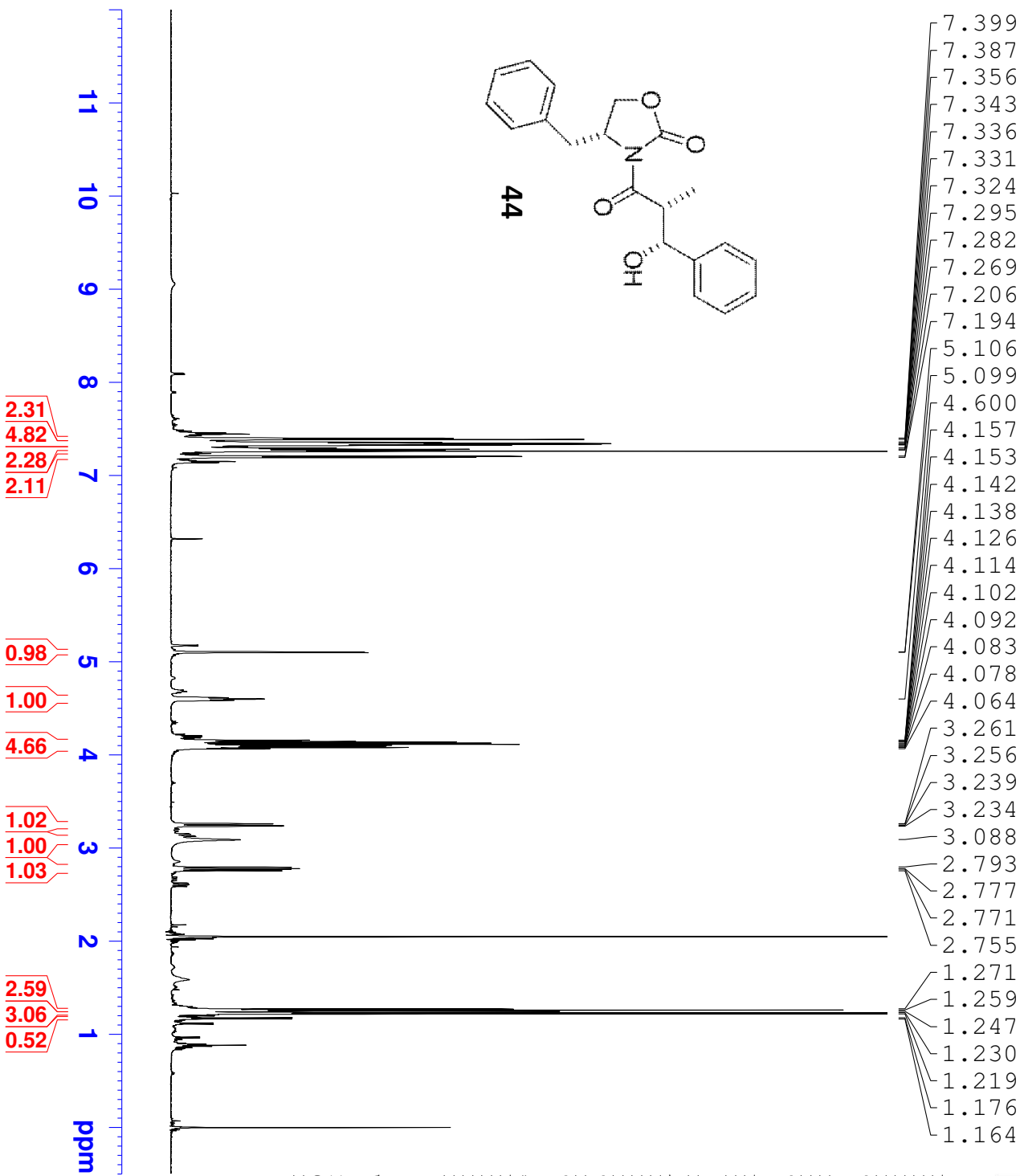


-Q1: Exp 2, 1.901 min from Sample 1 (DMB3-29f12) of DMB3-29f12.wiff (Turbo Spray)

Max. 4.1e4 cps.



DMB3-20f72-99

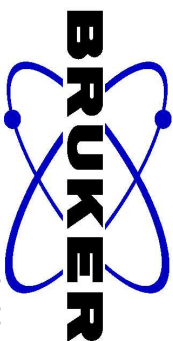
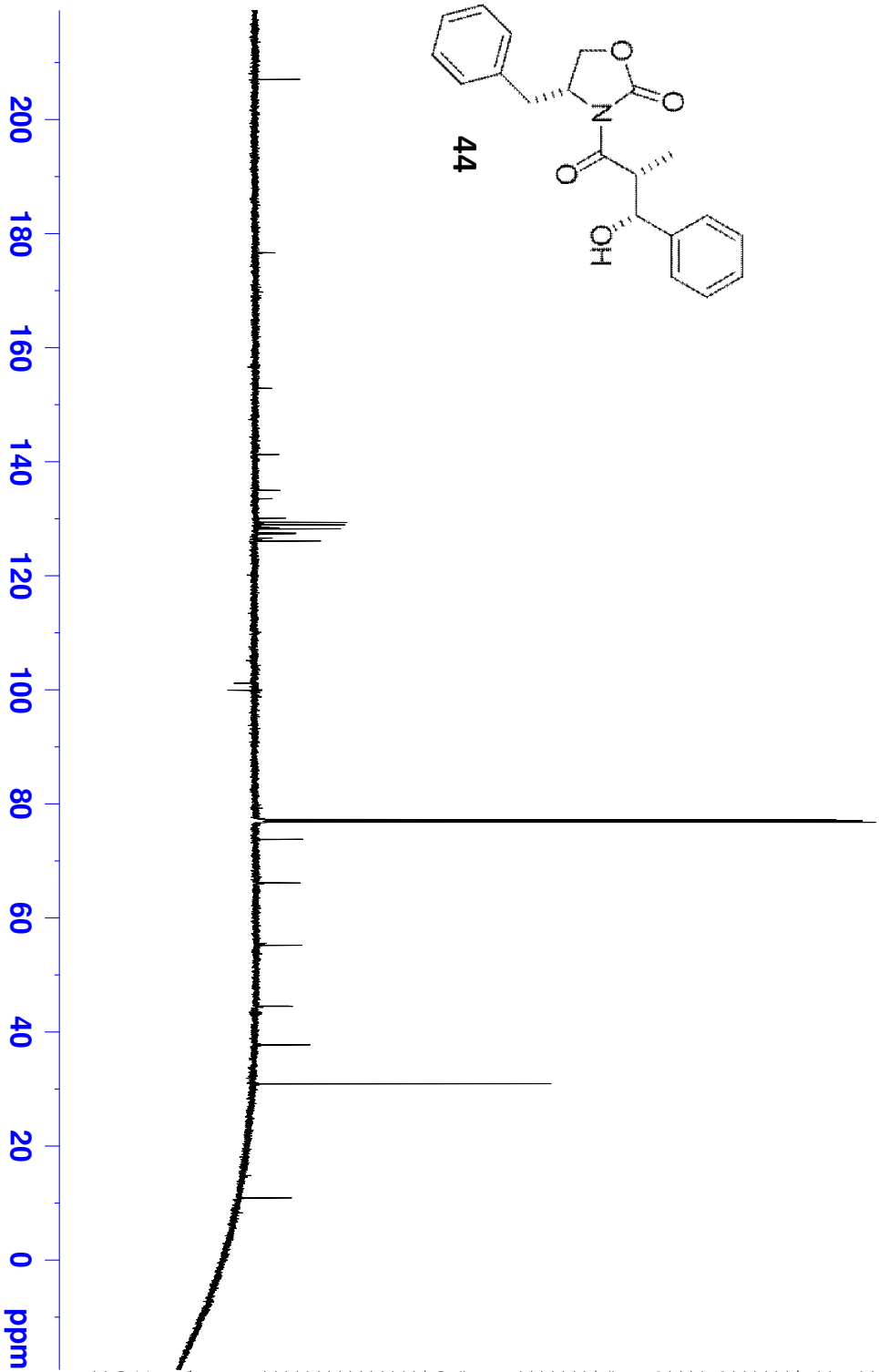
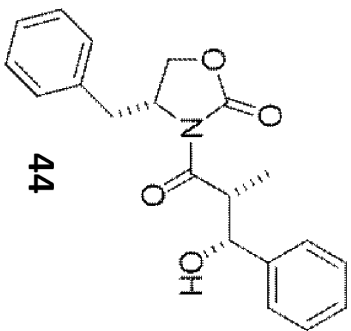
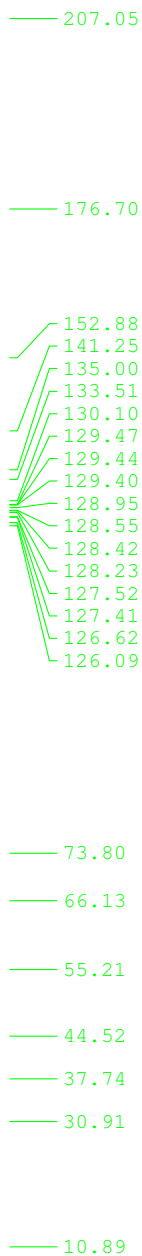


```

NAME          DMB3-20f72
EXPNO         1
PROCNO        1
Date_         20130206
Time          15.51
INSTRUM       spect
PROBHD        5 mm CPTCI 1H-
PULPROG       zg30
TD            65536
SOLVENT       CDCl3
NS            16
DS            2
SWH           12376.237 Hz
FIDRES        0.188846 Hz
AQ            2.6477449 sec
RG            16
DE            40.400 usec
TE            293.0 K
D1            1.00000000 sec
TD0           1

===== CHANNEL f1 =====
NUC1          1H
P1            8.00 usec
PL1           4.00 dB
PL1W          7.00000000 W
SFO1          600.1337060 MHz
SI            32768
SF            600.1300162 MHz
WDW           EM
SSB           0
LB            0.30 Hz
GB            0
PC            1.00
  
```

DMB3-20 Aldol Product



```

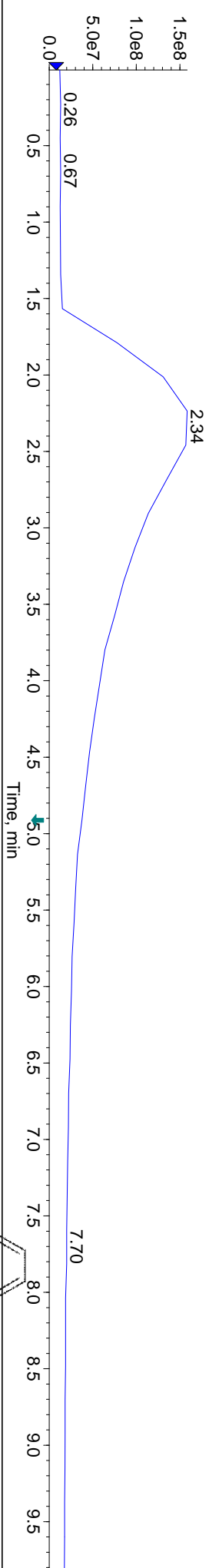
NAME DMB3-20
EXPNO 8
PROCNO 1
Date_ 20130827
Time 16.50
INSTRUM spect
PROBHD 5 mm CPIC1 1H-
PULPROG zgpg30
TD 65536
SOLVENT CDCl3
NS 512
DS 4
SWH 35971.223 Hz
FIDRES 0.548877 Hz
AQ 0.9110143 sec
RG 8
DW 13.900 usec
DE 6.50 usec
TE 298.0 K
D1 2.00000000 sec
D11 0.03000000 sec
TD0 1

===== CHANNEL f1 =====
NUC1 13C
P1 12.00 usec
PL1 -0.70 dB
PL1W 82.63385773 W
SFO1 150.9178988 MHz

===== CHANNEL f2 =====
CPDPRG2 waltz16
NUC2 1H
PCPD2 80.00 usec
PL2 4.00 dB
PL12 24.00 dB
PL13 27.00 dB
PL2W 7.00000000 W
PL12W 0.07000000 W
PL13W 0.03508311 W
SFO2 600.1324005 MHz
SI 32768
SF 150.9028147 MHz
WDW EM
SSB 0
LB 1.00 Hz
GB 0
PC 1.40
  
```

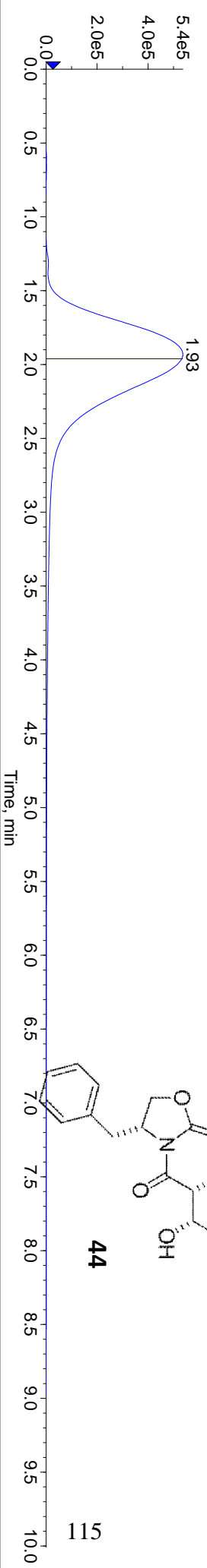
■ TIC: from Sample 1 (DMB3-20f100) of DMB3-20f100.wiff (Turbo Spray)

Max. 1.6e8 cps.



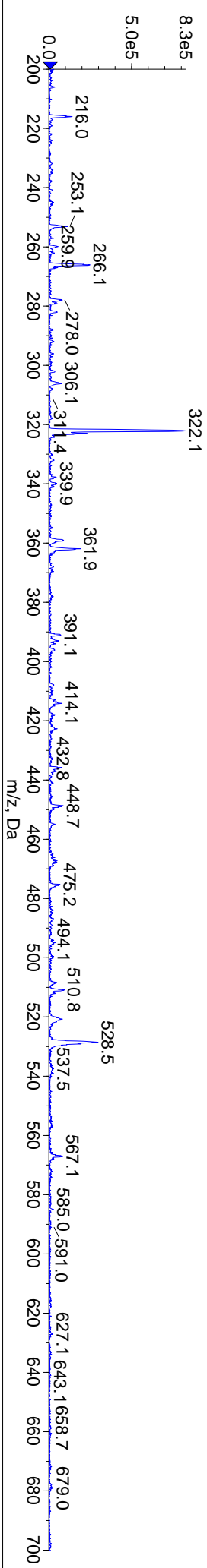
■ Shimadzu LC Controller Detector A, Channel 1 from Sample 1 (DMB3-20f100) of DMB3-20f100.wiff

Max. 5.4e5 .



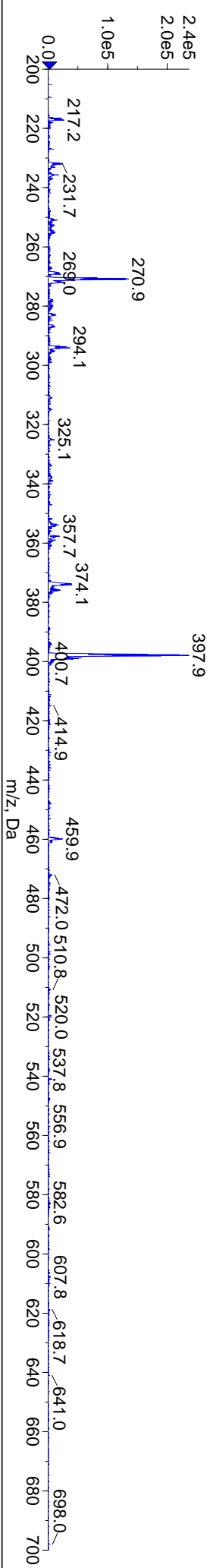
■ +Q1: Exp 1, 1.790 min from Sample 1 (DMB3-20f100) of DMB3-20f100.wiff (Turbo Spray)

Max. 8.3e5 cps.

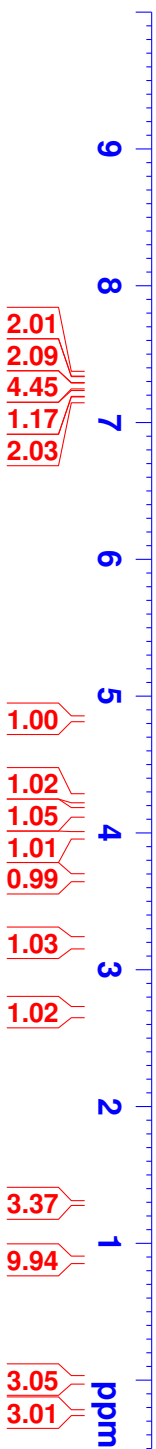
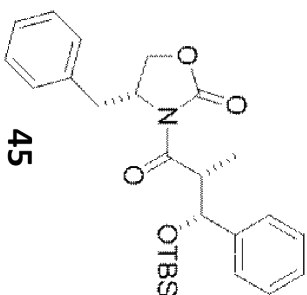
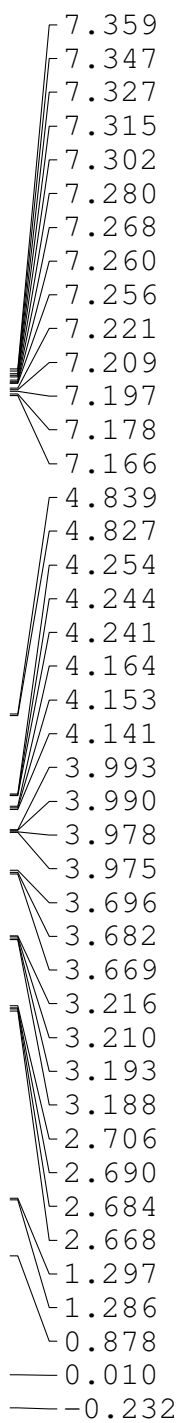


■ -Q1: Exp 2, 1.901 min from Sample 1 (DMB3-20f100) of DMB3-20f100.wiff (Turbo Spray)

Max. 2.4e5 cps.

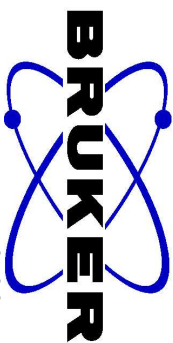
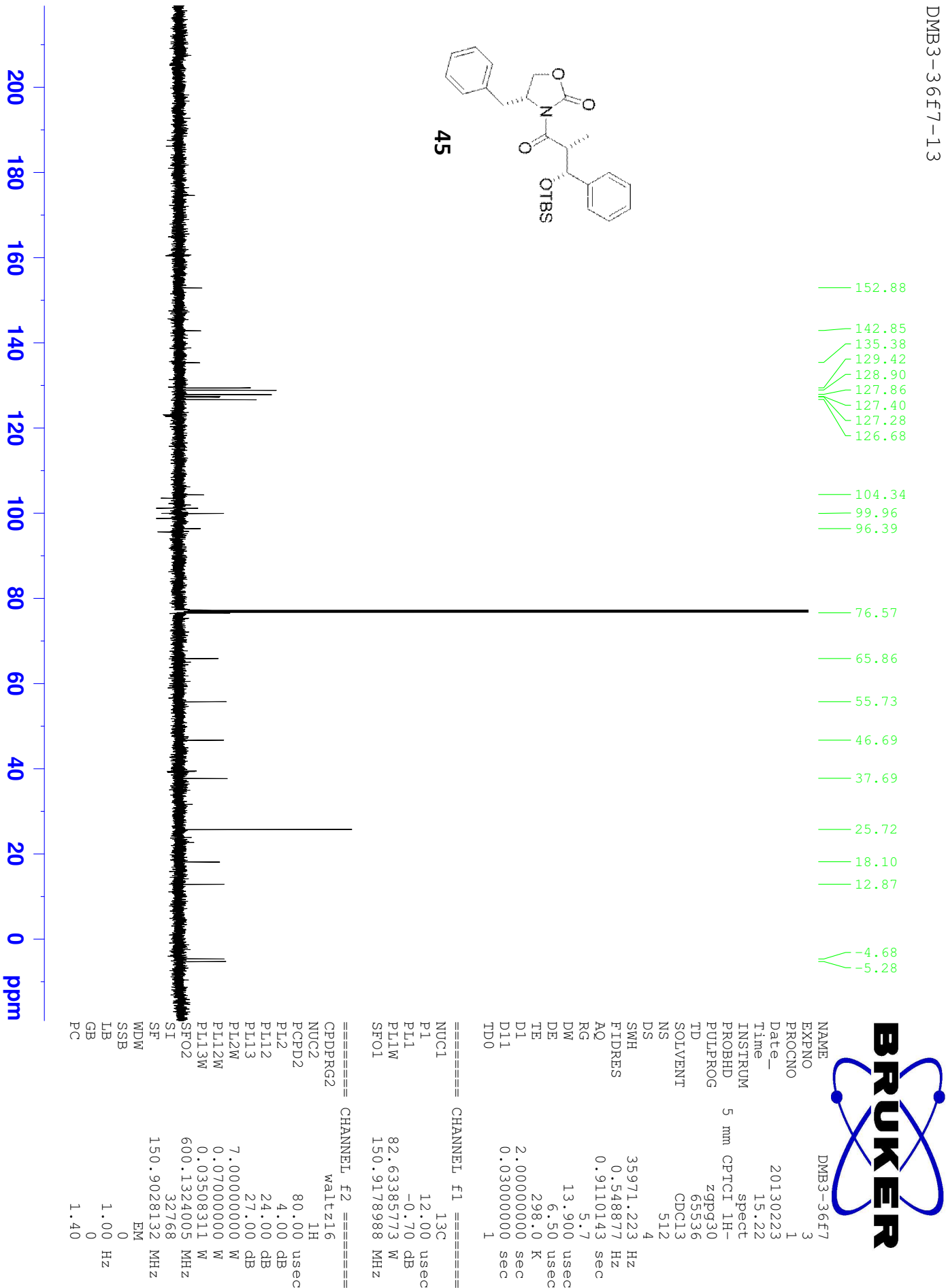
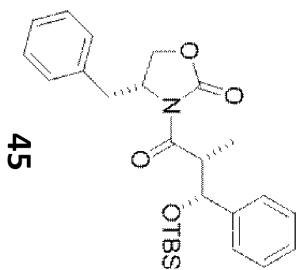


DMB3-36f7-13



NAME DMB3-36f7
EXPNO 2
PROCNO 1
Date_ 20130223
Time 14.53
INSTRUM spect
PROBHD 5 mm CPTCI 1H-
PULPROG zg30
TD 65536
SOLVENT CDCl3
NS 16
DS 2
SWH 12376.237 Hz
FIDRES 0.188846 Hz
AQ 2.6477449 sec
RG 14.3
DW 40.400 usec
DE 6.50 usec
TE 298.0 K
D1 1.0000000 sec
TD0 1

===== CHANNEL f1 =====
NUC1 1H
P1 8.00 usec
PL1 4.00 dB
PL1W 7.00000000 W
SFO1 600.1337060 MHz
SI 32768
SF 600.1300161 MHz
WDW EM
SSB 0
LB 0.30 Hz
GB 0
PC 1.00



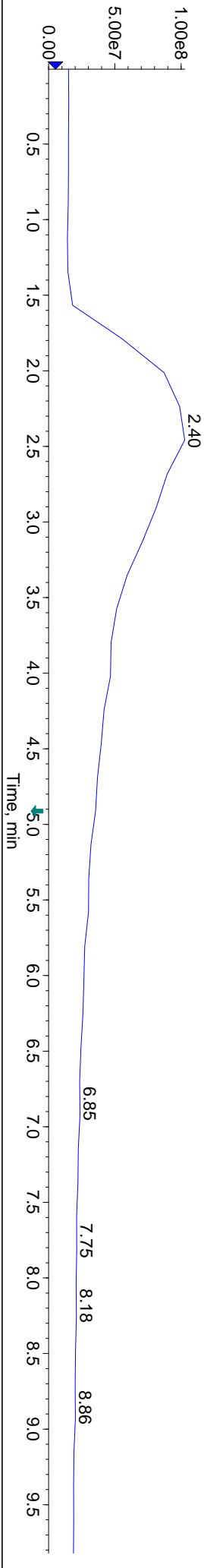
NAME DMB3-36f7
EXPNO 3
PROCNO 1
Date_ 20130223
Time 15.22
INSTRUM spect
PROBHD 5 mm CPTCI 1H-
PULPROG zgpg30
TD 65536
SOLVENT CDCl3
NS 512
DS 4
SWH 35971.223 Hz
FIDRES 0.548877 Hz
AQ 0.9110143 sec
RG 5.7
DW 13.900 usec
DE 6.50 usec
TE 298.0 K
D1 2.00000000 sec
D11 0.03000000 sec
TD0 1

===== CHANNEL f1 =====
NUC1 13C
P1 12.00 usec
PL1 -0.70 dB
PL1W 82.63385773 W
SFO1 150.9178988 MHz

===== CHANNEL f2 =====
CPDPRG2 waltz16
NUC2 1H
PCPD2 80.00 usec
PL2 4.00 dB
PL12 24.00 dB
PL13 27.00 dB
PL2W 7.00000000 W
PL12W 0.07000000 W
PL13W 0.03508311 W
SFO2 600.1324005 MHz
SI 32768
SF 150.9028132 MHz
WDW EM
SSB 0
LB 1.00 Hz
GB 0
PC 1.40

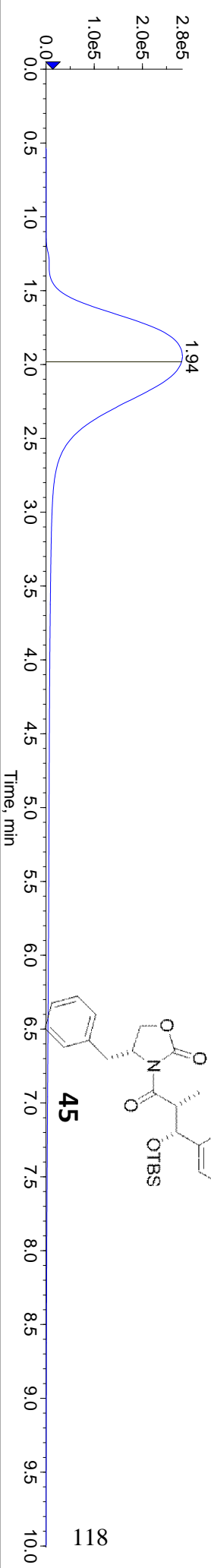
TIC: from Sample 1 (DMB3-36f) of DMB3-36f7-13.wiff (Turbo Spray)

Max. 1.0e8 cps.



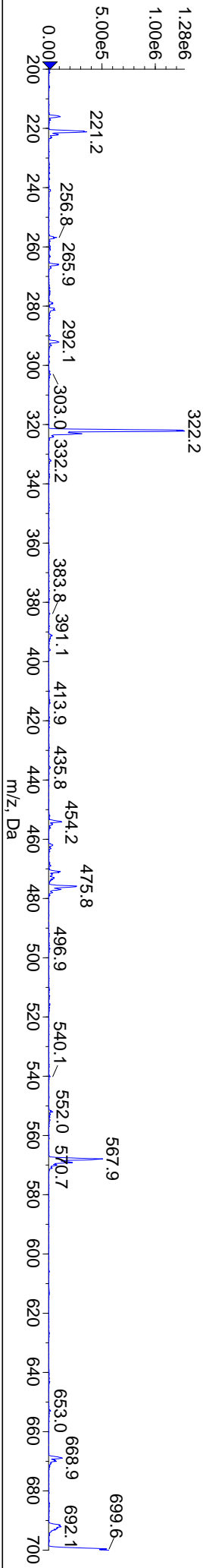
Shimadzu LC Controller Detector A, Channel 1 from Sample 1 (DMB3-36f) of DMB3-36f7-13.wiff

Max. 2.8e5



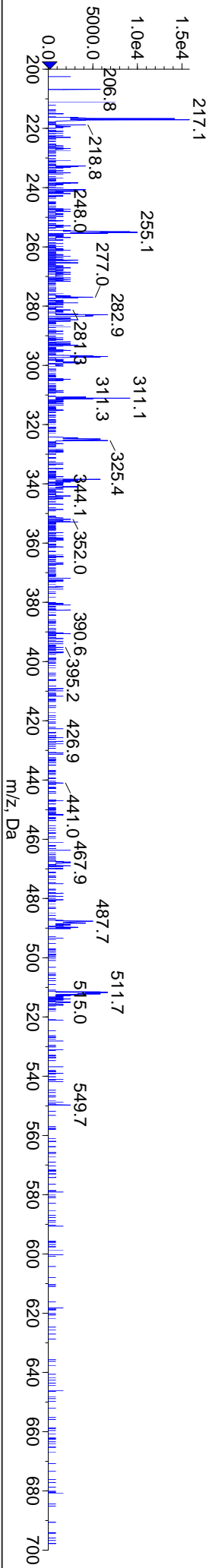
+Q1: Exp 1, 1.790 min from Sample 1 (DMB3-36f) of DMB3-36f7-13.wiff (Turbo Spray)

Max. 1.3e6 cps.

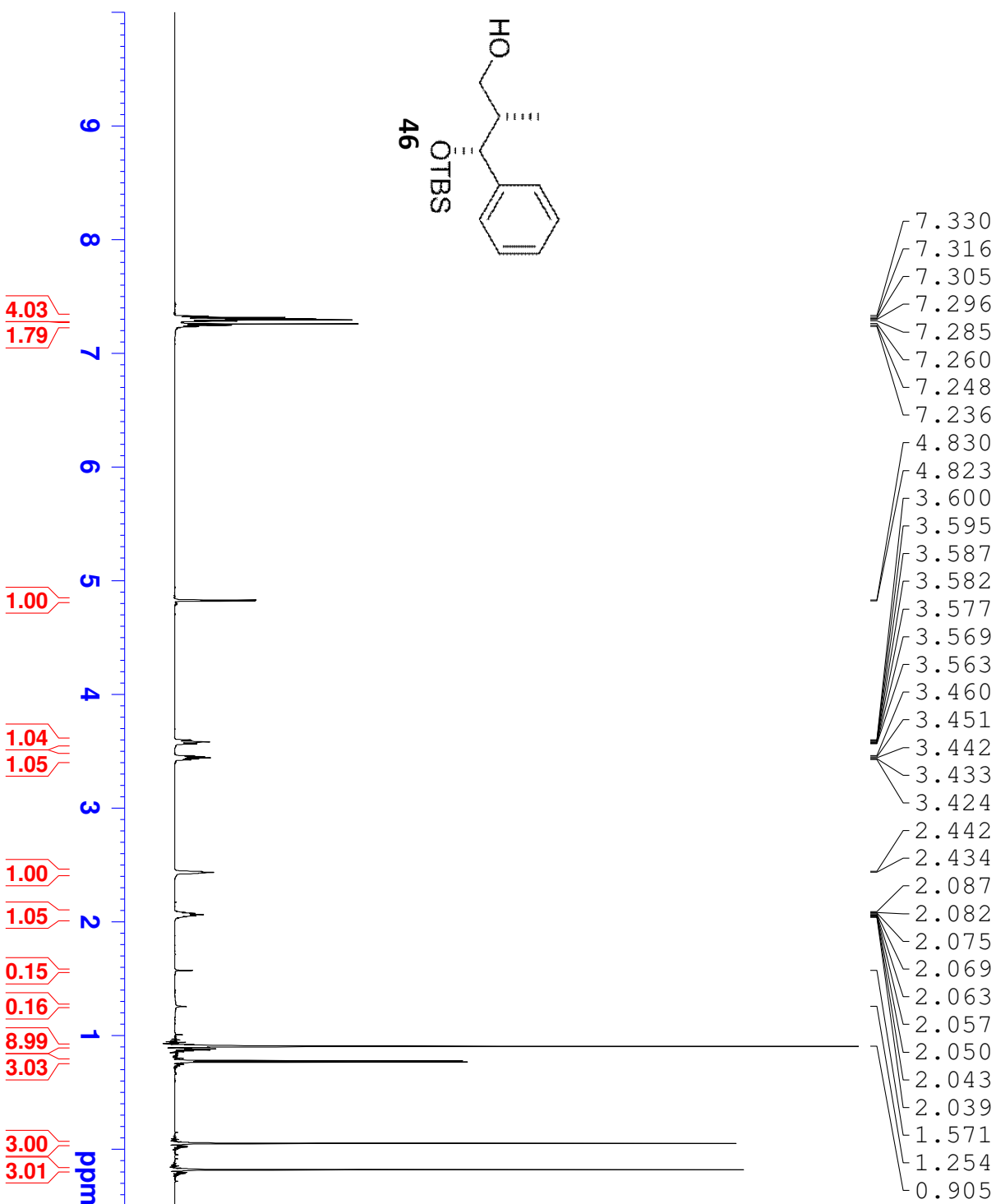


-Q1: Exp 2, 1.901 min from Sample 1 (DMB3-36f) of DMB3-36f7-13.wiff (Turbo Spray)

Max. 1.6e4 cps.



DMB3-26f8-17



NAME DMB3-26f8
EXPNO 2
PROCNO 1
Date_ 20130226
Time 11.55
INSTRUM spect
PROBHD 5 mm CPTCI 1H-
PULPROG zg30
TD 65536
SOLVENT CDCl3
NS 16
DS 2
SWH 12376.237 Hz
FIDRES 0.188846 Hz
AQ 2.6477449 sec
RG 14.3
DW 40.400 usec
DE 6.50 usec
TE 298.0 K
D1 1.00000000 sec
TD0 1

===== CHANNEL f1 =====
NUC1 1H
P1 8.00 usec
PL1 4.00 dB
PL1W 7.00000000 W
SFO1 600.1337060 MHz
SI 32768
SF 600.1300159 MHz
WDW EM
SSB 0
LB 0.30 Hz
GB 0
PC 1.00

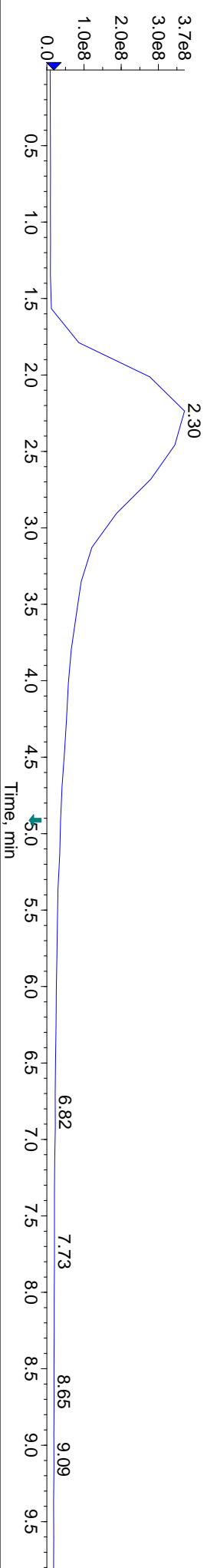
DMB3-26F8-17



NAME	DMB3-26f8
EXPNO	3
PROCNO	1
Date_	20130226
Time	12.10
INSTRUM	spect
PROBHD	5 mm CPTCI 1H-
PULPROG	zgpg30
TD	65536
SOLVENT	CDCl3
NS	256
DS	4
SMH	35971.223 Hz
FIDRES	0.548877 Hz
AQ	0.9110143 sec
RG	5.7
DW	13.900 usec
DE	6.50 usec
TE	298.0 K
D1	2.00000000 sec
D11	0.03000000 sec
TD0	1
===== CHANNEL f1 =====	
NUC1	13C
P1	12.00 usec
PL1	-0.70 dB
PL1W	82.63385773 W
SFO1	150.9178988 MHz
===== CHANNEL f2 =====	
CPDPRG2	waltz16
NUC2	1H
PCPD2	80.00 usec
P12	4.00 dB
PL12	24.00 dB
PL13	27.00 dB
PL1W	7.00000000 W
PL12W	0.07000000 W
PL13W	0.03508311 W
SFO2	600.1324005 MHz
SI	32768
SF	150.9028131 MHz
WDW	EM
SSB	0
LB	1.00 Hz
GB	0
PC	1.40

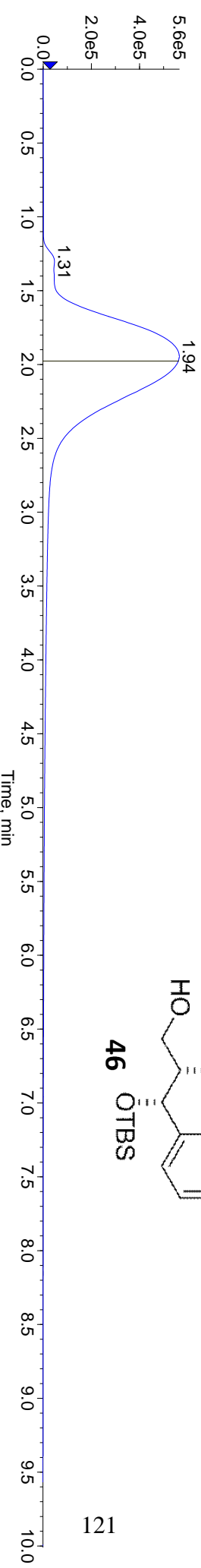
TIC: from Sample 1 (DMB3-26f8-22) of DMB3-26f8.wiff (Turbo Spray)

Max. 3.7e8 cps.



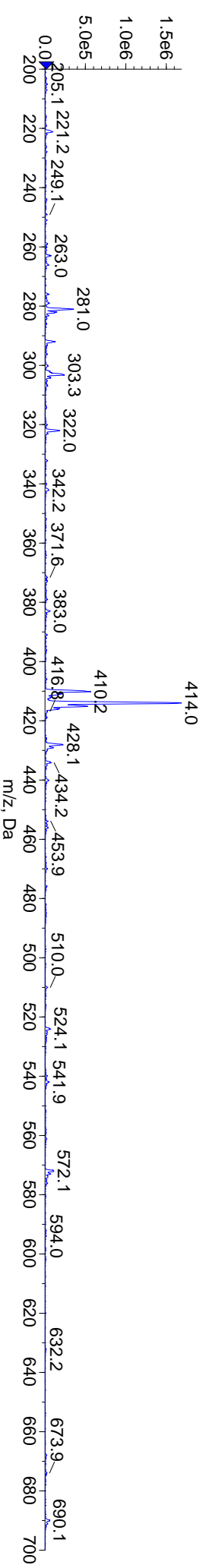
Shimadzu LC Controller Detector A, Channel 1 from Sample 1 (DMB3-26f8-22) of DMB3-26f8.wiff

Max. 5.6e5 .



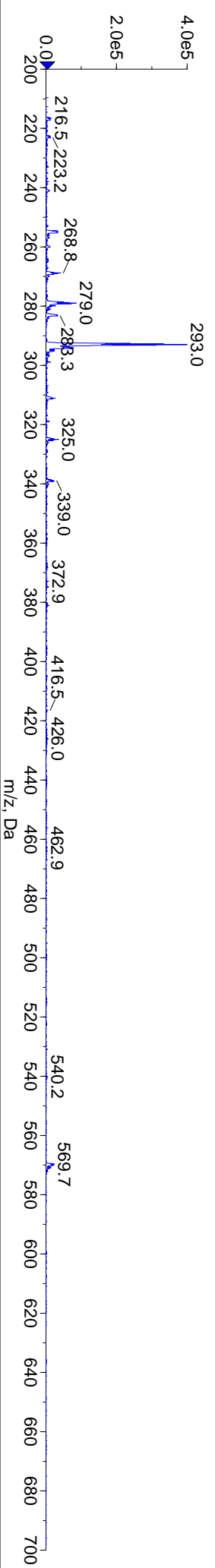
+Q1: Exp 1, 1.790 min from Sample 1 (DMB3-26f8-22) of DMB3-26f8.wiff (Turbo Spray)

Max. 1.7e6 cps.



-Q1: Exp 2, 1.901 min from Sample 1 (DMB3-26f8-22) of DMB3-26f8.wiff (Turbo Spray)

Max. 4.0e5 cps.



DMB3-59crude

9.765
9.764

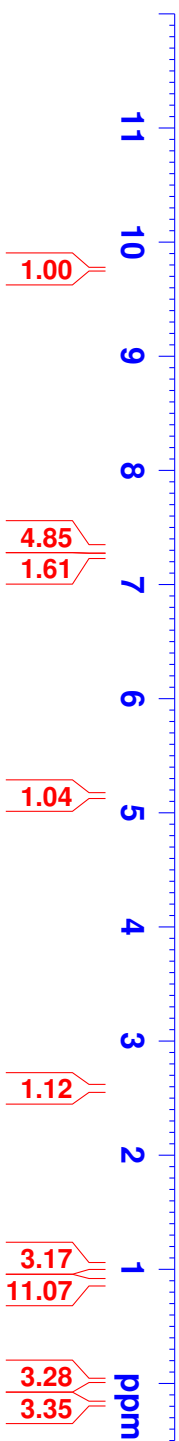
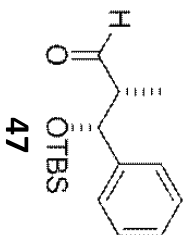
7.336
7.323
7.311
7.301
7.294
7.282
7.264
7.259
7.253

5.157
5.149

2.605
2.595
2.594
2.586
2.584
2.582
2.576
2.575
2.565
2.563

1.044
1.033
0.886

0.031
-0.175



NAME DMB3-59
EXPNO 1
PROCNO 1
Date_ 20130320
Time 9.41
INSTRUM spect
PROBHD 5 mm CPIC1 1H-
PULPROG zg30
TD 65536
SOLVENT CDCl3
NS 16
DS 2
SWH 12376.237 Hz
FIDRES 0.188846 Hz
AQ 2.6477449 sec
RG 14.3
DW 40.400 usec
DE 6.50 usec
TE 298.0 K
D1 1.00000000 sec
TD0 1

===== CHANNEL f1 =====
NUC1 1H
P1 8.00 usec
PL1 4.00 dB
PL1W 7.00000000 W
SFO1 600.1337060 MHz
SI 32768
SF 600.1300167 MHz
WDW EM
SSB 0
LB 0.30 Hz
GB 0
PC 1.00

DMB2-141f25-29

7.318
7.313
7.308
7.304
7.295
7.292
7.270
7.260
7.247
7.245
7.233
5.806
5.795
5.021
5.019
4.993
4.990
4.946
4.945
4.943
4.926
4.816
4.808
3.726
3.723
3.718
2.344
1.676
1.673
1.665
1.442
1.434
0.914
0.909
0.888
0.877
0.734
0.722
0.065
0.056
-0.176
-0.267



NAME DMB2-141f25

EXPNO 1

PROCNO 1

Date_ 20120529

Time 8.50

INSTRUM spect

PROBHD 5 mm CPTCI 1H-

PULPROG zg30

TD 65536

SOLVENT CDCl3

NS 16

DS 2

SWH 12376.237 Hz

FIDRES 0.188846 Hz

AQ 2.6477449 sec

RG 9

DW 40.400 usec

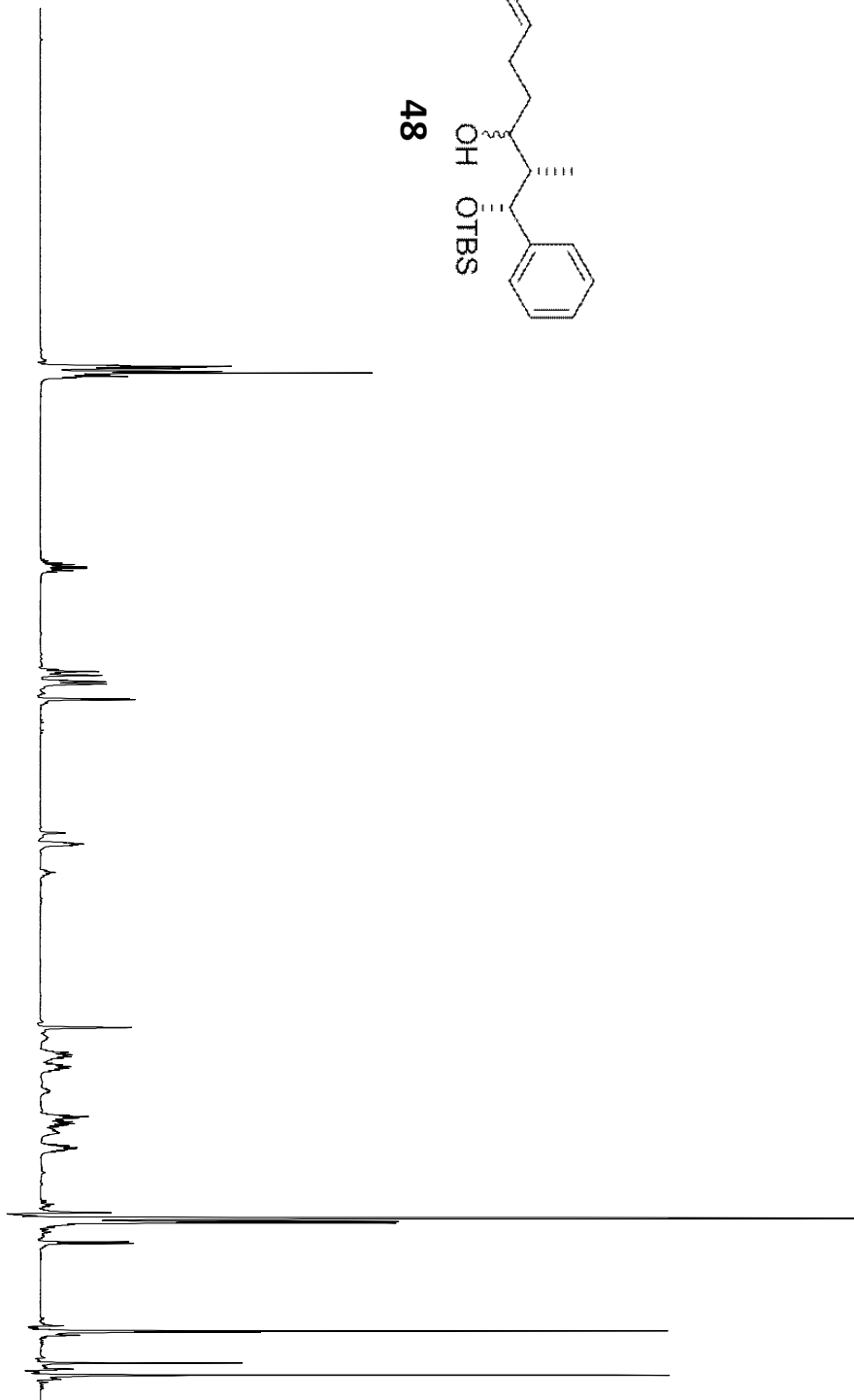
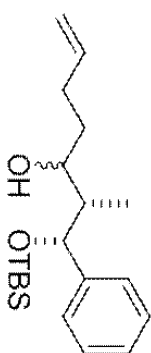
DE 6.50 usec

TE 298.0 K

D1 1.00000000 sec

TD0 1

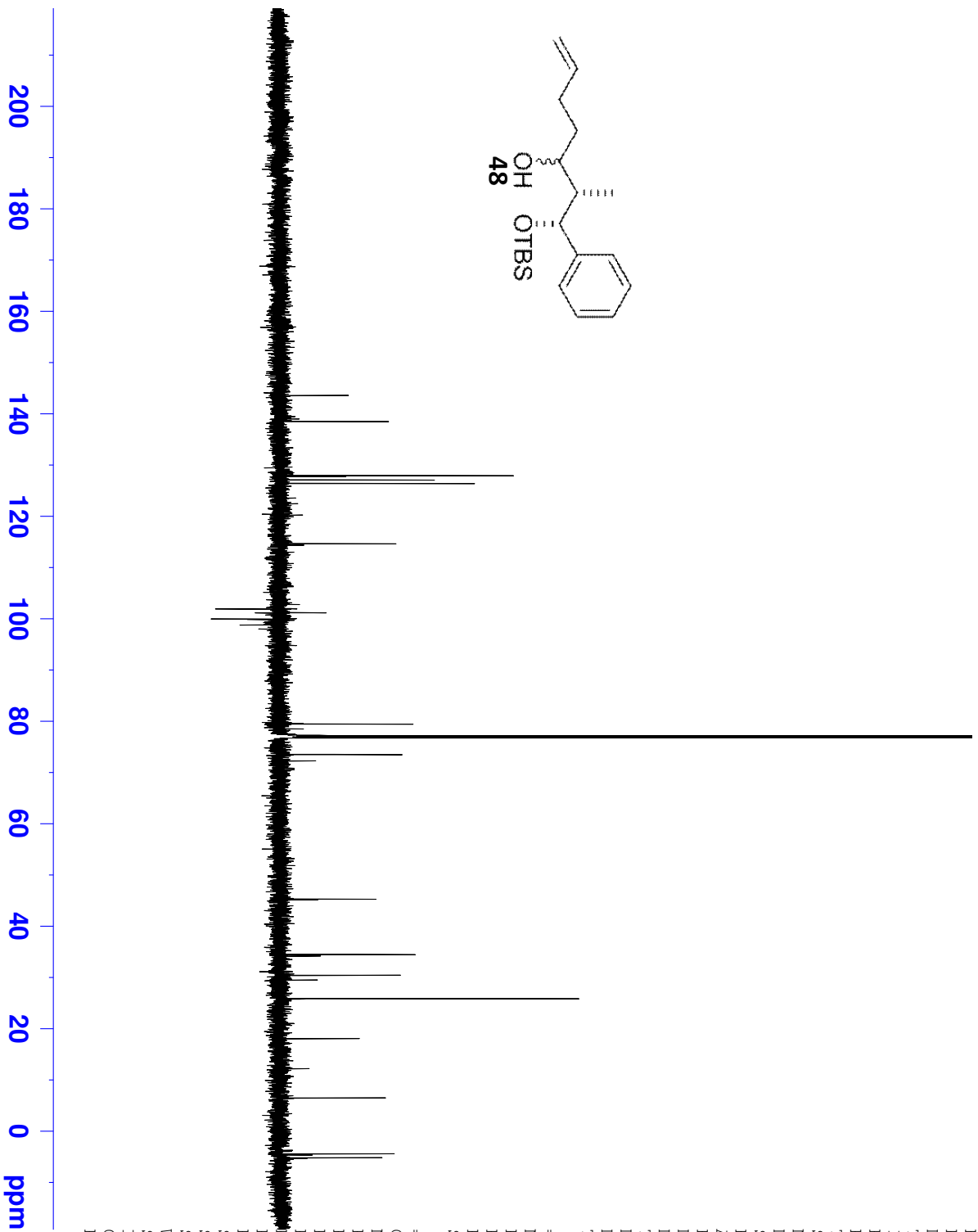
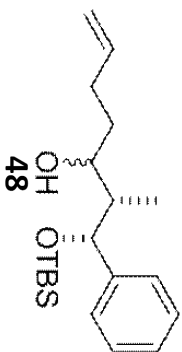
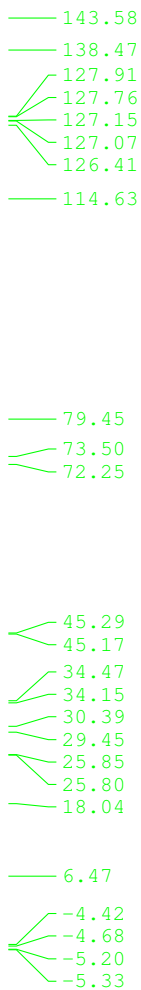
48



3.20
3.04
1.48
0.08
1.19
1.32
1.63
1.00
0.28
0.05
0.99
0.32
0.92
0.30
1.44
1.12
0.32
0.93
1.17
0.75
1.34
0.08
11.43
4.21
0.88
2.60
1.24

ppm

===== CHANNEL f1 =====
NUC1 1H
P1 8.00 usec
PL1 4.00 dB
PL1W 7.00000000 W
SFO1 600.1337060 MHz
SI 32768
SF 600.1300159 MHz
WDW EM
SSB 0
LB 0.30 Hz
GB 0
PC 1.00



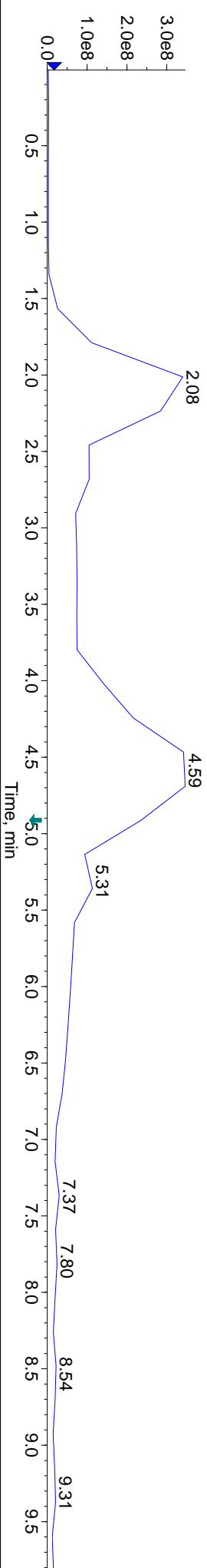
NAME DMB2-141f25
EXPNO 2
PROCNO 1
Date_ 20120529
Time 9.18
INSTRUM spect
PROBHD 5 mm CPTCI 1H-
PULPROG zgpg30
TD 65536
SOLVENT CDCl3
NS 512
DS 2
SWH 35971.223 Hz
FIDRES 0.548877 Hz
AQ 0.9110143 sec
RG 4.5
DE 13.900 usec
TE 298.0 K
D1 2.00000000 sec
D11 0.03000000 sec
TD0 1

===== CHANNEL f1 =====
NUC1 13C
P1 12.00 usec
PL1 -0.70 dB
PL1W 82.63385773 W
SFO1 150.9178988 MHz

===== CHANNEL f2 =====
CPDPRG2 waltz16
NUC2 1H
PCPD2 80.00 usec
PL2 4.00 dB
PL12 24.00 dB
PL13 27.00 dB
PL12W 7.00000000 W
PL12W 0.07000000 W
PL13W 0.03508311 W
SFO2 600.1324005 MHz
SI 32768
SF 150.9028132 MHz
WDW EM
SSB 0
LB 1.00 Hz
GB 0
PC 1.40

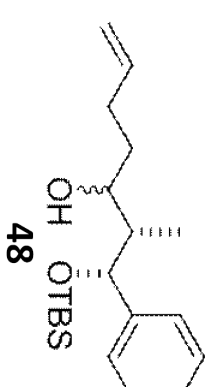
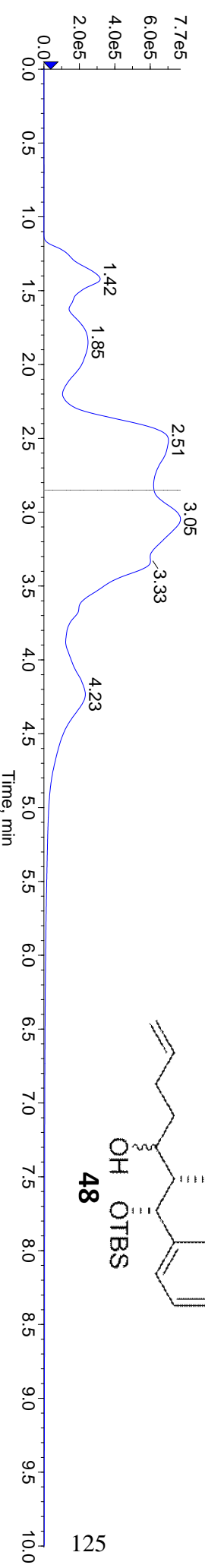
TIC: from Sample 1 (Sample002) of DMB2-48f6-8.wiff (Turbo Spray)

Max. 3.5e8 cps.



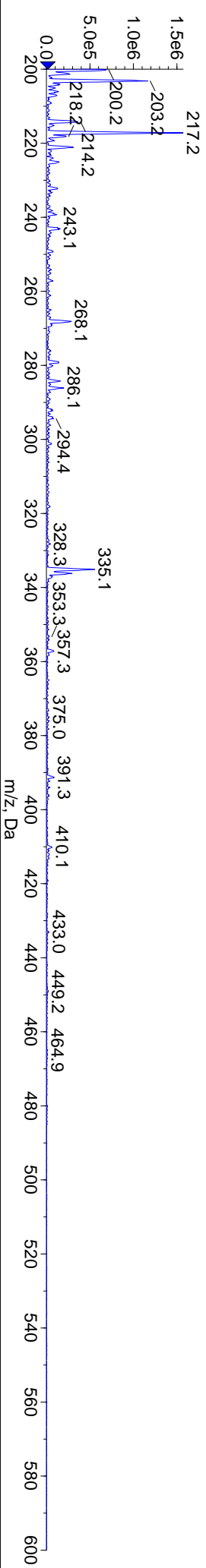
Shimadzu LC Controller Detector A, Channel 1 from Sample 1 (Sample002) of DMB2-48f6-8.wiff

Max. 7.7e5 .



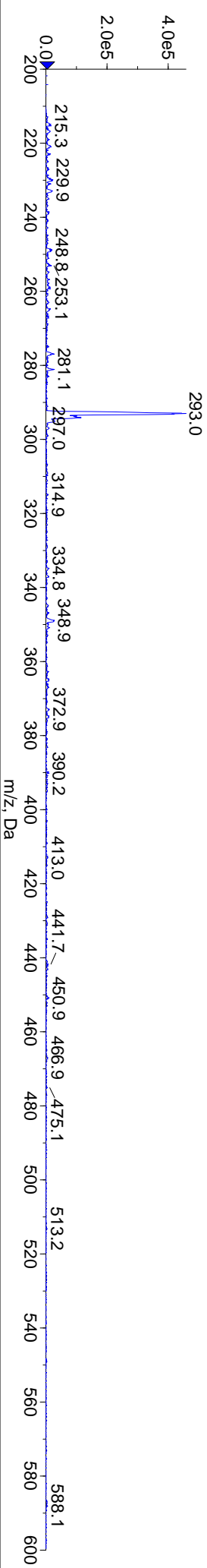
+Q1: Exp 1, 2.682 min from Sample 1 (Sample002) of DMB2-48f6-8.wiff (Turbo Spray)

Max. 1.6e6 cps.

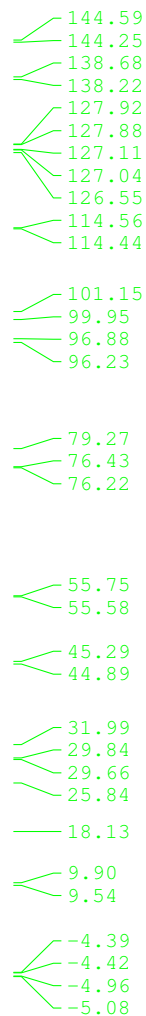


-Q1: Exp 2, 2.793 min from Sample 1 (Sample002) of DMB2-48f6-8.wiff (Turbo Spray)

Max. 4.6e5 cps.



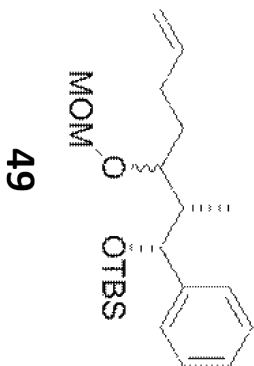
DMB2-89f26-30 C13



NAME DMB2-89f26
EXPNO 2
PROCNO 1
Date_ 20120125
Time 11.55
INSTRUM spect
PROBHD 5 mm CPTCI 1H-
PULPROG zgpg30
TD 65536
SOLVENT CDCl3
NS 512
DS 4
SWH 35971.223 Hz
FIDRES 0.54877 Hz
AQ 0.9110143 sec
RG 5
DW 13.900 usec
DE 6.50 usec
TE 298.0 K
D1 2.00000000 sec
D11 0.03000000 sec
TD0 1

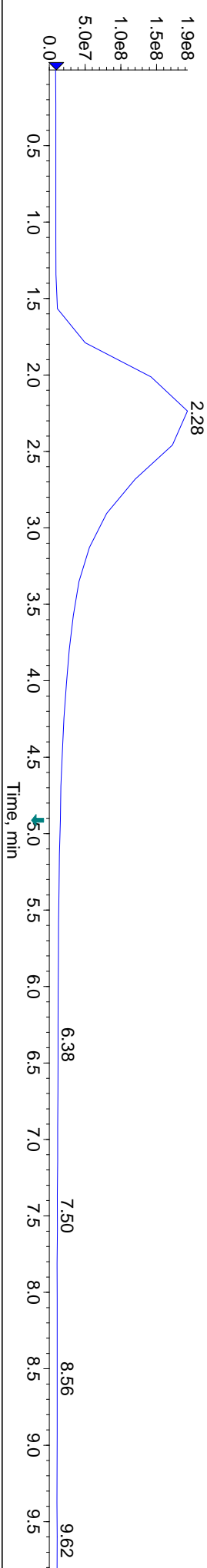
===== CHANNEL f1 =====
NUC1 13C
P1 12.00 usec
PL1 -0.70 dB
PL1W 82.63385773 W
SFO1 150.9178988 MHz

===== CHANNEL f2 =====
CPDPRG2 waltz16
NUC2 1H
PCPD2 80.00 usec
PL2 4.00 dB
PL12 24.00 dB
PL13 27.00 dB
PL2W 7.00000000 W
PL12W 0.07000000 W
PL13W 0.03508311 W
SFO2 600.1324005 MHz
SI 32768
SF 150.9028142 MHz
WDW EM
SSB 0
LB 1.00 Hz
GB 0
PC 1.40



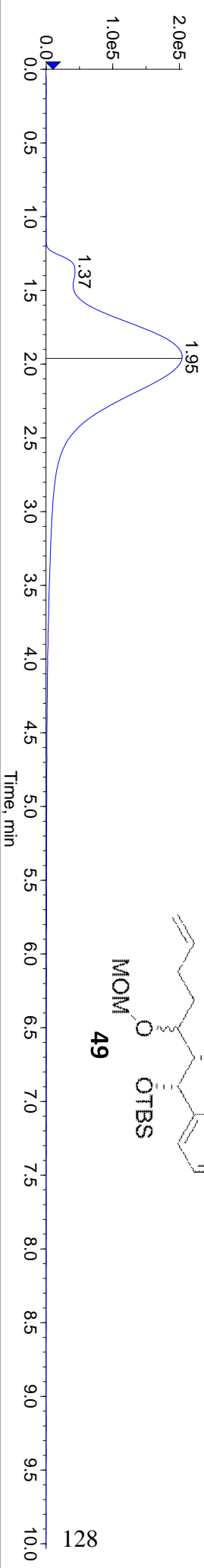
TIC: from Sample 1 (DMB2-125f6-7) of DMB2-125f6-7.wiff (Turbo Spray)

Max. 1.9e8 cps.



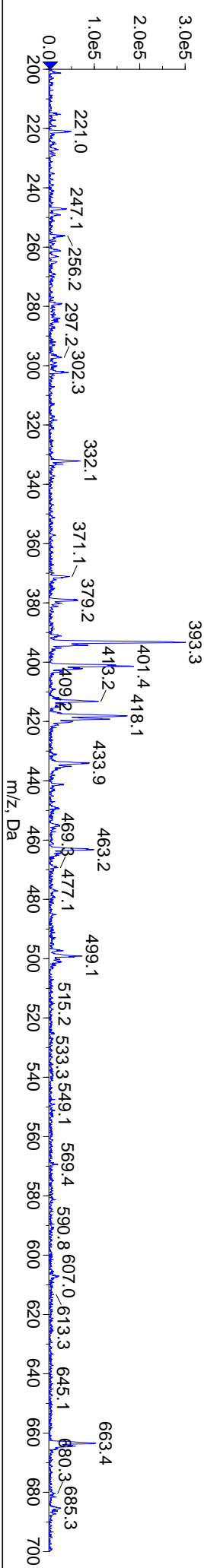
Shimadzu LC Controller Detector A, Channel 1 from Sample 1 (DMB2-125f6-7) of DMB2-125f6-7.wiff

Max. 2.0e5 .



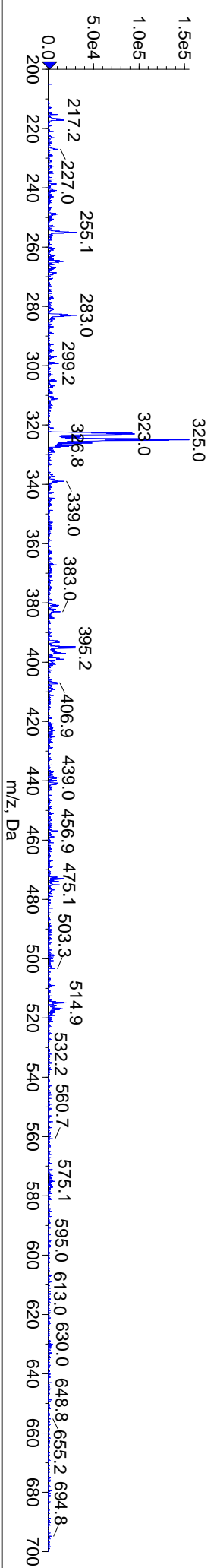
+Q1: Exp 1, 1.790 min from Sample 1 (DMB2-125f6-7) of DMB2-125f6-7.wiff (Turbo Spray)

Max. 3.0e5 cps.

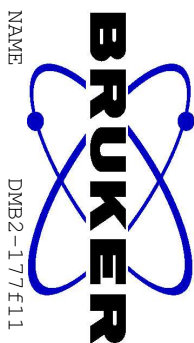


-Q1: Exp 2, 1.901 min from Sample 1 (DMB2-125f6-7) of DMB2-125f6-7.wiff (Turbo Spray)

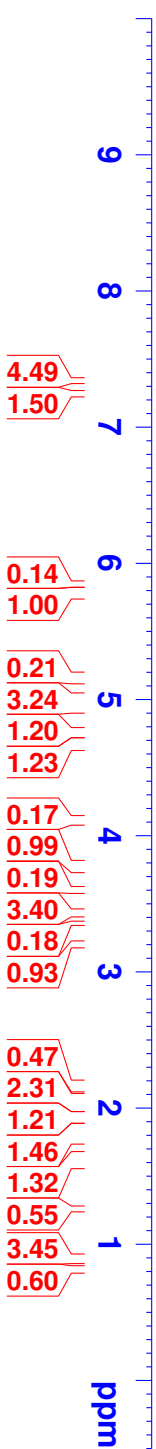
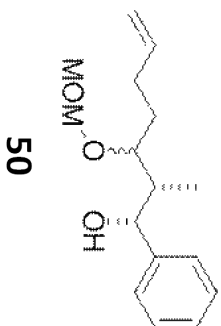
Max. 1.6e5 cps.



DMB2-177f11-12



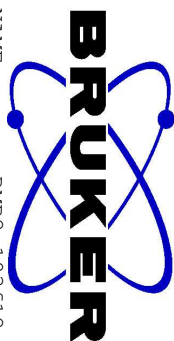
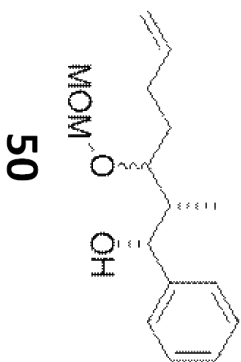
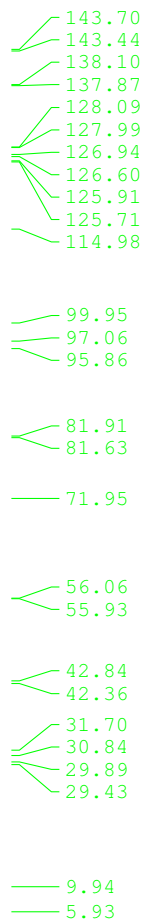
7.350
7.344
7.341
7.261
7.255
7.250
7.245
7.241
5.790
5.779
5.032
5.004
4.982
4.965
4.946
4.769
4.758
4.666
4.655
3.779
3.437
3.204
3.201
2.049
2.045
2.038
2.025
1.935
1.929
1.923
1.918
1.823
1.813
1.807
1.630
1.625
1.616
1.260
0.903
0.892
0.819
0.807



NAME DMB2-177f11
EXPNO 1
PROCNO 1
Date_ 20120719
Time 13.08
INSTRUM spect
PROBHD 5 mm CPTCI 1H-
PULPROG zg30
TD 65536
SOLVENT CDCl3
NS 16
DS 2
SWH 12376.237 Hz
FIDRES 0.188846 Hz
AQ 2.6477449 sec
RG 8
DW 40.400 usec
DE 6.50 usec
TE 298.0 K
D1 1.00000000 sec
TD0 1

===== CHANNEL f1 =====
NUC1 1H
P1 8.00 usec
PL1 4.00 dB
PL1W 7.00000000 W
SFO1 600.1337060 MHz
SI 32768
SF 600.1300147 MHz
WDW EM
SSB 0
LB 0.30 Hz
GB 0
PC 1.00

DMB2-103f12-13 13C



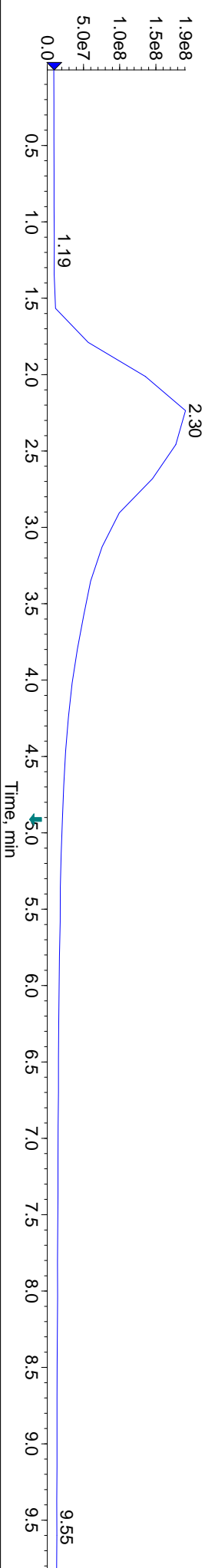
NAME DMB2-103f12
EXPNO 2
PROCNO 1
Date_ 20120202
Time 11.49
INSTRUM spect
PROBHD 5 mm CPTCI 1H-
PULPROG zgpg30
TD 65536
SOLVENT CDCl3
NS 512
DS 4
SWH 35971.223 Hz
FIDRES 0.548877 Hz
AQ 0.9110143 sec
RG 4.5
DW 13.900 usec
DE 6.50 usec
TE 298.0 K
D1 2.00000000 sec
D11 0.03000000 sec
TD0 1

===== CHANNEL f1 =====
NUC1 13C
P1 12.00 usec
PL1 -0.70 dB
PL1W 82.63385773 W
SFO1 150.9178988 MHz

===== CHANNEL f2 =====
CPDPRG2 waltz16
NUC2 1H
PCPD2 80.00 usec
PL2 4.00 dB
PL12 24.00 dB
PL13 27.00 dB
PL2W 7.00000000 W
PL12W 0.07000000 W
PL13W 0.03508311 W
SFO2 600.1324005 MHz
SI 32768
SF 150.9028175 MHz
WDW EM
SSB 0
LB 1.00 Hz
GB 0
PC 1.40

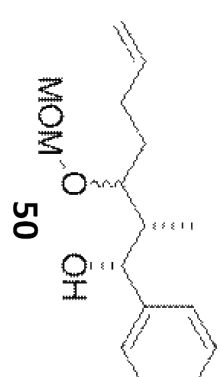
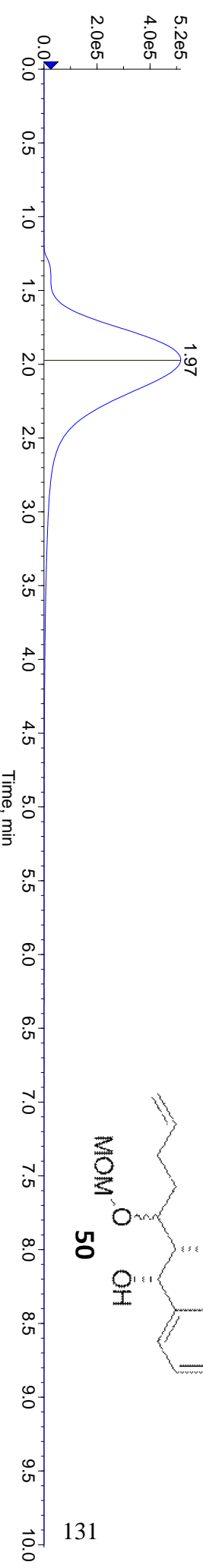
TIC: from Sample 1 (DMB2-125f10-12) of DMB2-125f10-12.wiff (Turbo Spray)

Max. 1.9e8 cps.



Shimadzu LC Controller Detector A, Channel 1 from Sample 1 (DMB2-125f10-12) of DMB2-125f10-12.wiff

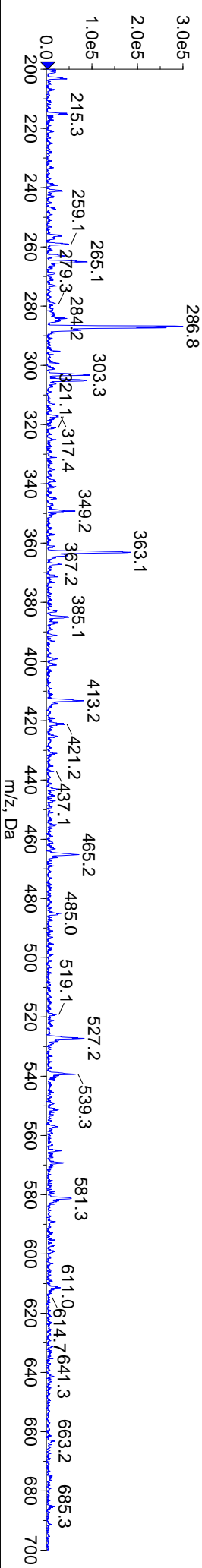
Max. 5.2e5 cps.



50

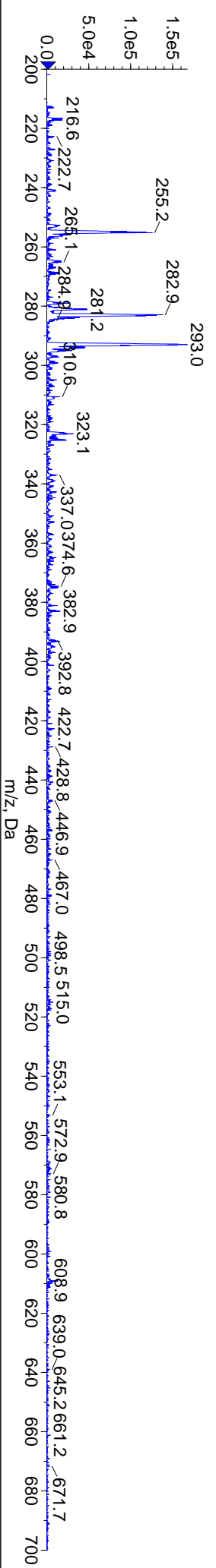
+Q1: Exp 1, 1.790 min from Sample 1 (DMB2-125f10-12) of DMB2-125f10-12.wiff (Turbo Spray)

Max. 3.0e5 cps.

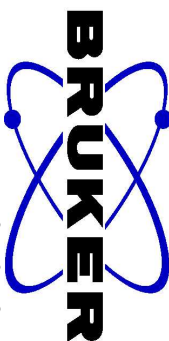


-Q1: Exp 2, 1.901 min from Sample 1 (DMB2-125f10-12) of DMB2-125f10-12.wiff (Turbo Spray)

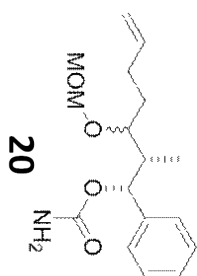
Max. 1.7e5 cps.



DMB2-197f31-47



7.344
7.331
7.319
7.310
7.298
7.283
7.280
7.269
7.260
5.745
5.741
5.733
5.723
5.712
4.969
4.966
4.940
4.938
4.916
4.899
4.657
4.608
4.601
4.590
4.519
4.508
3.397
3.253
3.247
2.111
2.105
2.002
1.990
1.978
1.693
1.682
1.643
1.632
1.619
1.590
1.251
1.037
1.026



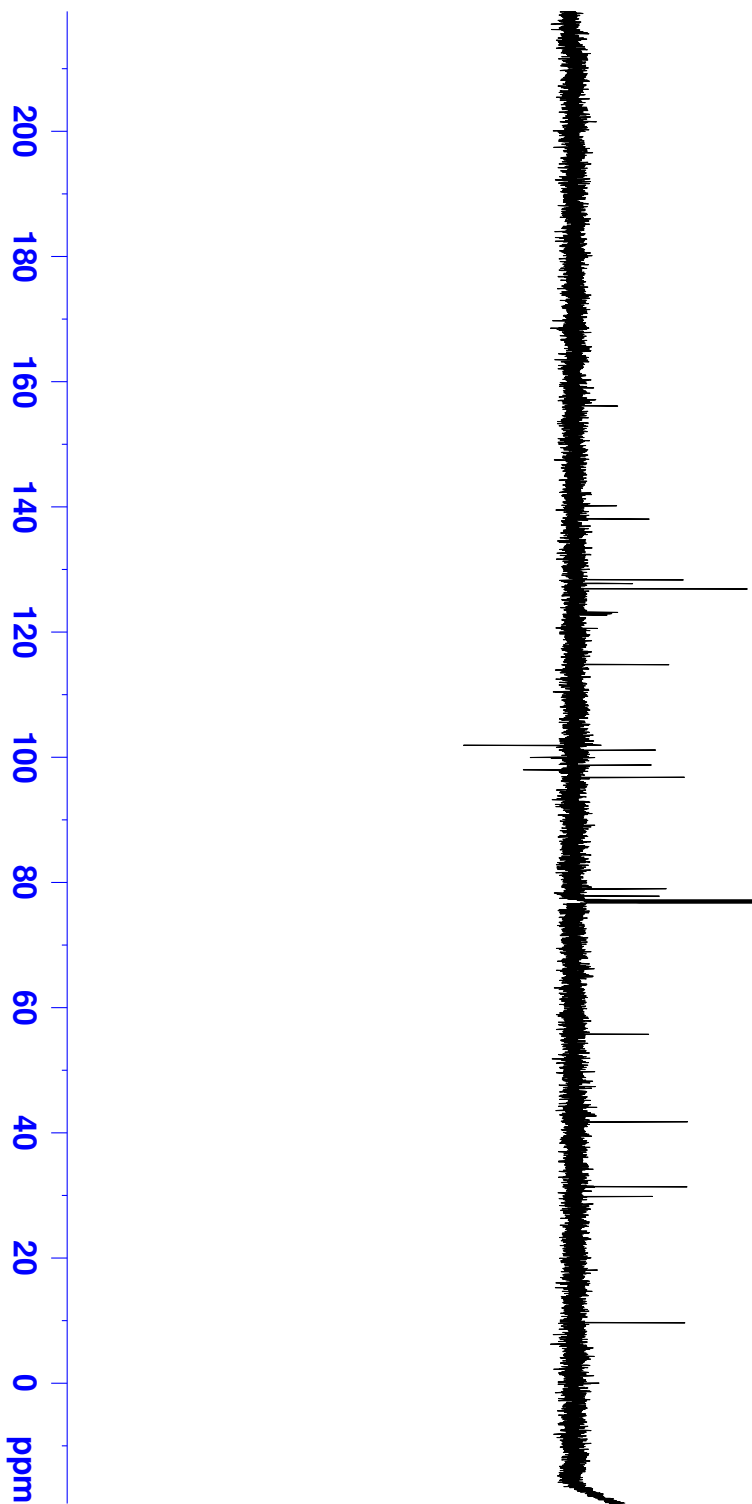
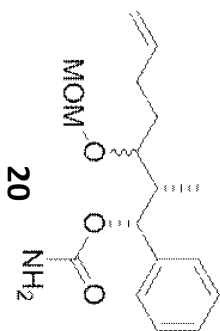
9 8 7 6 5 4 3 2 1 ppm

4.00
2.28
0.68
0.66
1.49
0.48
0.99
0.98
1.86
1.14
0.94
2.74
0.94
1.06
1.90
1.01
1.06
0.87
0.47
2.84
0.25

NAME DMB2-197f31
EXPNO 1
PROCNO 1
Date_ 20120822
Time 9.20
INSTRUM spect
PROBHD 5 mm CPTCI 1H-
PULPROG zg30
TD 65536
SOLVENT CDCl3
NS 16
DS 2
SWH 12376.237 Hz
FIDRES 0.188846 Hz
AQ 2.6477449 sec
RG 10.1
DW 40.400 usec
DE 6.50 usec
TE 298.0 K
D1 1.0000000 sec
TD0 1
===== CHANNEL f1 =====
NUC1 1H
P1 8.00 usec
PL1 4.00 dB
PL1W 7.00000000 W
SFO1 600.1337060 MHz
SI 32768
SF 600.1300156 MHz
WDW EM
SSB 0
LB 0.30 Hz
GB 0
PC 1.00

DMB2-197f31-47

156.14
140.20
138.08
128.35
127.79
126.92
123.14
122.94
122.72
114.82
101.16
98.77
96.78
78.96
77.81
55.75
41.75
31.39
29.83
9.64



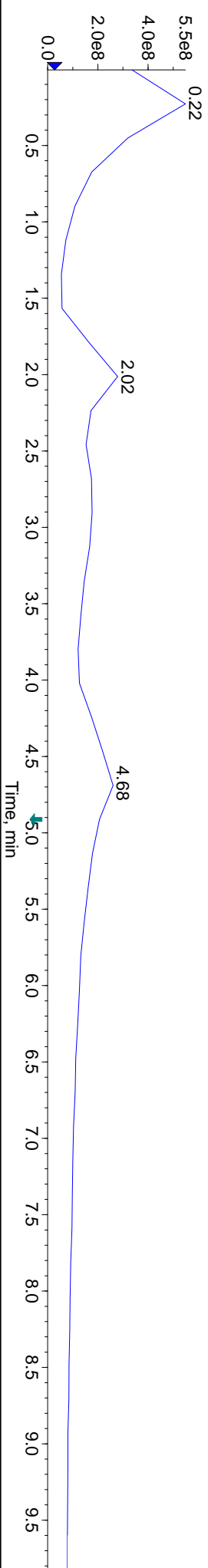
NAME DMB2-197f31
EXPNO 2
PROCNO 1
Date_ 20120822
Time 9.36
INSTRUM spect
PROBHD 5 mm CPTCI 1H-
PULPROG zgpg30
TD 65536
SOLVENT CDCl3
NS 256
DS 4
SWH 35971.223 Hz
FIDRES 0.548877 Hz
AQ 0.9110143 sec
RG 5.7
DE 13.900 usec
TE 298.0 K
D1 2.00000000 sec
D11 0.03000000 sec
TD0 1

===== CHANNEL f1 =====
NUC1 13C
P1 12.00 usec
PL1 -0.70 dB
PL1W 82.63385773 W
SFO1 150.9178988 MHz

===== CHANNEL f2 =====
CPDPRG2 waltz16
NUC2 1H
PCPD2 80.00 usec
PL2 4.00 dB
PL12 24.00 dB
PL13 27.00 dB
PL2W 7.00000000 W
PL12W 0.07000000 W
PL13W 0.03508311 W
SFO2 600.1324005 MHz
SI 32768
SF 150.9028132 MHz
WDW EM
SSB 0
LB 1.00 Hz
GB 0
PC 1.40

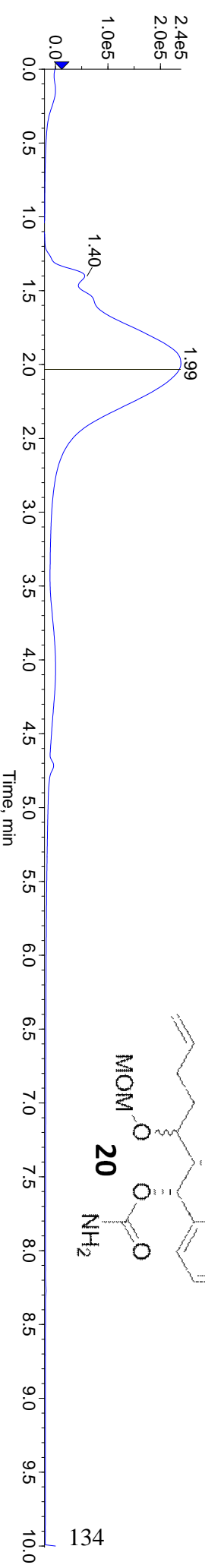
■ TIC: from Sample 1 (DMB2-197f31) of DMB2-197f31-47.wiff (Turbo Spray)

Max. 5.5e8 cps.



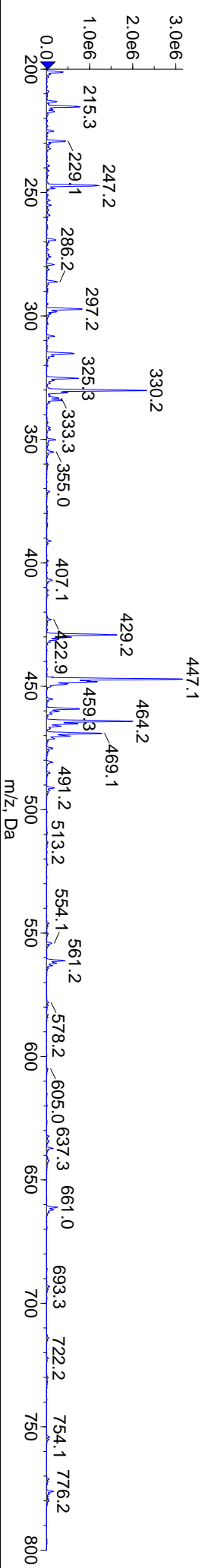
■ Shimadzu LC Controller Detector A, Channel 1 from Sample 1 (DMB2-197f31) of DMB2-197f31-47.wiff

Max. 2.4e5 .



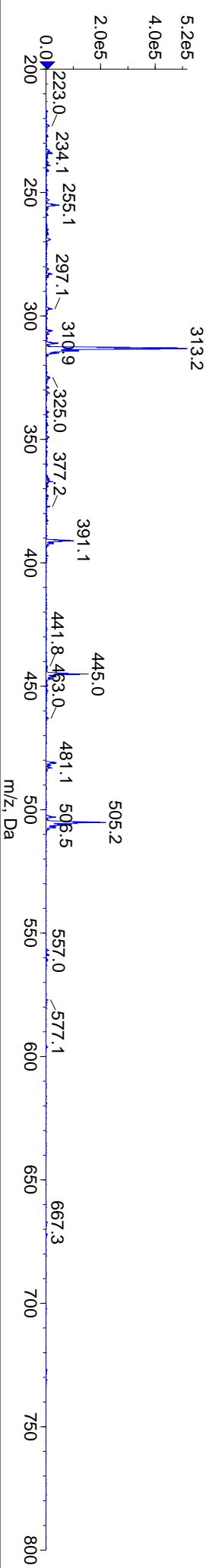
■ +Q1: Exp 1, 2.013 min from Sample 1 (DMB2-197f31) of DMB2-197f31-47.wiff (Turbo Spray)

Max. 3.2e6 cps.



■ -Q1: Exp 2, 2.124 min from Sample 1 (DMB2-197f31) of DMB2-197f31-47.wiff (Turbo Spray)

Max. 5.2e5 cps.





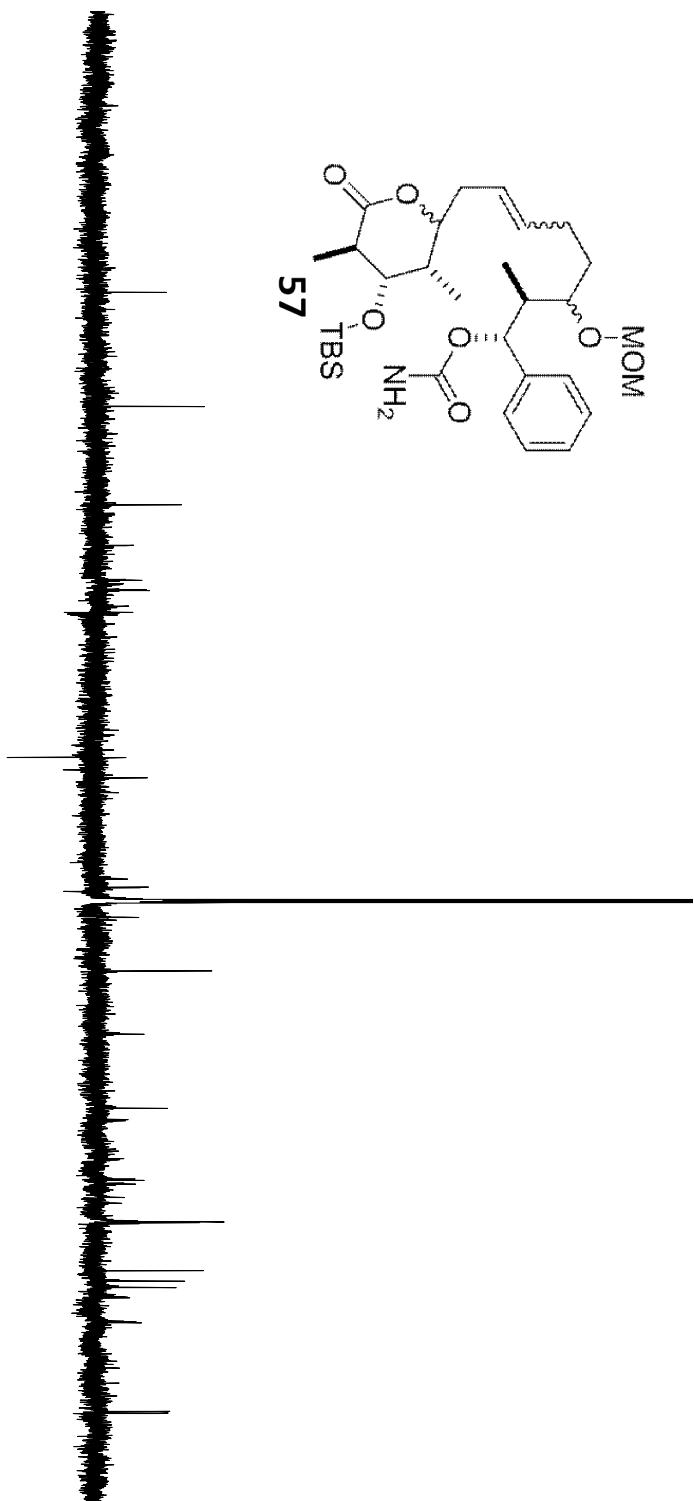
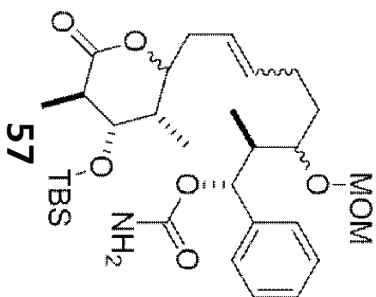
DMB3-75f41

57



DMB3-75f41-51

174.31
156.08
140.36
133.85
128.25
126.79
126.67
124.14
123.14
96.72
80.54
79.24
79.17
74.43
65.84
55.76
43.90
43.85
42.09
32.61
32.41
31.77
25.77
25.62
25.45
17.95
16.27
15.27
13.76
13.60
9.80
9.66
-4.55
-4.81



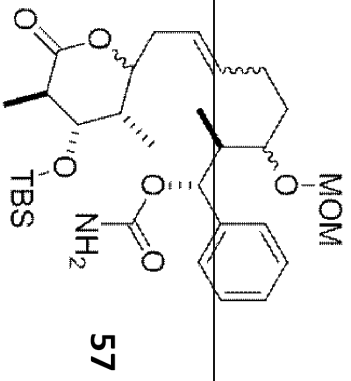
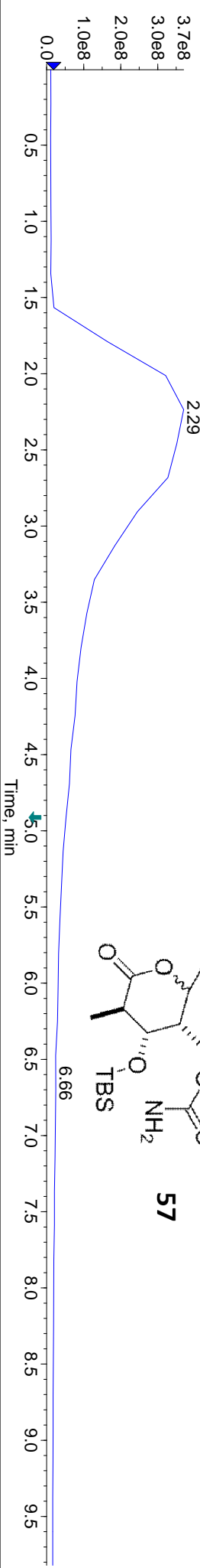
NAME DMB3-75f41
EXPNO 7
PROCNO 1
Date_ 20130413
Time 20.23
INSTRUM spect
PROBHD 5 mm CPTCI 1H-
PULPROG zgpg30
TD 65536
SOLVENT CDCl3
NS 3072
DS 4
SWH 35971.223 Hz
FIDRES 0.54877 Hz
AQ 0.9110143 sec
RG 5
DW 13.900 usec
DE 6.50 usec
TE 298.0 K
D1 2.00000000 sec
D11 0.03000000 sec
TD0 1

===== CHANNEL f1 =====
NUC1 13C
P1 12.00 usec
PL1 -0.70 dB
PL1W 82.63385773 W
SFO1 150.9178988 MHz

===== CHANNEL f2 =====
CPDPRG2 waltz16
NUC2 1H
PCPD2 80.00 usec
PL2 4.00 dB
PL12 24.00 dB
PL13 27.00 dB
PL2W 7.00000000 W
PL12W 0.07000000 W
PL13W 0.03508311 W
SFO2 600.1324005 MHz
SI 32768
SF 150.9028142 MHz
WDW EM
SSB 0
LB 1.00 Hz
GB 0
PC 1.40

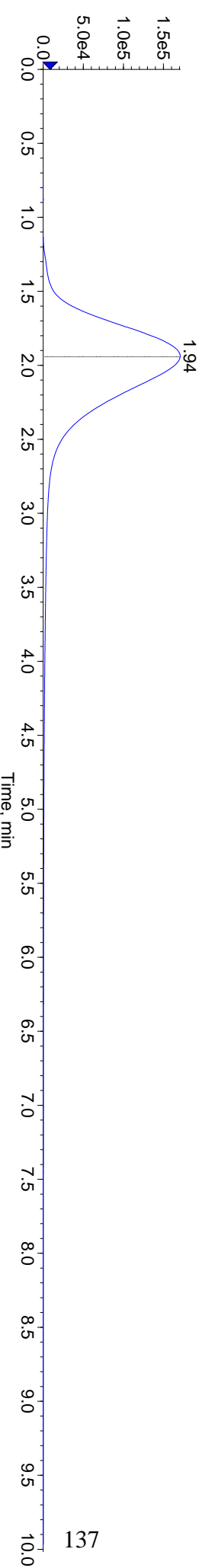
TIC: from Sample 1 (DMB3-75f41) of DMB3-75f41-51.wiff (Turbo Spray)

Max. 3.7e8 cps.



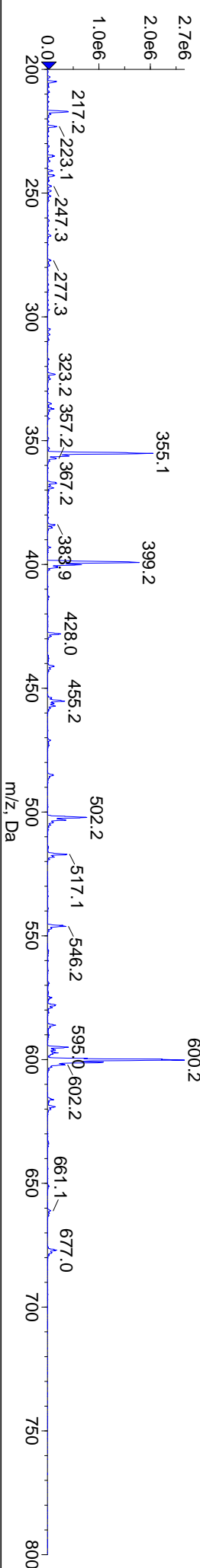
Shimadzu LC Controller Detector A, Channel 1 from Sample 1 (DMB3-75f41) of DMB3-75f41-51.wiff

Max. 1.7e5 .



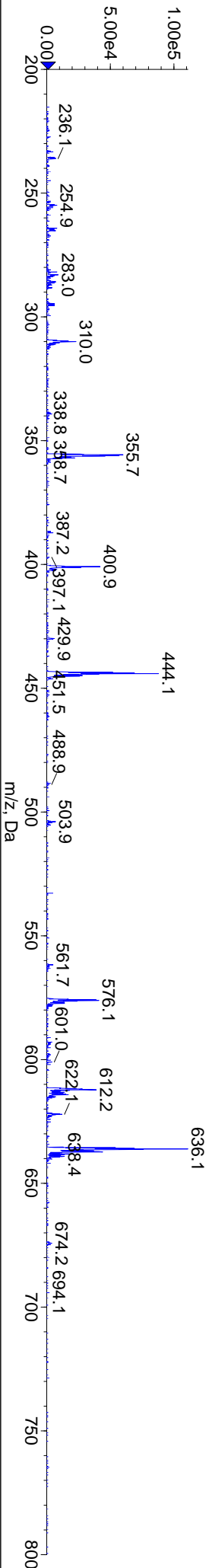
+Q1: Exp 1, 1.790 min from Sample 1 (DMB3-75f41) of DMB3-75f41-51.wiff (Turbo Spray)

Max. 2.7e6 cps.



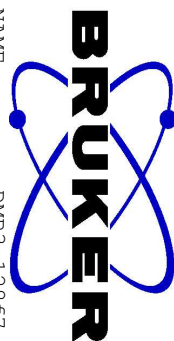
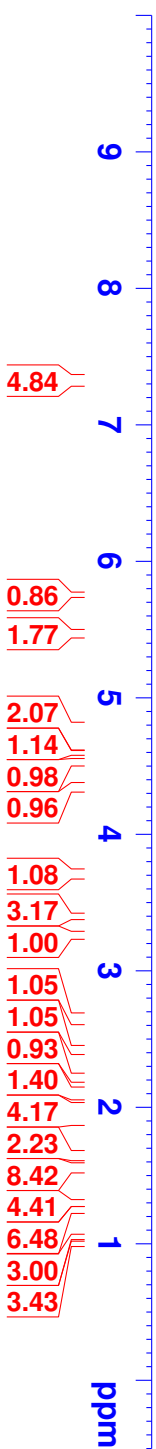
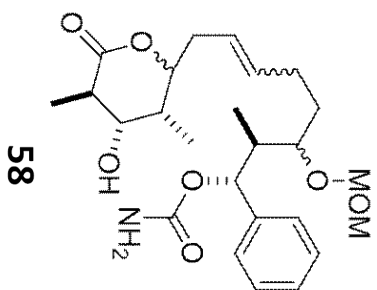
-Q1: Exp 2, 1.901 min from Sample 1 (DMB3-75f41) of DMB3-75f41-51.wiff (Turbo Spray)

Max. 1.1e5 cps.



DMB3-128f7-11

7.331
7.319
7.301
7.293
7.289
7.284
7.274
5.762
5.750
5.482
5.477
5.472
5.462
4.600
4.589
4.536
4.525
3.722
3.410
3.398
3.261
3.255
2.652
1.998
1.987
1.979
1.964
1.947
1.653
1.643
1.639
1.628
1.569
1.558
1.311
1.298
1.251
1.045
1.034
1.006
0.995
0.878

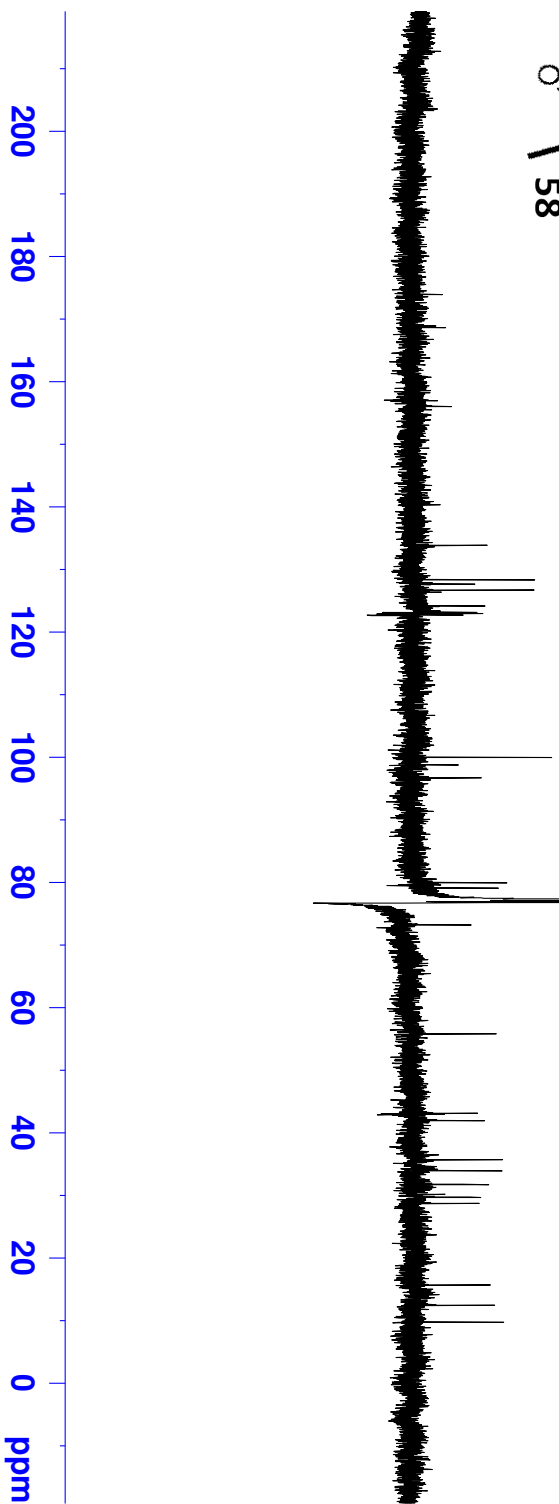
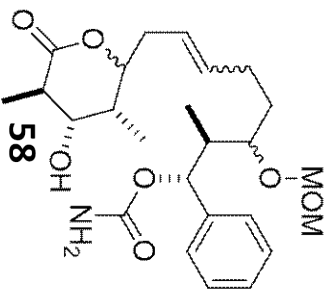


NAME DMB3-128f7
EXPNO 1
PROCNO 1
Date_ 20130801
Time 8.29
INSTRUM spect
PROBHD 5 mm CPTCI 1H-
PULPROG zg30
TD 65536
SOLVENT CDCl3
NS 128
DS 0
SWH 12376.237 Hz
FIDRES 0.188846 Hz
AQ 2.6477449 sec
RG 9
DW 40.400 usec
DE 6.50 usec
TE 298.0 K
D1 2.00000000 sec
TD0 1

===== CHANNEL f1 =====
NUC1 1H
P1 8.00 usec
PL1 4.00 dB
PL1W 7.00000000 W
SFO1 600.1337060 MHz
SI 32768
SF 600.1300157 MHz
WDW EM
SSB 0
LB 0.30 Hz
GB 0
PC 1.00

DMB3-128f7-11

156.09
133.90
128.34
127.68
126.73
124.19
123.16
122.95
122.74
99.97
98.77
96.70
79.97
79.11
73.20
55.80
43.09
41.93
35.69
33.92
31.75
29.70
28.69
15.65
12.41
9.71



```

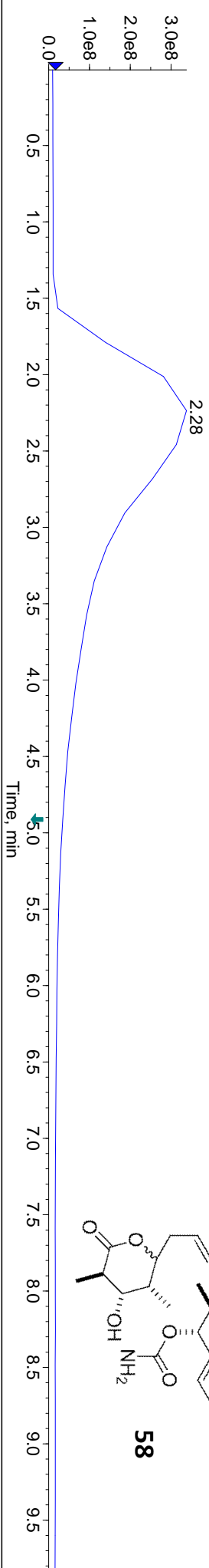
NAME DMB3-128f7
EXPNO 3
PROCNO 1
Date_ 20130801
Time 23.03
INSTRUM spect
PROBHD 5 mm CPTCI 1H-
PULPROG zgpg30
TD 65536
SOLVENT CDCl3
NS 4096
DS 4
SWH 35971.223 Hz
FIDRES 0.548877 Hz
AQ 0.9110143 sec
RG 7.1
DE 13.900 usec
TE 298.0 K
D1 2.00000000 sec
D11 0.03000000 sec
TD0 1

===== CHANNEL f1 =====
NUC1 13C
P1 12.00 usec
PL1 -0.70 dB
PL1W 82.63385773 W
SFO1 150.9178988 MHz

===== CHANNEL f2 =====
CPDPRG2 waltz16
NUC2 1H
PCPD2 80.00 usec
PL2 4.00 dB
PL12 24.00 dB
PL13 27.00 dB
PL2W 7.00000000 W
PL12W 0.07000000 W
PL13W 0.03508311 W
SFO2 600.1324005 MHz
SI 32768
SF 150.9028130 MHz
WDW EM
SSB 0
LB 1.00 Hz
GB 0
PC 1.40
  
```

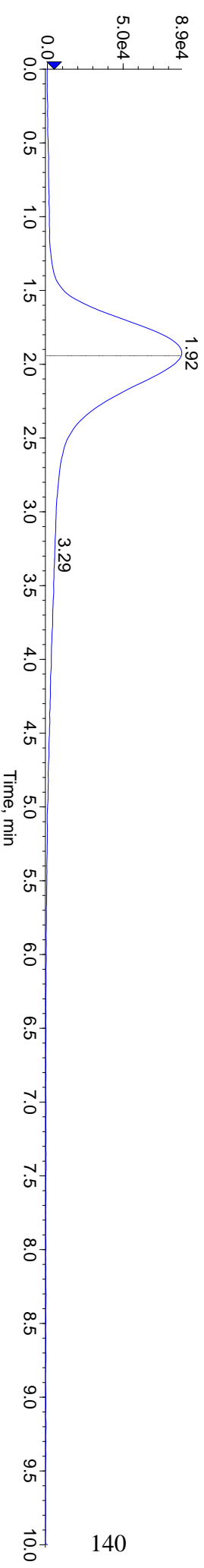
■ TIC: from Sample 1 (DMB3-128f7-11b) of DMB3-128f7-11b.wiff (Turbo Spray)

Max. 3.4e8 cps.



■ Shimadzu LC Controller Detector A, Channel 1 from Sample 1 (DMB3-128f7-11b) of DMB3-128f7-11b.wiff

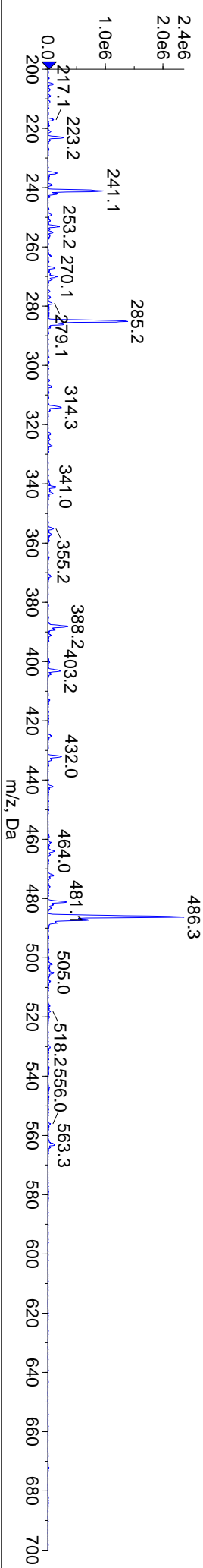
Max. 8.9e4 .



140

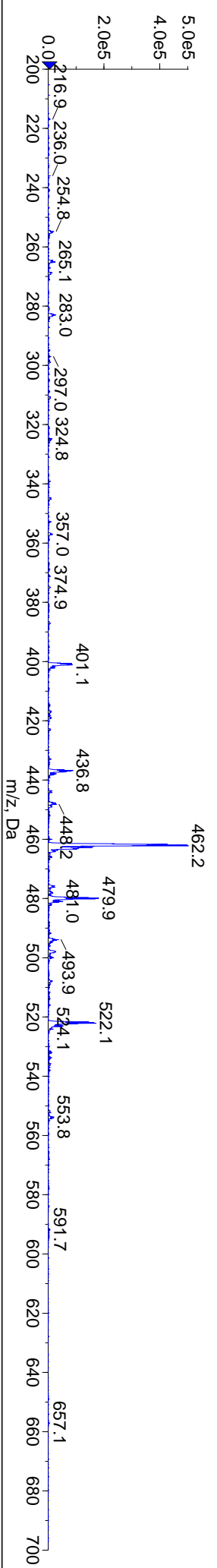
■ +Q1: Exp 1, 1.790 min from Sample 1 (DMB3-128f7-11b) of DMB3-128f7-11b.wiff (Turbo Spray)

Max. 2.4e6 cps.

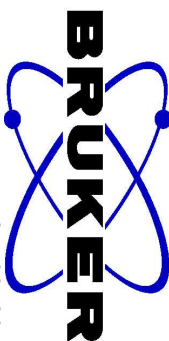


■ -Q1: Exp 2, 1.901 min from Sample 1 (DMB3-128f7-11b) of DMB3-128f7-11b.wiff (Turbo Spray)

Max. 5.0e5 cps.



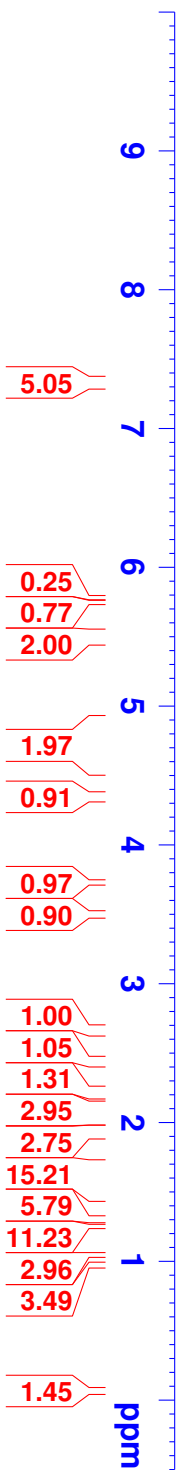
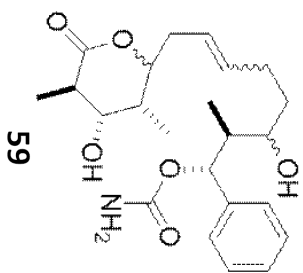
DMB3-128f20-27



7.340
7.328
7.313
7.301
7.284
5.753
5.742
5.510
5.503
5.495
4.345
3.736
3.731
3.725
3.501
3.350
2.670
2.664
2.658
2.234
2.045
1.950
1.944
1.940
1.934
1.929
1.924
1.918
1.588
1.576
1.566
1.552
1.547
1.541
1.534
1.527
1.514
1.311
1.299
1.051
1.040
0.984
0.972

NAME DMB3-128f20
EXPNO 1
PROCNO 1
Date_ 20130801
Time 8.44
INSTRUM spect
PROBHD 5 mm CPTCI 1H-
PULPROG zg30
TD 65536
SOLVENT CDCl3
NS 128
DS 0
SWH 12376.237 Hz
FIDRES 0.188846 Hz
AQ 2.6477449 sec
RG 9
DW 40.400 usec
DE 6.50 usec
TE 298.0 K
D1 2.0000000 sec
TD0 1

===== CHANNEL f1 =====
NUC1 1H
P1 8.00 usec
PL1 4.00 dB
PL1W 7.00000000 W
SFO1 600.1337060 MHz
SI 32768
SF 600.1300153 MHz
WDW EM
SSB 0
LB 0.30 Hz
GB 0
PC 1.00



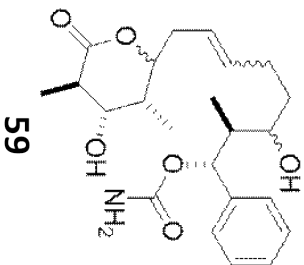
DMB3-128f20-27

139.98
133.92
128.39
128.34
127.68
126.40
124.38
123.16
122.95
120.35
104.34
101.96
98.77
79.96
78.67
73.38
71.37
44.04
43.25
35.61
34.42
33.80
29.70
29.12
15.82
12.50
8.58



NAME DMB3-128f20
EXPNO 3
PROCNO 1
Date_ 20130802
Time 2.36
INSTRUM spect
PROBHD 5 mm CPTCI 1H-
PULPROG zgpg30
TD 65536
SOLVENT CDCl3
NS 4096
DS 4
SWH 35971.223 Hz
FIDRES 0.548877 Hz
AQ 0.9110143 sec
RG 7.1
DE 13.900 usec
TE 298.0 K
D1 2.00000000 sec
D11 0.03000000 sec
TD0 1

===== CHANNEL f1 =====
NUC1 13C
P1 12.00 usec
PL1 -0.70 dB
PL1W 82.63385773 W
SFO1 150.9178988 MHz

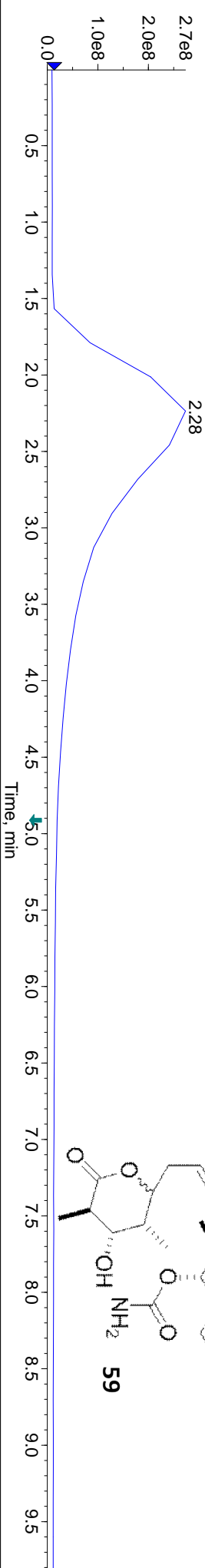


===== CHANNEL f2 =====
CPDPRG2 waltz16
NUC2 1H
PCPD2 80.00 usec
PL2 4.00 dB
PL12 24.00 dB
PL13 27.00 dB
PL2W 7.00000000 W
PL12W 0.07000000 W
PL13W 0.03508311 W
SFO2 600.1324005 MHz
SI 32768
SF 150.9028131 MHz
WDW EM
SSB 0
LB 1.00 Hz
GB 0
PC 1.40

200 180 160 140 120 100 80 60 40 20 0 ppm

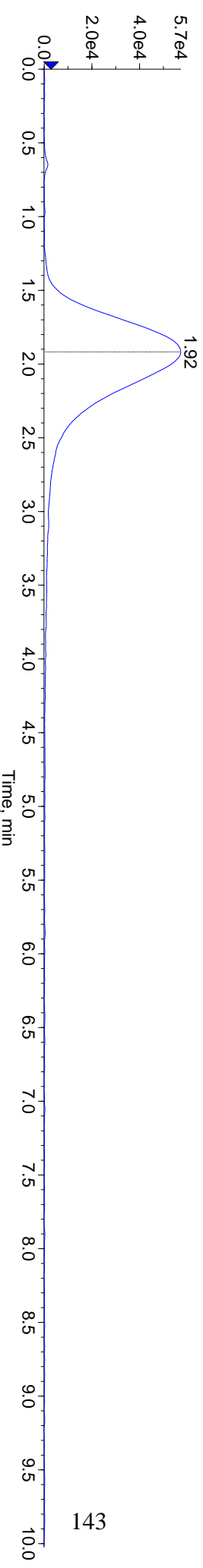
TIC: from Sample 1 (DMB3-128f20-27d) of DMB3-128f20-27d.wiff (Turbo Spray)

Max. 2.7e8 cps.



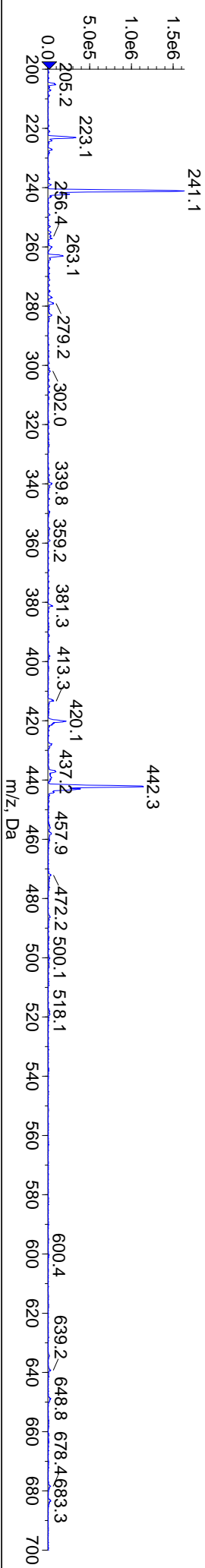
Shimadzu LC Controller Detector A, Channel 1 from Sample 1 (DMB3-128f20-27d) of DMB3-128f20-27d.wiff

Max. 5.7e4 .



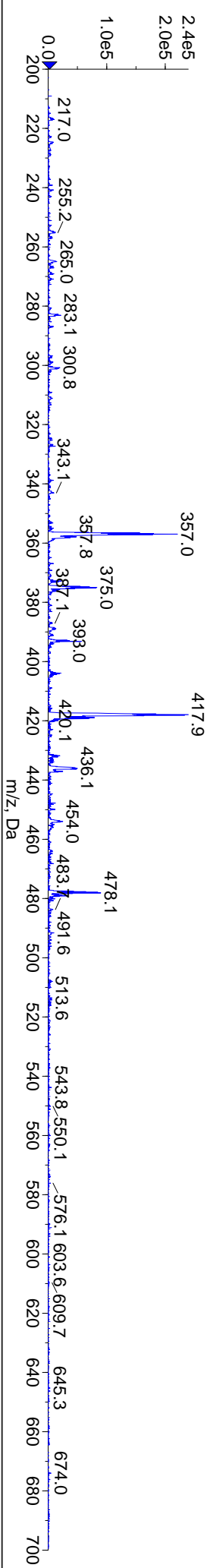
+Q1: Exp 1, 1.790 min from Sample 1 (DMB3-128f20-27d) of DMB3-128f20-27d.wiff (Turbo Spray)

Max. 1.6e6 cps.



-Q1: Exp 2, 1.901 min from Sample 1 (DMB3-128f20-27d) of DMB3-128f20-27d.wiff (Turbo Spray)

Max. 2.4e5 cps.





NAME DMB3-131f32

EXPNO 1

PROCNO 1

Date_ 20130723

Time 17.50

INSTRUM spect

PROBHD 5 mm CPTCI 1H-

PULPROG zg30

TD 65536

SOLVENT CDCl3

NS 16

DS 2

SWH 12376.237 Hz

FIDRES 0.188846 Hz

AQ 2.6477449 sec

RG 9

DW 40.400 usec

DE 6.50 usec

TE 298.0 K

D1 1.0000000 sec

TD0 1

===== CHANNEL f1 =====

NUC1 1H

P1 8.00 usec

PL1 4.00 dB

PL1W 7.0000000 W

SFO1 600.1337060 MHz

SI 32768

SF 600.1300156 MHz

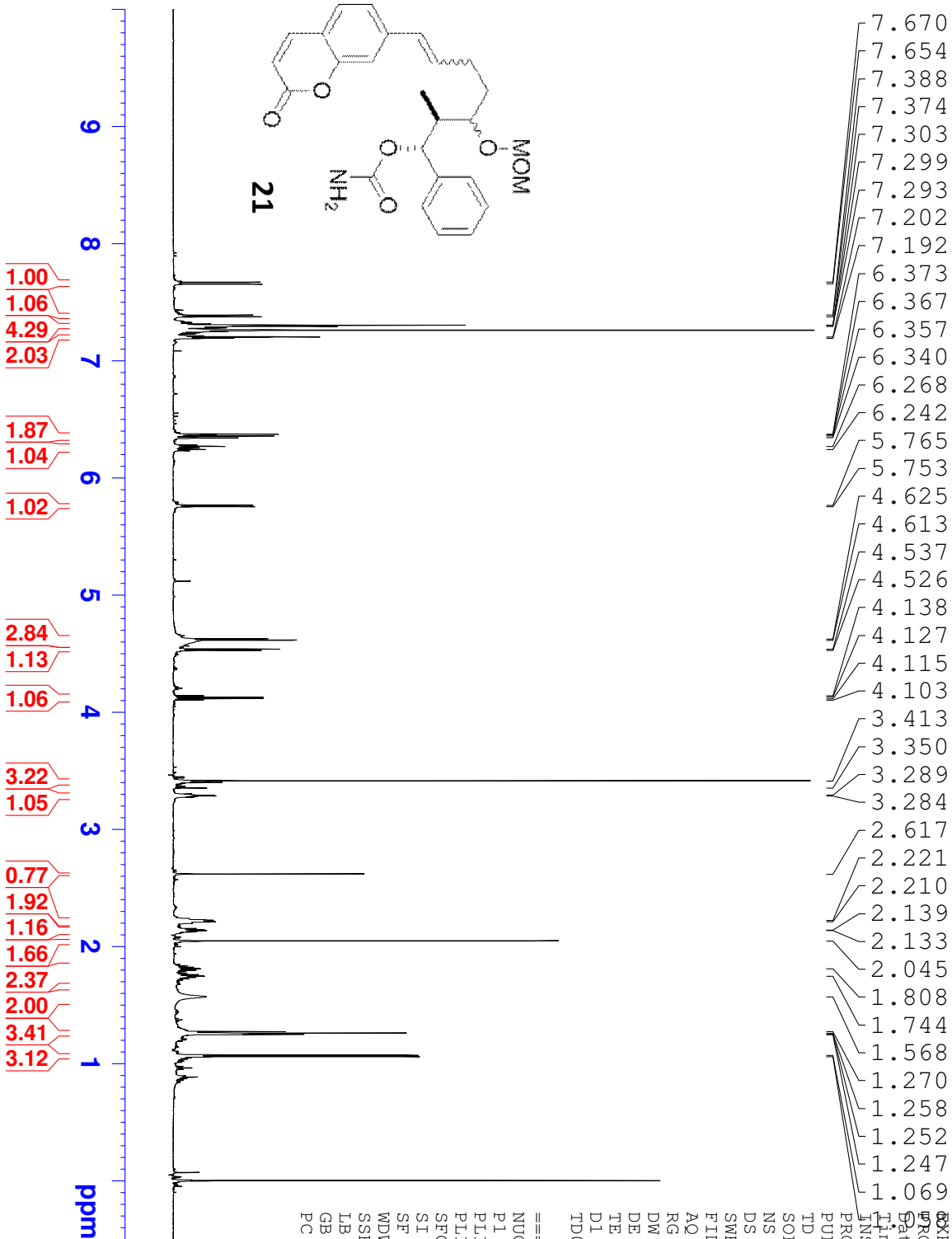
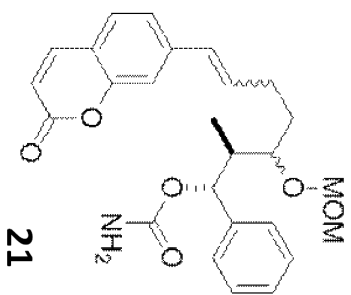
WDW EM

SSB 0

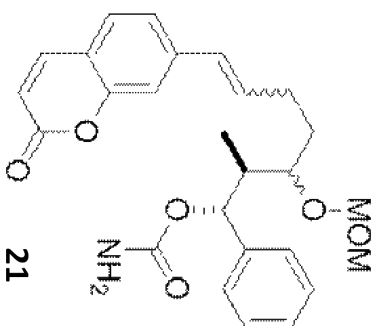
LB 0.30 Hz

GB 0

PC 1.00



143.12
133.86
129.05
128.39
127.87
127.79
126.90
122.18
115.70
113.79
101.16
99.97
96.91
78.91
77.74
55.82
41.89
31.64
29.24
9.72



21

NAME DMB3-131f32
EXPNO 2
PROCNO 1
Date_ 20130723
Time 18.18
INSTRUM spect
PROBHD 5 mm CPTCI 1H-
PULPROG zgpg30
TD 65536
SOLVENT CDCl3
NS 512
DS 4
SWH 35971.223 Hz
FIDRES 0.54877 Hz
AQ 0.9110143 sec
RG 7.1
DW 13.900 usec
DE 6.50 usec
TE 298.0 K
D1 2.00000000 sec
D11 0.03000000 sec
TD0 1

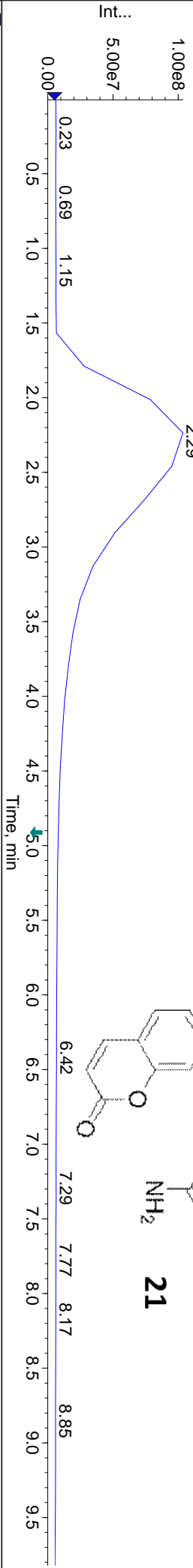
===== CHANNEL f1 =====
NUC1 13C
P1 12.00 usec
PL1 -0.70 dB
PL1W 82.63385773 W
SFO1 150.9178988 MHz

===== CHANNEL f2 =====
CPDPRG2 waltz16
NUC2 1H
PCPD2 80.00 usec
PL2 4.00 dB
PL12 24.00 dB
PL13 27.00 dB
PL2W 7.00000000 W
PL12W 0.07000000 W
PL13W 0.03508311 W
SFO2 600.1324005 MHz
SI 32768
SF 150.9028131 MHz
WDW EM
SSB 0
LB 1.00 Hz
GB 0
PC 1.40

200 180 160 140 120 100 80 60 40 20 0 ppm

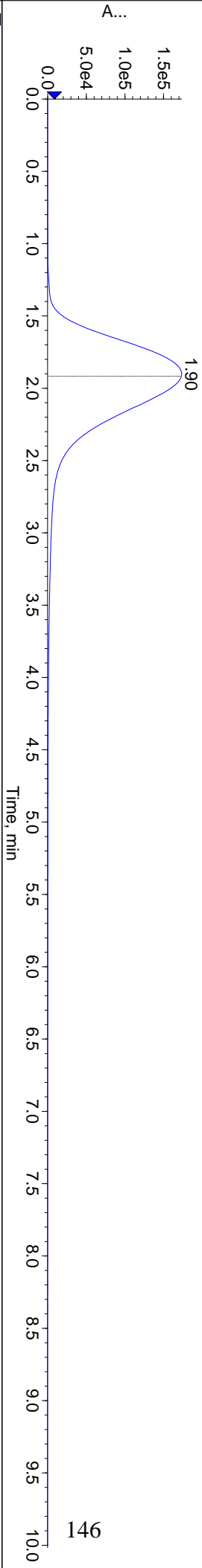
■ TIC: from Sample 1 (DMB3-131f32-36) of DMB3-131f32-36.wiff (Turbo Spray)

Max. 1.0e8 cps.



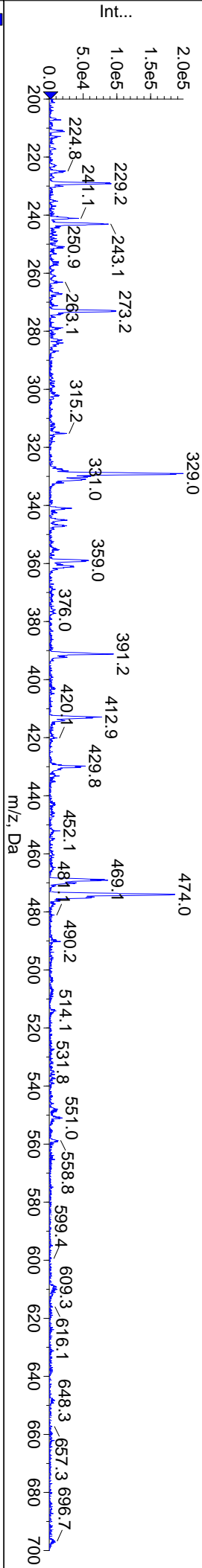
■ Shimadzu LC Controller Detector A, Channel 1 from Sample 1 (DMB3-131f32-36) of DMB3-131f32-36.wiff

Max. 1.7e5 .



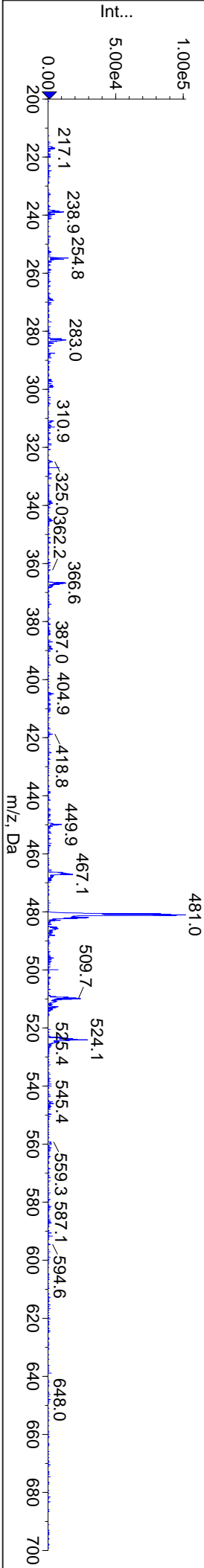
■ +Q1: Exp 1, 1.790 min from Sample 1 (DMB3-131f32-36) of DMB3-131f32-36.wiff (Turbo Spray)

Max. 2.0e5 cps.

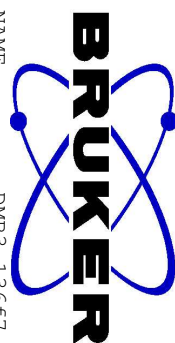


■ -Q1: Exp 2, 1.901 min from Sample 1 (DMB3-131f32-36) of DMB3-131f32-36.wiff (Turbo Spray)

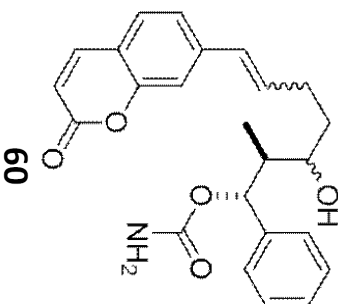
Max. 1.0e5 cps.



DMB3-136f7-12



7.668
7.652
7.432
7.388
7.374
7.326
7.319
7.285
7.216
7.211
7.208
7.197
7.083
6.372
6.356
6.310
5.738
5.117
3.350
2.173
1.636
1.626
1.621
1.459
1.117
1.099
1.080
1.068
1.044
1.032
1.020
1.008
0.996
0.898
0.890
0.879
0.867
0.855
0.839
0.828
0.815
0.712



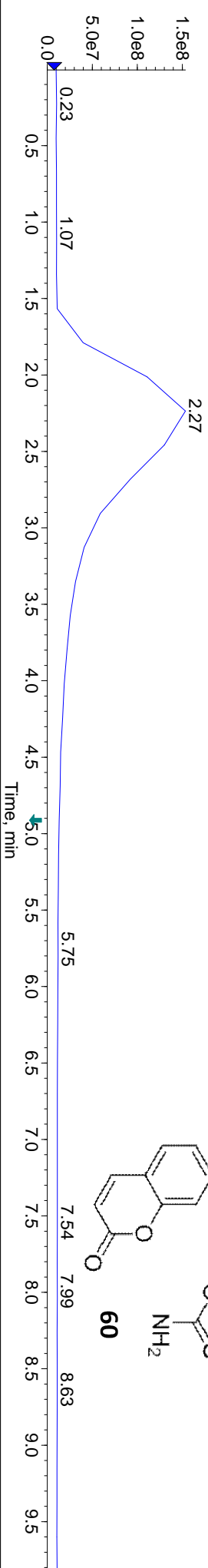
1.00
0.94
3.93
1.69
0.42
0.96
0.61
0.87
0.67
1.62
0.65
1.37
1.08
1.67
1.18
2.22
2.70
1.34
6.31
3.77

NAME DMB3-136f7
EXPNO 4
PROCNO 1
Date_ 20130819
Time 14.24
INSTRUM spect
PROBHD 5 mm CPTCI 1H-
PULPROG zg30
TD 65536
SOLVENT CDCl3
NS 256
DS 2
SWH 12376.237 Hz
FIDRES 0.188846 Hz
AQ 2.6477449 sec
RG 11.3
DW 40.400 usec
DE 6.50 usec
TE 298.0 K
D1 1.00000000 sec
TD0 1

===== CHANNEL f1 =====
NUC1 1H
P1 8.00 usec
PL1 4.00 dB
PL1W 7.00000000 W
SFO1 600.1337060 MHz
SI 32768
SF 600.1300156 MHz
WDW EM
SSB 0
LB 0.30 Hz
GB 0
PC 1.00

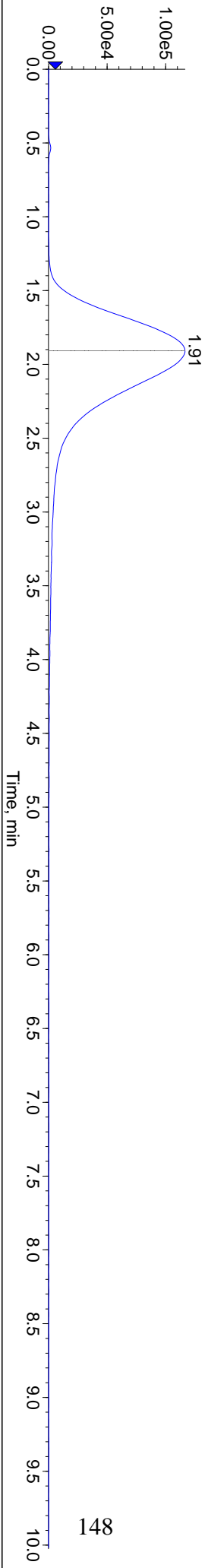
TIC: from Sample 1 (DMB3-136f7-12d) of DMB3-136f7-12d.wiff (Turbo Spray)

Max. 1.5e8 cps.



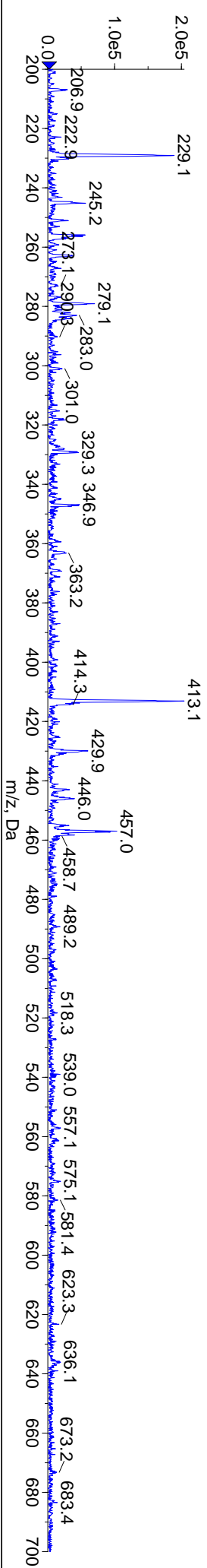
Shimadzu LC Controller Detector A, Channel 1 from Sample 1 (DMB3-136f7-12d) of DMB3-136f7-12d.wiff

Max. 1.2e5 .



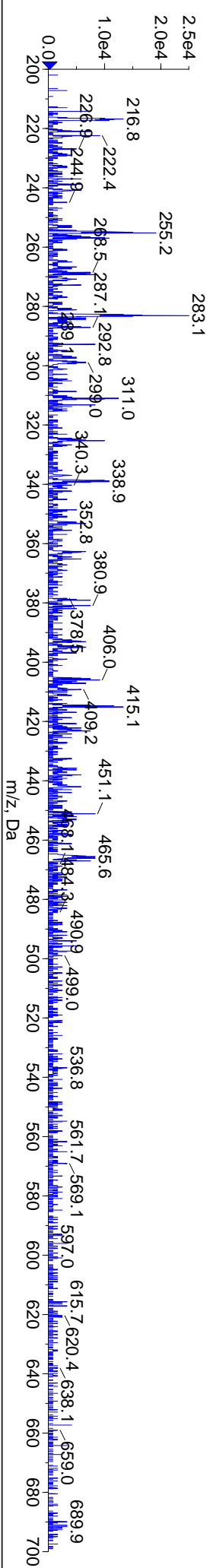
+Q1: Exp 1, 1.790 min from Sample 1 (DMB3-136f7-12d) of DMB3-136f7-12d.wiff (Turbo Spray)

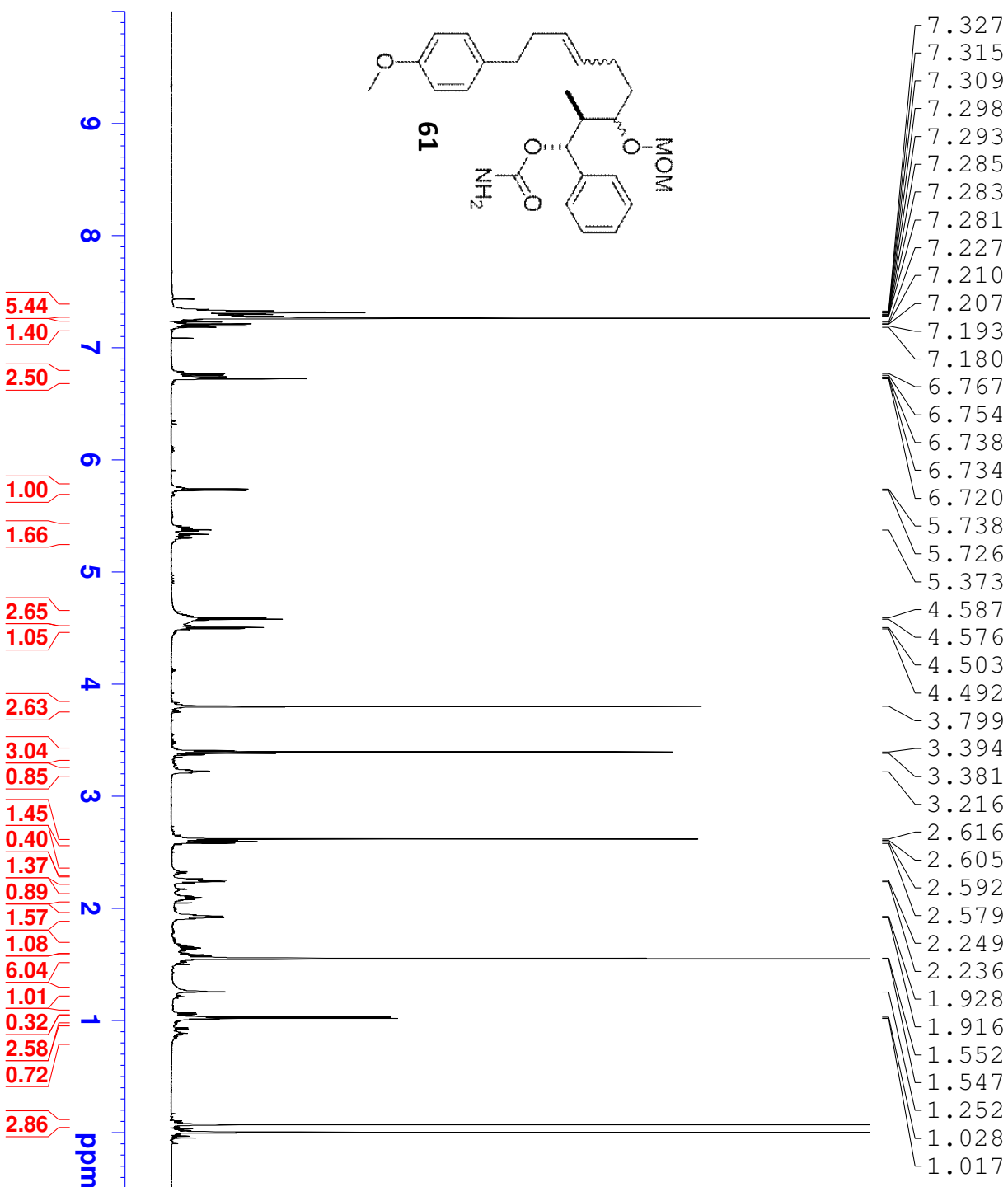
Max. 2.0e5 cps.



-Q1: Exp 2, 1.901 min from Sample 1 (DMB3-136f7-12d) of DMB3-136f7-12d.wiff (Turbo Spray)

Max. 2.5e4 cps.

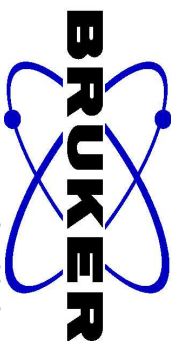
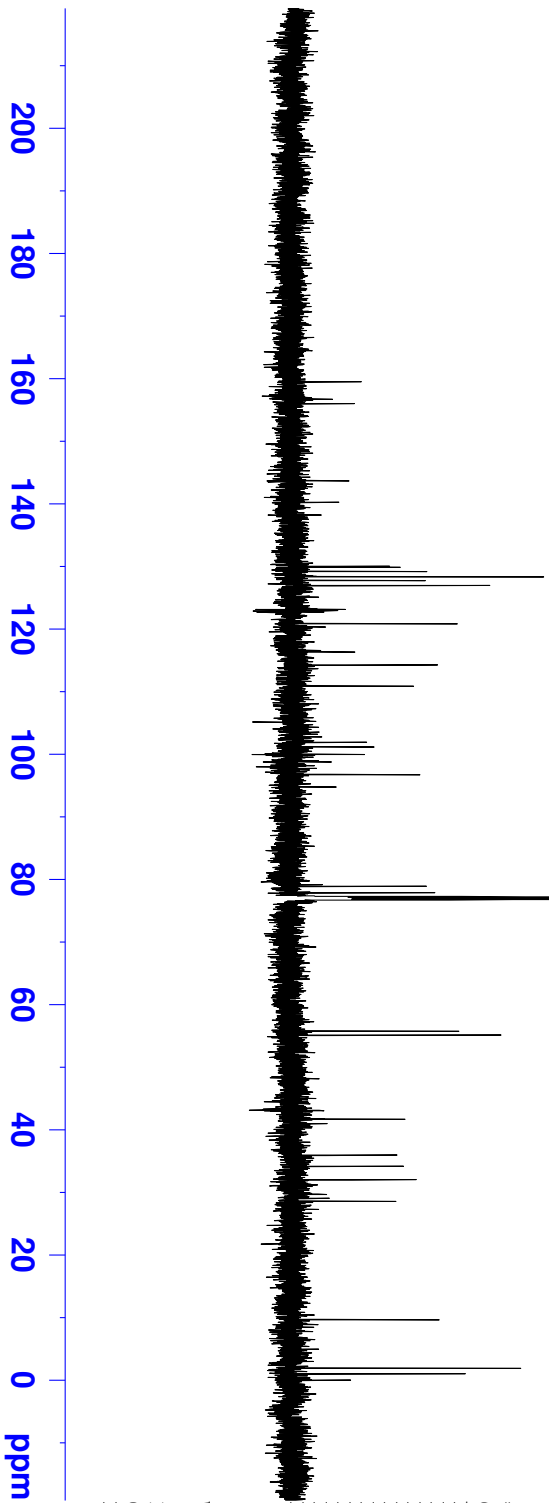
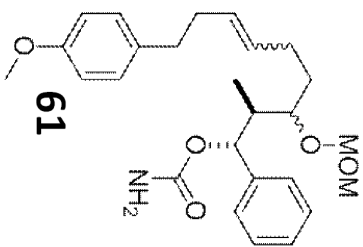




NAME DMB3-129f21
 EXPNO 1
 PROCNO 1
 Date_ 20130722
 Time 11.20
 INSTRUM spect
 PROBD 5 mm CPTCI 1H-
 PULPROG zg30
 TD 65536
 SOLVENT CDCl3
 NS 64
 DS 2
 SWH 12376.237 Hz
 FIDRES 0.188846 Hz
 AQ 2.6477449 sec
 RG 10.1
 DW 40.400 usec
 DE 6.50 usec
 TE 298.0 K
 D1 1.00000000 sec
 TD0 1

===== CHANNEL f1 =====
 NUC1 1H
 P1 8.00 usec
 PL1 4.00 dB
 PL1W 7.00000000 W
 SFO1 600.1337060 MHz
 SI 32768
 SF 600.1300159 MHz
 WDW EM
 SSB 0
 LB 0.30 Hz
 GB 0
 PC 1.00

159.52
156.04
143.72
140.25
130.03
129.92
129.18
128.33
127.77
126.96
120.87
116.35
114.24
110.91
101.95
101.16
99.96
98.78
96.76
94.79
78.89
77.88
55.74
55.11
41.71
35.98
34.17
32.01
28.58
9.65
1.90
1.00
-0.02



```

NAME DMB3-129f21
EXPNO 4
PROCNO 1
Date_ 20130722
Time 22.02
INSTRUM spect
PROBHD 5 mm CPTCI 1H-
PULPROG zgpg30
TD 65536
SOLVENT CDCl3
NS 2048
DS 4
SWH 35971.223 Hz
FIDRES 0.548877 Hz
AQ 0.9110143 sec
RG 7.1
DE 13.900 usec
TE 298.0 K
D1 2.00000000 sec
D11 0.03000000 sec
TD0 1

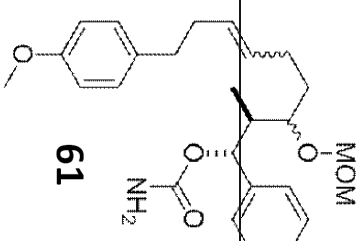
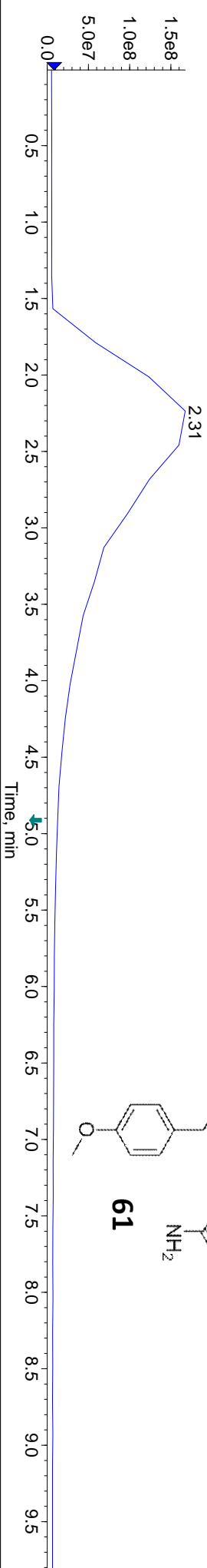
===== CHANNEL f1 =====
NUC1 13C
P1 12.00 usec
PL1 -0.70 dB
PL1W 82.63385773 W
SFO1 150.9178988 MHz

===== CHANNEL f2 =====
CPDPRG2 waltz16
NUC2 1H
PCPD2 80.00 usec
PL2 4.00 dB
PL12 24.00 dB
PL13 27.00 dB
PL2W 7.00000000 W
PL12W 0.07000000 W
PL13W 0.03508311 W
SFO2 600.1324005 MHz
SI 32768
SF 150.9028133 MHz
WDW EM
SSB 0
LB 1.00 Hz
GB 0
PC 1.40

```

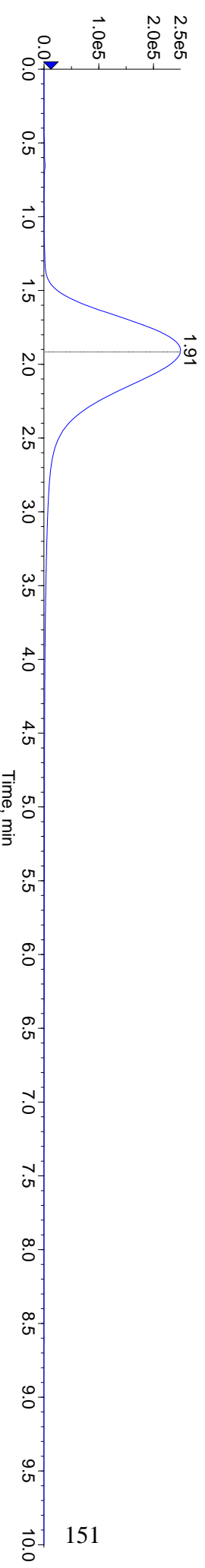

TIC: from Sample 1 (DMB3-129f21-23) of DMB3-129f21-23.wiff (Turbo Spray)

Max. 1.7e8 cps.



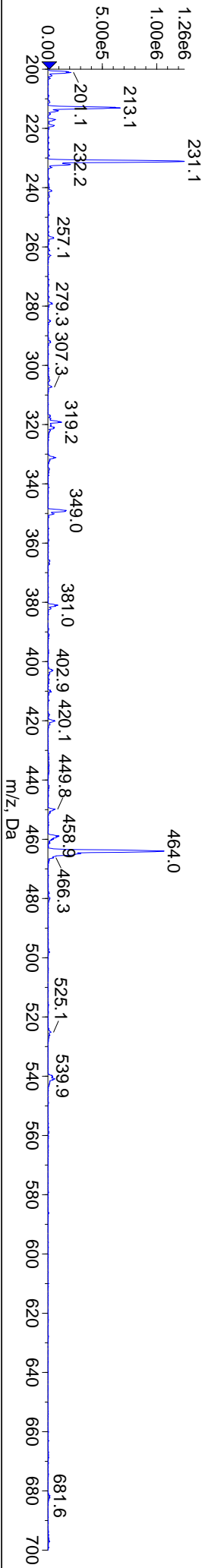
Shimadzu LC Controller Detector A, Channel 1 from Sample 1 (DMB3-129f21-23) of DMB3-129f21-23.wiff

Max. 2.5e5 .



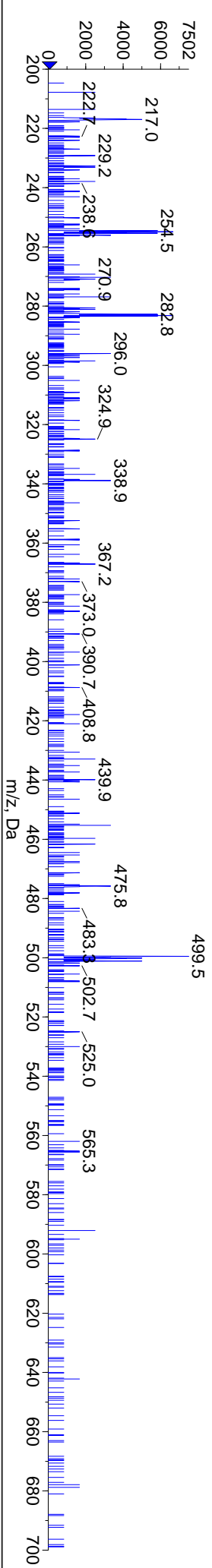
+Q1: Exp 1, 1.790 min from Sample 1 (DMB3-129f21-23) of DMB3-129f21-23.wiff (Turbo Spray)

Max. 1.3e6 cps.

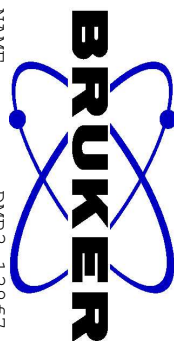
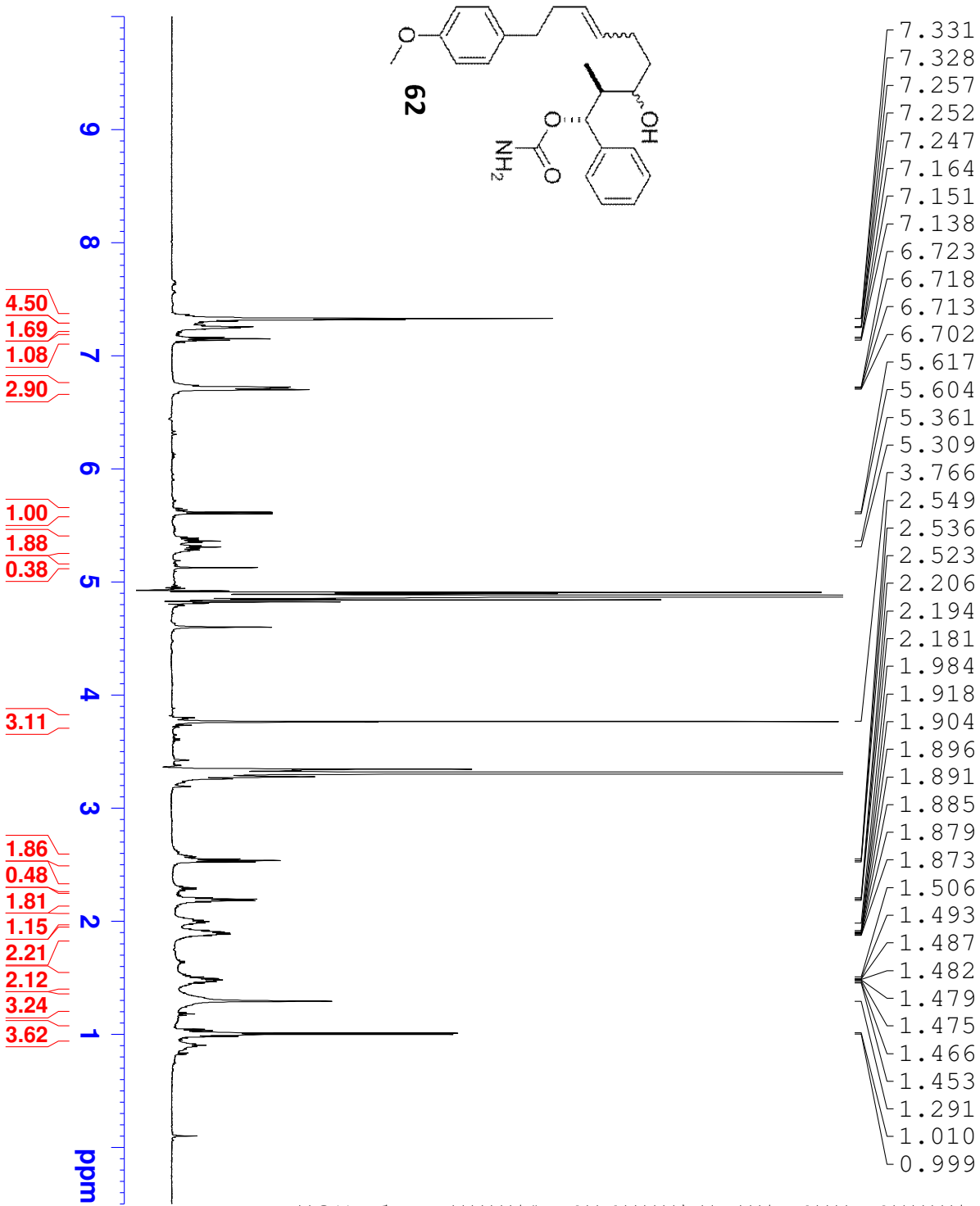


-Q1: Exp 2, 1.901 min from Sample 1 (DMB3-129f21-23) of DMB3-129f21-23.wiff (Turbo Spray)

Max. 7501.5 cps.



DMB3-138f7-13

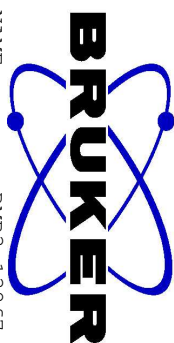


NAME DMB3-138f7
EXPNO 3
PROCNO 1
Date_ 20130823
Time 18.24
INSTRUM spect
PROBHD 5 mm CPTCI 1H-
PULPROG zg30
TD 65536
SOLVENT MeOD
NS 128
DS 0
SWH 12376.237 Hz
FIDRES 0.188846 Hz
AQ 2.6477449 sec
RG 12.7
DW 40.400 usec
DE 6.50 usec
TE 298.0 K
D1 2.0000000 sec
TD0 1

===== CHANNEL f1 =====
NUC1 1H
P1 8.00 usec
PL1 4.00 dB
PL1W 7.00000000 W
SFO1 600.1337060 MHz
SI 32768
SF 600.1292135 MHz
WDW EM
SSB 0
LB 0.30 Hz
GB 0
PC 1.00

DMB3-138f7-13

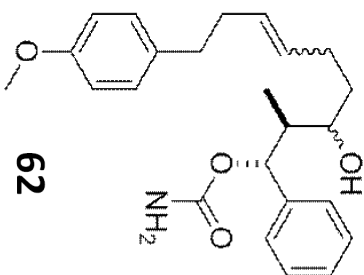
161.12
144.93
142.19
131.28
131.11
130.19
129.23
128.59
127.99
121.88
115.19
112.05
101.40
81.40
79.39
71.24
55.53
45.46
37.18
35.88
35.59
29.95
9.57



NAME DMB3-138f7
EXPNO 4
PROCNO 1
Date_ 20130824
Time 5.12
INSTRUM spect
PROBHD 5 mm CPTCI 1H-
PULPROG zgpg30
TD 65536
SOLVENT MeOD
NS 13000
DS 4
SWH 35971.223 Hz
FIDRES 0.548877 Hz
AQ 0.9110143 sec
RG 7.1
DW 13.900 usec
DE 6.50 usec
TE 298.0 K
D1 2.00000000 sec
D11 0.03000000 sec
TD0 1

===== CHANNEL f1 =====
NUC1 13C
P1 12.00 usec
PL1 -0.70 dB
PL1W 82.63385773 W
SFO1 150.9178988 MHz

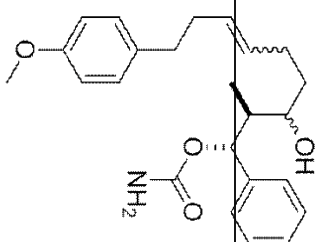
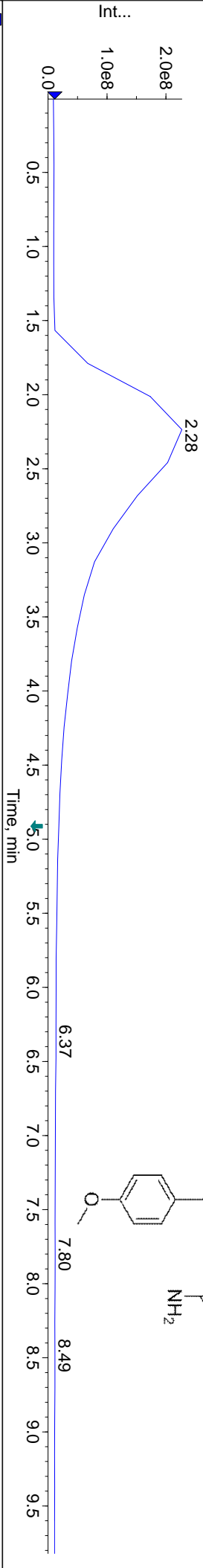
===== CHANNEL f2 =====
CPDPRG2 waltz16
NUC2 1H
PCPD2 80.00 usec
PL2 4.00 dB
PL12 24.00 dB
PL13 27.00 dB
PL2W 7.00000000 W
PL12W 0.07000000 W
PL13W 0.03508311 W
SFO2 600.1324005 MHz
SI 32768
SF 150.9025957 MHz
WDW EM
SSB 0
LB 1.00 Hz
GB 0
PC 1.40



200 180 160 140 120 100 80 60 40 20 0 ppm

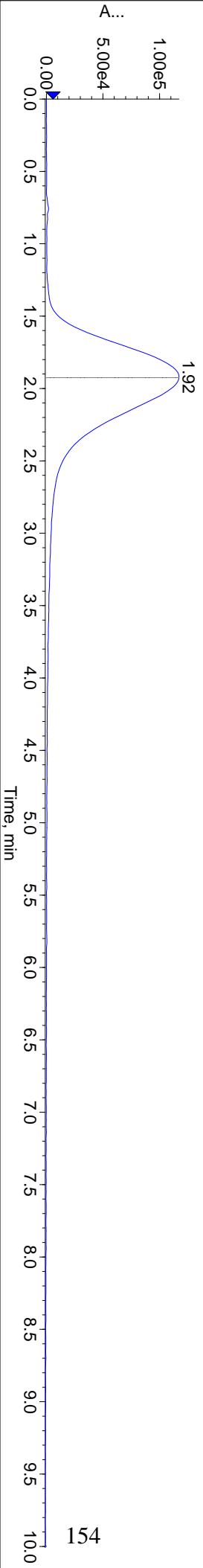
TIC: from Sample 1 (DMB3-138f7-13d) of DMB3-138f7-13d.wiff (Turbo Spray)

Max. 2.3e8 cps.



Shimadzu LC Controller Detector A, Channel 1 from Sample 1 (DMB3-138f7-13d) of DMB3-138f7-13d.wiff

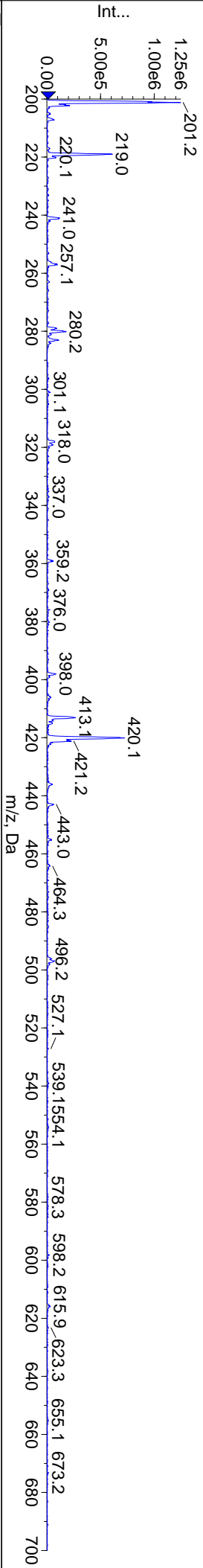
Max. 1.2e5 .



154

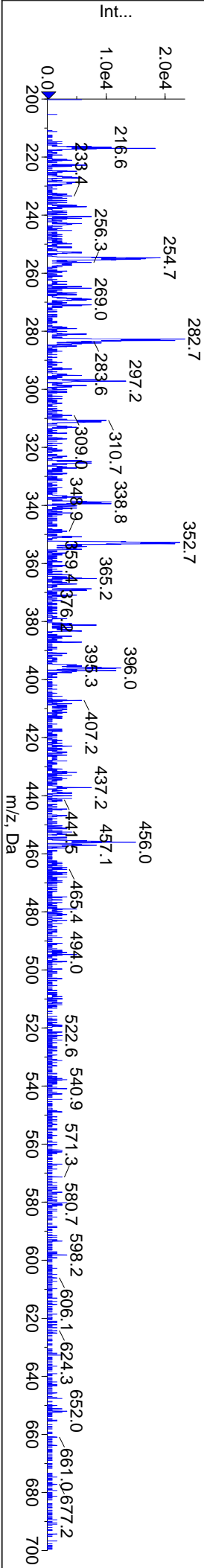
+Q1: Exp 1, 1.790 min from Sample 1 (DMB3-138f7-13d) of DMB3-138f7-13d.wiff (Turbo Spray)

Max. 1.2e6 cps.



-Q1: Exp 2, 1.901 min from Sample 1 (DMB3-138f7-13d) of DMB3-138f7-13d.wiff (Turbo Spray)

Max. 2.3e4 cps.



BIBLIOGRAPHY

- (1) Gunasekera, S. P.; Gunasekera, M.; Longley, R. E.; Schulte, G. K. *J. Org. Chem.* **1990**, *55*, 4912–4915.
- (2) Longley, R. E.; Caddigan, D.; Harmody, D.; Gunasekera, M.; Gunasekera, S. P. *Transplantation* **1991**, *52*, 650–656.
- (3) Longley, R. E.; Caddigan, D.; Harmody, D.; Gunasekera, M.; Gunasekera, S. P. *Transplantation* **1991**, *52*, 656–661.
- (4) Nerenberg, J. B.; Hung, D. T.; Somers, P. K.; Schreiber, S. L. *J. Org. Chem.* **1993**, *115*, 12621–12622.
- (5) Hung, D. T.; Nerenberg, J. B.; Schreiber, S. L. *Chem. Biol.* **1994**, *1*, 67–71.
- (6) Hung, D. T.; Nerenberg, J. B.; Schreiber, S. L. *J. Am. Chem. Soc.* **1996**, *118*, 11054–11080.
- (7) Smith III, A. B.; Qiu, Y.; Jones, D. R.; Kobayashi, K. *J. Am. Chem. Soc.* **1995**, *117*, 12011–12012.
- (8) Smith III, A. B.; Beauchamp, T. J.; Lamarche, M. J.; Kaufman, M. D.; Qiu, Y.; Arimoto, H.; Jones, D. R.; Kobayashi, K. *J. Am. Chem. Soc.* **2000**, *122*, 8654–8664.
- (9) Smith III, A. B.; Freeze, B. S.; Brouard, I.; Hirose, T. *Org. Lett.* **2003**, *5*, 4405–4408.
- (10) Smith III, A. B.; Freeze, B. S.; Xian, M.; Hirose, T. *Org. Lett.* **2005**, *7*, 1825–1828.
- (11) Mickel, S. J.; Sedelmeier, G. H.; Niederer, D.; Daeffler, R.; Osmani, A.; Schreiner, K.; Seeger-weibel, M.; Be, B.; Schaer, K.; Gamboni, R.; Chen, S.; Chen, W.; Jagoe, C. T.; Kinder, F. R.; Loo, M.; Prasad, K.; Repic, O.; Shieh, W.; Wang, R.; Waykole, L.; Xu, D. D.; Xue, S. *Org. Process Res. Dev.* **2004**, *8*, 92–100.
- (12) Mickel, S. J.; Sedelmeier, G. H.; Niederer, D.; Schuerch, F.; Grimler, D.; Koch, G.; Daeffler, R.; Osmani, A.; Hirni, A.; Schaer, K.; Gamboni, R.; Bach, A.; Chaudhary, A.; Chen, S.; Chen, W.; Hu, B.; Jagoe, C. T.; Kim, H.; Kinder, F. R.; Liu, Y.; Lu, Y.; Mckenna, J.; Prashad, M.; Ramsey, T. M. *Org. Process Res. Dev.* **2004**, *8*, 101–106.

- (13) Mickel, S. J.; Sedelmeier, G. H.; Niederer, D.; Schuerch, F.; Koch, G.; Kuesters, E.; Daeffler, R.; Osmani, A.; Seeger-weibel, M.; Schmid, E.; Hirni, A.; Schaer, K.; Gamboni, R.; Bach, A.; Chen, S.; Chen, W.; Geng, P.; Jagoe, C. T.; Kinder, F. R.; Lee, G. T.; Mckenna, J.; Ramsey, T. M.; Repic, O.; Rogers, L.; Shieh, W.; Wang, R. *Org. Process Res. Dev.* **2004**, 8, 107–112.
- (14) Mickel, S. J.; Sedelmeier, G. H.; Niederer, D.; Schuerch, F.; Seger, M.; Schreiner, K.; Daeffler, R.; Osmani, A.; Bixel, D.; Loiseleur, O.; Cercus, J.; Stettler, H.; Schaer, K.; Bach, A.; Chen, G.; Chen, W.; Geng, P.; Lee, G. T.; Loeser, E.; Mckenna, J.; Kinder, F. R.; Konigsberger, K.; Prasad, K.; Ramsey, T. M.; Reel, N.; Repic, O.; Rogers, L.; Shieh, W.; Wang, R.; Waykole, L.; Xue, S.; Florence, G.; Paterson, I. *Org. Process Res. Dev.* **2004**, 8, 113–121.
- (15) Mickel, S. J.; Niederer, D.; Daeffler, R.; Osmani, A.; Kuesters, E.; Schmid, E.; Schaer, K.; Chen, W.; Loeser, E.; Kinder, F. R.; Konigsberger, K.; Prasad, K.; Ramsey, T. M.; Florence, G.; Lyothier, I.; Paterson, I. *Org. Process Res. Dev.* **2004**, 8, 122–130.
- (16) Paterson, I.; Florence, G. J.; Gerlach, K.; Scott, J. P.; Sereinig, N. *J. Am. Chem. Soc.* **2001**, 123, 9535–9544.
- (17) Paterson, I.; Lyothier, I. *J. Org. Chem.* **2005**, 70, 5494–5507.
- (18) Harried, S. S.; Yang, G.; Strawn, M. A.; Myles, D. C. *J. Org. Chem.* **1997**, 62, 6098–6099.
- (19) Harried, S. S.; Lee, C. P.; Yang, G.; Lee, T. I. H.; Myles, D. C. *J. Org. Chem.* **2003**, 68, 6646–6660.
- (20) Marshall, J. A.; Johns, B. A. *J. Org. Chem.* **1998**, 63, 7885–7892.
- (21) Arefolov, A.; Panek, J. S. *J. Am. Chem. Soc.* **2005**, 127, 5596–5603.
- (22) De Lemos, E.; Porée, F.-H.; Bourin, A.; Barbion, J.; Agouridas, E.; Lannou, M.-I.; Commerçon, A.; Betzer, J.-F.; Pancrazi, A.; Ardisson, J. *Chemistry* **2008**, 14, 11092–112.
- (23) McGrogan, B. T.; Gilmartin, B.; Carney, D. N.; McCann, A. *Biochim. Biophys. Acta* **2008**, 1785, 96–132.
- (24) Gigant, B.; Cormier, A.; Dorléans, A.; Ravelli, R. B. G.; Knossow, M. *Top. Curr. Chem.* **2009**, 286, 259–278.
- (25) Jordan, M. A.; Wilson, L. *Nat Rev Cancer* **2004**, 4, 253–265.
- (26) Schiff, P. B.; Horwitz, S. B. *Proc. Natl. Acad. Sci. U. S. A.* **1980**, 77, 1561–1565.

- (27) Ter Haar, E.; Rosenkranz, H. S.; Hamel, E.; Day, B. W. *Bioorg. Med. Chem.* **1996**, *4*, 1659–1671.
- (28) Ter Haar, E.; Kowalski, R. J.; Hamel, E.; Lin, C. M.; Longley, R. E.; Gunasekera, S. P.; Rosenkranz, H. S.; Day, B. W.; Pierce, F. *Biochemistry* **1996**, *35*, 243–250.
- (29) Balachandran, R.; Grant, S. G.; Welsh, M. J.; Day, B. W. *Breast J.* **1998**, *4*, 409–419.
- (30) Kowalski, R. J.; Giannakakou, P.; Gunasekera, S. P.; Longley, R. E.; Day, B. W.; Hamel, E. *Mol. Pharmacol.* **1997**, *52*, 613–622.
- (31) Balachandran, R.; ter Haar, E.; Welsh, M. J.; Grant, S. G.; Day, B. W. *Anticancer. Drugs* **1998**, *9*, 67–76.
- (32) Klein, L. E.; Freeze, B. S.; Smith, A. B.; Horwitz, S. B. *Cell Cycle* **2005**, *4*, 501–507.
- (33) Martello, L. A.; LaMarche, M. J.; He, L.; Beauchamp, T. J.; Smith III, A. B.; Horwitz, S. B. *Chem. Biol.* **2001**, *8*, 843–855.
- (34) Bröker, L. E.; Huisman, C.; Ferreira, C. G.; Rodriguez, J. A.; Kruyt, F. A. E.; Giaccone, G. *Cancer Res.* **2002**, *62*, 4081–4088.
- (35) Chao, S. K.; Lin, J.; Brouwer-Visser, J.; Smith III, A. B.; Horwitz, S. B.; McDaid, H. M. *Proc. Natl. Acad. Sci. U. S. A.* **2011**, *108*, 391–396.
- (36) Martello, L. A.; McDaid, H. M.; Regl, D. L.; Yang, C.-P. H.; Meng, D.; Pettus, T. R. R.; Kaufman, M. D.; Arimoto, H.; Danishefsky, S. J.; Smith, A. B.; Horwitz, S. B. *Clin. Cancer Res.* **2000**, *6*, 1978–1987.
- (37) Honore, S.; Kamath, K.; Braguer, D.; Horwitz, S. B.; Wilson, L.; Briand, C.; Jordan, M. A. *Cancer Res.* **2004**, *64*, 4957–4964.
- (38) Wilmes, A.; O’Sullivan, D.; Chan, A.; Chandrasekhar, C.; Paterson, I.; Northcote, P. T.; La Flamme, A. C.; Miller, J. H. *Cancer Chemother. Pharmacol.* **2011**, *68*, 117–126.
- (39) Dabydeen, D. A.; Florence, G. J.; Paterson, I.; Hamel, E. *Cancer Chemother. Pharmacol.* **2004**, *53*, 397–403.
- (40) Mita, A.; Lockhart, A. C.; Chen, T.-L.; Bochinski, K.; Curtright, J.; Cooper, W.; Hammond, L.; Rothenberg, M.; Rowinsky, E.; Sharma, S. *ASCO Meet. Abstr.* **2004**, *22*, 2025.
- (41) Ojima, I.; Chakravarty, S.; Inoue, T.; Lin, S.; He, L.; Horwitz, S. B.; Kuduk, S. D.; Danishefsky, S. J. *Proc. Natl. Acad. Sci. U. S. A.* **1999**, *96*, 4256–4261.
- (42) Smith III, A. B.; LaMarche, M. J.; Falcone-Hindley, M. *Org. Lett.* **2001**, *3*, 695–698.

- (43) Monteagudo, E.; Cicero, D. O.; Cornett, B.; Myles, D. C.; Snyder, J. P. *J. Am. Chem. Soc.* **2001**, *123*, 6929–6930.
- (44) Sánchez-Pedregal, V. M.; Kubicek, K.; Meiler, J.; Lyothier, I.; Paterson, I.; Carlomagno, T. *Angew. Chem. Int. Ed. Engl.* **2006**, *45*, 7388–7394.
- (45) Canales, A.; Matesanz, R.; Gardner, N. M.; Andreu, J. M.; Paterson, I.; Díaz, J. F.; Jiménez-Barbero, J. *Chemistry* **2008**, *14*, 7557–7569.
- (46) Jogalekar, A. S.; Kriel, F. H.; Shi, Q.; Cornett, B.; Cicero, D.; Snyder, J. P. *J. Med. Chem.* **2010**, *53*, 155–165.
- (47) Díaz, J. F.; Barasoain, I.; Andreu, J. M. *J. Biol. Chem.* **2003**, *278*, 8407–8419.
- (48) Díaz, J. F.; Barasoain, I.; Souto, A. a; Amat-Guerri, F.; Andreu, J. M. *J. Biol. Chem.* **2005**, *280*, 3928–3937.
- (49) Buey, R. M.; Calvo, E.; Barasoain, I.; Pineda, O.; Edler, M. C.; Matesanz, R.; Cerezo, G.; Vanderwal, C. D.; Day, B. W.; Sorensen, E. J.; Lopez, J. A.; Andreu, J. M.; Hamel, E.; Diaz, J. F. *Nat Chem Biol* **2007**, *3*, 117–125.
- (50) Khrapunovich-Baine, M.; Menon, V.; Verdier-Pinard, P.; Smith, A. B.; Angeletti, R. H.; Fiser, A.; Horwitz, S. B.; Xiao, H. *Biochemistry* **2009**, *48*, 11664–77.
- (51) Gunasekera, S. P.; Longley, R. E.; Isbrucker, R. A. *J. Nat. Prod.* **2002**, *65*, 1830–1837.
- (52) Gunasekera, S. P.; Longley, R. E.; Isbrucker, R. A. *J. Nat. Prod.* **2001**, *64*, 171–174.
- (53) Gunasekera, S. P.; Paul, G. K.; Longley, R. E.; Isbrucker, R. A.; Pomponi, S. A. *J. Nat. Prod.* **2002**, *65*, 1643–1648.
- (54) Shaw, S. J.; Sundermann, K. F.; Burlingame, M. A.; Myles, D. C.; Freeze, B. S.; Xian, M.; Brouard, I.; Smith, A. B. *J. Am. Chem. Soc.* **2005**, *127*, 6532–6533.
- (55) Shaw, S. J.; Menzella, H. G.; Myles, D. C.; Xian, M.; Smith III, A. B. *Org. Biomol. Chem.* **2007**, *5*, 2753–2755.
- (56) Shaw, S. J.; Sundermann, K. F.; Burlingame, M. A.; Zhang, D.; Petryka, J.; Myles, D. C. *Bioorg. Med. Chem. Lett.* **2006**, *16*, 1961–1964.
- (57) Smith, A. B.; Freeze, B. S.; LaMarche, M. J.; Hirose, T.; Brouard, I.; Rucker, P. V.; Xian, M.; Sundermann, K. F.; Shaw, S. J.; Burlingame, M. A.; Horwitz, S. B.; Myles, D. C. *Org. Lett.* **2005**, *7*, 311–314.
- (58) Gunasekera, S. P.; Mickel, S. J.; Daeffler, R.; Niederer, D.; Wright, A. E.; Linley, P.; Pitts, T. *J. Nat. Prod.* **2004**, *67*, 749–756.

- (59) Smith, A. B.; Xian, M.; Liu, F. *Org. Lett.* **2005**, 7, 4613–4616.
- (60) Pettit, G. R.; Cichacz, A.; Gao, F.; Boydb, M. R.; Schmidt, J. M. *J. Chem. Soc. Chem. Comm.* **1994**, 1111–1112.
- (61) Paterson, I.; Britton, R.; Delgado, O.; Meyer, A.; Poullennec, K. G. *Angew. Chem. Int. Ed. Engl.* **2004**, 43, 4629–4633.
- (62) Shin, Y.; Fournier, J.-H.; Fukui, Y.; Brückner, A. M.; Curran, D. P. *Angew. Chem. Int. Ed. Engl.* **2004**, 43, 4634–4637.
- (63) Madiraju, C.; Edler, M. C.; Hamel, E.; Raccor, B. S.; Balachandran, R.; Zhu, G.; Giuliano, K. A.; Vogt, A.; Shin, Y.; Fournier, J.; Fukui, Y.; Curran, D. P.; Day, B. W. *Biochemistry* **2005**, 44, 15053–15063.
- (64) Zhu, W.; Jimenez, M.; Jung, W.-H.; Camarco, D. P.; Balachandran, R.; Vogt, A.; Day, B. W.; Curran, D. P. *J. Am. Chem. Soc.* **2010**, 132, 9175–9187.
- (65) Fukui, Y.; Brückner, A. M.; Shin, Y.; Balachandran, R.; Day, B. W.; Curran, D. P. *Org. Lett.* **2006**, 8, 301–304.
- (66) Shin, Y.; Fournier, J.; Balachandran, R.; Madiraju, C.; Raccor, B. S.; Zhu, G.; Edler, M. C.; Hamel, E.; Day, B. W.; Curran, D. P. *Org. Lett.* **2005**, 7, 2873–2876.
- (67) Shin, Y.; Choy, N.; Turner, T. R.; Balachandran, R.; Madiraju, C.; Day, B. W.; Curran, D. P. *Org. Lett.* **2002**, 4, 4443–4446.
- (68) Paterson, I.; Gardner, N. M. *Chem. Commun. (Camb)*. **2007**, 8, 49–51.
- (69) Paterson, I.; Naylor, G. J.; Wright, A. E. *Chem. Commun. (Camb)*. **2008**, 4628–4630.
- (70) Paterson, I.; Naylor, G. J.; Fujita, T.; Guzmán, E.; Wright, A. E. *Chem. Commun. (Camb)*. **2010**, 46, 261–263.
- (71) Smith, A. B.; Sugawara, K.; Atasoylu, O.; Yang, C.-P. H.; Horwitz, S. B. *J. Med. Chem.* **2011**, 54, 6319–6327.
- (72) Löwe, J.; Li, H.; Downing, K. H.; Nogales, E. *J. Mol. Biol.* **2001**, 313, 1045–1057.
- (73) Salum, L. B.; Dias, L. C.; Andricopulo, A. D. *QSAR Comb. Sci.* **2009**, 28, 325–337.
- (74) Day, B. W.; Kangani, C. O.; Avor, K. S. *Tetrahedron: Asymmetry* **2002**, 13, 1161–1165.
- (75) Loiseleur, O.; Koch, G.; Wagner, T. *Org. Process Res. Dev.* **2004**, 8, 597–602.
- (76) Loiseleur, O.; Koch, G.; Cercus, J.; Schürch, F. *Org. Process Res. Dev.* **2005**, 9, 259–271.

- (77) Gage, J. R.; Evans, D. A. *Org. Synth.* **1993**, 8, 528–531.
- (78) Hintermann, T.; Seebach, D. *Helv. Chim. Acta* **1998**, 81, 2093–2126.
- (79) Evans, D. A.; Fitch, D. M. *J. Org. Chem.* **1997**, 62, 454–455.
- (80) Smith, A. B.; Xian, M. *Org. Lett.* **2005**, 7, 5229–5232.
- (81) Schlosser, M.; Muller, G.; Christmann, K. F. *Angew. Chem. Int. Ed. Engl.* **1966**, 5, 667–668.
- (82) Xiao, Q.; Ren, W.-W.; Chen, Z.-X.; Sun, T.-W.; Li, Y.; Ye, Q.-D.; Gong, J.-X.; Meng, F.-K.; You, L.; Liu, Y.-F.; Zhao, M.-Z.; Xu, L.-M.; Shan, Z.-H.; Shi, Y.; Tang, Y.-F.; Chen, J.-H.; Yang, Z. *Angew. Chem. Int. Ed. Engl.* **2011**, 50, 7373–7377.
- (83) Anh, N. T.; Eisenstein, O.; Lefour, J.-M.; Tran Huu Dau, M. *J. Am. Chem. Soc.* **1973**, 95, 6146–6147.
- (84) Berliner, M. A.; Belecki, K. *J. Org. Chem.* **2005**, 70, 9618–9621.
- (85) Collington, E. W.; Finch, H.; Smith, I. J. *Tetrahedron Lett.* **1985**, 26, 681–684.
- (86) Oppolzer, W.; Snowden, R. L.; Simmons, D. P. *Helv. Chim. Acta* **1981**, 64, 2002–2021.
- (87) Kocovsky, P. *Tetrahedron Lett.* **1986**, 27, 5521–5524.
- (88) Smith, A. B.; Xian, M. *Org. Lett.* **2005**, 7, 5229–5232.
- (89) Hoveyda, A. H.; Malcolmson, S. J.; Meek, S. J.; Zhugralin, A. R. *Angew. Chem. Int. Ed. Engl.* **2010**, 49, 34–44.
- (90) Kangani, C. O.; Bruckner, A. M.; Curran, D. P. *Org. Lett.* **2005**, 7, 379–382.
- (91) Yu, M.; Wang, C.; Kyle, A. F.; Jakubec, P.; Dixon, D. J.; Schrock, R. R.; Hoveyda, A. H. *Nature* **2011**, 479, 88–93.
- (92) Yadav, J. S.; Venkatesh, M.; Swapnil, N.; Prasad, a. R. *Tetrahedron Lett.* **2013**, 54, 2336–2339.
- (93) Willwacher, J.; Kausch-Busies, N.; Fürstner, A. *Angew. Chem. Int. Ed. Engl.* **2012**, 12041–12046.
- (94) Chatterjee, A. K.; Choi, T.-L.; Sanders, D. P.; Grubbs, R. H. *J. Am. Chem. Soc.* **2003**, 125, 11360–11370.